A Model for Calculating EM Field in Layered Medium with Application to Biological Implants

A Thesis submitted for the degree of

Doctor of Philosophy

by

S.M. Salehi-Reyhani

Department of Electronic and Computer Engineering

Brunel University

July 10, 2001

To

My family

and
all scientists of this world.

Abstract

MODERN wireless telecommunication devices (GSM Mobile system)(cellular telephones and wireless modems on laptop computers) have the potential to interfere with implantable medical devices/prostheses and cause possible malfunction. An implant of resonant dimensions within a homogeneous dielectric lossy sphere can enhance local values of SAR (the specific absorption rate). Also antenna radiation pattern and other characteristics are significantly altered by the presence of the composite dielectric entities such as the human body. Besides, the current safety limits do not take into account the possible effect of hot spots arising from metallic implants resonant at mobile phone frequencies. Although considerable attention has been given to study and measurement of scattering from a dielectric sphere, no rigorous treatment using electromagnetic theory has been given to the implanted dielectric spherical head/cylindrical body.

This thesis aims to deal with the scattering of a plane electromagnetic wave from a perfectly conducting or dielectric spherical/cylindrical implant of electrically small radius (of resonant length), embedded eccentrically into a dielectric spherical head model. The method of dyadic Green's function (DGF) for spherical vector wave functions is used. Analytical expressions for the scattered fields of both cylindrical and spherical implants as well as layered spherical head and cylindrical torso models are obtained separately in different chapters. The whole structure is assumed to be uniform along the propagation direction.

To further check the accuracy of the proposed solution, the numerical results from the analytical expressions computed for the problem of implanted head/body

are compared with the numerical results from the Finite-Difference Time-Domain (FDTD) method using the EMU-FDTD Electromagnetic simulator. Good agreement is observed between the numerical results based on the proposed method and the FDTD numerical technique.

This research presents a new approach, away from simulation work, to the study of exact computation of EM fields in biological systems. Its salient characteristics are its simplicity, the saving in memory and CPU computational time and speed.

Contents

List of Figures

List of Tables

Acknowledgements

THE author wishes to express his sincere appreciation of the facilities placed at his disposal in the department of Electronic and Computer Engineering at BRUNEL University, as well as the helpful discussions with the project supervisor Dr. R.J. Glover to whom I am particularly grateful for his continual support and advice to tackle a variety of problems and investigations throughout the period of this project and preparation of this thesis.

I would also like to take this opportunity to express my gratitude to my other supervisor Dr. M. Berwick for all his guidance and encouragement throughout the research.

I am deeply grateful for the financial assistance given by Cochlear U.K Limited and EPSRC, and my sincere appreciation is extended to the support given by Dr. Barry Nevison of Cochlear U.K Limited.

Most of my knowledge of electromagnetics has been gained from the study of the work of other people, and there are a great many. To these people I am indebted and regret that I have not had an opportunity to meet with them.

I am also very grateful to my family for valuable help and providing me with financial support.

Last, but by no means least, thanks are due to fellow colleagues and friends for many helpful suggestions and comments throughout the various stages of this project.

Nomenclature

The symbols defined here are used throughout the dissertation.

$\overline{a}, \overline{b}$	Denotes Vectors
a_i	ith Element of Vector $\overline{a}$
Δx	A Small Change in x
δx	A Small Disturbance in x
dx	Derivative in x
$\sum$	Sum
$\prod$	Product
$\int$	Integral
$\oiint_S$	Surface (or Double) Contour Integral
$\iiint_V$	Volume (or Tripple) Integral
$\|.\|$	Absolute Value of
$\Re$	Real Component
$\Im$	Imaginary component
∞	Infinity
$=$	is Equal to
$\neq$	is Not Equal to
$\approx$	Approximately Equal to
log	Logarithm to the Base 10
ln	Natural Logarithm
$\Psi_{gmn}(\kappa)$	Denote the Spherical Characteristic Function

$\Psi_{ee_{o}^{e}n}(h)$	Denote the Cylindrical Characteristic Function
$\mathbf{B}$	Magnetic Flux Density (weber/m^2) (Teslas)
c	Conduction
c	Velocity of Light in Air
c_j	Current Moment of Dipole in any Direction
$\overline{c}$	Current Moment of Dipole
d	Displacement
$\mathbf{D}$	Electric Flux Density (Coulombs/m^2)
e	Subscript Denoting Electic Type
e	Subscripts "e" Stand for Even Character of the Generating Functions
$\mathbf{E}$	Subscript Identifies Electric Type
$\mathbf{E}$	Superscript Identifies TM Waves
$\mathbf{E}$	Electric Field Strength
E_x	x-Component of Electric Field Strength
E_y	y-Component of Electric Field Strength
E_z	z-Component of Electric Field Strength
$\mathbf{E}^{inc}$	Incident Electric Field Strength
$\mathbf{E}_{max}$	Positive Electric Field Strength Peak Value
$\mathbf{E}_{min}$	Negative Electric Field Strength Peak Value
$\mathbf{E}^{scat}$	Scattered Electric Field Strength
$\mathbf{E}_{tan}$	Tangential Electric Field Strength
$\mathbf{E}^{tot}$	Total Electric Field Strength
$\overline{E}_c(\overline{R}_o)$	Correction Term of Electric Type
f	Field Point or Observer Layer
f	Superscript Identifies Centrifugal Reflection or Transmission
$F_n^m(\cos\theta)$	Identifies the Associated Legendre Functions of the First Kind with Order (n, m)
$(\overline{\overline{F}})^{\intercal}$	Transpose of Dyadic $\overline{\overline{F}}$
$\overline{\overline{G}}$	Denotes Dyadic Green's Function

$\overline{\overline{G}}_{eo}^{00o}(\overline{R},\overline{R}')$	Free Space Dyadic Green's Function of Electric Type
$\overline{\overline{G}}_{es}^{Lfo}(\overline{R},\overline{R}')$	Scattering Dyadic Green's Function of Electric Type in Layered Media
$\overline{\overline{G}}_{ms}^{Lfso}(\overline{R},\overline{R}')$	Scattering Dyadic Green's Function of Magnetic Type in Layered Media
h	Eigenvalues
$h_n^{(1)}(kR)$	Spherical Hankel Function of the First Kind
$H_n^{(1)}(\eta_o r)$	Cylindrical Hankel Function of the First Kind
$\mathbf{H}$	Superscript Identifies TE Waves
$\mathbf{H}$	Magnetic Field Strength
H_x	x-Component of Magnetic Field Strength
H_y	y-Component of Magnetic Field Strength
H_z	z-Component of Magnetic Field Strength
$\mathbf{H}^{inc}$	Incident Magnetic Field Strength
$\mathbf{H}^{scat}$	Scattered Magnetic Field Strength
$\mathbf{H}^{tot}$	Total Magnetic Field Strength
i	Integer 1,2,3
$\mathbf{i}$	Unit Vector in the x-Direction
$\overline{\overline{I}}$	Idem Factor
j	Imaginary Numbers i.e $\sqrt{-1}$
j	Integer 1,2,3
$j_n(\kappa R)$	Spherical Bessel Functions of the Order n to Represent Both Out-Going and In-Coming Waves
$j_n(\lambda r)$	Cylindrical Bessel Functions of the Order n to Represent Both Out-Going and In-Coming Waves
$\mathbf{j}$	Unit Vector in the y-Direction
$\mathbf{J}$	Current Density (C/Sm^2) (A/m^2)
k	$\omega(\mu_o\varepsilon_o)^{1/2} = \frac{\omega}{c}$
$\mathbf{k}$	Unit Vector in the z-Direction

$\mathbf{K}$	Separation Constant
l	Length of the Torso/Implant
L	Last Inner Layer
$\overline{L}_{egnn}(k)$	Nonsolenoidal (Irrotational or Lamellar) Spherical Vector Wave Function
$\overline{L}_{oegn\lambda}(h)$	Nonsolenoidal (Irrotational or Lamellar) Cylindrical Vector Wave Function
$\overline{M}^{(R)}_{egnn}(k)$	Solenoidal (Rotational/Transverse) Spherical Vector Wave Function
n	Integer 0,1,2,3, ...
$\overline{N}^{(R)}_{egnn}(k)$	Solenoidal (Rotational/Transverse) Spherical Vector Wave Function
o	Subscripts "o" Stand for Odd Character of the Generating Functions
o	Subscript/Superscript Identifies Open Space
P	Superscript Identifies Centripetal Reflection or Transmission
$\mathbf{P}$	Power
$\mathbf{P}_{abs}$	Power Absorbed
$\mathbf{P}_{del}$	Real Power Delivered to the Antenna
$\mathbf{P}_{rad}$	Power Radiated
$\mathbf{P}_{tot}$	Total Power
$\overline{P}^{(z)}_{egnn}(h)$	Solenoidal (Rotational/Transverse) Cylindrical Vector Wave Function
$\mathbf{PV}_{tot}$	Principal Value
q	Integer 0,1,2,3, ...
$\overline{Q}^{(z)}_{egnn}(h)$	Solenoidal (Rotational/Transverse) Cylindrical Vector Wave Function
R	Radius of the Sphere
R	Reflection Coefficient
$\hat{R}$	Unit Vector in Spherical Coordinate
$\hat{R}\hat{R}$	Spherical Dyad
r	Radius of the Cylinder
$\hat{r}$	Unit Vector in Cylindrical Coordinate
$\hat{r}\hat{r}$	Cylindrical Dyad

s	Scattering
$^{\top}$	Transpose of a Matrix, Vector
T	Transmission Coefficient
$\overline{\overline{T}}_{\lambda}$	Dyadic Spatial Operator
x	x-Component of Rectangular Coordinate System
$\hat{x}$	Unit Vector in Rectangular Coordinate System
y	y-Component of Rectangular Coordinate System
$\hat{y}$	Unit Vector in Rectangular Coordinate System
$Y_n(k_r r)$	Neumann Function
z	z-Component of Rectangular Coordinate System
$\hat{z}$	Unit Vector in Rectangular Coordinate System
δ_f^o	The Free Space Kronecker Delta Function
δ_f^L	The Last Layer Kronecker Delta Function
δ_f^{fI}	Kronecker Delta Function where the Implant is Located
$\overline{\odot}$	Operator which Exploits the Symmetry of the DGF Expansion
$\delta(\overline{R}-\overline{R}')$	Weighted Dirac Delta Function in Three Dimensions
$-\frac{\hat{R}\hat{R}}{k_o^2}\delta(\overline{R}-\overline{R}')$	Isolated Singular Term
$\nabla\times[\overline{\overline{I}}\delta_e(\overline{R}-\overline{R}')]$	Source Function

Greek Symbols

α	Radius
ε	Dielectric Constant (Permittivity) (Farads/meter)
ε_o	Permittivity of Free Space (8.854×10^{-12} Farads/meter)
θ	Angle in Spherical Coordinate
$\hat{\theta}$	Unit Vector in Spherical Coordinate
κ	An Undetermined Wave Number
λ	Cylindrical Eigenvalue
λ	Wave-length

μ	Cylindrical Eigenvalue
μ	Permeability (Henrys/meter)
μ_o	Permeability of Free Space ($4\pi \times 10^{-7}$ Henrys/meter)
π	3.14
ρ	Mass Density (kgr/m^3) (gr/cm^3)
σ	Medium Conductivity (mho/m)
ϕ	Angle in Spherical/Cylindrical Coordinate
$\hat{\phi}$	Unit Vector in Cylindrical Coordinate
ψ	Denote a Characteristic Function
ω	Discrete Time Physical Frequency Variable
∇	Scalar to Vector Operator (Del) (Grad)
$\nabla\cdot$	Divergence (Vector to scalar) Operator (Div)
$\nabla\times$	Vector to Vector Operator (Curl)

Chapter 1

Introduction

COMPUTATIONAL electromagnetics (CEM) may be broadly defined as that branch of electromagnetics which intrinsically and routinely involves using a computer to obtain numerical results. With the evolutionary development of CEM during the past 30-plus years, two basic lines of improvement can be identified. One is due to advances taking place in computer hardware and software, providing tools of steadily growing power with little effort on the part of the electromagnetics community *per se*. The other line of improvement originates from within the electromagnetics discipline itself, where increasing awareness and utilization of numerical techniques has provided an expanding base of capability for solving problems in electromagnetics. The result has been to add the third tool of computational methods in electromagnetic (EM) specifically, and in science and engineering generally, to the two classical tools of experimental observation and mathematical analysis. The goal of this research is to create a model for calculating EM field in layered medium with application to biological implants.

1.1 Background and Motivation

Exposure to electromagnetic fields is not a new phenomenon. However, during the 20th century environmental exposure to man-made electromagnetic fields has been steadily increasing as growing electricity demand, ever-advancing technologies and

changes in social behaviour have created more and more artificial sources. Everyone is exposed to a complex mix of weak electric and magnetic fields, both at home and at work, from the generation and transmission of electricity, domestic appliances and industrial equipment, to telecommunications and broadcasting. Computer techniques have revolutionized the way in which EM problems are analyzed. EM engineers rely heavily on computer methods to analyze, for example, complex antenna-something systems, planar microwave devices, EMC/EMI problems, etc. A number of different numerical techniques for solving these EM problems are available. They are mostly based on full-wave analysis, either in the time or frequency domains, where one or two differential equations plus problem-specific boundary conditions are of interest. Each numerical technique is well suited for the analysis of a particular class of EM problem.

EM engineers must be very careful in applying these pure numerical techniques. Although they are powerful and can be applied to a variety of EM problems, their output may frequently mislead or be misinterpreted. As long as there are no numerical errors such as *overflow* or *underflow*, computers always give numbers as solutions. The problem is whether these numbers correspond to *real physics* of the problem at hand. EM engineers must always be aware of the assumptions made in the numerical technique that is being used. Under what conditions is this technique derived? What kind of a problem or problems can be handled via this technique? Are there any parametric limitations? What are the accuracy and numerical error limits? Without knowing the answers of these questions it is very dangerous to use these techniques.

One of the most powerful techniques in the frequency domain is the method of moments (MoM) [1]. The primary formulation of MoM is an integral equation obtained through the use of Green's functions. The technique is based on solving complex integral equations by reducing them to a system of linear equations and on applying *method of moments (weighted residuals).*

Mobile phone-human interaction is a current EM research topic [2] - [5]. It is

important from both human health and antenna performance points of view. It should be noted that, biomedical modeling via these techniques is very difficult. Only specific absorption rate (SAR) of human tissues can be calculated [5]. SAR is a measure of EM energy converted into heat in tissues. Discrete tissues are modeled with their electrical parameters (σ and ε_r), which are supplied by EM measurements. Different EM groups use quite different values. There are also discrepancies among the limits of SAR values declared to be safe by the international health organizations. Simulation results must therefore be carefully analyzed when human health is the concern.

Although limited with only idealized geometries, analytical solutions are very important to understand the physics behind the problem at hand. It is only then possible to use pure numerical techniques in analyzing complex EM problems.

The state-of-the-art in numerical modeling is progressing rapidly. On the other hand, practical EM problems are also becoming more and more complicated. It is, therefore, essential that EM engineers should

- have strong analytical background
- use numerical as well as analytical techniques at the same time.

Finally, it may be concluded that the trend in numerical simulation techniques is towards using some hybrid forms of analytical approximate and numerical methods.

As advances in numerical techniques for solutions to Maxwell's equations accelerate, larger and more complex EM problems are becoming tractable at an astounding rate. The science of computational electromagnetics (CEM) gains inertia with each passing day. In this exciting time, new and more efficient algorithms are being developed that augment the advances in computational facilities promising a bright future for CEM research.

The maturing field of CEM research has sprouted various branches of research. The FDTD method provides a simple and robust method for simulating the propagation of EM radiation through complex media, e.g., human tissue. Although the

FDTD method performs superbly for such propagation simulations, it is not very well suited for modeling complex metallic structures, e.g., antennas.

Conversely, a distinct branch of CEM research, MoM, is superior for modeling complex metallic structures and is not very well suited for propagation through complex media, such as human tissue. It is therefore paramount that a hybrid MoM/FDTD/DGF for simulating the interaction of antennas with humans should be researched.

An important problem in the study of the biological effects of microwave radiation is the prediction of the induced temperatures within irradiated, heat sensitive human organs. Animal experimentation has indicated that microwave heating can cause tissue damage. However, because of the general dissimilarity of animal and human organs, such work can not be exactly related to human exposure to microwaves. Direct human experimentation is not possible, in most instances, because of the possibility of injury to the test subject.

The recent efforts aimed at improving available personal communications services and allegedly their health hazards have generated an elevated interest in the performance of compact antenna structures mounted on hand-held devices. The characterization of such antennas is dependent upon the development of simulation tools which can accurately model general topologies including wires, dielectrics, conductors, and lumped elements. An important class of simulation tools which can accommodate these modeling requirements are derived dyadic Green's function (DGF) of Maxwell's equations. In this thesis, the formulation and application of this technique is investigated. First, the DGF for spherical head/cylindrical body is implemented to allow investigation of head/torso-antenna model. The resulting analytical tools are applied to determine the SAR when in proximity to antennas. The power absorption characteristics, SAR, within tissue are studied, and it is determined that approximately 48 to 68% of the power delivered to the antenna is absorbed in the human head.

The increasing use of electromagnetic (EM) equipment and devices, for applica-

tions such as radar communications, Nuclear Magnetic Resonance (NMR) imaging, radio frequency (RF) heaters and sealers, biomedical applications such as shortwave diathermy, hyperthermia devices for cancer therapy, etc., is causing the exposure of an increasing number of people to far- and near-field radiation. This has caused growing concern about possible health hazards produced by EM radiation. The concern has led to increased research aimed at identifying possible hazards due to EM radiation.

An important aspect of the application of this research is the determination of the deposition of EM energy in the human head/body when it is subjected to EM radiation.

The deposition of EM energy in the human head/body is usually quantified by the mass-normalized rate of energy absorption or the specific absorption rate (SAR), that includes the whole-body-averaged SAR, local SAR, etc. Whole-head/body-averaged SAR is the total energy absorbed per unit time, divided by the total mass of the body. Local SAR, on the other hand, is a point relationship describing the time rate of change of the energy absorbed in a differential volume of the absorbing body. The SI unit of SAR is watts per kilogram (W/kg).

In the past most of the researchers used frequency-domain techniques, such as the method of moments (MoM) [1], to calculate SARs within human models. Chen and Guru [6] used this method for a human model composed of 124 identical size cubical cells. However, the model was homogeneous. Hagmann, Gandhi, and Durney [7] also used the MoM on a more realistically shaped model. It was composed of 180 cells, allowed more freedom in defining the shape, and each cell was defined by fraction of 10 different tissue types. This model was used to calculate the average SAR of a human standing on a ground plane [8], and to study the effects of head resonance [9]. Borup used an improved MoM method and a supercomputer (CRAY-XMP) to calculate the SAR distribution in a 5600-cell inhomogeneous human model, but each run needs about 25 minutes of CPU time, a considerable expense. In general, the MoM method derives a set of linear equations for either field variables

or field expansion coefficients, and then solves the linear system with a suitable matrix-inversion scheme.

Also the use of numerical techniques for higher resolution models has been hindered by the fact that its need for computer resources increases rapidly with the number of cells used to model the body. Typically, computer storage requirements increase on the order of $(3N)^2$ and computation time increase as $(3N)^3$, where N is the number of cells. For the FFT-based MoM, the time requirements are reduced to $N \ln N$ [10].

A highly promising numerical method is the Finite-Difference Time-Domain (FDTD) method which is a direct implementation of the time-dependent Maxwell's curl equations. This method treats the irradiation of the scatterer as an initial value problem. At $t = 0$, a source of irradiation at frequency f is assumed to be turned on. The propagation of waves from this source is simulated by solving a finite-difference analog of the time-dependent Maxwell's equations on a lattice of points, including the scatterer. Time stepping is continued until the sinusoidal steady state is achieved at each point. The field envelope, or maximum absolute value, during the final half-wave cycle of time steps is recorded by the peak detectors as the magnitude of the phasor of the steady-state field. This method has two advantages relative to the frequency-domain approaches. First, and most important, its computer memory and running CPU time requirement is not proportional to $(3N)^2$ and $(3N)^3$, respectively, but increase linearly with $3N$, second, it is simple to implement for complicated scatterers, because arbitrary dielectric parameters may be assigned to each lattice point. The main advantages of such a method are that it can be easily applied to conducting obstacles and/or to dielectric and magnetic obstacles, which can be either homogeneous or inhomogeneous. The obstacles can be arbitrary shape. Furthermore, the FDTD technique provide a very efficient way of solving Maxwell's equations.

The FDTD method was first proposed by Yee [11] and later developed by Taflove [12] - [14], Holland [15], and Kunz and Lee [16]. Recently, it has been extended

for calculations of the distribution of electromagnetic fields in a human model for incident plane-wave at 100 MHz and 350 MHz [17, 18].

Analytical methods generally require less computation than numerical techniques. That makes them very powerful EM analysis tools.

This thesis presents a unified macroscopic theory of electromagnetic waves in accordance with the principle of DGFs from the point of view of the DGF form of Maxwell's equations and constitutive relations. We attempt to accomplish this extremely broad task by introducing only the detail needed to illustrate the central ideas involved and providing an alternative answer to CEM of biological modeling.

1.2 Organization of Thesis

In the remainder of this chapter we offer a brief outline of the rest of this thesis, and give a short (but important) remark on notation. The organization of this thesis is as follows:

Chapter 1, gives a brief introduction to the work undertaken in this thesis and how it is organized. Original contribution of this work is also itemized in this chapter. Although each chapter, in itself, outlines the problems addressed by its contents, overall justifications for the direction taken during the author's PhD study are also contained in this chapter. An overview of computational electromagnetics and a few of the available popular numerical modeling techniques have been presented in chapter 1. Methods included in this review are categorized in terms of time or frequency domain FDTD, TLM and MoM techniques.

Chapter 2, discusses DGF, a mathematical and conceptual method applicable in the analysis of the electromagnetic fields.

Chapter 3 has been published as a paper in the Journal of Electromagnetics, 2000, and its concise version was presented in a Colloquium in IEE Savoy Place. It introduces a model for human head or any organ resembling an sphere using spherical DGF. The principle objectives in this chapter are three-fold. An exact general

expression of dyadic Green's function (DGF) for the problem of electromagnetic radiation from a source of excitation in the presence of a layered spherical dielectric head model, which is valid everywhere, including the source region was outlined. The medium is assumed to be homogeneous, isotropic, linear, non-dispersive and stationary. The DGFs obtained by employing the method of scattering superposition. Furthermore, the question of incompleteness of previously related studies with regard to the E and H modes in the source region were discussed. We consider that one should explicitly extract the singularity term for the expansion to be valid both inside and outside the source region. This follows because the primary interest can be the development of a formulation to evaluate the electromagnetic fields away from the source. Also, a compact alternative general representation has been developed to determine the electric and magnetic type DGFs giving clarity as well as more efficient and economical computation in terms of speed, time and memory.

Chapter 4, further investigates human torso model using cylindrical DGF. Antenna radiation pattern and other characteristics are significantly altered by the presence of the human body. This chapter aims to express a general representation of dyadic Green's function (DGF) for the problem of electromagnetic radiation from a source of excitation in the presence of a human torso model (multi-layered homogeneous lossy dielectric circular cylinder of finite length) as well as any part of the body assuming the shape of a cylinder. The whole structure is assumed to be uniform along the propagation direction. Chapter 4 has been submitted to Electromagnetic Journal for publication, and a short version was presented in the 11th International Conference on EMC (IEE EMC York 99) University of York, UK.

Chapter 5, (presented in the 3rd IMACS/IEEE International Multiconference on: Circuits, Systems, Communications and Computers (CSCC'99) (IMACS/IEEE CSCC'99), Athens, Greece), investigates the extension of the cylindrical DGF method to electromagnetic DGF of an implantable medical device model. Comprehensive understanding of EM interactions between implanted human and modern personal communication antennas is essential for the hand held transceiver design. Since the

human head is usually located in the reactive or near-field region of the antenna, the performance of an antenna may be severely affected by the presence of conducting medical devices/prostheses in the head. Also, significant portion of the antenna delivered power may be absorbed in the head. The principle objective of this chapter is to outline a general expression of dyadic Green's function (DGF) for the problem of electromagnetic radiation from a source of excitation in the presence of a finite length of perfectly conducting circular cylinder of any size as well as of resonant length, which is valid everywhere, including the source region. The whole structure is assumed to be uniform along the propagation direction. The DGFs are obtained by employing the method of scattering superposition.

Chapter 6, discusses an alternative formulation of electromagnetic modeling of implantable medical devices using cylindrical DGFs. GSM (global system for mobile communication) and PCS's (personal communication services) can interfere with implantable medical devices/prostheses particularly for systems using TDMA (time-division multiple access) and cause possible malfunction. Also the performance of an antenna is significantly altered by the presence of conducting medical devices/prostheses. The objective of this chapter is to propose an alternative general expression of dyadic Green's function (DGF) for the problem of electromagnetic radiation from a source of excitation in the presence of a finite length "l" of perfectly conducting thin circular cylinder of radius "a" concentric along z-axis of any size as well as of resonant length, which is valid everywhere, including the source region. The whole structure is assumed to be uniform along the propagation direction. The advantage of the proposed analysis is its simplicity and efficiency in computation. This chapter was accepted for publication in 7th International Symposium on Recent Advances in Microwave Technology ISRAMT 99/IEEE, Malaga, Spain.

Chapter 7, develops an insulated implantable medical device model using electromagnetic dyadic Green's function. Modern wireless telecommunication devices (GSM Mobile system and PCS's) can interfere with implantable medical devices or prostheses and cause possible malfunction. Also the performance of an antenna is

significantly altered by the presence of these conducting medical devices/prostheses. Dielectric-coated medical devices are preferable over bare ones for use in a human body. The reason is that the often undesirable contact (hyperthermic/heating effect) between the prostheses and the surrounding tissue is avoided and, more importantly, the radiation efficiency of the antenna can be improved by insulating all or part of the medical devices surface. The principle objective of this chapter is to outline a general expression of dyadic Green's function (DGF) for the problem of electromagnetic radiation from a source of excitation in the presence of a finite length of insulated perfectly conducting circular cylinder of any size as well as of resonant length, which is valid everywhere, including the source region. The whole structure is assumed to be uniform along the propagation direction. The DGFs are obtained by employing the method of scattering superposition. The advantage of the proposed analysis is its simplicity and efficiency in computation. Chapter 7 was presented in AP2000 Millennium Conference on Antennas and Propagation in Davos, Switzerland.

Chapter 8 was presented in the International Conference on EMC (EMC York 2000) University of York, UK. It deals with the far field electromagnetic modeling of implantable medical devices using cylindrical DGFs. Electromagnetic pollution is increasing due to the massive increase in both mobile and fixed electronic equipments, whilst at the same time, industry is producing devices with ever increasing clock speeds. Modern wireless telecommunication devices (GSM Mobile system) can interfere with implantable medical devices/prostheses and cause possible malfunction. Also the performance of an antenna is significantly altered by the presence of conducting medical devices/prostheses. Hence the need to consider electromagnetic compatibility (EMC) becomes ever more important. The principle objective of this chapter is to outline a far field general expression of dyadic Green's function (DGF) for the problem of electromagnetic radiation from a source of excitation in the presence of a finite length of perfectly conducting circular cylinder of any size as well as of resonant length, which is valid everywhere, including the source region. The whole structure is assumed to be uniform along the propagation direction. The DGFs are

obtained by employing the eigenfunction expansion (EFE) and the method of scattering superposition. The advantage of the proposed analysis is its simplicity and efficiency in computation.

Chapter 9 will be submitted as a journal paper to IEEE Transaction on Microwave Theory and Techniques. In this chapter we have dealt with the implanted spherical head model for numerical EMC investigation. Recent years have seen an unprecedented increase in the number and diversity of sources of electric and magnetic fields (EMF) used for individual, industrial and commercial purposes. Such sources include television, radio, computers, mobile cellular phones, microwave ovens, radars and equipment used in industry, medicine and commerce.

All these technologies have made our life richer and easier. Modern society is inconceivable without computers, television and radio. Mobile phones have greatly enhanced the ability of individuals to communicate with each other and have facilitated the dispatch of emergency medical and police aid to persons in both urban and rural environments. Radars make air traveling much safer.

At the same time, these technologies have brought with them concerns about possible health risks associated with their use. Such concerns have been raised about the safety of cellular mobile telephones, electric power lines and police speed-control "radar guns". Scientific reports have suggested that exposure to electromagnetic fields emitted from these devices could have adverse health effects, such as cancer, reduced fertility, memory loss, and adverse changes in the behaviour and development of children. However, the actual level of health risk is not known, although for certain types of EMF, at levels found in the community, it may be very low or non-existent.

These technologies can interfere with implantable medical devices/prostheses and cause possible malfunction. Also antenna radiation pattern and other characteristics are significantly altered by the presence of the composite dielectric entities such as the human body. This chapter aims to deal with the scattering of a plane electromagnetic wave from a perfectly conducting or dielectric spherical/cylindrical

implant of electrically small radius (of resonant length), embedded eccentrically into a dielectric spherical head model. The method of dyadic Green's function (DGF) for spherical vector wave functions is used. Analytical expressions for the scattered fields of both cylindrical and spherical implants embedded in head model are obtained. The whole structure is assumed to be uniform along the propagation direction.

Numerical computations and results are discussed in chapter 10.

Finally, the thesis is concluded in chapter 11, which summarizes the important results of the work presented, before suggestions for further work are given in chapter 12.

1.3 Contributions of Thesis

Original contributions presented within this thesis that have been all published in journals or presented at conferences include;

1. Electromagnetic Dyadic Green's Function for a Multi-layered Homogeneous Lossy Dielectric Spherical Head Model for Numerical EMC Investigation.

2. Electromagnetic Dyadic Green's Function for a Human Torso Model for Numerical EMC Investigation.

3. Electromagnetic Dyadic Green's Function of an Implantable Medical Device Model for Numerical EMC Investigation.

4. An alternative Electromagnetic Modeling of Implantable Medical Devices Using Cylindrical DGFs.

5. Insulated Implantable Medical Device Model Using Electromagnetic Dyadic Green's Function.

6. Far Field Electromagnetic Modeling of Implantable Medical Devices Using Cylindrical DGFs.

7. Implanted Spherical Head Model for Numerical EMC Investigation.

8. Electromagnetic Fields due to Electric and Magnetic Current Distributions using Dyadic Green's Functions. This contribution, although not directly related to this project was investigated while working on the analytical expressions. This is included in Appendix B.

This research presents a new approach away from simulation work to the study of exact computation of EM fields in biological systems. Its salient characteristics are its simplicity, the saving in memory and CPU computational time and speed.

1.4 A Remark about Notation

Notation, where not defined explicitely, is standard (for example, we use the traditional symbols i, j, and k, for the unit vectors in the x, y, and z directions). Note that we use $\hat{r}\hat{r}$ to denote the cylindrical dyad, and RR to represent the spherical dyad. Also, the letter ω only ever denotes the discrete time physical frequency variable

Chapter 2

Dyadic Green's Functions

THE present chapter discusses a mathematical and conceptual method applicable in the analysis of the electromagnetic fields. The leading tone is dyadic algebra. It is in the form originated by J.Willard Gibbs (the American physicist called the American Maxwell) more than one hundred years ago. Dyadic algebra is seen especially as an aid in solving EM problems involving different linear media. In various chapters of this thesis, Green dyadics for different kind of media are discussed and a systematic method for their solution is given.

Dyadics are linear functions of vectors. In real vector space they can be visualized through their operation on vectors, which for real vectors consists of turning and stretching the vector arrow. In complex vector space they correspondingly rotate and deform ellipses. Dyadic notation was introduced by Gibbs in 1884, Tai [19] or Collin [21].

2.1 Dyadic analysis

In this section we will introduce some essential formulae in dyadic analysis, which is an extension of vector analysis to a higher level.

A vector or a vector function $\overline{F}$ expressed in a Cartesian system is defined by

$$\overline{F} = \sum_{i=1}^{3} F_i \hat{x}_i \tag{2.1}$$

where F_i with $i = (1, 2, 3)$ denotes the three scalar components of $\overline{F}$ and $\hat{x}_i$ denotes the three unit vectors in the direction of $\overline{x}_i$. We use x_i throughout this section to denote the Cartesian variables (x, y, z), so the summation sign can be applied to $\overline{F}$ as in (2.1). From now on, it is understood that the summation index always runs from 1 to 3 unless specified otherwise.

Now we consider three distinct vector functions, denoted by

$$\overline{F}_j = \sum_i F_{ij}\hat{x}_i, \qquad j = (1, 2, 3); \tag{2.2}$$

then a *dyadic* or dyadic function, denoted by $\overline{\overline{F}}$, can be formed and is defined by

$$\overline{\overline{F}} = \sum_j \overline{F}_j \hat{x}_j, \tag{2.3}$$

where $\overline{F}_j$ with $j = (1, 2, 3)$ are designated as the three vector components of $\overline{\overline{F}}$. In (2.3) the positioning of $\overline{F}_j$ and $\hat{x}_j$ must be kept in that order. By substituting (2.2) into (2.3) we can write $\overline{\overline{F}}$ in the form

$$\overline{\overline{F}} = \sum_i \sum_j F_{ij}\hat{x}_i\hat{x}_j \tag{2.4}$$

where F_{ij} are designated as the nine scalar components of $\overline{\overline{F}}$ and the doublet $\hat{x}_i\hat{x}_j$ as the nine unit dyadics or *dyads*, each being formed by a pair of unit vectors in that order, which are not commutative; that is,

$$\hat{x}_i\hat{x}_j \neq \hat{x}_j\hat{x}_i. \tag{2.5}$$

The *transpose of a dyadic* $\overline{\overline{F}}$ expressed by (2.3) will be denoted by $(\overline{\overline{F}})^\intercal$ and is defined by

$$(\overline{\overline{F}})^\intercal = \sum_j \hat{x}_j\overline{F}_j = \sum_i \sum_j F_{ij}\hat{x}_j\hat{x}_i = \sum_j \sum_i F_{ji}\hat{x}_i\hat{x}_j. \tag{2.6}$$

Comparing (2.6) with (2.2) into (2.3) we see that the positions of $\overline{F}_j$ and $\hat{x}_j$ in $\overline{\overline{F}}$ has been interchanged, or the scalar component F_{ij} in $\overline{\overline{F}}$ has been replaced by F_{ji} in $(\overline{\overline{F}})^\intercal$; hence the nomenclature "transpose".

A *symmetrical dyadic*, denoted by $\overline{\overline{F}}_s$, is characterized by $F_{ji} = F_{ij}$; hence

$$(\overline{\overline{F}}_s)^{\mathsf{T}} = \overline{\overline{F}}_s. \tag{2.7}$$

A symmetrical dyadic therefore has only six distinct scalar components, although it still has nine terms or nine dyadic components.

An *anti-symmetrical dyadic*, designated by $\overline{\overline{F}}_a$, is characterized by $F_{ij} = -F_{ji}$; hence $F_{ii} = 0$ for $i = (1, 2, 3)$ and

$$(\overline{\overline{F}}_a)^{\mathsf{T}} = -\overline{\overline{F}}_a. \tag{2.8}$$

An anti-symmetric dyadic, therefore has only three distinct scalar components if we do not consider the negative sign as being distinct, and it has six non-vanishing dyadic components.

One special case of a symmetric dyadic is described by

$$\begin{aligned} F_{ij} &= 1, \qquad i = j \\ F_{ij} &= 0, \qquad i \neq j \end{aligned} \tag{2.9}$$

or

$$F_{ij} = \delta_{ij}, \tag{2.10}$$

where δ_{ij} denotes the Kronecker delta function. This dyadic is denoted by $\overline{\overline{I}}$, and it is called an *idem factor*. Its explicit expression is

$$\overline{\overline{I}} = \sum_i \hat{x}_i \hat{x}_i. \tag{2.11}$$

A dyadic by itself, like a matrix, has no algebraic property. It plays the role of an operator when certain products are formed. In particular, we can define two scalar products between a vector $\overline{a}$ and a dyadic $\overline{\overline{F}}$.

1. The *anterior scalar product*, denoted by $\overline{a} \cdot \overline{F}$, is defined by

$$\overline{a} \cdot \overline{\overline{F}} = \sum_j (\overline{a} \cdot \overline{F}_j)\hat{x}_j = \sum_i \sum_j a_i F_{ij} \hat{x}_j, \tag{2.12}$$

which is a vector.

2. The *posterior scalar product*, distinguished by $\overline{F} \cdot \overline{a}$, is defined by

$$\begin{aligned} \overline{\overline{F}} \cdot \overline{a} &= \sum_j \overline{F}_j (\hat{x}_j \cdot \overline{a}) = \sum_i \sum_j a_j F_{ij} \hat{x}_i \\ &= \sum_i \sum_j a_i F_{ji} \hat{x}_j , \end{aligned} \tag{2.13}$$

which is also a vector.

In general, the above scalar products are not equal unless $\overline{\overline{F}}$ is a symmetrical dyadic. For any dyadic we have the relation

$$\overline{a} \cdot (\overline{\overline{F}})^{\intercal} = \overline{\overline{F}} \cdot \overline{a}. \tag{2.14}$$

This is an important identity in dyadic analysis. Consequently as a result of (2.7) and (2.8), one deducts that

$$\overline{a} \cdot \overline{\overline{F}}_s = \overline{\overline{F}}_s \cdot \overline{a}. \tag{2.15}$$

$$\overline{a} \cdot \overline{\overline{F}}_a = -\overline{\overline{F}}_a \cdot \overline{a}. \tag{2.16}$$

If a symmetric dyadic $\overline{\overline{F}}_s = \overline{\overline{I}}$, the idem factor, then

$$\overline{a} \cdot \overline{\overline{I}} = \overline{\overline{I}} \cdot \overline{a} = \overline{a}. \tag{2.17}$$

This is the reason why $\overline{\overline{I}}$ is designated as the idem factor.

There are also two vector products between a vector $\overline{a}$ and a dyadic $\overline{\overline{F}}$.

1. The *anterior vector product*, denoted by $\overline{a} \times \overline{F}$, is defined by

$$\overline{a} \times \overline{\overline{F}} = \sum_{j=1}^{3} (\overline{a} \times \overline{F}_j) \hat{x}_j ; \tag{2.18}$$

2. The *posterior vector product*, indicated by $\overline{a} \times \overline{F}$, is defined by

$$\overline{\overline{F}} \times \overline{a} = \sum_{j=1}^{3} \overline{F}_j (\hat{x}_j \times \overline{a}). \tag{2.19}$$

These vector products are both dyadics, and there is no relation similar to (2.14) for these two products.

In the following, we draw attention to some definitions and formulae involving the differentiation and the integration of dyadic functions.

The *divergence of a dyadic function*, denoted by $\nabla \cdot \overline{\overline{F}}$, is defined by

$$\nabla \cdot \overline{\overline{F}} = \sum_j (\nabla \cdot \overline{F}_j)\hat{x}_j = \sum_i \sum_j \frac{\partial F_{ij}}{\partial x_i}\hat{x}_j \tag{2.20}$$

which is a vector function.

The *curl of a dyadic function*, denoted by $\nabla \times \overline{\overline{F}}$, is defined by

$$\nabla \times \overline{\overline{F}} = \sum_j (\nabla \times \overline{F}_j)\hat{x}_j = \sum_i \sum_j (\nabla F_{ij} \times \hat{x}_i)\hat{x}_j, \tag{2.21}$$

where we have used the vector identity

$$\nabla \times (F_{ij} \times \hat{x}_j) = \nabla F_{ij} \times \hat{x}_j \tag{2.22}$$

to derive (2.21), which is a dyadic function. In addition to these two functions, we will encounter the *gradient of a vector function*, denoted by $\nabla \overline{F}$, which is defined by

$$\nabla \overline{F} = \sum_j (\nabla \overline{F}_j)\hat{x}_j = \sum_i \sum_j \frac{\partial F_j}{\partial x_i}\hat{x}_i\hat{x}_j \tag{2.23}$$

which is a dyadic.

When a dyadic function is constructed with an idem factor $\overline{\overline{I}}$ and a scalar function f in the form

$$\overline{\overline{F}} = f\overline{\overline{I}}, \tag{2.24}$$

then

$$\begin{aligned} \nabla \cdot \overline{\overline{F}} = \nabla \cdot (f\overline{\overline{I}}) &= \sum_i \nabla \cdot (f\hat{x}_i)\hat{x}_i = \sum_i \frac{\partial f}{\partial x_i}\hat{x}_i \\ &= \nabla f \end{aligned} \tag{2.25}$$

and

$$\begin{aligned}\nabla \times \overline{\overline{F}} = \nabla \times (f\overline{\overline{I}}) &= \sum_i \nabla \times (f\hat{x}_i)\hat{x}_i \\ &= \sum_i (\nabla f \times \hat{x}_i)\hat{x}_i = \nabla f \times \overline{\overline{I}},\end{aligned} \tag{2.26}$$

which is a dyadic.

2.2 Dyadic Green's Functions of Electric and Magnetic Type

This section introduces the concept of dyadic Green's functions in electromagnetic theory. In order to introduce the concept of dyadic Green's functions in electromagnetic theory in a coherent manner, Maxwell's equations have to be elevated to a dyadic form. We assume three sets of harmonically oscillating fields with the same frequency and in the same environment, which are produced by three distinct current distributions $\overline{J}_j$ with $j = (1, 2, 3)$. Maxwell's equations for these fields can then be written in the form

$$\nabla \times \overline{E}_{ej}(\overline{R}) = i\omega\mu_o \overline{H}_{ej}(\overline{R}) \tag{2.27}$$

$$\nabla \times \overline{H}_{ej}(\overline{R}) = \overline{J}_{ej}(\overline{R}) - i\omega\varepsilon_o \overline{E}_{ej}(\overline{R}) \tag{2.28}$$

$$\nabla \cdot \overline{J}_{ej} = i\omega\rho_j \tag{2.29}$$

$$\nabla \cdot (\varepsilon_o \overline{E}_{ej}) = \rho_j \tag{2.30}$$

$$\nabla \cdot (\mu_o \overline{H}_{ej}) = 0 \tag{2.31}$$

The medium under consideration is assumed to be air. For other isotropic homogeneous media we simply replace the constants μ_o and ε_o by μ and ε. We now change the notation (x, y, z) to (x_1, y_2, z_3). By juxtaposing a unit vector $\hat{x}_j$ at the posterior position of (2.27) to (2.31) and summing the three sets of equations with respect to j, we obtain Maxwell's equations in dyadic form; namely,

$$\nabla \times \overline{\overline{E}}_e(\overline{R}) = i\omega\mu_o \overline{\overline{H}}_e(\overline{R}) \tag{2.32}$$

$$\nabla \times \overline{\overline{H}}_e(\overline{R}) = \overline{J}_e(\overline{R}) - i\omega\epsilon_o \overline{\overline{E}}_e(\overline{R}) \tag{2.33}$$

$$\nabla \cdot \overline{\overline{J}}_e = i\omega\overline{\rho} \tag{2.34}$$

$$\nabla \cdot (\varepsilon_o \overline{\overline{E}}_e) = \overline{\rho} \tag{2.35}$$

$$\nabla \cdot (\mu_o \overline{\overline{H}}_e) = 0 \tag{2.36}$$

$$\overline{\overline{E}}_e = \sum \overline{E}_{ej}\hat{x}_j = \sum\sum \overline{E}_{eij}\hat{x}_i\hat{x}_j \tag{2.37}$$

$$\overline{\overline{H}}_e = \sum_j \overline{H}_{ej}\hat{x}_j = \sum_i\sum_j \overline{H}_{eij}\hat{x}_i\hat{x}_j \tag{2.38}$$

$$\overline{\overline{J}}_e = \sum_j \overline{J}_{ej}\hat{x}_j = \sum_i\sum_j \overline{J}_{eij}\hat{x}_i\hat{x}_j \tag{2.39}$$

$$\overline{\rho}_e = \sum_j \rho_{ej}\hat{x}_j \tag{2.40}$$

According to the nomenclature of dyadic analysis in the previous section, a dyadic function like $\overline{\overline{E}}_e$ has three vector components, $\overline{E}_{ej}$ with $j = (1,2,3)$, and the vector charge density function $\overline{\rho}_e$ contains three distinct scalar charge distributions. $\overline{\rho}_e$ does not have the normal physical meaning of a vector quantity. For example, the magnitude of $\overline{\rho}_e$ does not have any physical significance.

Let us consider the three current distributions which correspond to that of three infinitesimal electric dipoles located at $\overline{R} = \overline{R}'$ and oriented in the direction of $(\hat{x},\hat{y},\hat{z})$ to $(\hat{x}_1,\hat{y}_2,\hat{z}_3)$; then

$$\overline{J}_{ej} = c_j\delta(\overline{R}-\overline{R}')\hat{x}_j, \qquad j = (1,2,3), \tag{2.41}$$

where c_j denotes the current moment of the dipoles; that is,

$$\iiint \overline{J}_{ej}\,dv = c_j\hat{x}_j \tag{2.42}$$

We now normalize the current moment such that

$$i\omega\mu_o c_j = 1; \tag{2.43}$$

then

$$\begin{aligned} i\omega\mu_o\overline{J}_{ej} &= i\omega\mu_o c_j\delta(\overline{R}-\overline{R}')\hat{x}_j \\ &= \delta(\overline{R}-\overline{R}')\hat{x}_j \end{aligned} \tag{2.44}$$

Under this condition, we introduce a set of new notations for the various dyadic functions. They are

$$\overline{\overline{E}}_e = \overline{\overline{G}}_e \tag{2.45}$$

$$i\omega\mu_o\overline{\overline{H}}_e = \overline{\overline{G}}_m \tag{2.46}$$

$$i\omega\mu_o\overline{\overline{J}}_e = \overline{\overline{I}}\delta(\overline{R}-\overline{R}') \tag{2.47}$$

$$\begin{aligned}\overline{\rho}_e &= \frac{1}{i\omega}\nabla\cdot\overline{\overline{J}}_e = \frac{-1}{\omega^2\mu_o}\nabla\cdot[\overline{\overline{I}}\delta(\overline{R}-\overline{R}')] \\ &= -\frac{\varepsilon_o}{k^2}\nabla\delta(\overline{R}-\overline{R}')\end{aligned} \tag{2.48}$$

where

$$k = \omega(\mu_o\varepsilon_o)^{1/2} = \frac{\omega}{c}$$

$$c = (\mu_o\varepsilon_o)^{\frac{1}{2}} = \text{velocity of light in air}$$

The expression for $\overline{\rho}_e$ in the form of the gradient of a delta function is a consequence of (2.25). With this change of notation, equations (2.32)-(2.36) can be written in the form

$$\nabla\times\overline{\overline{G}}_e = \overline{\overline{G}}_m \tag{2.49}$$

$$\nabla\times\overline{\overline{G}}_m = \overline{\overline{I}}\delta(\overline{R}-\overline{R}') + k^2\overline{\overline{G}}_e \tag{2.50}$$

$$\begin{aligned}\nabla\cdot\overline{\overline{G}}_e &= -\frac{1}{k^2}\nabla\cdot[\overline{\overline{I}}\delta(\overline{R}-\overline{R}')] \\ &= -\frac{1}{k^2}\nabla\delta(\overline{R}-\overline{R}')\end{aligned} \tag{2.51}$$

$$\nabla\cdot\overline{\overline{G}}_m = 0. \tag{2.52}$$

The relation between $\overline{\overline{J}}_e$ and $\overline{\rho}_e$ is described by (2.34). The function of $\overline{\overline{G}}_e$ so defined is designed as the DGF of electric type or electric DGF, and the function $\overline{\overline{G}}_m$ is designated as the DGF of magnetic type or the magnetic DGF. If one writes these two functions in the form

$$\overline{\overline{G}}_e = \sum_j \overline{G}_{ej}\hat{x}_j \tag{2.53}$$

$$\overline{\overline{G}}_m = \sum_j \overline{G}_{mj}\hat{x}_j \tag{2.54}$$

then $\overline{G}_{ej}$ and $\overline{G}_{mj}$ denote, respectively, the vector Green function of the electric type and the vector Green function of the magnetic type. Physically, $\overline{G}_{ej}$ represents the electric field due to an infinitesimal electric dipole oriented in the direction of $\hat{x}_j$ and $\overline{R} = \overline{R}'$, that is,

$$\overline{\overline{G}}_e = \overline{\overline{G}}_e(\overline{R} - \overline{R}') \tag{2.55}$$

$$\overline{\overline{G}}_m = \overline{\overline{G}}_m(\overline{R} - \overline{R}') \tag{2.56}$$

where $\overline{R}$ denotes the position vector of the field point and $\overline{R}'$ that of the point source.

2.3 Fields due to Electric and Magnetic Current Distributions

In this section we draw attention to electromagnetic fields due to electric and magnetic current distributions using dyadic Green's functions. The general relation for $(\overline{E}_f)$ and $(\overline{H}_f)$ for the case of two types of current sources such as $\overline{J}_e$ and $\overline{J}_m$ radiating in an isotropic, homogeneous medium is quite simple and may be usefully applied to various problems of propagation in media.

Here, the time-harmonic convention of $e^{-i\omega t}$ is used. Consider electric $(\overline{E}_e)$ and magnetic $(\overline{H}_e)$ vectors to be generated by an electric current described by the current density vector $\overline{J}_e$. The vectors $\overline{E}_e$ and $\overline{H}_e$ are then the solutions of Maxwell's equations, (2.57) and (2.58).

$$\nabla \times \overline{E}_e(\overline{R}) = i\omega\mu_o \overline{H}_e(\overline{R}) \qquad \text{(Faraday's law)} \tag{2.57}$$

$$\nabla \times \overline{H}_e(\overline{R}) = \overline{J}_e(\overline{R}) - i\omega\varepsilon_o \overline{E}_e(\overline{R}) \qquad \text{(Maxwell-Ampère law)} \tag{2.58}$$

Similarly $\overline{E}_m$ and $\overline{H}_m$ are generated by a non-physical magnetic current density vector $\overline{J}_m$

$$\nabla \times \overline{E}_m(\overline{R}) = i\omega\mu_o\overline{H}_m(\overline{R}) - \overline{J}_m(\overline{R}) \tag{2.59}$$

$$\nabla \times \overline{H}_m(\overline{R}) = -i\omega\varepsilon_o\overline{E}_m(\overline{R}) \tag{2.60}$$

The use of the magnetic current density vector ensures symmetric Maxwell's equations. It is sometimes necessary to calculate the electromagnetic fields due to both electric and equivalent magnetic current sources.

Assuming $\overline{H}_e + \overline{H}_m = \overline{H}_f$ and $\overline{E}_e + \overline{E}_m = \overline{E}_f$. Therefore Maxwell's equations with a magnetic current density $\overline{J}_m$ could be written as

$$\nabla \times \overline{E}_f(\overline{R}) = i\omega\mu_f\overline{H}_f(\overline{R}) - \overline{J}_m(\overline{R}) \tag{2.61}$$

$$\nabla \times \overline{H}_f(\overline{R}) = \overline{J}_e(\overline{R}) - i\omega\varepsilon_f\overline{E}_f(\overline{R}). \tag{2.62}$$

Since electromagnetic fields are vector fields, the general wave equation is a vector wave equation. For a homogeneous isotropic medium, the general form of the vector wave equation is given by:

$$\nabla\times\nabla\times\overline{E}_f - k_f^2\overline{E}_f = (i\omega\mu_f\overline{J}_e - \nabla\times\overline{J}_m)\delta_f^s \tag{2.63}$$

$$\nabla\times\nabla\times\overline{H}_f - k_f^2\overline{H}_f = (i\omega\varepsilon_f\overline{J}_m + \nabla\times\overline{J}_e)\delta_f^s \tag{2.64}$$

The above equations follow directly from the duality principle. We can now introduce the use of dyadic Green's functions. To obtain the electromagnetic fields due to these electric and magnetic current distributions, one first constructs $\overline{\overline{G}}_e^{fs}(\overline{R},\overline{R}')$ and $\overline{\overline{G}}_m^{fs}(\overline{R},\overline{R}')$, the electric and magnetic dyadic Green's functions respectively [19] and [21]. These two DGFs are the solutions of the following dyadic differential equations (taking into account the discontinuous nature of magnetic or electric DGF with respect to electric or magnetic dipole respectively at $R = R'$ i.e., $\nabla\times\overline{\overline{I}}\delta_{\substack{e\\m}}(\overline{R}-\overline{R}') = 0$ and in case of cavities the source term $\overline{J}_{\substack{e\\m}} = 0$ on the surface):

$$\nabla\times\nabla\times\overline{\overline{G}}_{\substack{e\\m}}^{(fs)}(\overline{R},\overline{R}') - k_f^2\overline{\overline{G}}_{\substack{e\\m}}^{(fs)}(\overline{R},\overline{R}') = i\omega\vartheta\overline{\overline{I}}\delta_{\substack{e\\m}}(\overline{R}-\overline{R}')\delta_f^s \tag{2.65}$$

Where ϑ represents ε or μ in the electric or magnetic DGF equations respectively. Here a unit current density at $\overline{R}'$ in the direction of e or m has the space form

$\delta_{\substack{e\\m}}(\overline{R}-\overline{R}')$. This requires that both DGFs satisfy the nonsolenoidal condition $\nabla \cdot \overline{\overline{G}}^{fs}_{\substack{e\\m}}(\overline{R},\overline{R}') \neq 0$ because

$$\nabla \cdot \overline{E} = \frac{\overline{\rho}_e}{\varepsilon} = \frac{\nabla \cdot \overline{J}_e}{i\omega\varepsilon} \tag{2.66}$$

and

$$\nabla \cdot \overline{H} = \frac{\overline{\rho}_m}{\mu} = \frac{\nabla \cdot \overline{J}_m}{i\omega\mu} \tag{2.67}$$

Chapter 3

Head Model Using Spherical DGF

THE principle objectives of this chapter are threefold. We outline an exact general expression of dyadic Green's function (DGF) for the problem of electromagnetic radiation from a source of excitation in the presence of a layered spherical dielectric head model, which is valid everywhere, including the source region. The medium is assumed to be homogeneous, isotropic, linear, nondispersive and stationary. The DGFs are obtained by employing the method of scattering superposition. Furthermore, we have made an attempt to discuss the question of incompleteness of previously related studies with regard to the E and H modes in the source region. We consider that one should explicitly extract the singularity term for the expansion to be valid both inside and outside the source region. This follows because the primary interest can be the development of a formulation to evaluate the electromagnetic fields away from the source. Also, a compact alternative general representation has been developed to determine the electric- and magnetic-type DGFs, giving clarity as well as more efficient and economical computation in terms of speed, time and memory.

3.1 Introduction

The objective of modeling biological bodies exposed in near as well as in the far-field is to assess the induced and scattered fields. However, near-field exposure is of considerably higher complexity because:

i) the field distribution is extremely nonuniform in the vicinity of the source as well as inside the body;

ii) in many cases, the interaction of the scattered field on the source is not small enough to be negligible.

The dyadic Green's function (DGF) was introduced by Schwinger in the early 1940's and has been extensively discussed by Tai [19, 20], Collin [21], Samii [22], Yaghjian [23, 24], and others. This technique was presented mainly to formulate various canonical electromagnetic problems in a systematic manner and to enable many special cases to be treated as one general problem. If the current source in these problems has some specific distributions, we have to consider these distributions as special cases, for example, excitation by a transversal electric dipole or a longitudinal or a magnetic dipole. The DGF, which relates the current source and the field, is singular in the source region.

The format of this chapter is as follows. The complete set of spherical vector wave functions are introduced in section 3.2.

In section 3.3, we start with the unbounded case, in which the point source radiates with no interface present, and construct the corresponding DGF, $\overline{\overline{G}}_{eo}^{00o}(\overline{R},\overline{R}')$, in terms of an integral over the spectra of plane waves that constitute the continuous eigenfunction expansion (EFE) in which the eigenfunctions are guided in the preferred R-coordinate direction, using the procedures described in Tai [19] or Collin [21]. This expansion also contains an explicit dyadic delta function term which is required for completeness at the source point. It is considered as a correction to the general solenoidal EFE, which is valid outside the source point.

The procedure required to derive the complete EFE of the general scattering DGF for the multilayered media in terms of only the solenoidal eigenfunctions is shown to be a simple and straightforward general expression. The DGF for the multilayered media $\overline{\overline{G}}_{e}^{Lfo}(\overline{R},\overline{R}')$, is then constructed from the principle of the superposition, which involves the sum of the fields of, first, the source in free-space (or

the free space Green's function $\overline{\overline{G}}^{00o}_{eo}(\overline{R},\overline{R}')$ and, second, the fields scattered by the layered media $\overline{\overline{G}}^{Lfo}_{es}(\overline{R},\overline{R}')$. A radically new and generic method for deriving the scattering formulae is described in this section, giving an idea of the computational burden involved in the general method described in this chapter. This represents one of the main contributions of this study. Magnetic-type DGF can be found by invoking duality. Once the electric field is obtained the magnetic field is derivable by taking the curl of the electric field, and vice versa.

Conclusions are then presented in section 10.3, which summarize the important points contained in this work.

3.2 Spherical Hansen Vector Wave Functions

The spherical vector wave functions which were introduced by Hansen [25] are the building blocks of the EFE of various kinds of DGF. They are denoted by $\overline{L}^{e}_{o}{}_{mn}$, $\overline{M}^{e}_{o}{}_{mn}$, and $\overline{N}^{e}_{o}{}_{mn}$, which are solutions of the homogeneous vector Helmholtz equation. The generating functions or eigenfunctions, which are solutions of the spherical scalar wave equation $\nabla^2\Psi + k^2\Psi=0$, can be written in the form

$$\Psi_{\substack{e\\o}mn}(k) = j_n(kR)P_n^m(\cos\theta)^{\cos}_{\sin}m\phi, \tag{3.1}$$

Here k is an undetermined wave number and R is the piloting radial vector. Subscripts "e" stands for even, and "o" is the odd character of the generating functions.

$P_n^m(\cos\theta)$ identifies the associated Legendre functions of the first kind with order (n,m), and $j_n(kR)$ denotes the spherical Bessel functions of the order n to represent both outgoing and incoming waves. Spherical vector wave functions are akin to the Debye potentials:

$$\overline{L}_{\substack{e\\o}mn}(k) = \nabla\Psi_{\substack{e\\o}mn}, \tag{3.2}$$

$$\overline{M}_{\substack{e\\o}mn}(k) = \nabla\times[\Psi_{\substack{e\\o}mn}\overline{R}], \tag{3.3}$$

$$\overline{N}_{\substack{e\\o}mn}(k) = \frac{1}{k}\nabla\times\nabla\times[\Psi_{\substack{e\\o}mn}\overline{R}]. \tag{3.4}$$

To satisfy the symmetrical properties of DGF,

$$\overline{N}_{emn}(k) = \frac{1}{k}\nabla\times\overline{M}_{emn}(k), \tag{3.5}$$

$$\overline{M}_{emn}(k) = \frac{1}{k}\nabla\times\overline{N}_{emn}(k). \tag{3.6}$$

Green's functions for bounded regions are usually given in the form of modal expansions. Modal series are unsuitable for use in numerical algorithms which require the computation of the electric field inside the source region. In this case, the Green's function must be computed at points $\overline{R}'$ close to $\overline{R}$, where the convergence of the series is very poor due to the singularity of $\overline{\overline{G}}_e(\overline{R},\overline{R}')$ at point source $R = R'$. This drawback can be avoided by using expressions where a diverging term, expressed in closed form, is extracted from the modal expansion of $\overline{\overline{G}}_e(\overline{R},\overline{R}')$, so that the remaining series represents a function finite at point source $R = R'$; see Bressan and Conciauro [26].

The complete expressions for the solenoidal or rotational or transverse functions are given by Collin [21]:

$$\overline{M}_{emn}(k) = \left\{ \begin{array}{c} 0 \\ \mp\frac{m}{\sin\theta} j_n(kR) P_n^m(\cos\theta)^{\sin}_{\cos} m\phi\hat{\theta} \\ -j_n(kR)(\frac{\partial P_n^m(\cos\theta)}{\partial\theta})^{\cos}_{\sin} m\phi\hat{\phi} \end{array} \right\}, \tag{3.7}$$

$$\overline{N}_{emn}(k) = \left\{ \begin{array}{c} \frac{n(n+1)}{kR} j_n(kR) P_n^m(\cos\theta)^{\cos}_{\sin} m\phi\hat{R} \\ \frac{1}{kR}\frac{\partial}{\partial R}[Rj_n(kR)](\frac{\partial P_n^m(\cos\theta)}{\partial\theta})^{\cos}_{\sin} m\phi\hat{\theta} \\ \frac{1}{kR}\frac{\partial}{\partial R}[Rj_n(kR)][\mp\frac{m}{\sin\theta} P_n^m(\cos\theta)^{\sin}_{\cos} m\phi\hat{\phi}] \end{array} \right\}, \tag{3.8}$$

and the complete expressions for the nonsolenoidal or irrotational or lamellar functions are given by Collin [21]:

$$\overline{L}_{emn}(k) = \left\{ \begin{array}{c} \frac{\partial}{\partial R} j_n(kR) P_n^m(\cos\theta)^{\cos}_{\sin} m\phi\hat{R} \\ (\frac{j_n(kR)}{R}\frac{\partial P_n^m(\cos\theta)}{\partial\theta})^{\cos}_{\sin} m\phi\hat{\theta} \\ \mp\frac{m j_n(kR)}{R\sin\theta} P_n^m(\cos\theta)^{\sin}_{\cos} m\phi\hat{\phi} \end{array} \right\}. \tag{3.9}$$

Note that in the set of spherical vector wave functions, only $\overline{M}_{omn}$ do not possess the radial component. m and n are the eigenvalues associated with the ϕ and θ

coordinates, respectively, when for problems involving spheres, they are integers. The $\hat{R}$, $\hat{\theta}$, and $\hat{\phi}$ are the spherical unit vectors.

The orthogonal properties of these vector wave functions have been discussed by Tai [19, 20] and Collin [21]. $\overline{L}_{e^{o}mn}$ functions are not required to derive the eigenfunction expansion of the magnetic DGF that are solenoidal and satisfy the vector wave equation, but to find the EFE of the electric DGF, the $\overline{L}_{e^{o}mn}$ functions are also necessary, because $\overline{\overline{G}}_{e}^{Lfo}(\overline{R},\overline{R}')$, unlike $\overline{\overline{G}}_{m}^{Lfo}(\overline{R},\overline{R}')$, the dyadic Green's functions of electric- and magnetic-type, respectively, is a nonsolenoidal dyadic function.

The spherical vector wave functions in x, y and z-directions and their mutual relationships are given in Appendix A (A.1) where $\overline{M}_{e^{o}mn}^{(x)}(k)$, $\overline{N}_{e^{o}mn}^{(x)}(k)$, $\overline{M}_{e^{o}mn}^{(y)}(k)$, $\overline{N}_{e^{o}mn}^{(y)}(k)$, $\overline{M}_{e^{o}mn}^{(z)}(k)$, and $\overline{N}_{e^{o}mn}^{(z)}(k)$ are derived in relation to $\overline{M}_{e^{o}mn}(k)$ and $\overline{N}_{e^{o}mn}(k)$ which are the even or odd spherical vector wave functions in R-direction.

The method for deriving the magnetic/electric DGF given in the following section for spherical configurations uses the Ohm-Rayleigh (G_m) procedure. However, there exist several alternative derivations, which will not be discussed further.

3.3 General Representation of Dyadic Green's Function

Before we develop the analysis of electromagnetic wave propagation in the multilayered head model, it is convenient to examine the media firstly with no scatterer and then secondly with one-, two-, three-, and four-layer head models. Consider a multilayered homogeneous lossy dielectric concentric sphere with radii as shown in Figure 1 illuminated by an electromagnetic wave. A time dependence $e^{j\omega t}$ is assumed and suppressed throughout.

3.3.1 Free Space DGF for an Electric Dipole in Unbounded Medium

The electric and magnetic fields due to an electric dipole located at R' in an infinite homogeneous space without the presence of an scatterer (obstacle) can be computed in spherical coordinates. There are various methods that can be utilized to achieve

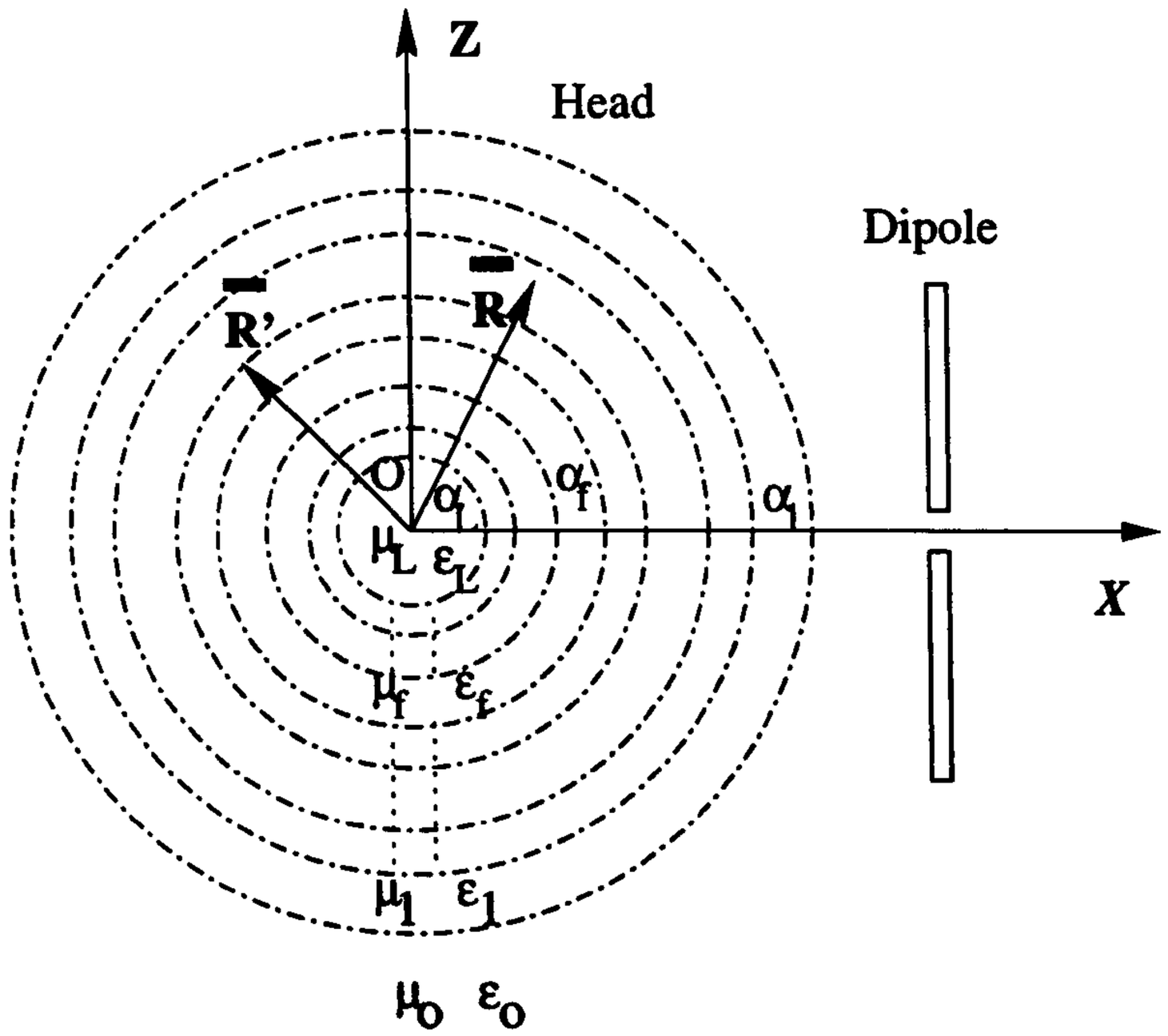

Figure 1: Test Position of a Dipole and Cross Section of Spherical Head Model

this. The expansion of the electric field requires both the transverse and longitudinal vector eigenfunctions and hence the DGF must also have both sets of eigenfunctions in its expansion [19]:

$$\overline{\overline{G}}^{00o}_{eo}(\overline{R},\overline{R}') = -\frac{\hat{R}\hat{R}}{k_o^2}\delta(\overline{R}-\overline{R}') + \frac{ik_o}{4\pi}\sum_{n=1}^{\infty}\sum_{m=0}^{n} C_{mn}$$

$$\cdot\begin{cases} \left\{ \begin{array}{l} [\overline{M}^{(1)}_{\substack{e\\o}mn}(k_o)\overline{M}'_{\substack{e\\o}mn}(k_o)] \\ [\overline{N}^{(1)}_{\substack{e\\o}mn}(k_o)\overline{N}'_{\substack{e\\o}mn}(k_o)] \end{array} \right\}, & R > R', \\ \left\{ \begin{array}{l} [\overline{M}_{\substack{e\\o}mn}(k_o)\overline{M}'^{(1)}_{\substack{e\\o}mn}(k_o)] \\ [\overline{N}_{\substack{e\\o}mn}(k_o)\overline{N}'^{(1)}_{\substack{e\\o}mn}(k_o)] \end{array} \right\}, & R < R'. \end{cases} \tag{3.10}$$

Here the first term presents the singularity term specifying inside the source region and the second term outside the source region.

Where, the prime on the vector wave functions indicates that, functions are defined with respect to the co-ordinates of the position vector $\overline{R}'$, co-ordinates

(R', θ', ϕ'). The superscript "1" in $\overline{M}^{(1)}_{\substack{e\\o}mn}(k_o)$ and $\overline{N}^{(1)}_{\substack{e\\o}mn}(k_o)$, $\overline{M}'^{(1)}_{\substack{e\\o}mn}(k_o)$, and $\overline{N}'^{(1)}_{\substack{e\\o}mn}(k_o)$ is present to indicate the substitution of spherical Hankel function of the first kind (spherical Bessel functions of the third kind) "$h_n(kR)$" for "$j_n(kR)$" in the generating function $\Psi_{\substack{e\\o}mn}(k)$. It is important to note the singularity of the Hankel function at the origin. $\hat{R}\hat{R}$ is a dyad (dyadic product of the unit vectors) [27]:

$$\hat{R}\hat{R} = (\frac{\hat{x}x}{R} + \frac{\hat{y}y}{R} + \frac{\hat{z}z}{R})(\frac{\hat{x}x}{R} + \frac{\hat{y}y}{R} + \frac{\hat{z}z}{R}) \tag{3.11}$$

and $\delta(\overline{R} - \overline{R}')$ is weighted Dirac delta function in three dimensions. Subscripts "o" and "e" stand for unbounded (open) space and electric component respectively.

The dyadic delta function term at the source point is included explicitly as a correction to the general solenoidal EFE which is valid outside the source point.

$$C_{mn} = (2 - \delta_o^m)\frac{2n+1}{n(n+1)}\frac{(n-m)!}{(n+m)!} \tag{3.12}$$

Coefficient C_{mn} depends on the value of m and n, where δ_o^m is the Kronecker delta functions, when

$$\delta = \begin{cases} 1, & \text{if } m = o, \\ 0, & \text{if } m \neq o \end{cases}. \tag{3.13}$$

3.3.2 Scattering DGFs for an Electric Dipole in the Presence of Spherical Head Model

When a biological system is illuminated by an electromagnetic wave, an electromagnetic field is induced inside the system and an electromagnetic wave is scattered externally by the system. Since the biological system is an irregularly shaped heterogeneous imperfectly conducting medium with frequency-dependent permittivity and conductivity, the distribution of the internal electromagnetic field and the scattered electromagnetic wave will depend on the body's physiological parameters and geometry, as well as the frequency and polarization of the incident wave. The mathematical complexity of the problem has led researchers to investigate simple models.

Several theoretical studies have analyzed these models (Reyhani [28] - [33]). In this chapter, the medium is assumed to be homogeneous, isotropic, linear, nondispersive, and stationary.

Having expressed the DGF for an unbounded medium in terms of spherical vector wave functions, we may now use that result to construct one for a spherical head model.

DGF for a Single-layer Spherical Head Model

This can be considered as the contribution of the reflections and transmissions of a single layer sphere of radius α_1 centered at O, superimposed in an unbounded homogeneous medium with the radiation source located outside the sphere at R'. The medium is characterized by (μ_o, ε_o), and material properties of sphere is represented by $(\mu_{h1}, \varepsilon_{h1})$, where subscripts "$o$" and "$h$" stand for unbounded (open) space and head, respectively.

The Scattered DGF terms for this case was examined by [19]:

$$\overline{\overline{G}}^{10o}_{es}(\overline{R},\overline{R}') = \frac{ik_o}{4\pi}\sum_{n=1}^{\infty}\sum_{m=0}^{n} C_{mn}\cdot\begin{bmatrix} A^{10o}_{eM}\overline{M}^{(1)}_{emn}(k_o)\overline{M}'^{(1)}_{emn}(k_o) \\ A^{10o}_{eN}\overline{N}^{(1)}_{emn}(k_o)\overline{N}'^{(1)}_{emn}(k_o)\end{bmatrix}, \tag{3.14}$$

$$\overline{\overline{G}}^{11o}_{es}(\overline{R},\overline{R}') = \frac{ik_o}{4\pi}\sum_{n=1}^{\infty}\sum_{m=0}^{n} C_{mn}\cdot\begin{bmatrix} B^{11o}_{eM}\overline{M}_{emn}(k_1)\overline{M}'^{(1)}_{emn}(k_o) \\ B^{11o}_{eN}\overline{N}_{emn}(k_1)\overline{N}'^{(1)}_{emn}(k_o)\end{bmatrix}. \tag{3.15}$$

Where the first number of triple superscripts signifies the last inner layer in the model and the second number identifies the region where the function is defined, that is the observation or field point, and the third number corresponds to the location of the source, i.e., the source point, which in this case is denoted by the letter "o". Subscripts M and N attribute the coefficients to the excitation functions.

The choice of $\overline{M}^{(1)}_{emn}$ and $\overline{N}^{(1)}_{emn}$ as the field functions in $\overline{\overline{G}}^{10o}_{es}(\overline{R},\overline{R}')$ is dictated by the radiation condition that the scattered field must consist of outgoing waves,

and the choice of $\overline{M}'^{(1)}_{\substack{e\\o}mn}$ and $\overline{N}'^{(1)}_{\substack{e\\o}mn}$ as the excitation functions is guided by the expression for $\overline{\overline{G}}^{00o}_{eo}(\overline{R},\overline{R}')$ and the boundary condition that at $R=\alpha_1$, $\overline{\overline{G}}^{Lfo}_{e}(\overline{R},\overline{R}')$ must satisfy the Dirichlet boundary condition, which can be satisfied only if the excitation functions are the same as that of $\overline{\overline{G}}^{00o}_{eo}(\overline{R},\overline{R}')$ for $R<R'$.

The field functions for $\overline{\overline{G}}^{11o}_{es}(\overline{R},\overline{R}')$ are so chosen because they are the solutions for the vector wave equation in region 1, and they must be finite like that of $\overline{\overline{G}}^{00o}_{eo}(\overline{R},\overline{R}')$ for $R<R'$.

Also, the expanded version of a typical combination is [34, p. 380]:

$$A^{10o}_{\substack{e\\o}M}\overline{M}^{(1)}_{\substack{e\\o}mn}(k_o)\overline{M}'^{(1)}_{\substack{e\\o}mn}(k_o)=\left\{\begin{array}{l} A^{10o}_{eM}\overline{M}^{(1)}_{emn}(k_o)\overline{M}'^{(1)}_{emn}(k_o)\\ A^{10o}_{oM}\overline{M}^{(1)}_{omn}(k_o)\overline{M}'^{(1)}_{omn}(k_o)\end{array}\right\}. \tag{3.16}$$

Double-layer Spherical Head model

We consider two concentric spheres centered at O, superimposed by an unbounded homogeneous medium with the current distribution source located outside the sphere at R'. The medium is characterized by (μ_b,ε_o), and material properties of the outer sphere are represented by $(\mu_{h1},\varepsilon_{h1})$ and that of the inner sphere by $(\mu_{h2},\varepsilon_{h2})$. The radii of outer to inner spheres are α_1 and α_2, respectively.

In this case the Scattered DGF terms can be shown by

$$\overline{\overline{G}}^{20o}_{es}(\overline{R},\overline{R}')=\frac{ik_o}{4\pi}\sum_{n=1}^{\infty}\sum_{m=0}^{n}C_{mn}\cdot\left[\begin{array}{l} A^{20o}_{\substack{e\\o}M}\overline{M}^{(1)}_{\substack{e\\o}mn}(k_o)\overline{M}'^{(1)}_{\substack{e\\o}mn}(k_o)\\ A^{20o}_{\substack{e\\o}N}\overline{N}^{(1)}_{\substack{e\\o}mn}(k_o)\overline{N}'^{(1)}_{\substack{e\\o}mn}(k_o)\end{array}\right], \tag{3.17}$$

$$\overline{\overline{G}}^{21o}_{es}(\overline{R},\overline{R}')=\frac{ik_o}{4\pi}\sum_{n=1}^{\infty}\sum_{m=0}^{n}C_{mn}\cdot\left\{\begin{array}{l} B^{21o}_{\substack{e\\o}M}\overline{M}^{(1)}_{\substack{e\\o}mn}(k_1)\overline{M}'^{(1)}_{\substack{e\\o}mn}(k_o)\\ B^{21o}_{\substack{e\\o}N}\overline{N}^{(1)}_{\substack{e\\o}mn}(k_1)\overline{N}'^{(1)}_{\substack{e\\o}mn}(k_o)\\ C^{21o}_{\substack{e\\o}M}\overline{M}_{\substack{e\\o}mn}(k_1)\overline{M}'^{(1)}_{\substack{e\\o}mn}(k_o)\\ C^{21o}_{\substack{e\\o}N}\overline{N}_{\substack{e\\o}mn}(k_1)\overline{N}'^{(1)}_{\substack{e\\o}mn}(k_o)\end{array}\right\}, \tag{3.18}$$

$$\overline{\overline{G}}^{22o}_{es}(\overline{R},\overline{R}')=\frac{ik_o}{4\pi}\sum_{n=1}^{\infty}\sum_{m=0}^{n}C_{mn}\cdot\left[\begin{array}{l} D^{22o}_{\substack{e\\o}M}\overline{M}_{\substack{e\\o}mn}(k_2)\overline{M}'^{(1)}_{\substack{e\\o}mn}(k_o)\\ D^{22o}_{\substack{e\\o}N}\overline{N}_{\substack{e\\o}mn}(k_2)\overline{N}'^{(1)}_{\substack{e\\o}mn}(k_o)\end{array}\right]. \tag{3.19}$$

The choice of the field and excitation functions in $\overline{\overline{G}}^{21o}_{es}(\overline{R},\overline{R}')$ are governed by the fact that the electromagnetic fields consist of radial wave-modes propagating outwards and inwards. Therefore

$$\overline{\overline{G}}^{21o}_{es} = \alpha \cdot \overline{\overline{G}}^{20o}_{es} + \beta \cdot \overline{\overline{G}}^{22o}_{es} . \tag{3.20}$$

Trilayer Spherical Head Model

In this case three concentric spheres centered at O, superimposed by an unbounded homogeneous medium with the radiation source located outside the sphere at R' are considered. The material properties of the outer to inner spheres are represented by $(\mu_{h1},\varepsilon_{h1})$, $(\mu_{h2},\varepsilon_{h2})$ and $(\mu_{h3},\varepsilon_{h3})$, respectively. The radii of outer to inner spheres are α_1, α_2 and α_3, respectively.

The Scattered DGF terms for $\overline{\overline{G}}^{30o}_{es}$ and $\overline{\overline{G}}^{31o}_{es}$ are the same as those in the last section and the rest can be expressed by

$$\overline{\overline{G}}^{32o}_{es}(\overline{R},\overline{R}') = \frac{ik_o}{4\pi}\sum_{n=1}^{\infty}\sum_{m=0}^{n} C_{mn}\cdot \left\{ \begin{array}{l} D^{32o}_{e_o M}\overline{M}^{(1)}_{e_o mn}(k_2)\overline{M}'^{(1)}_{e_o mn}(k_o) \\ D^{32o}_{e_o N}\overline{N}^{(1)}_{e_o mn}(k_2)\overline{N}'^{(1)}_{e_o mn}(k_o) \\ E^{32o}_{e_o M}\overline{M}_{e_o mn}(k_2)\overline{M}'^{(1)}_{e_o mn}(k_o) \\ E^{32o}_{e_o N}\overline{N}_{e_o mn}(k_2)\overline{N}'^{(1)}_{e_o mn}(k_o) \end{array} \right\}, \tag{3.21}$$

and for the inner layer,

$$\overline{\overline{G}}^{33o}_{es}(\overline{R},\overline{R}') = \frac{ik_o}{4\pi}\sum_{n=1}^{\infty}\sum_{m=0}^{n} C_{mn}\cdot \left[\begin{array}{l} F^{33o}_{e_o M}\overline{M}_{e_o mn}(k_3)\overline{M}'^{(1)}_{e_o mn}(k_o) \\ F^{33o}_{e_o N}\overline{N}_{e_o mn}(k_3)\overline{N}'^{(1)}_{e_o mn}(k_o) \end{array} \right] . \tag{3.22}$$

Quad-layer Spherical Head Model

Similarly, the case of four concentric spheres centered at O, superimposed by an unbounded homogeneous medium with the dipole source of radiation located outside the sphere at R', is considered. The material properties of the outer to inner spheres are, respectively, represented by $(\mu_{h1},\varepsilon_{h1})$, $(\mu_{h2},\varepsilon_{h2})$, $(\mu_{h3},\varepsilon_{h3})$ and $(\mu_{h4},\varepsilon_{h4})$. The radii of outer to inner spheres are α_1, α_2, α_3 and α_4, respectively.

The scattered DGF terms for $\overline{\overline{G}}_{es}^{40o}$, $\overline{\overline{G}}_{es}^{41o}$ and $\overline{\overline{G}}_{es}^{42o}$ are the same as those in the previous section and the rest can be presented by

$$\overline{\overline{G}}_{es}^{43o}(\overline{R},\overline{R}') = \frac{ik_o}{4\pi}\sum_{n=1}^{\infty}\sum_{m=0}^{n} C_{mn}\cdot\begin{Bmatrix} F_{\substack{e\\o}M}^{43o}\overline{M}_{\substack{e\\o}mn}^{(1)}(k_3)\overline{M}'^{(1)}_{\substack{e\\o}mn}(k_o) \\ F_{\substack{e\\o}N}^{43o}\overline{N}_{\substack{e\\o}mn}^{(1)}(k_3)\overline{N}'^{(1)}_{\substack{e\\o}mn}(k_o) \\ G_{\substack{e\\o}M}^{43o}\overline{M}_{\substack{e\\o}mn}(k_3)\overline{M}'^{(1)}_{\substack{e\\o}mn}(k_o) \\ G_{\substack{e\\o}N}^{43o}\overline{N}_{\substack{e\\o}mn}(k_3)\overline{N}'^{(1)}_{\substack{e\\o}mn}(k_o) \end{Bmatrix}. \tag{3.23}$$

The final inner layer gives

$$\overline{\overline{G}}_{es}^{44o}(\overline{R},\overline{R}') = \frac{ik_o}{4\pi}\sum_{n=1}^{\infty}\sum_{m=0}^{n} C_{mn}\cdot\begin{bmatrix} H_{\substack{e\\o}M}^{44o}\overline{M}_{\substack{e\\o}mn}(k_4)\overline{M}'^{(1)}_{\substack{e\\o}mn}(k_o) \\ H_{\substack{e\\o}N}^{44o}\overline{N}_{\substack{e\\o}mn}(k_4)\overline{N}'^{(1)}_{\substack{e\\o}mn}(k_o) \end{bmatrix}. \tag{3.24}$$

3.3.3 General Expression of Scattering DGFs for an Electric Dipole in the Presence of a Multilayered Spherical Head Model

Observation and analysis of the above expressions for the scattering equations allows an efficient formulation of the general scattering DGF for a multilayer spherical head as:

$$\overline{\overline{G}}_{es}^{Lfo}(\overline{R},\overline{R}') = \frac{ik_o}{4\pi}\sum_{n=1}^{\infty}\sum_{m=0}^{n} C_{mn}\cdot\begin{Bmatrix} A_{\substack{e\\o}M}^{Lfo}(1-\delta_f^L)\overline{M}_{\substack{e\\o}mn}^{(1)}(k_f)\overline{M}'^{(1)}_{\substack{e\\o}mn}(k_o) \\ A_{\substack{e\\o}N}^{Lfo}(1-\delta_f^L)\overline{N}_{\substack{e\\o}mn}^{(1)}(k_f)\overline{N}'^{(1)}_{\substack{e\\o}mn}(k_o) \\ B_{\substack{e\\o}M}^{Lfo}(1-\delta_f^o)\overline{M}_{\substack{e\\o}mn}(k_f)\overline{M}'^{(1)}_{\substack{e\\o}mn}(k_o) \\ B_{\substack{e\\o}N}^{Lfo}(1-\delta_f^o)\overline{N}_{\substack{e\\o}mn}(k_f)\overline{N}'^{(1)}_{\substack{e\\o}mn}(k_o) \end{Bmatrix}. \tag{3.25}$$

"L" is the symbol for last inner layer in the head. "f" is the field point or observer layer. Superscript/subscript "o" stands for source point at open space while subscript "s" is scattering. Where $k_f^2 = \omega^2(\mu_f\varepsilon_f)$ and $k_o^2 = \omega^2(\mu_o\varepsilon_o)$.

δ_f^L and δ_f^o are the Kronecker delta functions, where

$$\delta = \begin{cases} 1, & \text{if } L/o = f \\ 0, & \text{if } L/o \neq f \end{cases} \tag{3.26}$$

$A^{Lfo}_{\substack{e\\o}M}$, $A^{Lfo}_{\substack{e\\o}N}$, $B^{Lfo}_{\substack{e\\o}M}$ and $B^{Lfo}_{\substack{e\\o}N}$ are the amplitude coefficients of scattered DGF to be calculated by applying the boundary condition at the surface ($f = 0, 1, 2, ..., L$) of the sphere. These boundary conditions are;

$$\hat{R} \times \overline{\overline{G}}^{Lfo}_{e} = \hat{R} \times \overline{\overline{G}}^{L(f+1)o}_{e} \tag{3.27}$$

and

$$\frac{1}{\mu_f} \hat{R} \times \nabla \times \overline{\overline{G}}^{Lfo}_{e} = \frac{1}{\mu_{(f+1)}} \hat{R} \times \nabla \times \overline{\overline{G}}^{L(f+1)o}_{e} \tag{3.28}$$

In this section we list a few of the coefficients of the scattering DGF for the cases of two and three layered media when the source is located outside the spherical body.

All the local reflection coefficients are given by

$$R^{E}_{Pf} = \frac{V_\vartheta}{L}, \qquad R^{E}_{Ff} = \frac{V_\vartheta}{M} \tag{3.29}$$

$$R^{H}_{Pf} = \frac{W_\vartheta}{N}, \qquad R^{H}_{Ff} = \frac{W_\vartheta}{S} \tag{3.30}$$

And for the local transmission coefficients,

$$T^{E}_{Pf} = \frac{\nu}{L}, \qquad T^{E}_{Ff} = \frac{\varpi}{M} \tag{3.31}$$

$$T^{H}_{Pf} = \frac{\varpi}{N}, \qquad T^{H}_{Ff} = \frac{\nu}{S} \tag{3.32}$$

The superscripts E and H in the above equations denote TE and TM waves, whereas the subscripts P and F define the centripetal and centrifugal reflection or transmission respectively. Here

$$L = \mu_f k_{f+1} j_{ff} h'_{(f+1)f} - \mu_{f+1} k_f j'_{ff} h_{(f+1)f} \tag{3.33}$$

$$M = \mu_f k_{f+1} j'_{(f+1)f} h_{ff} - \mu_{f+1} k_f j_{(f+1)f} h'_{ff} \tag{3.34}$$

$$N = \mu_f k_{f+1} j'_{ff} h_{(f+1)f} - \mu_{f+1} k_f j_{ff} h'_{(f+1)f} \tag{3.35}$$

$$S = \mu_f k_{f+1} j_{(f+1)f} h'_{ff} - \mu_{f+1} k_f j'_{(f+1)f} h_{ff} \tag{3.36}$$

$$V_\vartheta = \mu_f k_{f+1} \vartheta'_{(f+1)f} \vartheta_{ff} - \mu_{f+1} k_f \vartheta'_{ff} \vartheta_{(f+1)f} \tag{3.37}$$

$$W_\vartheta = \mu_f k_{f+1} \vartheta_{(f+1)f} \vartheta'_{ff} - \mu_{f+1} k_f \vartheta_{ff} \vartheta'_{(f+1)f} \tag{3.38}$$

Besides ϑ represents j or h in the (Pf) or (Ff) mode representations respectively, while ϑ' represents j' or h' in the relationships for V and W.

$$\nu = \mu_f k_{f+1}(j_{(f+1)f} h'_{(f+1)f} - j'_{(f+1)f} h_{(f+1)f}) \tag{3.39}$$

$$\varpi = \mu_f k_{f+1}(j'_{(f+1)f} h_{(f+1)f} - j_{(f+1)f} h'_{(f+1)f}) \tag{3.40}$$

Where we have assumed the following abbreviations:

$$\begin{aligned} j_{fl} &= j_n(k_f \alpha_l), \qquad & j'_{fl} &= \frac{1}{k_f \alpha_l} j'_n(k_f \alpha_l) \\ h_{fl} &= h_n^{(1)}(k_f \alpha_l), \qquad & h'_{fl} &= \frac{1}{k_f \alpha_l} h'^{(1)}_n(k_f \alpha_l) \end{aligned} \tag{3.41}$$

Furthermore $\hat{j}_n(x) = x j_n(x)$ and $\hat{h}_n^{(1)}(x) = x h_n^{(1)}(x)$. In the above, the Wronskian of the spherical Bessel functions is

$$i = j_{ff} h'_{(f+1)f} - j'_{ff} h_{(f+1)f}. \tag{3.42}$$

If the source is located outside the spherical body, the coefficients of the scattering DGF is given by

i) For the case of two layered media the coefficients are

$$A^{10o}_{\substack{e\\o}M,N} = -R^{E,H}_{F0} \tag{3.43}$$

$$B^{11o}_{\substack{e\\o}M,N} = \frac{1}{T^{E,H}_{P0}} \left[1 - R^{E,H}_{F0} R^{E,H}_{P0}\right] \tag{3.44}$$

Where $R^{E,H}_{F0}$, $R^{E,H}_{P0}$ and $T^{E,H}_{P0}$ can be obtained from (3.29) to (3.32) by letting $f = 0$.

ii) For the case of three layered media the coefficients are

$$A^{20o}_{\substack{e\\o}M,N} = -\frac{T^{E,H}_{F0} R^{E,H}_{F0} + T^{E,H}_{F0} R^{E,H}_{F1}}{T^{E,H}_{F0} + T^{E,H}_{P0}} \tag{3.45}$$

$$A^{21o}_{\substack{e\\o}M,N} = \frac{R^{E,H}_{F0} + R^{E,H}_{F1}}{T^{E,H}_{F0} + T^{E,H}_{P0}} \tag{3.46}$$

$$B^{21o}_{\substack{e\\o}M,N} = \frac{1}{T^{E,H}_{P0}} \left[1 + R^{E,H}_{P0} A^{20o}_{\substack{e\\o}M,N}\right] \tag{3.47}$$

$$B^{22o}_{\substack{e\\o}M,N} = \frac{1}{T^{E,H}_{P1}} \left[R^{E,H}_{P1} A^{21o}_{\substack{e\\o}M,N} + B^{21o}_{\substack{e\\o}M,N}\right] \tag{3.48}$$

Where $R_{F0}^{E,H}$, $R_{F1}^{E,H}$, $R_{P0}^{E,H}$, $R_{P1}^{E,H}$ and $T_{F0}^{E,H}$, $T_{F1}^{E,H}$, $T_{P0}^{E,H}$ and $T_{P1}^{E,H}$ can be obtained from (3.29) to (3.32) by letting $f = 0, 1, 2$.

iii) For the case of four layered media the coefficients are

$$A_{\substack{e\\o}M,N}^{30o} = \frac{-1}{\varrho}\big[\big(T_{P0}^{E,H} R_{F0}^{E,H} + T_{F0}^{E,H} R_{F1}^{E,H}\big) T_{P1}^{E,H} + \big(T_{F0}^{E,H} + T_{P0}^{E,H} R_{P1}^{E,H} R_{F0}^{E,H}\big) T_{F1}^{E,H} R_{F2}^{E,H}\big] \tag{3.49}$$

with

$$\varrho = \left(T_{P0}^{E,H} + T_{F0}^{E,H} R_{F1}^{E,H} R_{P0}^{E,H}\right) T_{P1}^{E,H} + \left(T_{P0}^{E,H} R_{P1}^{E,H} + T_{F0}^{E,H} R_{P0}^{E,H}\right) T_{F1}^{E,H} R_{F2}^{E,H} \tag{3.50}$$

$$A_{\substack{e\\o}M,N}^{31o} = \frac{1}{T_{F0}^{E,H}}\left[A_{\substack{e\\o}M,N}^{30o} + R_{F0}^{E,H}\right] \tag{3.51}$$

$$B_{\substack{e\\o}M,N}^{31o} = \frac{1}{T_{P0}^{E,H}}\left[1 + R_{P0}^{E,H} A_{\substack{e\\o}M,N}^{30o}\right] \tag{3.52}$$

$$A_{\substack{e\\o}M,N}^{32o} = \frac{1}{T_{F1}^{E,H}}\left[A_{\substack{e\\o}M,N}^{31o} + R_{F1}^{E,H} B_{\substack{e\\o}M,N}^{31o}\right] \tag{3.53}$$

$$B_{\substack{e\\o}M,N}^{32o} = \frac{1}{T_{P1}^{E,H}}\left[R_{P1}^{E,H} A_{\substack{e\\o}M,N}^{31o} + B_{\substack{e\\o}M,N}^{31o}\right] \tag{3.54}$$

$$B_{\substack{e\\o}M,N}^{33o} = \frac{1}{T_{P2}^{E,H}}\left[R_{P2}^{E,H} A_{\substack{e\\o}M,N}^{32o} + B_{\substack{e\\o}M,N}^{32o}\right] \tag{3.55}$$

Where $R_{F0}^{E,H}$, $R_{F1}^{E,H}$, $R_{F2}^{E,H}$, $R_{P0}^{E,H}$, $R_{P1}^{E,H}$, $R_{P2}^{E,H}$ and $T_{F0}^{E,H}$, $T_{F1}^{E,H}$, $T_{F2}^{E,H}$, $T_{P0}^{E,H}$, $T_{P1}^{E,H}$ and $T_{P2}^{E,H}$ can be obtained from (3.29) to (3.32) by letting $f = 0, 1, 2, 3$.

For more details on the evaluation of coefficients, readers are referred to Cavalcante et-al [35] and Li et-al [36, 37].

3.3.4 A Novel General Expression of Scattering DGFs for an Electric Dipole in the Presence of a Multilayered Spherical Head Model

It is a well known fact that integral equation methods can solve unbounded problems very effectively. They are often referred to as exact techniques, because they

guarantee convergence for sufficiently dense discretizations. However, they have the disadvantage of being difficult to implement for complex objects, and generally result in the use of full matrices, whose treatment requires a large amount of memory and CPU time. The computational difficulties can be surmounted by more convenient and compact general equations. General formulations for scattering DGFs can be expressed by introducing the $\overline{\odot}$ operator which exploits the symmetry of the principle terms in the DGF expansion to give a general formulation applicable to a wide range of geometrical configurations [38] when one can significantly reduce the number of field samples needed for the field calculation. As shown below

$$\overline{\overline{G}}_{es}^{Lfo}(\overline{R},\overline{R}') = \frac{ik_o}{4\pi}\sum_{n=1}^{\infty}\sum_{m=0}^{n} C_{mn}\begin{bmatrix} A_{\substack{e\\o}M}^{Lfo}\,\overline{\overline{\odot}}_{es\,M}^{Lfo} \\ A_{\substack{e\\o}N}^{Lfo}\,\overline{\overline{\odot}}_{es\,N}^{Lfo}\end{bmatrix} \tag{3.56}$$

We give a direct and conceptually simple algorithm whose chief benefit is great computational efficiency. Where

$$\overline{\overline{\odot}}_{es\,M}^{L0o} = 0, \qquad \text{for } L = 0$$

(This means that, there is only infinite open space in the absence of a scattering body.) and

$$\overline{\overline{\odot}}_{es\,M}^{L0o} = \overline{M}_{\substack{e\\o}mn}^{(1)}(k_f)\overline{M}'^{(1)}_{\substack{e\\o}mn}(k_o), \qquad \text{for } f = 0 \text{ and } L > 0$$

$$\overline{\overline{\odot}}_{es\,M}^{Lfo} = \begin{bmatrix}\alpha\overline{M}_{\substack{e\\o}mn}^{(1)}(k_f)\overline{M}'^{(1)}_{\substack{e\\o}mn}(k_o)\\ \beta\overline{M}_{\substack{e\\o}mn}(k_f)\overline{M}'^{(1)}_{\substack{e\\o}mn}(k_o)\end{bmatrix}, \qquad \text{for} f \neq \begin{cases}0\\ or\\ L\end{cases}$$

and

$$\overline{\overline{\odot}}_{es\,M}^{LLo} = \overline{M}_{\substack{e\\o}mn}(k_f)\overline{M}'^{(1)}_{\substack{e\\o}mn}(k_o), \qquad \text{for } f = L$$

$\overline{\overline{\odot}}_{es\,N}^{Lfo}$ can be calculated from the same procedure as for $\overline{\overline{\odot}}_{es\,M}^{Lfo}$.

3.3.5 Electric DGF in the Antenna-Head Configuration

The electric DGF in the system can be computed by means of the method of scattering superposition expressed as the sum of incident (free-space) DGF and another contribution to account for the field scattered by layered media (secondary DGF), i.e.

$$\overline{\overline{G}}_e^{Lfo}(\overline{R},\overline{R}') = \overline{\overline{G}}_{eo}^{00o}(\overline{R},\overline{R}')\delta_f^o + \overline{\overline{G}}_{es}^{Lfo}(\overline{R},\overline{R}') \tag{3.57}$$

substituting in the above equation yields the electric DGF in the system:

$$\begin{aligned}\overline{\overline{G}}_e^{Lfo}(\overline{R},\overline{R}') = &-\frac{\hat{R}\hat{R}}{k_o^2}\delta(\overline{R}-\overline{R}')\delta_f^o + \frac{ik_o}{4\pi}\sum_{n=1}^{\infty}\sum_{m=0}^{n} C_{mn} \\ &\times \begin{Bmatrix} \begin{bmatrix} [\overline{M}_{\substack{e\\o}mn}^{(1)}(k_o)\overline{M}'_{\substack{e\\o}mn}(k_o)]\delta_f^o \\ [\overline{N}_{\substack{e\\o}mn}^{(1)}(k_o)\overline{N}'_{\substack{e\\o}mn}(k_o)]\delta_f^o \\ A_{\substack{e\\o}M}^{Lfo}(1-\delta_f^L)\overline{M}_{\substack{e\\o}mn}^{(1)}(k_f)\overline{M}'^{(1)}_{\substack{e\\o}mn}(k_o) \\ A_{\substack{e\\o}N}^{Lfo}(1-\delta_f^L)\overline{N}_{\substack{e\\o}mn}^{(1)}(k_f)\overline{N}'^{(1)}_{\substack{e\\o}mn}(k_o) \\ B_{\substack{e\\o}M}^{Lfo}(1-\delta_f^o)\overline{M}_{\substack{e\\o}mn}(k_f)\overline{M}'^{(1)}_{\substack{e\\o}mn}(k_o) \\ B_{\substack{e\\o}N}^{Lfo}(1-\delta_f^o)\overline{N}_{\substack{e\\o}mn}(k_f)\overline{N}'^{(1)}_{\substack{e\\o}mn}(k_o) \end{bmatrix}, & R>R', \\ \begin{bmatrix} [\overline{M}_{\substack{e\\o}mn}(k_o)\overline{M}'^{(1)}_{\substack{e\\o}mn}(k_o)]\delta_f^o \\ [\overline{N}_{\substack{e\\o}mn}(k_o)\overline{N}'^{(1)}_{\substack{e\\o}mn}(k_o)]\delta_f^o \\ A_{\substack{e\\o}M}^{Lfo}(1-\delta_f^L)\overline{M}_{\substack{e\\o}mn}^{(1)}(k_f)\overline{M}'^{(1)}_{\substack{e\\o}mn}(k_o) \\ A_{\substack{e\\o}N}^{Lfo}(1-\delta_f^L)\overline{N}_{\substack{e\\o}mn}^{(1)}(k_f)\overline{N}'^{(1)}_{\substack{e\\o}mn}(k_o) \\ B_{\substack{e\\o}M}^{Lfo}(1-\delta_f^o)\overline{M}_{\substack{e\\o}mn}(k_f)\overline{M}'^{(1)}_{\substack{e\\o}mn}(k_o) \\ B_{\substack{e\\o}N}^{Lfo}(1-\delta_f^o)\overline{N}_{\substack{e\\o}mn}(k_f)\overline{N}'^{(1)}_{\substack{e\\o}mn}(k_o) \end{bmatrix}, & R<R'. \end{Bmatrix} \end{aligned} \tag{3.58}$$

using the novel general method

$$\overline{\overline{G}}_e^{Lfo}(\overline{R},\overline{R}') = -\frac{\hat{R}\hat{R}}{k_o^2}\delta(\overline{R}-\overline{R}')\delta_f^o + \frac{ik_o}{4\pi}\sum_{n=1}^{\infty}\sum_{m=0}^{n} C_{mn}$$

$$\times \begin{cases} \left\{ \begin{array}{c} [\overline{M}_{\substack{e\\o}mn}^{(1)}(k_o)\overline{M}'_{\substack{e\\o}mn}(k_o)]\delta_f^o \\ [\overline{N}_{\substack{e\\o}mn}^{(1)}(k_o)\overline{N}'_{\substack{e\\o}mn}(k_o)]\delta_f^o \\ A_{\substack{e\\o}M}^{Lfo}\,\overline{\overline{\odot}}_{es}^{Lfo}\,M \\ A_{\substack{e\\o}N}^{Lfo}\,\overline{\overline{\odot}}_{es}^{Lfo}\,N \end{array} \right\}, & R > R', \\ \left\{ \begin{array}{c} [\overline{M}_{\substack{e\\o}mn}(k_o)\overline{M}'^{(1)}_{\substack{e\\o}mn}(k_o)]\delta_f^o \\ [\overline{N}_{\substack{e\\o}mn}(k_o)\overline{N}'^{(1)}_{\substack{e\\o}mn}(k_o)]\delta_f^o \\ A_{\substack{e\\o}M}^{Lfo}\,\overline{\overline{\odot}}_{es}^{Lfo}\,M \\ A_{\substack{e\\o}N}^{Lfo}\,\overline{\overline{\odot}}_{es}^{Lfo}\,N \end{array} \right\}, & R < R'. \end{cases} \tag{3.59}$$

If our concern is only with the region exterior to the source, then the singular term, which is important only in the source region can be dropped from the expression for the Green's function.

3.3.6 Magnetic DGF in the Antenna-Head Configuration

The principle of duality states that once the electric DGF is obtained, the magnetic DGF is derivable by interchanging the field functions $\overline{M}_{\substack{e\\o}mn} \rightarrow k\overline{N}_{\substack{e\\o}mn}$ and $\overline{N}_{\substack{e\\o}mn} \rightarrow k\overline{M}_{\substack{e\\o}mn}$ and omitting the singularity term contribution and vice versa.

On the other hand, the corresponding total magnetic DGF at any point in the system can be calculated from $\nabla \times \overline{\overline{G}}_e^{Lfo} = \overline{\overline{G}}_m^{Lfo}$, bearing in mind the discontinuous nature of magnetic DGF across a point source at $R = R'$ and the Ampère-Maxwell equation relating $\overline{\overline{G}}_e^{Lfo}$ and $\overline{\overline{G}}_m^{Lfo}$ in the dyadic form i.e.,

$$\nabla \times \overline{\overline{G}}_m^{Lfo} = \overline{\overline{I}}\delta(\overline{R}-\overline{R}') + k^2\overline{\overline{G}}_e^{Lfo} \tag{3.60}$$

$$\overline{\overline{G}}_m^{Lfo}(\overline{R},\overline{R}') = +\frac{ik_o^2}{4\pi}\sum_{n=1}^{\infty}\sum_{m=0}^{n} C_{mn}$$

$$\left\{\begin{array}{c} \left\{\begin{array}{c} [\overline{N}^{(1)}_{\substack{e\\o}mn}(k_o)\overline{M}'_{\substack{e\\o}mn}(k_o)]\delta_f^o \\ [\overline{M}^{(1)}_{\substack{e\\o}mn}(k_o)\overline{N}'_{\substack{e\\o}mn}(k_o)]\delta_f^o \\ A^{Lfo}_{\substack{e\\o}M}(1-\delta_f^L)\overline{N}^{(1)}_{\substack{e\\o}mn}(k_f)\overline{M}'^{(1)}_{\substack{e\\o}mn}(k_o) \\ A^{Lfo}_{\substack{e\\o}N}(1-\delta_f^L)\overline{M}^{(1)}_{\substack{e\\o}mn}(k_f)\overline{N}'^{(1)}_{\substack{e\\o}mn}(k_o) \\ B^{Lfo}_{\substack{e\\o}M}(1-\delta_f^o)\overline{N}_{\substack{e\\o}mn}(k_f)\overline{M}'^{(1)}_{\substack{e\\o}mn}(k_o) \\ B^{Lfo}_{\substack{e\\o}N}(1-\delta_f^o)\overline{M}_{\substack{e\\o}mn}(k_f)\overline{N}'^{(1)}_{\substack{e\\o}mn}(k_o) \end{array}\right\}, & R>R', \\ \times \\ \left\{\begin{array}{c} [\overline{N}_{\substack{e\\o}mn}(k_o)\overline{M}'^{(1)}_{\substack{e\\o}mn}(k_o)]\delta_f^o \\ [\overline{M}_{\substack{e\\o}mn}(k_o)\overline{N}'^{(1)}_{\substack{e\\o}mn}(k_o)]\delta_f^o \\ A^{Lfo}_{\substack{e\\o}M}(1-\delta_f^L)\overline{N}^{(1)}_{\substack{e\\o}mn}(k_f)\overline{M}'^{(1)}_{\substack{e\\o}mn}(k_o) \\ A^{Lfo}_{\substack{e\\o}N}(1-\delta_f^L)\overline{M}^{(1)}_{\substack{e\\o}mn}(k_f)\overline{N}'^{(1)}_{\substack{e\\o}mn}(k_o) \\ B^{Lfo}_{\substack{e\\o}M}(1-\delta_f^o)\overline{N}_{\substack{e\\o}mn}(k_f)\overline{M}'^{(1)}_{\substack{e\\o}mn}(k_o) \\ B^{Lfo}_{\substack{e\\o}N}(1-\delta_f^o)\overline{M}_{\substack{e\\o}mn}(k_f)\overline{N}'^{(1)}_{\substack{e\\o}mn}(k_o) \end{array}\right\}, & R<R'. \end{array}\right. \tag{3.61}$$

Notice that the magnetic DGF does not contain the singularity term because this term is canceled by the derivatives of the delta function and the unit function at the source point. The above equations can be used to accommodate any number of layers in the model system.

3.3.7 Electric and Magnetic Field at any Point in the Antenna-Head Configuration

The use of DGF technique allows us to determine the expansion of the electric and magnetic fields in a head/antenna configuration in a direct and elegant manner.

For any current source with current density function $\overline{J}(\overline{R}')$ located outside the

head, the electric or magnetic field radiated by such a dipole can be calculated using the formulae,

$$\overline{E}^{Lfo}(\overline{R}) = i\omega\mu_f \iiint_V \overline{\overline{G}}_e^{Lfo}(\overline{R},\overline{R}') \cdot \overline{J}(\overline{R}')dV' \tag{3.62}$$

$$\overline{H}^{Lfo}(\overline{R}) = i\omega\varepsilon_f \iiint_V \overline{\overline{G}}_m^{Lfo}(\overline{R},\overline{R}') \cdot \overline{J}(\overline{R}')dV'. \tag{3.63}$$

These signify the computation of the E and H-fields in the structure, which states the superposition of the incident field $\overline{E}_i(\overline{R})$ or $\overline{H}_i(\overline{R})$ and the scattered field $\overline{E}_s(\overline{R})$ or $\overline{H}_s(\overline{R})$ is given by

$$\overline{E}^{Lfo}(\overline{R}) = \overline{E}_i^{00o}(\overline{R})\delta_f^o + \overline{E}_s^{Lfo}(\overline{R}) \tag{3.64}$$

$$.\overline{H}^{Lfo}(\overline{R}) = \overline{H}_i^{00o}(\overline{R})\delta_f^o + \overline{H}_s^{Lfo}(\overline{R}). \tag{3.65}$$

3.4 Scattering DGF for a Perfectly Conducting Spherical Implant

When a perfectly conducting sphere of radius α is illuminated by an electromagnetic wave, the scattered terms can be written in the form

$$\overline{\overline{G}}_{es}(\overline{R},\overline{R}') = \frac{ik_o}{4\pi}\sum_{n=1}^{\infty}\sum_{m=0}^{n} C_{mn} \cdot \begin{bmatrix} \alpha_{\substack{e\\o}M}\overline{M}^{(1)}_{\substack{e\\o}mn}(k_o)\overline{M}'^{(1)}_{\substack{e\\o}mn}(k_o) \\ \beta_{\substack{e\\o}N}\overline{N}^{(1)}_{\substack{e\\o}mn}(k_o)\overline{N}'^{(1)}_{\substack{e\\o}mn}(k_o) \end{bmatrix}, \tag{3.66}$$

Applying the principle of scattering superposition, we obtain

$$\overline{\overline{G}}_e(\overline{R},\overline{R}') = \overline{\overline{G}}_{eo}(\overline{R},\overline{R}') + \overline{\overline{G}}_{es}(\overline{R},\overline{R}') \tag{3.67}$$

Where we consider the function for a conducting sphere in a region $0 \leq \alpha \leq \infty$. After applying the boundary condition one can determine the unknown coefficients. In order to satisfy the boundary condition at interface $r = \alpha$,

$$\hat{r} \times \left[\overline{M}_{\substack{e\\o}mn}(k_o)\overline{M}'^{(1)}_{\substack{e\\o}mn}(k_o) + \alpha_{\substack{e\\o}M}\overline{M}^{(1)}_{\substack{e\\o}mn}(k_o)\overline{M}'^{(1)}_{\substack{e\\o}mn}(k_o)\right]_{r=\alpha} \tag{3.68}$$

$$\hat{r} \times \left[\overline{N}_{\substack{e\\o}mn}(k_o)\overline{N}'^{(1)}_{\substack{e\\o}mn}(k_o) + \beta_{\substack{e\\o}N}\overline{N}^{(1)}_{\substack{e\\o}mn}(k_o)\overline{N}'^{(1)}_{\substack{e\\o}mn}(k_o)\right]_{r=\alpha} \tag{3.69}$$

$$\hat{r}\times\left[\overline{M}_{\substack{e\\o}mn}(k_o)+\alpha_{\substack{e\\o}M}\overline{M}^{(1)}_{\substack{e\\o}mn}(k_o)\right]_{r=\alpha}=0 \tag{3.70}$$

$$\hat{r}\times\left[\overline{N}_{\substack{e\\o}mn}(k_o)+\beta_{\substack{e\\o}N}\overline{N}^{(1)}_{\substack{e\\o}mn}(k_o)\right]_{r=\alpha}=0 \tag{3.71}$$

substituting for $\overline{M}_{\substack{e\\o}mn}(k_o)$ and $\overline{M}^{(1)}_{\substack{e\\o}mn}(k_o)$

$$\overline{M}_{\substack{e\\o}mn}(k_o)=\nabla\times[j_n(kR)P_n^m(\cos\theta)^{\cos}_{\sin}m\phi\overline{R}], \tag{3.72}$$

$$\overline{M}^{(1)}_{\substack{e\\o}mn}(k_o)=\nabla\times[h_n^{(1)}(kR)P_n^m(\cos\theta)^{\cos}_{\sin}m\phi\overline{R}], \tag{3.73}$$

in equation (3.70) produces $\alpha_{\substack{e\\o}M}=-\frac{[j_n(k_o\alpha)]}{[h_n^{(1)}(k_o\alpha)]}$.

Similarly inserting for $\overline{N}_{\substack{e\\o}mn}(k_o)$ and $\overline{N}^{(1)}_{\substack{e\\o}mn}(k_o)$

$$\overline{N}_{\substack{e\\o}mn}(k_o)=\frac{1}{k}\nabla\times\nabla\times[j_n(kR)P_n^m(\cos\theta)^{\cos}_{\sin}m\phi\overline{R}], \tag{3.74}$$

$$\overline{N}^{(1)}_{\substack{e\\o}mn}(k_o)=\frac{1}{k}\nabla\times\nabla\times[h_n^{(1)}(kR)P_n^m(\cos\theta)^{\cos}_{\sin}m\phi\overline{R}], \tag{3.75}$$

in equation (3.71) produces $\beta_{\substack{e\\o}N}=-\frac{\partial[(k_o\alpha)j_n(k_o\alpha)]/\partial(k_o\alpha)}{\partial[(k_o\alpha)h_n^{(1)}(k_o\alpha)]/\partial(k_o\alpha)}$.

3.5 Discussions and Comparison of General Representation of DGFs with Other Authors' Related Works

A fundamental problem in electromagnetic theory is the calculation of the field at source point. It arises in the evaluation of the antenna impedance, the power radiation pattern, the induced current on a scatterer, and other situations.

A DGF is highly singular. Inside the source region the field is not solenoidal so the $\overline{L}_{\substack{e\\o}mn}$ functions must also be included. The singular behaviour of the DGF at the source point caused considerable difficulty in the early development of the theory. Many authors examined this elusive singular nature of DGF [19] - [24], [26], [27], [39] - [66].

Collin [39] has shown that, "a relatively straight-forward analysis using the complete set of eigenfunctions described by Tai led to the discovery that there was a sub-spectrum of zero frequency or "static-like" modes that were part of the spectrum of the transverse eigenfunctions (the N functions of Hansen). These zero frequency

modes cancel the longitudinal mode spectrum outside the source region. Inside the source region the cancellation is not complete but the non-cancellating part can be expressed as a delta function contribution".

A symbolic way to represent a point source of excitation is the use of Dirac's three-dimensional delta function expressed in spherical polar coordinates if R' is (R', θ', ϕ'); thus

$$\delta(\overline{R} - \overline{R}') = \frac{1}{R'^2 \sin\theta'} \delta(\overline{R} - \overline{R}')\delta(\overline{\theta} - \overline{\theta}')\delta(\overline{\phi} - \overline{\phi}') \tag{3.76}$$

The free space scalar Green function has an R^{-1} singularity, where R is the distance between source and observation points.

Tai [19] pointed out that the method of expressing the point source dyadics only in terms of the transverse (divergenceless) vector functions $\overline{M}_{\substack{e \\ o}mn}$ and $\overline{N}_{\substack{e \\ o}mn}$ can lead to a contradiction: the left hand side of the vector wave equation is solenoidal, but the right hand side is not. A remedy for this dilemma, is by including the longitudinal wave functions, or the discontinuous nature of $\overline{\overline{G}}_m(\overline{R}, \overline{R}')$ at $R = R'$. $\overline{\overline{G}}_e(\overline{R}, \overline{R}')$ unlike $\overline{\overline{G}}_m(\overline{R}, \overline{R}')$ is not a solenoidal dyadic function because

$$\begin{aligned} \nabla \cdot \overline{\overline{G}}_e(\overline{R}, \overline{R}') &= -\frac{1}{k^2} \nabla \cdot [\overline{\overline{I}} \delta(\overline{R} - \overline{R}')] \\ &= -\frac{1}{k^2} \nabla \delta(\overline{R} - \overline{R}') \end{aligned} \tag{3.77}$$

which is not zero except for $R \neq R'$.

In the present work, we have derived a complete eigenfunction expansion of the DGF for the multilayered dielectric head-antenna model using the R-directed solenoidal electric and magnetic (TM and TE) eigenfunctions. The DGF for this canonical problem can be constructed in several ways using methods such as G_m, G_e or G_A. Furthermore, it is demonstrated that the formula is particularly suitable for the numerical evaluation of the field at the source point, because it allows the exclusion of a finite region around the singular point from the integration volume. This feature is not shared by a few of the previous results on the DGF, such as work done by Bowman [34], Ruoss [67], Buttler [68], Jones [70], and a few others.

The singularity [24], [27] of the DGF depends on the shape of the infinitesimal exclusion volume. Assuming the correlation function for the random medium to be spherically symmetric and choose a spherically-shaped exclusion volume. the DGF can be decomposed into

$$\overline{\overline{G}}_e(\overline{R},\overline{R}') = PV\overline{\overline{G}}_e(\overline{R},\overline{R}') - \overline{\overline{I}}\frac{1}{3k^2}\delta(\overline{R}-\overline{R}') \tag{3.78}$$

Where PV stands for principal value.

If $\overline{R}$ and the $\overline{R}'$ coincide we must account for the singularities of the DGF. Thus, to make use of DGF when the observation point is in the source region, extreme caution must be exercized. We write for $\overline{R}'$ in the source region,

$$\overline{E}(\overline{R}_o) = PV\iiint_V \overline{\overline{G}}_e(\overline{R}_o,\overline{R}')\cdot\overline{J}(\overline{R}')dV + \overline{E}_c(\overline{R}_o) \tag{3.79}$$

Where the correction term, $\overline{E}_c(\overline{R}_o)$ depends on the shape of ΔV, but the final result which is the sum of the principal value integral and correction term, however is independent of the shape of ΔV.

The principal value integral is obtained by performing the volume integration over the source region excluding a small exclusion volume with spherical shape and containing the observation point. The size of exclusion volume is allowed to shrink to zero eventually. Thus, the first term can be thought of as the contribution to the field at the observation point due to the source outside the exclusion volume. The latter term is the contribution to the field at the observation point due to the source inside the exclusion volume, which can be shown to be non-vanishing event when the exclusion volume shrinks to zero. The two terms on the right-hand side of the above equation depend on the shape of the exclusion volume. Since the exclusion volume is vanishingly small, we can assume that $\overline{J}(\overline{R}')$ is uniform inside the exclusion volume.

Two of the sources of error are to be found in Tai's technical reports and his book [20]. The first edition of Tai [20] had made no allowance for the singularity

term, and in the second edition, one should notice that he has not considered this term for a cone and also for a cone with a spherical sector in [19, chap.10, pages 223 and 224 respectively]. The term involving δ had not been included in Tai's earlier works until 1973 [46] and has been a subject of discussions by many authors, Tai [46], Rahmat-Samii [22], Collin [21] and [47].

In 1971 Tai [20] assumed that for the vector wave equation the eigenfunction expansion would be complete without including the irrotational modes. Further investigation of the subject by the above mentioned author uncovered the necessity to add a term to the expansion in order to achieve a complete expansion for the DGF in the source region [19].

Since understanding the properties of the singularity is essential to the use of the DGF in numerical analyses, it is highly desirable to resolve and clarify the apparent incongruities. Samii [22] stated that "Care must be exercized in defining the derivatives in the sense of distribution and in using the correct completeness relation in order to compute the correct DGF". Proper handling of the electric DGF in the source region is essential when using it in numerical analyses involving dielectric scatterer. The difficulty arises in the computation of the "self-cell" or self-coupling matrix element that must be generated when using the method of moments.

Yaghjian [24] explained the difference in the delta function terms between Tai et al. [52] and Samii [22] caused by their different choices of the principal volume and emphasized the need to include in $\overline{\overline{G}}_e(\overline{R}, \overline{R}')$ the shape of the principal volume involved. Yaghjian [24] and Lee et al. [56] outlined proofs to show that singularity associated with the electric DGF in a bounded region is exactly the same as that for the free space.

Wang [60] has also attempted to clarify some of the apparent discrepancies in the literature regarding the singular behaviour of $\overline{\overline{G}}_e(\overline{R}, \overline{R}')$ and seeking a unified and consistent view on this important subject.

According to the homogeneous vector Helmholtz decomposition theorem and its

manifestation in field theory, a general E-field can be decomposed into an irrotational (lamellar) and a rotational (solenoidal) component:

$$E = E_{irr} + E_{rot} \tag{3.80}$$

The E_{irr} describes current source's near field, the field lines for which emanate from and terminate on the dipole electrodes while the E_{rot} approximately describes the far field, the field lines for which neither touch nor encompass the dipole. Also in Ampère's law

$$\nabla \times H = J, \tag{3.81}$$

where $J = J_c + J_d$, and here the displacement current density, J_d, can be decomposed in an irrotational component $J_{d_{irr}}$ and a rotational component $J_{d_{rot}} \cdot J_c$ is the conduction-current density. $J_{d_{irr}}$ represents the quasi-static displacement-current density completing J_c to form a closed current loop, thereby satisfying the continuity law $\nabla \cdot (J_c + J_{d_{irr}}) = 0$. The $J_{d_{rot}}$ represents the far field. Hence the true current density of the non-stationary case consists of three components

$$J = J_c + J_{d_{irr}} + J_{d_{rot}}, \tag{3.82}$$

where $J_c + J_{d_{irr}}$ represent the quasi-static true current density corresponding to the applied excitation. The total displacement-current density $J_d = J_{d_{irr}} + J_{d_{rot}}$, consists of $J_{d_{irr}}$, driven by the applied voltage and $J_{d_{rot}}$ existing isolated from the applied voltage source, so that $J_{d_{rot}}$ remains in existent also after disconnecting the voltage source [71].

In numerical codes, based on the method of moments, the integration domain is limited to the conductor surfaces, hence the integration of the quasi-static displacement current density $J_{d_{irr}}$ is excluded.

In using the method of $\overline{\overline{G}}_m$ to find the electric DGF, the key step is to obtain an expression of $\nabla \times \overline{\overline{G}}_e(\overline{R}, \overline{R}')$ while taking into consideration of the discontinuous behaviour of $\overline{\overline{G}}_m$ at $R = R'$.

Our purpose here is to bring to light the importance of characteristics of the delta function term in source region. These comparisons may prove valuable in estimating the effect of the delta term.

In this section we highlight five different discrepancies in other authors' works in comparison to ours, taking into account to what was mentioned above.

3.5.1 The Isolated Singular Term in $\overline{\overline{G}}_e$ in the Form of Delta Term $-\frac{\hat{R}\hat{R}}{k_o^2}\delta(\overline{R}-\overline{R}')$

Since the primary interest can be to develop a formulation for the evaluation of the electromagnetic fields away from the source, $\overline{\overline{G}}_{eo}^{00o}(\overline{R},\overline{R}')$ can be given only by the second term on the right side of $\overline{\overline{G}}_{eo}^{00o}(\overline{R},\overline{R}')$ i.e. the non-delta terms outside the source region. But on the other hand, it is well known that the solenoidal modes do not form a complete set for expanding an electric field. This has been proven by Kurokawa [41] as early as 1958 and of course by others later on/afterwards.

The electric and magnetic dyadic Green's components given in Ruoss' [67] work appears to be closely related to those electric and magnetic dyadic Green's components which have been derived by Bowman [34], Butler [68], and Jones [70] utilizing the usual boundary conditions at each of the interfaces but not the proper condition at the source point. Ruoss did not utilize the vector wave functions to derive the complete eigenfunction expansion of the electric DGF which contains a physical interpretation at source region. Therefore the expansion (15) in Ruoss' paper does not contain an explicit dyadic delta function term which is required for completeness at the source region even though he has referred to Tai's second edition [19] that contains the corrected version. The correct expressions are given here using the eigenfunction expansions method.

These discrepancies can be eliminated by recognizing the distribution or principal volume theory.

One of the most confusing aspects of the above paper deals with the generalization of DGF for electric as well as magnetic type which is really the DGFs for an

electric dipole in the presence of a sphere plus that of a dipole in unbounded space similar to Butler's work [68] who referred to both Bowman [34] and Jones [70].

This delta term does not exist in Li's paper [72] who has referred to Tai [46] whom has declared/announced his error about the singular behaviour of the eigenfunction expansion of the DGF in his publication [20] presenting his improved method for deriving the residue series. This communication of Li [72] has a couple of printing errors and in his general representation of scattering DGF.

Bohren [73] did not manage to extract the singularity term in the source region explicitly, even though he has added the radial term to $\overline{M}_{o_{mn}}$ function by the addition of $\overline{M}_{e_{mn}}$ and $\overline{N}_{e_{mn}}$ functions. Consequently, Engheta [74] who used the same technique lacks the same expression. Also the dyadic delta function term, which makes the DGF representation complete at the source point, was not explicitly extracted in Bagby [75]; Viola and Nyquist [76], slightly modified that analysis later to properly extract the dyadic delta function term.

A paper by Pearson [77] gives an expansion of the DGFs in cylindrical coordinates. Unfortunately, several delta function terms were missed in that expansion. When the static like modes cancel, the results reduce to those obtained by Tai [19]. Stubenrauch [78] has the same problem.

3.5.2 The Limits of Summing Series Indices

Care must be taken in choosing the values of indices in double series in order to satisfy the physically required series condition. It is noted that, for any value of the double summation index n, there is a different value of m. Infinite series consist of terms slowly convergent with m and n. When indices m and n are both equal to zero, the functions $\overline{M}_{o_{mn}}$ and $\overline{N}_{e_{mn}}$ are null functions, and their normalization factors are equal zero, therefore we start n with unity and m begins from zero to avoid this situation.

Li's expressions [36] which have a couple of typographical errors containing double infinite series, which is evaluated by a summation technique over the contribu-

tions from all the individual modes. The limits of these summing series are taken as n and m both equal zero. Therefore as mentioned above, these limits are incorrect and would drive $C_{mn} = (2 - \delta_o^m)\frac{2n+1}{n(n+1)}\frac{(n-m)!}{(n+m)!}$ to an infinite value. This error also exists throughout Li's other paper [72].

Butler's summing series indices n equal zero and m starting from $-n$, at one time m and n can become zero where coefficient C_{mn}, and also $\overline{M}_{o^e_o mn}$ and $\overline{N}_{o^e_o mn}$ vector wave functions can become null vector [68].

3.5.3 The Range for R and R'

After correcting an error in the sign in Li's [36] expression for free space electric DGF, the ranges $R \geq R'$ and $R \leq R'$ are also incorrect because when $R = R'$ the operational property that Delta $\delta(\overline{R} - \overline{R}') = \infty$, and the operational property that Delta $\delta(\overline{R} - \overline{R}') = 0$ for $R \neq R'$ and for any vector function $F(R')$ that is continuous at $R = R'$;

$$\iiint_V F(\overline{R})\delta(\overline{R} - \overline{R}')dV = \begin{cases} F(\overline{R}'), & R' \text{ in V}, \\ 0, & R' \text{ not in V} \end{cases} \tag{3.83}$$

and

$$\int_{R-\alpha}^{R+\alpha} \delta(R - R')dR' = 1 \tag{3.84}$$

where the product of delta functions is used to represent a unit source.

The factor $\delta(R-R')$ shows that the impulse occurs at $R = R'$, i.e. $\delta(\overline{R}-\overline{R}') = \infty$, as a result of which free space electric DGF also becomes infinite. Therefore, the correct ranges are $R > R'$ and $R < R'$.

Another of Li's papers [79] which has a great deal of mistakes in its general scattering DGF expression for the radially multilayered chiral media also suffers from this problem.

3.5.4 The Range for z and z'

Li-Bennett et al and one of their references Cavalcante et al have the same problem as in IV-C in [35] and [37] respectively by assuming $z \geq z'$ and $z \leq z'$ for the DGF in free space. A similar analogy following 3.5.3 applies here as well, but in this occasion the $z = z'$ makes the delta function to become infinite.

Li's other paper [80] " On the eigenfunction expansion of electromagnetic dyadic Green's functions in rectangular cavities and waveguides", also suffers from this problem.

3.5.5 The Integration of Delta Term in Field Equations

Notice that the integral representations of E-fields given in Tai [19] throughout his book do not have Dirac delta singularity integrated and no explanation have been also expressed. But by evaluating one of the integrals in the representation, a singularity can be explicitly integrated from the vector wave function representations. For example looking at one of these examples in Tai [19, chap.10, page 213] for an infinitesimal horizontal electric dipole with current moment c pointed in the x-direction and located at $R' = b$, $\theta' = 0$ and $\phi' = 0$ the electric field produced by this dipole in the presence of a perfectly conducting sphere with radius α is then given by:

$$\overline{E}(\overline{R}) = \frac{-kc\omega\mu_o}{4\pi} \sum_{n=1}^{\infty} \frac{2n+1}{n(n+1)}$$

$$\times \begin{cases} \begin{Bmatrix} [j_n(\rho_b) + \alpha_n h_n^{(1)}(\rho_b)]\overline{M}^{(1)}(k) \\ \frac{1}{\rho_b}([\rho_b j_n(\rho_b)]' + \beta_n[\rho_b h_n^{(1)}(\rho_b)]')\overline{N}^{(1)}(k) \end{Bmatrix}, & R > b, \\ \begin{Bmatrix} h_n^{(1)}(\rho_b)[\overline{M}(k) + \alpha_n \overline{M}^{(1)}(k)] \\ \frac{[\rho_b j_n(\rho_b)]'}{\rho_b}[\overline{N}(k) + \beta_n \overline{N}^{(1)}(k)]' \end{Bmatrix}, & R < b. \end{cases} \tag{3.85}$$

Of course the explanation can be given as in the previous section, because when

one is not interested in the source region, the singular term in the expression for G_e may be dropped.

The answer including consideration of the integration of the delta function term and the use of generalized function in 3.5.3 provides

$$\overline{E}(\overline{R}) = -\frac{\hat{R}\hat{R}}{k^2}J(\overline{R}) - \frac{kc\omega\mu_o}{4\pi}\sum_{n=1}^{\infty}\frac{2n+1}{n(n+1)}$$
$$\times \begin{cases} \left\{ \begin{array}{c} [j_n(\rho_b) + \alpha_n h_n^{(1)}(\rho_b)]\overline{M}^{(1)}(k) \\ \frac{1}{\rho_b}([\rho_b j_n(\rho_b)]' + \beta_n[\rho_b h_n^{(1)}(\rho_b)]')\overline{N}^{(1)}(k) \end{array} \right\}, & R > b, \\ \left\{ \begin{array}{c} h_n^{(1)}(\rho_b)[\overline{M}(k) + \alpha_n\overline{M}^{(1)}(k)] \\ \frac{[\rho_b h_n(\rho_b)]'}{\rho_b}[\overline{N}(k) + \beta_n\overline{N}^{(1)}(k)] \end{array} \right\}, & R < b. \end{cases} \tag{3.86}$$

Examination of the two equations show that apart from the term in source region, the derivative sign in the last line of his equation (3.85) should be removed.

It must be pointed out that Tai's second edition [19] has many typographical errors throughout the book. Jones [70] and Bowman [34] also do not have the complete solutions to the total E-fields throughout their books because they have not included the delta terms in their representations of eigenfunction expansions of DGFs. Bohren [73] and Stubenrauch [78] suffers from the same problem/situation.

3.6 Concluding Remarks

A theoretical analysis of antenna/layered head configuration is demonstrated. An improved general multilayered homogeneous lossy dielectric spherical head/antenna model of DGF for numerical EMC investigation has been proposed and compared with the models by various authors. The DGFs are obtained by employing the method of scattering superposition. This study enables one to assess the influence of the presence of a close-by biological head upon the operating characteristics of a mobile phone, antennas input impedance, SAR values inside the head, the power

absorbed, the total radiated power, the thermal emission, the induced current on a scatterer, novel antenna design, the electric and magnetic near-/far-fields patterns, and also other situations.

In this communication we have also drawn attention to the fact that the singular behaviour of the eigenfunction expansion of the DGF is incorrectly formulated in some authors' related works. This is significant because this expansion is used in the numerical calculation of the electric field in the source region.

Furthermore, by defining a symmetry operator the required memory for efficient numerical computations using the method of moments can be reduced drastically by formulating a new compact general expression. The validity of the general model is verified by the DGF of the specific models, which agrees with other authors' study. Further work is in hand to find a reduced general formulation for electromagnetic DGF in spherically multilayered media by utilizing the technique presented in this chapter.

The results of this study could be useful for a further analysis of the problem. Both GSM (global system for mobile communication) and PCS (personal communication services) pose potential problems with regard to interactions with the human body and implanted medical devices. Interaction/interference-free antenna design is useful and, increasingly, becoming necessary. Since anything that conducts can be considered as an antenna and two antennas interact with each other, the interaction problem could potentially be solved by using the mobile phone (handset transceiver) user (human body) as an antenna and transmitting at frequency levels (for example, noise) unharmful to humans. This would make possible the design of antenna-less PCS, receiving/transmitting signals only in close proximity to biological antennas (users).

Chapter 4

Human Torso Model Using Cylindrical DGF

ANTENNA radiation pattern, performance and other characteristics in modern wireless telecommunication devices (GSM Mobile system) are significantly altered by the presence of the human body as a volume conductor. This chapter aims to express a general representation of dyadic Green's function (DGF) for the problem of electromagnetic radiation from a source of excitation in the presence of a human torso model (multilayered homogeneous lossy dielectric circular cylinder of finite length) as well as any part of the body assuming the shape of a cylinder. The whole structure is assumed to be uniform along the propagation direction and stationary. The DGFs are obtained by employing the method of scattering superposition.

4.1 Introduction

Antenna-body interaction is of interest with the use of chest-mounted 418 MHz biotelemetry transmitters for medical applications. Short range telemeters being developed for medical applications increasingly operate at UHF, taking advantage of greater spectrum availability and reduced levels of synthetic noise. Transmitting devices built for the patient-end of the radio link are invariably battery powered so must be lightweight and compact to ensure user comfort. Such physical limitations on packaging mean that even built-in antennas at UHF are electrically small, with

correspondingly low efficiencies. Further problems arise as the telemeter is usually worn next to the skin at chest or abdominal level, so the transmitting antenna is in close proximity to the body tissue. Power dissipation in the body and impedance mismatches induced by effects of proximity presents additional system losses, so the risk of signal drop-out in the link is increased. The most important operational parameters for a closed-coupled antenna-body interaction for biotelemetry are its antenna efficiency and radiation pattern in the azimuthal plane.

This chapter is organized as follows. The complete set of finite cylindrical vector wave functions are introduced in section 4.2 and the orthogonal behaviour of these functions are investigated in section 4.3.

In section 4.4, we begin to formulate the problem for a torso model (finite circular cylinder) and in subsection 4.4.1, we set out with the case, in which we construct the DGF, $\overline{\overline{G}}_{e1}(\overline{R}, \overline{R}')$, in terms that constitute the continuous eigenfunction expansion (EFE) in which the eigenfunctions are guided in the preferred r and z-coordinate directions, using the procedures described in Tai [19] or Collin [21]. This expansion also contains an explicit dyadic delta function term which is required for completeness at the source point. It is considered as a correction to the general solenoidal EFE which is valid outside the source point.

The procedure required to derive the complete EFE of the general scattering DGF for the torso model (finite multilayered circular cylinder), in terms of only the solenoidal eigenfunctions is shown to be a simple and straightforward general expression and is summarized in subsections 4.4.2 and 4.4.3.

Subsection 4.4.3, presents the final construction of the DGFs expansions (4.56). It is in this development that the principal point of this chapter is identified.

Magnetic type DGF can be found by invoking duality. Once the electric field is obtained the magnetic field is derivable by taking the curl of the electric field, and vice versa.

Conclusions are then presented in section 4.7 summarizing the important points contained in this work.

4.2 Vector Wave Functions for a Circular Cylinder of Finite Length

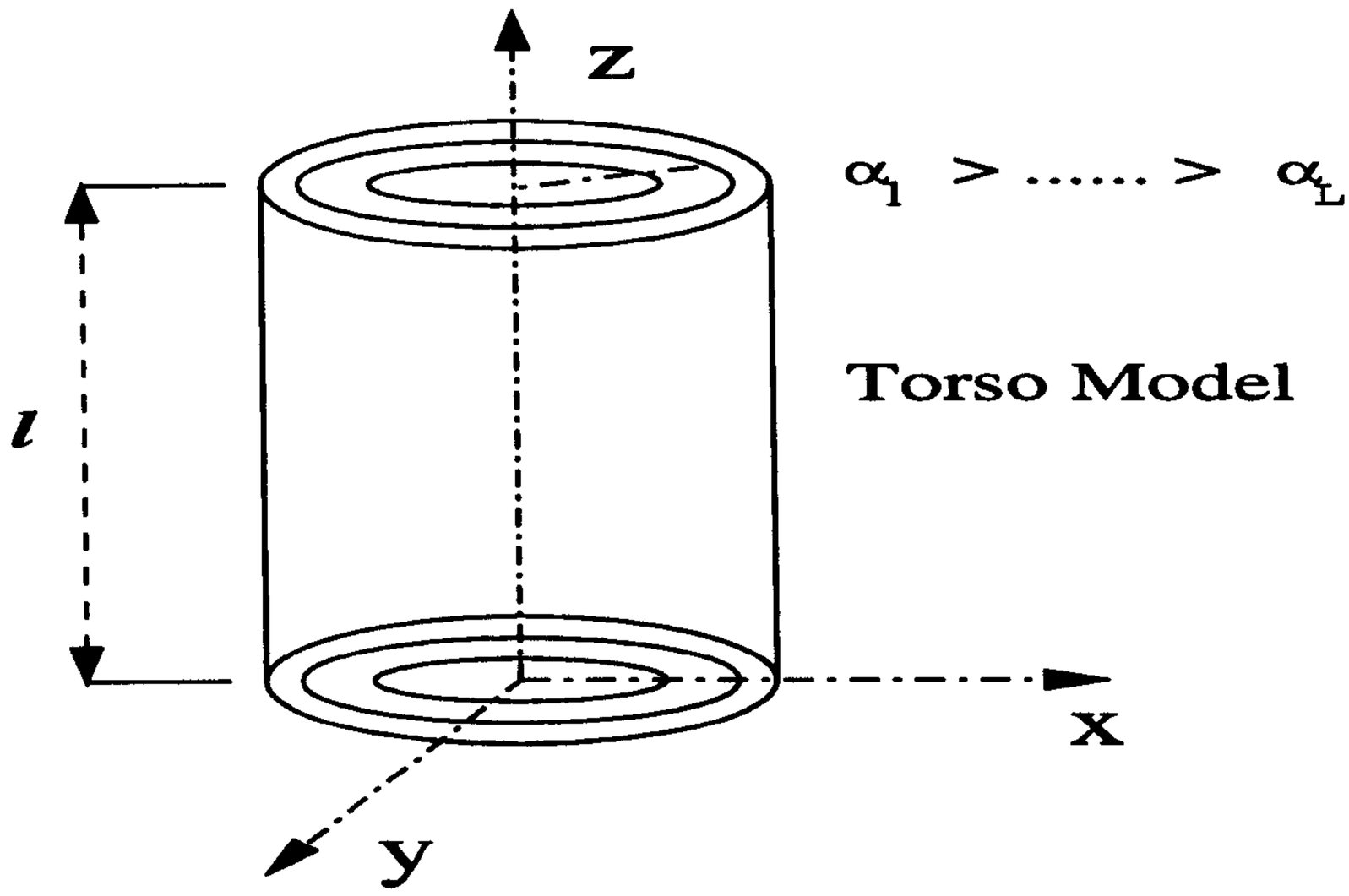

Figure 2: Diagram of a Finite Cylindrical Human Torso

The cylindrical vector wave functions are the building blocks of the EFE of various kinds of DGF. They are denoted by $\overline{L}_{\substack{ee\\oo}n\lambda}$, $\overline{P}_{\substack{ee\\oo}n\lambda}$, and $\overline{Q}_{\substack{ee\\oo}n\lambda}$, that are solutions of the homogeneous vector Helmholtz equation. The generating functions or eigenfunctions, which are solutions of the cylindrical scalar wave equation $\nabla^2\Psi + k_\lambda^2\Psi = 0$, with the differential equation in the cylindrical coordinate system

$$\frac{1}{r}\frac{\partial}{\partial r}(r\frac{\partial\Psi}{\partial r}) + \frac{1}{r^2}\frac{\partial^2\Psi}{\partial\phi^2} + \frac{\partial^2\Psi}{\partial\phi^2} + \frac{\partial^2\Psi}{\partial z^2} + K^2\Psi = 0 \tag{4.1}$$

with K, the separation constant and k_λ being an undetermined wave number. Implementation of the method of separation of variables in this system results, in letting $\Psi = R\Phi z$ to be a solution of the basic differential equation, and substitution in (4.1) and dividing by $R\Phi z$, one establishes

$$\frac{1}{R}\frac{d^2R}{dr^2} + \frac{1}{rR}\frac{dR}{dr} + \frac{1}{r^2\Phi}\frac{d^2\Phi}{d\phi^2} + \frac{1}{Z}\frac{d^2Z}{dz^2} + K^2 = 0 \tag{4.2}$$

Solving for Z-component, one obtains

$$Z = A\cos\sqrt{K^2 - k_r^2}z + B\sin\sqrt{K^2 - k_r^2}z \tag{4.3}$$

where k_r is a separation constant still to be determined. The equation we are left with is of the form

$$\frac{r^2}{R}\frac{d^2R}{dr^2} + \frac{r^2}{rR}\frac{dR}{dr} + k_r^2 r^2 + \frac{1}{\Phi}\frac{d^2\Phi}{d\phi^2} = 0 \tag{4.4}$$

and permits us to solve for the ϕ-component,

$$\Phi = C\cos k_\phi\phi + D\sin k_\phi\phi \tag{4.5}$$

In order to ensure the uniqueness of the Φ function, the function must be single-valued for $0 \leq \phi \leq 2\pi$. This condition gives a value of k_ϕ which can not be arbitrary but has to be an integer and therefore

$$k_\phi = n \qquad n = 0, 1, 2, ...$$

Whence

$$\Phi = C\cos n\phi + D\sin n\phi \tag{4.6}$$

The differential equation for the r-component,

$$\frac{d^2R}{dr^2} + \frac{1}{r}\frac{dR}{dr} + (k_r^2 - \frac{n^2}{r^2})R = 0, \tag{4.7}$$

has for its solution the cylindrical Bessel functions $j_n(k_r r)$ and the Neumann functions $Y_n(k_r r)$. The latter solution has been rejected because we require a finite solution at the origin. We will designate $k_r = \lambda$, where p_{nm} are the roots of the equation $j_n(x) = 0$ and $\lambda = p_{nm}/\alpha$ for $r = \alpha$.

Finally, the generating function can be written in the form

$$\Psi_{\substack{e\\o}\,mn}(h) = j_n(\lambda r)^{\cos}_{\sin} n\phi^{\cos}_{\sin} hz, \tag{4.8}$$

Here subscripts "*e*" stands for even and "*o*" is the odd character of the generating functions. $h = \frac{q\pi}{l}$ are the eigenvalues in the z-direction with $q = 0, 1, 2, ...$ and l is the length of cylinder. $j_n(\lambda r)$ identifies the cylindrical Bessel functions of the order n to represent both out-going and in-coming waves. λ is the continuous eigenvalue. Cylindrical vector wave functions are akin to the Debye potentials.

$$\overline{L}_{\substack{ee\\oo}n\lambda}(h) = \nabla\Psi_{\substack{ee\\oo}n}, \tag{4.9}$$

$$\overline{P}_{\substack{ee\\oo}n\lambda}(h) = \nabla\times[\Psi_{\substack{ee\\oo}n}\hat{z}], \tag{4.10}$$

$$\overline{Q}_{\substack{ee\\oo}n\lambda}(h) = \frac{1}{k_\lambda}\nabla\times\nabla\times[\Psi_{\substack{ee\\oo}n}\hat{z}]. \tag{4.11}$$

Where $\hat{z}$ is the piloting vector. To satisfy the symmetrical properties of DGF

$$\overline{Q}_{\substack{ee\\oo}n\lambda}(h) = \frac{1}{k_\lambda}\nabla\times\overline{P}_{\substack{ee\\oo}n\lambda}(h), \tag{4.12}$$

$$\overline{P}_{\substack{ee\\oo}n\lambda}(h) = \frac{1}{k_\lambda}\nabla\times\overline{Q}_{\substack{ee\\oo}n\lambda}(h). \tag{4.13}$$

Green's functions for bounded regions are usually given in the form of modal expansions. Modal series are unsuitable for use in numerical algorithms which require the computation of the electric field inside the source region. In this case, the Green's function must be computed at points $\overline{R}'$ close to $\overline{R}$, where the convergence of the series is very poor due to the singularity of $\overline{\overline{G}}_e(\overline{R}, \overline{R}')$ at point source $R = R'$. This drawback can be avoided by using expressions where a diverging term, expressed in closed form, is extracted from the modal expansion of $\overline{\overline{G}}_e(\overline{R}, \overline{R}')$, so that the remaining series represents a function finite at point source $R = R'$ Bressan [26].

The complete expressions for the solenoidal (rotational or transverse) functions are represented by

$$\overline{P}_{\substack{ee\\oo}n\lambda}(h) = \left\{ \begin{array}{c} \mp\frac{n}{r}j_n(\lambda r)^{\sin}_{\cos} n\phi^{\cos}_{\sin} hz\hat{r} \\ -(\frac{\partial j_n(\lambda r)}{\partial r})^{\cos}_{\sin} n\phi^{\cos}_{\sin} hz\hat{\phi} \\ 0 \end{array} \right\}, \tag{4.14}$$

and

$$\overline{Q}_{\substack{ee\\oo}n\lambda}(h) = \left\{ \begin{array}{c} \mp h\left[\frac{\partial j_n(\lambda r)}{\partial r}\right]^{\cos}_{\sin} n\phi^{\sin}_{\cos} hz\hat{r} \\ \frac{hn}{r}[j_n(\lambda r)]^{\sin}_{\cos} n\phi^{\sin}_{\cos} hz\hat{\phi} \\ \lambda^2[j_n(\lambda r)]^{\cos}_{\sin} n\phi^{\cos}_{\sin} hz\hat{z} \end{array} \right\} \frac{1}{k_\lambda}, \tag{4.15}$$

and the complete expressions for the non-solenoidal (irrotational or lamellar) functions are

$$\overline{L}_{\substack{ee\\oo}n\lambda}(h) = \left\{ \begin{array}{c} \frac{\partial}{\partial r}[j_n(\lambda r)]^{\cos}_{\sin} n\phi^{\cos}_{\sin} hz\hat{r} \\ \mp\frac{n}{r}[j_n(\lambda r)]^{\sin}_{\cos} n\phi^{\cos}_{\sin} hz\hat{\phi} \\ \mp h[j_n(\lambda r)]^{\cos}_{\sin} n\phi^{\sin}_{\cos} hz\hat{z} \end{array} \right\}, \tag{4.16}$$

where $k_\lambda^2 = \lambda^2 + h^2$ and in these vector wave functions one should be careful with the sign of the elements in the matrices when cross-multiplying the terms from "e" to "o" and vice-versa e.g. "sin sin" always remains negative while "cos cos" positive. Also "$-$ cos sin" and "$-$ sin cos" in second elements of matrices in $\overline{P}_{eo}$ and $\overline{P}_{oe}$ respectively. In $\overline{L}_{eo}$ and $\overline{L}_{oe}$ both "cos sin" and "sin cos" are positive in the first element of their respective matrix. For $\overline{Q}_{eo}$, "$-$ sin cos" in second element of matrix, while "$+$ cos sin" in the third element. For $\overline{Q}_{oe}$, "$-$ cos sin" and "$+$ sin cos" in the elements 2 and 3 respectively. "$\mp$" applies the negative to the top line while positive to the bottom line.

Note that in the set of cylindrical vector wave functions only $\overline{P}_{\substack{ee\\oo}n\lambda}$ do not possess the z component. The $\hat{r}$, $\hat{\phi}$ and $\hat{z}$ are the cylindrical unit vectors. These functions are defined in the entire space, corresponding to $0 \leq r \leq \infty$, $0 \leq \phi \leq 2\pi$ and $0 < z < l$.

Cylindrical vector wave functions in x and y-directions and their mutual relationships are given in Appendix A (A.2) where $\overline{P}^{(x)}_{\substack{ee\\oo}n\lambda}(h)$ and $\overline{Q}^{(x)}_{\substack{ee\\oo}n\lambda}(h)$ are derived in relation to $\overline{P}_{\substack{ee\\oo}n\lambda}(h)$ and $\overline{Q}_{\substack{ee\\oo}n\lambda}(h)$ which are the even or odd Cylindrical vector wave functions in z-direction.

$\overline{L}_{\substack{ee\\oo}n\lambda}$ functions are not required to derive the EFE of the magnetic DGF that are solenoidal and satisfy the vector wave equation, but to find the EFE of the

electric DGF, then the $\overline{L}_{ee_{oo}n\lambda}$ functions are also necessary, because $\overline{\overline{G}}_e(\overline{R},\overline{R}')$ unlike $\overline{\overline{G}}_m(\overline{R},\overline{R}')$, the DGFs of electric- and magnetic-type, respectively, is a non-solenoidal dyadic function.

The method for deriving the magnetic/electric DGF given in the following sections for cylindrical configurations used the Ohm-Rayleigh (G_m) procedure. However, there exist several alternative derivations, which will not be discussed further.

4.3 Orthogonal Properties of Vector Wave Functions for a Circular Cylinder of Finite Length

Having defined the vector wave functions, we will now investigate the orthogonal behaviour of these functions. A volume integral of the product of the cylindrical vector wave functions is clearly zero if $n \neq n'$ and $h \neq h'$ because of the orthogonal property of the $\cos n\phi$ and $\sin n\phi$ functions and the Fourier integral relation. Hence it suffices to consider the case $n = n'$ and $h = h'$, $\lambda \neq \lambda'$. The orthogonality of these functions can be shown below

$$
\begin{aligned}
I &= \iiint_V \overline{P}_{een\lambda}(h) \cdot \overline{Q}_{oon\lambda'}(h) dV \\
&= \frac{1}{k_{\lambda'}} \Bigg[\iiint_V - \frac{hn}{r} [j_n(\lambda r) \frac{\partial j_n(\lambda' r)}{\partial r} \sin^2 n\phi \cos^2 hz] \\
&\qquad\qquad - \frac{hn}{r} [j_n(\lambda' r) \frac{\partial j_n(\lambda r)}{\partial r} \cos^2 n\phi \cos^2 hz] \Bigg] dV \\
&= -\frac{(1+\delta_o^n)\pi}{k_{\lambda'}} \int_0^\infty \frac{hn}{r} r dr \int_0^l dz \cos^2 hz \\
&\qquad\qquad \cdot \left[j_n(\lambda r) \frac{\partial j_n(\lambda' r)}{\partial r} + j_n(\lambda' r) \frac{\partial j_n(\lambda r)}{\partial r} \right] \\
&= -\frac{(1+\delta_o^n)}{k_{\lambda'}} \frac{q\pi^2}{2} \\
&\qquad\qquad \cdot \int_0^\infty \frac{n}{r} \left[j_n(\lambda r) \frac{\partial j_n(\lambda' r)}{\partial r} + j_n(\lambda' r) \frac{\partial j_n(\lambda r)}{\partial r} \right] r dr \\
&= -\frac{(1+\delta_o^n)}{k_{\lambda'}} \frac{qn\pi^2}{2} \Big[j_n(\lambda r) j_n(\lambda' r) \Big]_0^\infty = 0
\end{aligned}
\tag{4.17}
$$

The proofs for the other combinations are very similar to the above solution. Such as

$$\iiint_V \overline{P}^{e_o e}_{o^e n\lambda}(h) \cdot \overline{Q}^{e_o o}_{o^o n'\lambda'}(h')dV = 0 \tag{4.18}$$

The normalization factor for these functions can be found as follows.

$$\begin{aligned} I &= \iiint_V \overline{Q}_{een\lambda}(h) \cdot \overline{Q}_{een\lambda'}(h)dV \\ &= \frac{1}{k_\lambda k_{\lambda'}} \iiint_V \Big[h^2 \frac{\partial j_n(\lambda r)}{\partial r} \frac{\partial j_n(\lambda' r)}{\partial r} \cos^2 n\phi \sin^2 hz \\ &\qquad + \frac{h^2 n^2}{r^2} j_n(\lambda r) j_n(\lambda' r) \sin^2 n\phi \sin^2 hz \\ &\qquad + \lambda^2 \lambda'^2 j_n(\lambda r) j_n(\lambda' r) \cos^2 n\phi \cos^2 hz \Big] dV, \end{aligned} \tag{4.19}$$

The integrations with respect to ϕ and z yield

$$\begin{aligned} I = \frac{(1+\delta_o^n)\pi l}{2k_\lambda k_{\lambda'}} \int_0^\infty \Big[& h^2 \frac{\partial j_n(\lambda r)}{\partial r} \frac{\partial j_n(\lambda' r)}{\partial r} \\ & + \Big(\frac{h^2 n^2}{r^2} + \lambda^2 \lambda'^2\Big) j_n(\lambda r) j_n(\lambda' r) \Big] r dr. \end{aligned} \tag{4.20}$$

Using the recurrence relations of the Bessel functions,

$$j_n(x) = \frac{x}{2n}[j_{n-1}(x) + j_{n+1}(x)] \tag{4.21}$$

$$\frac{dj_n(x)}{dx} = \frac{1}{2}[j_{n-1}(x) - j_{n+1}(x)], \tag{4.22}$$

the above integral (4.20) changes into the form

$$\begin{aligned} I = \frac{(1+\delta_o^n)\pi l}{2k_\lambda k_{\lambda'}} \int_0^\infty \Big[& \frac{1}{2}\lambda\lambda' h^2 [j_{n-1}(\lambda r) j_{n-1}(\lambda' r) \\ & + j_{n+1}(\lambda r) j_{n+1}(\lambda' r)] \\ & + \lambda^2 \lambda'^2 j_n(\lambda r) j_n(\lambda' r) \Big] r dr. \end{aligned} \tag{4.23}$$

As a result of the integral representation of the weighted delta function [19] given by

$$\frac{\delta(\lambda - \lambda')}{\lambda} = \int_0^\infty j_n(\lambda r) j_n(\lambda' r) r dr, \tag{4.24}$$

$$I = \frac{1}{2k_\lambda k_{\lambda'}} (1+\delta_o^n)\pi l(\lambda' h^2 + \lambda\lambda'^2)\delta(\lambda - \lambda') \tag{4.25}$$

Because of the presence of the delta function $\delta(\lambda - \lambda')$, it is not necessary to distinguish λ' and k' from λ and k in the coefficient in the function. Therefore

$$I = \frac{1}{2}(1 + \delta_o^n)\pi l \lambda \delta(\lambda - \lambda') \tag{4.26}$$

This is the normalization factor for the finite cylindrical vector wave functions of the same species.

The proofs for the other combinations are practically the same.

$$\iiint_V \overline{P}^{ee}_{o\,n\lambda}(h) \cdot \overline{P}^{eo}_{o\,n'\lambda'}(h) dV = \begin{cases} 0, & n \neq n' \\ or & \\ (1 + \delta_o^n)\frac{l\pi}{2}\lambda\delta(\lambda - \lambda'), & n = n' \end{cases} \tag{4.27}$$

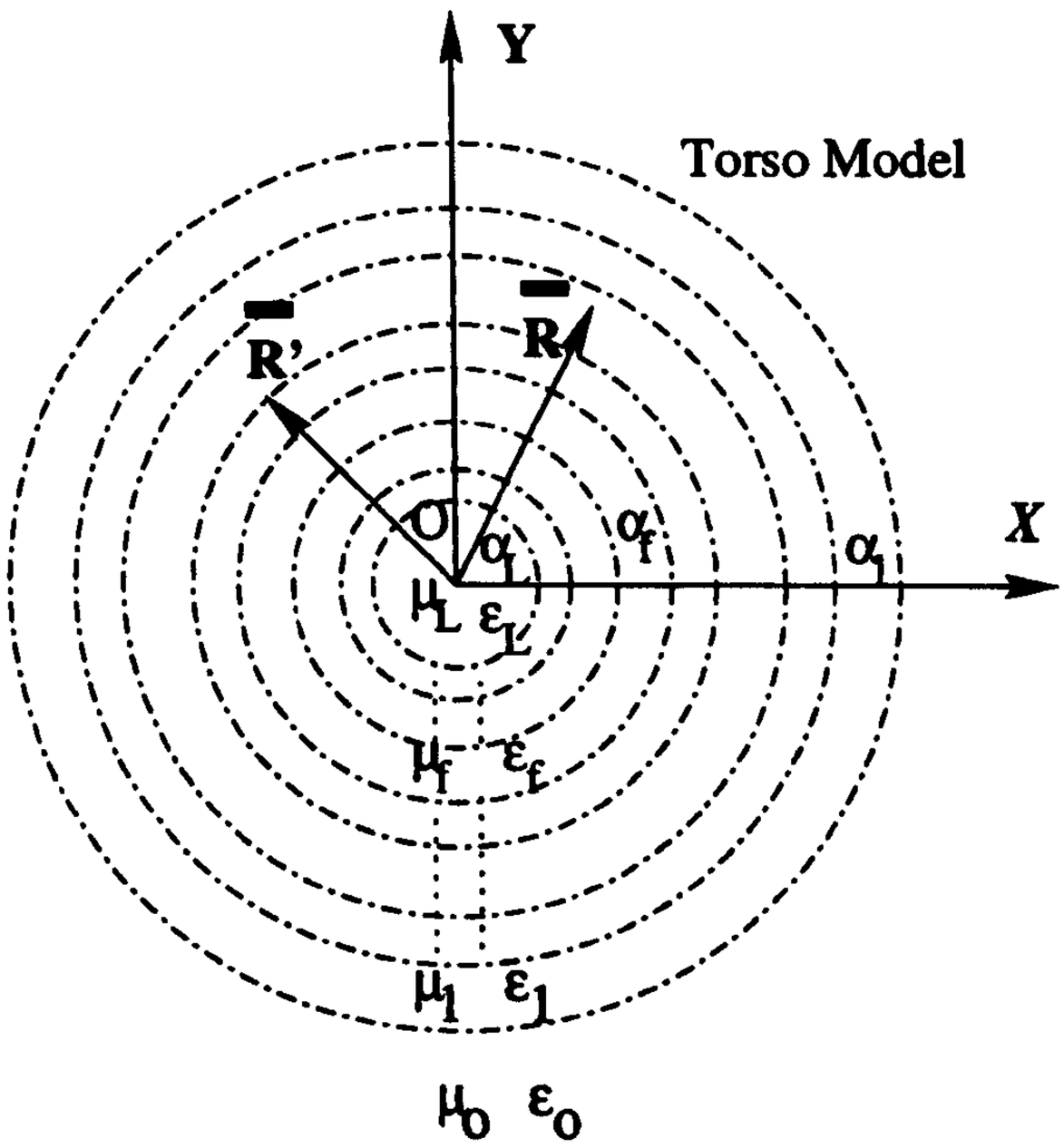

Figure 3: Cross Section of a Human Torso Model

4.4 Formulation of the Problem

Consider a torso model represented by a multilayered cylinder in Figure 2 with radii "α_f" as shown in Figure 3 concentric along z-axis with length "l" is illuminated by

an electromagnetic wave. An electromagnetic field is induced inside the system and an electromagnetic wave is scattered by the system.

A time dependence $e^{j\omega t}$ is assumed and suppressed throughout.

4.4.1 DGF for a finite Length Cylinder of Circular Cross-Section

Because the dyadic $\nabla \times [\bar{\bar{I}}\delta_e(\overline{R} - \overline{R}')]$ is solenoidal, it can be expanded in terms of solenoidal vector wave functions; $\overline{P}_{\substack{ee\\oo}n\lambda}$ and $\overline{Q}_{\substack{ee\\oo}n\lambda}$ defined previously.

Applying the method of (G_m) and according to the Ohm-Rayleigh procedure, an EFE for the source function $\nabla \times [\bar{\bar{I}}\delta_e(\overline{R} - \overline{R}')]$ using the solenoidal vector wave functions. Thus we let

$$\nabla \times [\bar{\bar{I}}\delta_e(\overline{R} - \overline{R}')] = \int_0^\infty d\lambda \int_0^l dh \sum_{n=0}^\infty \begin{bmatrix} \overline{Q}_{\substack{eo\\o}n\lambda}(h)\overline{A}_{\substack{eo\\o}n\lambda}(h) \\ \overline{P}_{\substack{ee\\o}n\lambda}(h)\overline{B}_{\substack{ee\\o}n\lambda}(h) \end{bmatrix}, \tag{4.28}$$

where λ and h are continuous eigenvalues and $\overline{A}_{\substack{eo\\o}n\lambda}(h)$ and $\overline{B}_{\substack{ee\\o}n\lambda}(h)$ are two unknown vector functions to be determined. This is a three-dimensional problem with a dyadic singular function, therefore the above equation can be treated as the Fourier transform and the Fourier-Bessel transform or the Hankel transform of $\nabla \times [\bar{\bar{I}}\delta_e(\overline{R} - \overline{R}')]$. By taking the anterior scalar product of the above equation with $\overline{Q}_{\substack{eo\\o}n'\lambda'}(h')$ and integrating the resultant equation through the entire space and as a result of the orthogonal relationships and repeating the same routine with the $\overline{P}_{\substack{ee\\o}n'\lambda'}(h')$ we obtain the EFE,

$$\nabla \times [\bar{\bar{I}}\delta_e(\overline{R} - \overline{R}')] = \int_0^\infty d\lambda \int_0^l dh \sum_{n=0}^\infty Ck_\lambda \cdot \begin{bmatrix} \overline{Q}_{\substack{eo\\o}n\lambda}(h)\overline{P}'_{\substack{eo\\o}n\lambda}(h) \\ \overline{P}_{\substack{ee\\o}n\lambda}(h)\overline{Q}'_{\substack{ee\\o}n\lambda}(h) \end{bmatrix}, \tag{4.29}$$

here,

$$C = \frac{(2 - \delta_o^n)}{l\pi\lambda} \tag{4.30}$$

Where the primed functions are defined with respect to the primed variables r', ϕ' and z' pertaining to the position vector $\overline{R}'$.

The DGF of the magnetic type satisfy the differential relation

$$\nabla\times\nabla\times\overline{\overline{G}}_{m2}(\overline{R},\overline{R}')-k^2\overline{\overline{G}}_{m2}(\overline{R},\overline{R}')=\nabla\times[\overline{\overline{I}}\delta_e(\overline{R}-\overline{R}')]. \tag{4.31}$$

In view of the above relation (4.31), the EFE of $\overline{\overline{G}}_{m2}(\overline{R},\overline{R}')$, therefore is given by

$$\overline{\overline{G}}_{m2}(\overline{R},\overline{R}')=\int_0^\infty d\lambda\int_0^l dh\sum_{n=0}^\infty C\frac{k_\lambda}{k_\lambda^2-k^2}\cdot\begin{bmatrix}\overline{Q}_{o^{e^o}n\lambda}(h)\overline{P}'_{o^{e^o}n\lambda}(h)\\ \overline{P}_{o^{e^e}n\lambda}(h)\overline{Q}'_{o^{e^e}n\lambda}(h)\end{bmatrix}, \tag{4.32}$$

To perform the integration with respect to λ in (4.32) we can write the dyadics in an operational form provided $\frac{\overline{\overline{T}}_\lambda}{\lambda}$ has no poles in λ-plane. Thus we have

$$\overline{Q}_{o^{e^o}n\lambda}(h)\overline{P}'_{o^{e^o}n\lambda}(h)=\overline{\overline{T}}_\lambda[j_n(\lambda r)j_n(\lambda r')] \tag{4.33}$$

$\overline{\overline{T}}_\lambda$ represents a dyadic spatial operator.

$$\int_0^\infty\frac{k_\lambda\overline{Q}_{o^{e^o}n\lambda}(h)\overline{P}'_{o^{e^o}n\lambda}(h)}{\lambda(k_\lambda^2-k^2)}d\lambda=\int_0^\infty\frac{k_\lambda\overline{\overline{T}}_\lambda[j_n(\lambda r)j_n(\lambda r')]}{\lambda(k_\lambda^2-k^2)}d\lambda \tag{4.34}$$

where $\lambda^2=(k_\lambda^2-h^2)$

$$\begin{aligned}\frac{ik\pi}{2\eta_o^2}&\begin{cases}\overline{\overline{T}}_{\eta_o}[H_n^{(1)}(\eta_o r)j_n(\eta_o r')], & r>r',\\ \overline{\overline{T}}_{\eta_o}[j_n(\eta_o r)H_n^{(1)}(\eta_o r')], & r<r'.\end{cases}\\ =\frac{ik\pi}{2\eta_o^2}&\begin{cases}[\overline{Q}^{(1)}_{o^{e^o}\eta_o}(h)\overline{P}'_{o^{e^o}\eta_o}(h)], & r>r',\\ [\overline{Q}_{o^{e^o}\eta_o}(h)\overline{P}'^{(1)}_{o^{e^o}\eta_o}(h)], & r<r'.\end{cases}\end{aligned} \tag{4.35}$$

here $\eta_o^2=(k^2-h^2)$ and the superscript "1" in $\overline{P}^{(1)}_{\substack{ee\\oo}n\eta_o}(h;\eta_o)$ and $\overline{Q}^{(1)}_{\substack{ee\\oo}n\eta_o}(h;\eta_o)$, $\overline{P}'^{(1)}_{\substack{ee\\oo}n\eta_o}(h;\eta_o)$ and $\overline{Q}'^{(1)}_{\substack{ee\\oo}n\eta_o}(h;\eta_o)$ is present to indicate the substitution of cylindrical Hankel function of the first kind (cylindrical Bessel functions of the third kind) "$H_n^{(1)}(\eta_o r)$" for "$j_n(\eta_o r)$" in the generating function $\Psi^{(1)}_{\substack{ee\\oo}n}$.

$$\Psi^{(1)}_{\substack{ee\\oo}n}(h)=H_n^{(1)}(\eta_o r)^{\cos}_{\sin}n\phi^{\cos}_{\sin}hz, \tag{4.36}$$

$$\Psi'^{(1)}_{\substack{ee\\oo}n}(h)=H_n^{(1)}(\eta_o r')^{\cos}_{\sin}n\phi'^{\cos}_{\sin}hz', \tag{4.37}$$

These functions are now defined with respect to the cylindrical Hankel function of the first kind;

$$\overline{Q}^{(1)}_{\substack{ee\\oo}n\eta_o}(h;\eta_o) = \frac{1}{k_\lambda}\nabla\times\nabla\times[\Psi^{(1)}_{\substack{ee\\oo}n}\hat{z}], \tag{4.38}$$

$$\overline{P}'^{(1)}_{\substack{ee\\oo}n\eta_o}(h;\eta_o) = \nabla'\times[\Psi'^{(1)}_{\substack{ee\\oo}n}\hat{z}]. \tag{4.39}$$

The Fourier integration in the equation (4.32) can be evaluated in a closed form by the method of contour integration with the aid of residue theorem in the h-plane. The final expression for the equation (4.32) is given by

$$\overline{\overline{G}}^{\pm}_{m2}(\overline{R},\overline{R}') = \int_0^l dh \sum_{n=0}^{\infty} C_\lambda k \cdot \begin{cases} \left\{ \begin{array}{l} [\overline{Q}^{(1)}_{\substack{eo\\oe}\eta_o}(h;\eta_o)\overline{P}'_{\substack{eo\\oe}\eta_o}(h;\eta_o)] \\ [\overline{P}^{(1)}_{\substack{ee\\oo}\eta_o}(h;\eta_o)\overline{Q}'_{\substack{ee\\oo}\eta_o}(h;\eta_o)] \end{array} \right\}, & r > r', \\ \left\{ \begin{array}{l} [\overline{Q}_{\substack{eo\\oe}\eta_o}(h;\eta_o)\overline{P}'^{(1)}_{\substack{eo\\oe}\eta_o}(h;\eta_o)] \\ [\overline{P}_{\substack{ee\\oo}\eta_o}(h;\eta_o)\overline{Q}'^{(1)}_{\substack{ee\\oo}\eta_o}(h;\eta_o)] \end{array} \right\}, & r < r'. \end{cases} \tag{4.40}$$

Where we have preserved the Fourier integration. The plane of discontinuity for the magnetic DGF is located at $r = r'$.

$$C_\lambda = \frac{i(2-\delta^n_o)}{2l\eta_o^2} \tag{4.41}$$

Coefficient C_λ depends on the value of δ^n_o which is the Kronecker delta function defined with respect to n, when

$$\delta^n_o = \begin{cases} 1, & \text{if } n = o \\ 0, & \text{if } n \neq o \end{cases} \tag{4.42}$$

By means of method of (G_m) the expression for $(\overline{\overline{G}}_{e1})$ for a finite cylinder of

radius "α" concentric with the z-axis can now be written in the form

$$\overline{\overline{G}}_{e1}(\overline{R},\overline{R}') = -\frac{\hat{r}\hat{r}}{k^2}\delta_e(\overline{R}-\overline{R}') + \int_0^l dh \sum_{n=0}^{\infty} C_\lambda$$

$$\cdot \begin{cases} \left\{ \begin{array}{l} [\overline{P}^{(1)}_{\substack{e_o \\ o_e}\eta_o}(h;\eta_o)\overline{P}'_{\substack{e_o \\ o_e}\eta_o}(h;\eta_o)] \\ [\overline{Q}^{(1)}_{\substack{e_e \\ o_o}\eta_o}(h;\eta_o)\overline{Q}'_{\substack{e_e \\ o_o}\eta_o}(h;\eta_o)] \end{array} \right\}, & r > r', \\ \left\{ \begin{array}{l} [\overline{P}_{\substack{e_o \\ o_e}\eta_o}(h;\eta_o)\overline{P}'^{(1)}_{\substack{e_o \\ o_e}\eta_o}(h;\eta_o)] \\ [\overline{Q}_{\substack{e_e \\ o_o}\eta_o}(h;\eta_o)\overline{Q}'^{(1)}_{\substack{e_e \\ o_o}\eta_o}(h;\eta_o)] \end{array} \right\}, & r < r'. \end{cases} \tag{4.43}$$

Comparing the DGFs for a finite cylinder developed here with those presented by other authors e.g. Tai [19] for an infinite cylinder, one can notice that they are similar in mathematical form but different in the calculations of Ps and Qs and the limits of integration for a finite cylinder.

Here $\hat{r}\hat{r}$ is a dyad (dyadic product of the unit vectors) and $\delta(\overline{R}-\overline{R}')$ is weighted Dirac delta function in three dimensions. This is included explicitly as a correction to the general solenoidal EFE which is valid outside the source point. The dyadic delta function term at the source point in cylindrical coordinates

$$\delta(\overline{R}-\overline{R}') = \frac{1}{r'}\delta(\overline{r}-\overline{r}')\delta(\overline{\phi}-\overline{\phi}')\delta(\overline{z}-\overline{z}') \tag{4.44}$$

4.4.2 Scattering DGFs for an Electric Dipole in the Presence of Cylindrical Torso Model i.e. a Dielectric Cylinder of Circular Cross-Section of Finite Length

When a biological system is illuminated by an electromagnetic wave, an electromagnetic field is induced inside the system and an electromagnetic wave is scattered externally by the system. Since the biological system is an irregularly shaped heterogeneous imperfectly conducting medium with frequency dependent permittivity and conductivity, the distribution of the internal electromagnetic field and the scattered electromagnetic wave will depend on the body's physiological parameters and

geometry, as well as the frequency and polarization of the incident wave. The mathematical complexity of the problem has led researchers to investigate simple models. In this chapter the medium is assumed to be homogeneous, isotropic, linear, non-dispersive and stationary.

Having expressed the DGF for a medium in terms of finite cylindrical vector wave functions, we may now use that result to set up the scattered terms for the cylinder of finite length for a cylindrical torso model.

DGF for a Single-layer Cylindrical Torso Model

This can be considered as the contribution of the reflections and transmissions of a single-layer cylinder of radius α_1 concentric along z-axis with length "l" centered at O, superimposed in an unbounded homogeneous medium with the radiation source located outside the cylinder at R'. The medium is characterized by (μ_o, ε_o), and material properties of the cylinder are represented by $(\mu_{t1}, \varepsilon_{t1})$, where subscripts "$o$" and "$t$" stand for unbounded (open) space and torso, respectively.

The Scattered DGF term for the exterior of torso in this case has the form

$$\overline{\overline{G}}_{es}^{10o}(\overline{R},\overline{R}') = \int_0^l dh \sum_{n=0}^{\infty} C_\lambda \left\{ \begin{array}{l} [A_{\substack{e_o o \\ o}}^{10o}{}_{\eta_o} \overline{P}_{\substack{e_o o \\ o}}^{(1)}{}_{\eta_o}(h;\eta_o) + B_{\substack{o_o o \\ e}}^{10o}{}_{\eta_o} \overline{Q}_{\substack{o_o o \\ e}}^{(1)}{}_{\eta_o}(h;\eta_o)]\overline{P}'^{(1)}_{\substack{e_o o \\ o}}{}_{\eta_o}(h;\eta_o) \\ [C_{\substack{e_e o \\ o}}^{10o}{}_{\eta_o} \overline{Q}_{\substack{e_e o \\ o}}^{(1)}{}_{\eta_o}(h;\eta_o) + D_{\substack{o_e o \\ e}}^{10o}{}_{\eta_o} \overline{P}_{\substack{o_e o \\ e}}^{(1)}{}_{\eta_o}(h;\eta_o)]\overline{Q}'^{(1)}_{\substack{e_e o \\ o}}{}_{\eta_o}(h;\eta_o) \end{array} \right\}, \tag{4.45}$$

and for the interior region,

$$\overline{\overline{G}}_{es}^{11o}(\overline{R},\overline{R}') = \int_0^l dh \sum_{n=0}^{\infty} C_\lambda \left\{ \begin{array}{l} [a_{\substack{e_o o \\ o}}^{10o}{}_{\eta_1} \overline{P}_{\substack{e_o o \\ o}}{}_{\eta_1}(h;\eta_1) + b_{\substack{o_o o \\ e}}^{10o}{}_{\eta_1} \overline{Q}_{\substack{o_o o \\ e}}{}_{\eta_1}(h;\eta_1)]\overline{P}'^{(1)}_{\substack{e_o o \\ o}}{}_{\eta_o}(h;\eta_o) \\ [c_{\substack{e_e o \\ o}}^{10o}{}_{\eta_1} \overline{Q}_{\substack{e_e o \\ o}}{}_{\eta_1}(h;\eta_1) + d_{\substack{o_e o \\ e}}^{10o}{}_{\eta_1} \overline{P}_{\substack{o_e o \\ e}}{}_{\eta_1}(h;\eta_1)]\overline{Q}'^{(1)}_{\substack{e_e o \\ o}}{}_{\eta_o}(h;\eta_o) \end{array} \right\}. \tag{4.46}$$

Where the first number of triple superscripts signifies the last inner layer in the model and the second number identifies the region where the function is defined, that is the observation or field point, and the third number corresponds to the location

of the source, i.e., the source point, which in this case denotes by the letter "o". Subscript η_1 attribute the coefficients to the observer layer.

The choice of $\overline{P}^{(1)}_{\substack{ee\\oo}\eta_o}(h;\eta_o)$ and $\overline{Q}^{(1)}_{\substack{ee\\oo}\eta_o}(h;\eta_o)$ as the field functions in $\overline{\overline{G}}^{10o}_{es}(\overline{R},\overline{R}')$ is dictated by the radiation condition that the scattered field must consist of outgoing waves, and the choice of $\overline{P}'^{(1)}_{\substack{ee\\oo}\eta_o}(h;\eta_o)$ and $\overline{Q}'^{(1)}_{\substack{ee\\oo}\eta_o}(h;\eta_o)$ as the excitation functions is guided by the expression for $\overline{\overline{G}}_{e1}(\overline{R},\overline{R}')$ and the boundary condition that at $r=\alpha_1$, $\overline{\overline{G}}^{Lfo}_{e}(\overline{R},\overline{R}')$ must satisfy the Dirichlet boundary condition which can be satisfied only if the excitation functions are the same as that of $\overline{\overline{G}}_{e1}(\overline{R},\overline{R}')$ for $r<r'$.

The field functions for $\overline{\overline{G}}^{11o}_{es}(\overline{R},\overline{R}')$ are so chosen because they are the solutions for the vector wave equation in region 1, and they must be finite like that of $\overline{\overline{G}}_{e1}(\overline{R},\overline{R}')$ for $r<r'$.

Also the expanded version of a typical combination in DGF can be written in the form

$$[A^{10o}_{\substack{eo\\oe}\eta_o}\overline{P}^{(1)}_{\substack{eo\\oe}\eta_o}(h;\eta_o)+B^{10o}_{\substack{oo\\ee}\eta_o}\overline{Q}^{(1)}_{\substack{oo\\ee}\eta_o}(h;\eta_o)]\overline{P}'^{(1)}_{\substack{eo\\oe}\eta_o}(h;\eta_o)=$$
$$\left\{\begin{array}{l}[A^{10o}_{eo\eta_o}\overline{P}^{(1)}_{eo\eta_o}(h;\eta_o)+B^{10o}_{oo\eta_o}\overline{Q}^{(1)}_{oo\eta_o}(h;\eta_o)]\overline{P}'^{(1)}_{eo\eta_o}(h;\eta_o)\\ [A^{10o}_{oo\eta_o}\overline{P}^{(1)}_{oo\eta_o}(h;\eta_o)+B^{10o}_{eo\eta_o}\overline{Q}^{(1)}_{eo\eta_o}(h;\eta_o)]\overline{P}'^{(1)}_{oo\eta_o}(h;\eta_o)\end{array}\right\}. \quad (4.47)$$

Double-layer Cylindrical Torso model

We consider two concentric cylinders centered at O, superimposed by an unbounded homogeneous medium with the current distribution source located outside the cylinder at R'. The medium is characterized by (μ_o,ϵ_o), and material properties of the outer cylinder are represented by (μ_{t1},ϵ_{t1}) and those of the inner cylinder by (μ_{t2},ϵ_{t2}). The radii of outer to inner cylinders are α_1 and α_2, respectively.

In this case the Scattered DGFs terms can be shown by

$$\overline{\overline{G}}^{20o}_{es}(\overline{R},\overline{R}')=\int_0^l dh\sum_{n=0}^{\infty}C_\lambda$$
$$\left\{\begin{array}{l}[A^{20o}_{\substack{eo\\oe}\eta_o}\overline{P}^{(1)}_{\substack{eo\\oe}\eta_o}(h;\eta_o)+B^{20o}_{\substack{oo\\ee}\eta_o}\overline{Q}^{(1)}_{\substack{oo\\ee}\eta_o}(h;\eta_o)]\overline{P}'^{(1)}_{\substack{eo\\oe}\eta_o}(h;\eta_o)\\ [C^{20o}_{\substack{ee\\oo}\eta_o}\overline{Q}^{(1)}_{\substack{ee\\oo}\eta_o}(h;\eta_o)+D^{20o}_{\substack{oe\\eo}\eta_o}\overline{P}^{(1)}_{\substack{oe\\eo}\eta_o}(h;\eta_o)]\overline{Q}'^{(1)}_{\substack{ee\\oo}\eta_o}(h;\eta_o)\end{array}\right\}, \quad (4.48)$$

$$\overline{\overline{G}}_{es}^{21o}(\overline{R},\overline{R}') = \int_0^l dh \sum_{n=0}^{\infty} C_\lambda \left\{ \begin{array}{l} \left[\begin{array}{l} A_{\substack{e^o \\ o^o}\eta_1}^{21o} \overline{P}_{\substack{e^o \\ o^o}\eta_1}^{(1)}(h;\eta_1) + B_{\substack{o^o \\ e^o}\eta_1}^{21o} \overline{Q}_{\substack{o^o \\ e^o}\eta_1}^{(1)}(h;\eta_1) \\ a_{\substack{e^o \\ o^o}\eta_1}^{21o} \overline{P}_{\substack{e^o \\ o^o}\eta_1}(h;\eta_1) + b_{\substack{o^o \\ e^o}\eta_1}^{21o} \overline{Q}_{\substack{o^o \\ e^o}\eta_1}(h;\eta_1) \end{array} \right] \overline{P}'^{(1)}_{\substack{e^o \\ o^o}\eta_o}(h;\eta_o) \\ \\ \left[\begin{array}{l} C_{\substack{e^e \\ o^e}\eta_1}^{21o} \overline{Q}_{\substack{e^e \\ o^e}\eta_1}^{(1)}(h;\eta_1) + D_{\substack{o^e \\ e^e}\eta_1}^{21o} \overline{P}_{\substack{o^e \\ e^e}\eta_1}^{(1)}(h;\eta_1) \\ c_{\substack{e^e \\ o^e}\eta_1}^{21o} \overline{Q}_{\substack{e^e \\ o^e}\eta_1}(h;\eta_1) + d_{\substack{o^e \\ e^e}\eta_1}^{21o} \overline{P}_{\substack{o^e \\ e^e}\eta_1}(h;\eta_1) \end{array} \right] \overline{Q}'^{(1)}_{\substack{e^e \\ o^e}\eta_o}(h;\eta_o) \end{array} \right\}, \tag{4.49}$$

and the final inner layer gives

$$\overline{\overline{G}}_{es}^{22o}(\overline{R},\overline{R}') = \int_0^l dh \sum_{n=0}^{\infty} C_\lambda \left\{ \begin{array}{l} [a_{\substack{e^o \\ o^o}\eta_2}^{22o} \overline{P}_{\substack{e^o \\ o^o}\eta_2}(h;\eta_2) + b_{\substack{o^o \\ e^o}\eta_2}^{22o} \overline{Q}_{\substack{o^o \\ e^o}\eta_2}(h;\eta_2)] \overline{P}'^{(1)}_{\substack{e^o \\ o^o}\eta_o}(h;\eta_o) \\ [c_{\substack{e^e \\ o^e}\eta_2}^{22o} \overline{Q}_{\substack{e^e \\ o^e}\eta_2}(h;\eta_2) + d_{\substack{o^e \\ e^e}\eta_2}^{22o} \overline{P}_{\substack{o^e \\ e^e}\eta_2}(h;\eta_2)] \overline{Q}'^{(1)}_{\substack{e^e \\ o^e}\eta_o}(h;\eta_o) \end{array} \right\}. \tag{4.50}$$

The choice of the field and excitation functions in $\overline{\overline{G}}_{es}^{21o}(\overline{R},\overline{R}')$ are governed by the fact that the electromagnetic fields consist of wave-modes propagating outwards and inwards. Therefore,

$$\overline{\overline{G}}_{es}^{21o} = \alpha \cdot \overline{\overline{G}}_{es}^{20o} + \beta \cdot \overline{\overline{G}}_{es}^{22o}. \tag{4.51}$$

Trilayer Cylindrical Torso Model

In this case three concentric cylinders centered at O, superimposed by an unbounded homogeneous medium with the radiation source located outside the cylinder at R' are considered. The material properties of the outer to inner cylinders are represented by $(\mu_{t1},\varepsilon_{t1})$, $(\mu_{t2},\varepsilon_{t2})$, and $(\mu_{t3},\varepsilon_{t3})$, respectively. The radii of outer to inner cylinders are α_1, α_2, and α_3, respectively.

The Scattered DGF terms for $\overline{\overline{G}}_{es}^{30o}$ and $\overline{\overline{G}}_{es}^{31o}$ are the same as those in the last section, and the rest can be expressed by

e.g. for the middle layer,

$$\overline{\overline{G}}^{32o}_{es}(\overline{R},\overline{R}') = \int_0^l dh \sum_{n=0}^{\infty} C_\lambda \left\{ \begin{array}{l} \left[A^{32o}_{\substack{eo\\ o}\eta_2} \overline{P}^{(1)}_{\substack{eo\\ o}\eta_2}(h;\eta_2) + B^{32o}_{\substack{oo\\ e}\eta_2} \overline{Q}^{(1)}_{\substack{oo\\ e}\eta_2}(h;\eta_2) \right] \overline{P}'^{(1)}_{\substack{eo\\ o}\eta_o}(h;\eta_o) \\ \\ \left[C^{32o}_{\substack{ee\\ o}\eta_2} \overline{Q}^{(1)}_{\substack{ee\\ o}\eta_2}(h;\eta_2) + D^{32o}_{\substack{oe\\ e}\eta_2} \overline{P}^{(1)}_{\substack{oe\\ e}\eta_2}(h;\eta_2) \right] \overline{Q}'^{(1)}_{\substack{ee\\ o}\eta_o}(h;\eta_o) \end{array} \right\}, \tag{4.52}$$

and for the inner layer,

$$\overline{\overline{G}}^{33o}_{es}(\overline{R},\overline{R}') = \int_0^l dh \sum_{n=0}^{\infty} C_\lambda \left\{ \begin{array}{l} [a^{33o}_{\substack{eo\\ o}\eta_3} \overline{P}_{\substack{eo\\ o}\eta_3}(h;\eta_3) + b^{33o}_{\substack{oo\\ e}\eta_3} \overline{Q}_{\substack{oo\\ e}\eta_3}(h;\eta_3)] \overline{P}'^{(1)}_{\substack{eo\\ o}\eta_o}(h;\eta_o) \\ [c^{33o}_{\substack{ee\\ o}\eta_3} \overline{Q}_{\substack{ee\\ o}\eta_3}(h;\eta_3) + d^{33o}_{\substack{oe\\ e}\eta_3} \overline{P}_{\substack{oe\\ e}\eta_3}(h;\eta_3)] \overline{Q}'^{(1)}_{\substack{ee\\ o}\eta_o}(h;\eta_o) \end{array} \right\}. \tag{4.53}$$

Quad-layer Cylindrical Torso Model

Similarly, the case of four concentric cylinders centered at O, superimposed by an unbounded homogeneous medium with the dipole source of radiation located outside the cylinder at R' is considered. The material properties of the outer to inner cylinders are, respectively, represented by $(\mu_{t1},\varepsilon_{t1})$, $(\mu_{t2},\varepsilon_{t2})$, $(\mu_{t3},\varepsilon_{t3})$, and $(\mu_{t4},\varepsilon_{t4})$. The radii of outer to inner cylinders are α_1, α_2, α_3, and α_4 respectively.

The scattered DGFs terms for $\overline{\overline{G}}^{40o}_{es}$, $\overline{\overline{G}}^{41o}_{es}$, and $\overline{\overline{G}}^{42o}_{es}$ are the same as those in the previous section and the rest can be presented by

$$\overline{\overline{G}}^{43o}_{es}(\overline{R},\overline{R}') = \int_0^l dh \sum_{n=0}^{\infty} C_\lambda \left\{ \begin{array}{l} \left[A^{43o}_{\substack{eo\\ o}\eta_3} \overline{P}^{(1)}_{\substack{eo\\ o}\eta_3}(h;\eta_3) + B^{43o}_{\substack{oo\\ e}\eta_3} \overline{Q}^{(1)}_{\substack{oo\\ e}\eta_3}(h;\eta_3) \right] \overline{P}'^{(1)}_{\substack{eo\\ o}\eta_o}(h;\eta_o) \\ \\ \left[C^{43o}_{\substack{ee\\ o}\eta_3} \overline{Q}^{(1)}_{\substack{ee\\ o}\eta_3}(h;\eta_3) + D^{43o}_{\substack{oe\\ e}\eta_3} \overline{P}^{(1)}_{\substack{oe\\ e}\eta_3}(h;\eta_3) \right] \overline{Q}'^{(1)}_{\substack{ee\\ o}\eta_o}(h;\eta_o) \end{array} \right\}. \tag{4.54}$$

The final inner layer gives

$$\overline{\overline{G}}_{es}^{44o}(\overline{R},\overline{R}') = \int_0^l dh \sum_{n=0}^{\infty} C_\lambda \left\{ \begin{array}{l} [a_{\substack{e_o e_o \\ o_o \eta_4}}^{44o} \overline{P}_{\substack{e_o \\ o_o}\eta_4}(h;\eta_4) + b_{\substack{o_o e_o \\ e_o \eta_4}}^{44o} \overline{Q}_{\substack{o_o \\ e_o}\eta_4}(h;\eta_4)] \overline{P}'^{(1)}_{\substack{e_o e_o \\ o_o \eta_o}}(h;\eta_o) \\ [c_{\substack{e_e e_o \\ o_e \eta_4}}^{44o} \overline{Q}_{\substack{e_e \\ o_e}\eta_4}(h;\eta_4) + d_{\substack{o_e e_o \\ e_e \eta_4}}^{44o} \overline{P}_{\substack{o_e \\ e_e}\eta_4}(h;\eta_4)] \overline{Q}'^{(1)}_{\substack{e_e e_o \\ o_e \eta_o}}(h;\eta_o) \end{array} \right\}. \tag{4.55}$$

4.4.3 General Expression of Scattering DGFs for an Electric Dipole in the Presence of a Multilayered Cylindrical Torso Model

Observation and analysis of the above expressions for the scattering equations (4.45) to (4.55) allows an efficient formulation of the general scattering dyadic Green's function (DGF) for a multilayer cylindrical torso (Figure 3) as:

$$\overline{\overline{G}}_{es}^{Lfo}(\overline{R},\overline{R}') = \int_0^l dh \sum_{n=0}^{\infty} C_\lambda \cdot \left\{ \begin{array}{l} \left\{ \begin{array}{l} (1-\delta_f^L) \begin{bmatrix} A_{\substack{e_o e_o \\ o_o \eta_f}}^{Lfo} \overline{P}_{\substack{e_o \\ o_o}\eta_f}^{(1)}(h;\eta_f) \\ B_{\substack{o_o e_o \\ e_o \eta_f}}^{Lfo} \overline{Q}_{\substack{o_o \\ e_o}\eta_f}^{(1)}(h;\eta_f) \end{bmatrix} \\ (1-\delta_f^o) \begin{bmatrix} a_{\substack{e_o e_o \\ o_o \eta_f}}^{Lfo} \overline{P}_{\substack{e_o \\ o_o}\eta_f}(h;\eta_f) \\ b_{\substack{o_o e_o \\ e_o \eta_f}}^{Lfo} \overline{Q}_{\substack{o_o \\ e_o}\eta_f}(h;\eta_f) \end{bmatrix} \end{array} \right\} \overline{P}'^{(1)}_{\substack{e_o e_o \\ o_o \eta_o}}(h;\eta_o) \\ \left\{ \begin{array}{l} (1-\delta_f^L) \begin{bmatrix} C_{\substack{e_e e_o \\ o_e \eta_f}}^{Lfo} \overline{Q}_{\substack{e_e \\ o_e}\eta_f}^{(1)}(h;\eta_f) \\ D_{\substack{o_e e_o \\ e_e \eta_f}}^{Lfo} \overline{P}_{\substack{o_e \\ e_e}\eta_f}^{(1)}(h;\eta_f) \end{bmatrix} \\ (1-\delta_f^o) \begin{bmatrix} c_{\substack{e_e e_o \\ o_e \eta_f}}^{Lfo} \overline{Q}_{\substack{e_e \\ o_e}\eta_f}(h;\eta_f) \\ d_{\substack{o_e e_o \\ e_e \eta_f}}^{Lfo} \overline{P}_{\substack{o_e \\ e_e}\eta_f}(h;\eta_f) \end{bmatrix} \end{array} \right\} \overline{Q}'^{(1)}_{\substack{e_e e_o \\ o_e \eta_o}}(h;\eta_o) \end{array} \right\}. \tag{4.56}$$

Where $k_f^2 = \omega^2(\mu_f \epsilon_f)$ and $\eta_f^2 = (k_f^2 - h^2)$.

For the general case, when the current source is located in different layers of the

media, one obtains a different general expression of DGF.

$$\overline{\overline{G}}_{es}^{Lfso}(\overline{R},\overline{R}') = \int_0^l dh \sum_{n=0}^{\infty} C_\lambda$$

$$\left\{ \begin{array}{l} \left\{ \begin{array}{l} (1-\delta_f^L)\begin{bmatrix} A^{Lfo}_{\substack{e^o\\o^o}\eta_f}\,\overline{P}^{(1)}_{\substack{e^o\\o^o}\eta_f}(h;\eta_f) \\ B^{Lfo}_{\substack{o^o\\e^o}\eta_f}\,\overline{Q}^{(1)}_{\substack{o^o\\e^o}\eta_f}(h;\eta_f) \end{bmatrix} \\ (1-\delta_f^o)\begin{bmatrix} a^{Lfo}_{\substack{e^o\\o^o}\eta_f}\,\overline{P}_{\substack{e^o\\o^o}\eta_f}(h;\eta_f) \\ b^{Lfo}_{\substack{o^o\\e^o}\eta_f}\,\overline{Q}_{\substack{o^o\\e^o}\eta_f}(h;\eta_f) \end{bmatrix} \end{array} \right\} \begin{bmatrix} (1-\delta_s^L)\overline{P}'^{(1)}_{\substack{e^o\\o^o}\eta_s}(h;\eta_s) \\ (1-\delta_s^o)\overline{P}'_{\substack{e^o\\o^o}\eta_s}(h;\eta_s) \end{bmatrix} \\ \\ \left\{ \begin{array}{l} (1-\delta_f^L)\begin{bmatrix} C^{Lfo}_{\substack{e^e\\o^e}\eta_f}\,\overline{Q}^{(1)}_{\substack{e^e\\o^e}\eta_f}(h;\eta_f) \\ D^{Lfo}_{\substack{o^e\\e^e}\eta_f}\,\overline{P}^{(1)}_{\substack{o^e\\e^e}\eta_f}(h;\eta_f) \end{bmatrix} \\ (1-\delta_f^o)\begin{bmatrix} c^{Lfo}_{\substack{e^e\\o^e}\eta_f}\,\overline{Q}_{\substack{e^e\\o^e}\eta_f}(h;\eta_f) \\ d^{Lfo}_{\substack{o^e\\e^e}\eta_f}\,\overline{P}_{\substack{o^e\\e^e}\eta_f}(h;\eta_f) \end{bmatrix} \end{array} \right\} \begin{bmatrix} (1-\delta_s^L)\overline{Q}'^{(1)}_{\substack{e^e\\o^e}\eta_s}(h;\eta_s) \\ (1-\delta_s^o)\overline{Q}'_{\substack{e^o\\o^o}\eta_s}(h;\eta_s) \end{bmatrix} \end{array} \right\}. \tag{4.57}$$

"L" is the symbol for last inner layer in the torso; "f", $(f = 0, 1, 2, ..., L)$ is the field point or observer layer. Superscript/subscript "o" stands for source point at open space. Subscript "s" is scattering, while its superscript represents the layer at which the source is located.

δ_f^L and δ_f^o are the Kronecker delta functions, where

$$\delta = \begin{cases} 1, & \text{if } L/o = f \\ 0, & \text{if } L/o \neq f \end{cases}. \tag{4.58}$$

$A^{Lfo}_{\substack{e^o\\o^o}\eta_f}$, $a^{Lfo}_{\substack{e^o\\o^o}\eta_f}$, $B^{Lfo}_{\substack{o^o\\e^o}\eta_f}$, $b^{Lfo}_{\substack{o^o\\e^o}\eta_f}$, $C^{Lfo}_{\substack{e^e\\o^e}\eta_f}$, $c^{Lfo}_{\substack{e^e\\o^e}\eta_f}$, $D^{Lfo}_{\substack{o^e\\e^e}\eta_f}$, and $d^{Lfo}_{\substack{o^e\\e^e}\eta_f}$ are the amplitude coefficients of scattered DGF to be determined by applying the boundary condition at the

interfaces $r = \alpha_l$, $(l = 1, 2, ..., L)$. These boundary conditions are

$$\hat{r} \times \overline{\overline{G}}_e^{Lfo} = \hat{r} \times \overline{\overline{G}}_e^{L(f+1)o} \tag{4.59}$$

and

$$\frac{1}{\mu_f} \hat{r} \times \nabla \times \overline{\overline{G}}_e^{Lfo} = \frac{1}{\mu_{(f+1)}} \hat{r} \times \nabla \times \overline{\overline{G}}_e^{L(f+1)o}. \tag{4.60}$$

All the local reflection coefficients are given by

$$R_{Pf}^{E,H} = \frac{1}{N_\vartheta} \left(\vartheta_{f+1} \eta_f H_{ff} H'_{f+1,f} - \vartheta_f \eta_{f+1} H_{f+1,f} H'_{ff} \right) \tag{4.61}$$

$$R_{Ff}^{E,H} = \frac{1}{N_\vartheta} \left(\vartheta_{f+1} \eta_f j_{ff} j'_{f+1,f} - \vartheta_f \eta_{f+1} j_{f+1,f} j'_{ff} \right) \tag{4.62}$$

And for the local transmission coefficients,

$$T_{Pf}^{E,H} = \frac{-2i\vartheta_f \eta_{f+1}}{(\pi \eta_f r_f) N_\vartheta} \tag{4.63}$$

$$T_{Ff}^{E,H} = \frac{-2i\vartheta_{f+1} \eta_f}{(\pi \eta_{f+1} r_f) N_\vartheta} \tag{4.64}$$

Where we have assumed the following abbreviations.

$$j_{fl} = j_n(\eta_f \alpha_l), \qquad j'_{fl} = j'_n(\eta_f \alpha_l)$$
$$H_{fl} = H_n^{(1)}(\eta_f \alpha_l), \qquad H'_{fl} = H_n'^{(1)}(\eta_f \alpha_l)$$

The superscripts E and H in the above equations denote TM and TE waves, whereas the subscripts P and F define the centripetal and centrifugal reflection or transmission respectively. Here

$$N_\vartheta = \vartheta_{f+1} \eta_f H_{f+1,f} j'_{ff} - \vartheta_f \eta_{f+1} j_{ff} H'_{f+1,f} \tag{4.65}$$

Besides ϑ represents ϵ or μ in the E (TM) or H (TE) mode representations respectively.

Furthermore $\hat{j}_n(x) = x j_n(x)$ and $\hat{H}_n^{(1)}(x) = x h_n^{(1)}(x)$. In the above, the Wronskian of the cylindrical Hankel functions is

$$\frac{2i}{\pi x} = j_{ff} H'_{f+1,f} - H_{f+1,f} j'_{ff}. \tag{4.66}$$

If the source is located outside the cylindrical body for axial symmetry $n = 0$, the scattering DGF is given by

i) For the case of two layered media the coefficients are

$$A^{10o}_{\substack{eo\\o}\eta_o} = R^H_{F1}, \qquad C^{10o}_{\substack{ee\\o}\eta_o} = R^E_{F1}$$

$$a^{10o}_{\substack{eo\\o}\eta_1} = T^H_{F1}, \qquad c^{10o}_{\substack{ee\\o}\eta_1} = T^E_{F1}$$

Where $R^{E,H}_{F1}$ and $T^{E,H}_{F1}$ can be obtained from (4.62) and (4.64) by letting $f = 1$.

ii) For the case of three layered media the coefficients are

$$c^{22o}_{\substack{ee\\o}\eta_2} = \frac{T^E_{P2}T^E_{P1}}{1 - R^E_{F1}R^E_{P2}}, \qquad c^{21o}_{\substack{ee\\o}\eta_1} = \frac{T^E_{P2}}{(1 - R^E_{F1}R^E_{P2})^2}$$

$$a^{22o}_{\substack{eo\\o}\eta_2} = \frac{T^H_{P2}T^H_{P1}}{1 - R^H_{F1}R^H_{P2}}, \qquad a^{21o}_{\substack{eo\\o}\eta_1} = \frac{T^H_{P2}}{(1 - R^H_{F1}R^H_{P2})^2}$$

$$C^{21o}_{\substack{ee\\o}\eta_1} = \frac{R^E_{F1}T^E_{P2}}{(1 - R^E_{F1}R^E_{P2})^2}, \qquad C^{20o}_{\substack{ee\\o}\eta_o} = R^E_{F2} + \frac{R^E_{F1}T^E_{F2}T^E_{P2}}{1 - R^E_{F1}R^E_{P2}}$$

$$A^{21o}_{\substack{eo\\o}\eta_1} = \frac{R^H_{F1}T^H_{P2}}{(1 - R^H_{F1}R^H_{P2})^2}, \qquad A^{20o}_{\substack{eo\\o}\eta_o} = R^H_{F2} + \frac{R^H_{F1}T^H_{F2}T^H_{P2}}{1 - R^H_{F1}R^H_{P2}}$$

Where $R^{E,H}_{F1}$, $R^{E,H}_{P2}$ and $T^{E,H}_{F2}$, $T^{E,H}_{P1}$ and $T^{E,H}_{P2}$ can be obtained from (4.61) to (4.64) by letting $f = 1$.

The results for these specific cases agree with those given by other authors [81], showing the validity of our DGF representation.

We can obtain the total DGF by applying the principle of scattering superposition,

$$\overline{\overline{G}}^{Lfo}_{E1}(\overline{R}, \overline{R}') = \delta^o_f \overline{\overline{G}}_{e1}(\overline{R}, \overline{R}') + \overline{\overline{G}}^{Lfo}_{cs}(\overline{R}, \overline{R}'). \tag{4.67}$$

If our concern is only with the region exterior to the source, then the singular term, which is important only in the source region can be dropped from the expression for the Green's function.

When more than one source is present in a system, the field of a source is affected by the presence of others, i.e. there is some interaction which needs to be taken into account. Moreover, the above expression can be used to give a more accurate field model on the kind of scatterer (such as human torso/head) to take into

account the radiation condition by the sources inside the scatterer due to moving cells bioelectromagnetics [82] causing internal electromagnetic fields, resulting in the

$$\overline{E}_{\text{(total sources)}} = \overline{E}_{\text{(external sources)}} + \sum \overline{E}_{\text{(internal sources)}} \tag{4.68}$$

4.5 Magnetic DGF in the Antenna-Torso Configuration

The principle of duality states that once the electric DGF is obtained, the magnetic DGF is derivable by interchanging the field functions $\overline{P}^{ee}_{oo} \rightarrow k\overline{Q}^{ee}_{oo}$ and $\overline{Q}^{ee}_{oo} \rightarrow k\overline{P}^{ee}_{oo}$ and omitting the singularity term contribution and vice versa.

On the other hand the corresponding total magnetic DGF at any point in the system can be calculated from $\nabla \times \overline{\overline{G}}_e = \overline{\overline{G}}_m$, bearing in mind the discontinuous nature of magnetic DGF across a point source at $R = R'$ and the Ampère-Maxwell equation relating $\overline{\overline{G}}_e$ and $\overline{\overline{G}}_m$ in the dyadic form i.e.: $\nabla \times \overline{\overline{G}}_m = \overline{\overline{I}}\delta_e(\overline{R} - \overline{R}') + k^2\overline{\overline{G}}_e$.

4.6 Electric and Magnetic Field at any Point in the Configuration

Since electromagnetic fields are vector fields, the general wave equation is a vector wave equation. For an homogeneous isotropic medium, the general form of the vector wave equation is given by:

$$\nabla \times \nabla \times \overline{E}_f - k_f^2 \overline{E}_f = (i\omega\mu_f \overline{J}_e - \nabla \times \overline{J}_m)\delta_f^s \tag{4.69}$$

$$\nabla \times \nabla \times \overline{H}_f - k_f^2 \overline{H}_f = (i\omega\varepsilon_f \overline{J}_m + \nabla \times \overline{J}_e)\delta_f^s \tag{4.70}$$

The above equations follow directly from duality principle [19], [21]. To obtain the electromagnetic fields due to these electric and magnetic current distributions, one first constructs $\overline{\overline{G}}_e^{Lfs}(\overline{R}, \overline{R}')$ and $\overline{\overline{G}}_m^{Lfs}(\overline{R}, \overline{R}')$, the electric and magnetic dyadic Green's functions respectively. These two DGFs are the solutions of the following dyadic differential equations (taking into account the discontinuous nature of magnetic or electric DGF with respect to electric or magnetic dipole respectively at

$R = R'$ i.e., $\nabla \times \overline{\overline{I}} \delta_{\substack{e \\ m}}(\overline{R} - \overline{R}') = 0$ and in the case when the source term $\overline{J}_{\substack{e \\ m}} = 0$ on the surface):

$$\nabla \times \nabla \times \overline{\overline{G}}^{(Lfs)}_{\substack{e \\ m}}(\overline{R}, \overline{R}') - k_f^2 \overline{\overline{G}}^{(Lfs)}_{\substack{e \\ m}}(\overline{R}, \overline{R}') = i\omega\vartheta \overline{\overline{I}} \delta_{\substack{e \\ m}}(\overline{R} - \overline{R}')\delta_f^s \tag{4.71}$$

Here a unit current density at $\overline{R}'$ in the direction of e or m has the space form $\delta_{\substack{e \\ m}}(\overline{R} - \overline{R}')$. This requires both DGFs satisfy the non-solenoidal condition $\nabla \cdot \overline{\overline{G}}^{Lfs}_{\substack{e \\ m}}(\overline{R}, \overline{R}') \neq 0$ because

$$\nabla \cdot \overline{E} = \frac{\overline{\rho}_e}{\varepsilon} = \frac{\nabla \cdot \overline{J}_e}{i\omega\varepsilon} \tag{4.72}$$

and

$$\nabla \cdot \overline{H} = \frac{\overline{\rho}_m}{\mu} = \frac{\nabla \cdot \overline{J}_m}{i\omega\mu} \tag{4.73}$$

Therefore the use of DGF technique allows us to determine the expansion of the electric and magnetic fields in a body (cylinder)/antenna configuration in a direct and elegant manner.

For any current source with current density function $\overline{J}(\overline{R}')$ located outside the body, the electric or magnetic field radiated by such a dipole can be evaluated using the formulae,

$$\overline{E}^{Lfo}(\overline{R}) = i\omega\mu_f \iiint_V \overline{\overline{G}}^{Lfo}_{E1}(\overline{R}, \overline{R}') \cdot \overline{J}(\overline{R}')dV', \tag{4.74}$$

$$\overline{H}^{Lfo}(\overline{R}) = i\omega\varepsilon_f \iiint_V \overline{\overline{G}}^{Lfo}_{M1}(\overline{R}, \overline{R}') \cdot \overline{J}(\overline{R}')dV'. \tag{4.75}$$

These signify the computation of the E and H-fields in the structure, which states the superposition of the incident field $\overline{E}_i(\overline{R})$ or $\overline{H}_i(\overline{R})$ and the scattered field $\overline{E}_s(\overline{R})$ or $\overline{H}_s(\overline{R})$ is given by

$$\overline{E}^{Lfo}(\overline{R}) = \overline{E}_i^{00o}(\overline{R})\delta_f^o + \overline{E}_s^{Lfo}(\overline{R}), \tag{4.76}$$

$$\overline{H}^{Lfo}(\overline{R}) = \overline{H}_i^{00o}(\overline{R})\delta_f^o + \overline{H}_s^{Lfo}(\overline{R}). \tag{4.77}$$

4.7 Concluding Remarks

We have derived general electromagnetic representations for a human torso model (in simple form for the multilayered homogeneous lossy dielectric circular cylinder of finite length) in order to evaluate deterioration of the antennas performance and obtain the rates of RF energy deposition (SAR), the power absorbed, the total power radiated, the thermal emission and the current induced on a scatterer. The representations may be used to optimize antenna design, ascertain potential health hazards, and compliance with standards legislation. The DGFs are obtained by employing the EFE and the method of scattering superposition.

Scattering from complex bodies is often used for detecting possible internal inhomogeneities and non-symmetries. By observing the field scattered by a body on which radiation is impinging it is possible to obtain information about its internal structure. Investigation of cells and of biological bodies, remote sensing techniques and detection of imperfections inside optical waveguides and lenses are straightforward examples.

The results of this chapter could be useful for a further analysis of the problem of an implant such as heart pace-maker embedded in the body and biotelemetry transmitters for medical applications and could easily be expanded so as to handle any scatterer having finite radius and length. They can also be applied to problems of optical fibers and waveguides for the investigation of inhomogeneities or obstacles inside them or by considering the cylinder as an excitation or scatterer.

Chapter 5

Electromagnetic DGF of an Implantable Medical Device Model

COMPREHENSIVE understanding of EM interactions between implanted human and modern personal communication antennas is essential for the hand held transceiver design. Since the human head is usually located in the reactive or near-field region of the antenna, the performance of an antenna may be severely affected by the presence of conducting medical devices/prostheses in the head. Also, significant portion of the antenna delivered power may be absorbed in the head. This chapter extends the method developed in the previous chapter to outline a general expression of dyadic Green's function (DGF) for the problem of electromagnetic radiation from a source of excitation in the presence of a finite length of perfectly conducting circular cylinder of any size as well as of resonant length, which is valid everywhere, including the source region. The whole structure is assumed to be uniform along the propagation direction. The DGFs are obtained by employing the method of scattering superposition.

5.1 Introduction

Although electromagnetic scattering by a finite cylinder is a well known canonical problem, published work does not include the effects of arbitrary placed source point. The derivations presented here are motivated by the need to understand

the behaviour of antennas near to or embedded in living tissue. The eigenfunction expansion (EFE) of DGFs in electromagnetic theory provide a systematic means of constructing and interpreting these dyadics. The pioneering work by Tai [20] has set the stage for most of what has been achieved over the last two and a half decades. The expansion of DGFs in terms of the Hansen [25] vector wave functions must be carried out carefully in order to ensure that one is dealing with a complete expansion.

The organization of this chapter is as follows. The complete set of cylindrical vector wave functions are introduced in section 5.2. This material is included here in order to explicitly define notation and to call attention to a few points in connection with these expansions.

In section 5.3 we begin to formulate the problem for a finite circular cylinder and in subsection 5.3.1, we set out with the case, in which we construct the DGF, $\overline{\overline{G}}_{e1}(\overline{R}, \overline{R}')$, in terms that constitute the continuous eigenfunction expansion (EFE) in which the eigenfunctions are guided in the preferred r and z-coordinate directions, using the procedures described in Tai [19] or Collin [21]. This expansion also contains an explicit dyadic delta function term which is required for completeness at the source point. It is considered as a correction to the general solenoidal EFE which is valid outside the source point.

The procedure required to derive the complete EFE of the scattering DGF for the finite circular cylinder, in terms of only the solenoidal eigenfunctions is shown to be a simple and straightforward general expression and is summarized in section 5.4. The DGF for a finite conducting cylinder, $\overline{\overline{G}}_{E1}(\overline{R}, \overline{R}')$ can be constructed from the principle of the superposition, where it satisfies the boundary conditions.

Magnetic type DGF discussed in section 5.5, can be found by invoking duality or once the electric field is obtained the magnetic field is derivable by taking the curl of the electric field, and vice versa.

Conclusions are then presented in section 5.7 summarizing the important points contained in this work.

5.2 Vector Wave Functions for a Circular Cylinder of Finite Length

The cylindrical vector wave functions are the building blocks of the EFE of various kinds of DGF. They are denoted by $\overline{L}_{\substack{ee\\oo}n\lambda}$, $\overline{P}_{\substack{ee\\oo}n\lambda}$ and $\overline{Q}_{\substack{ee\\oo}n\lambda}$, that are solutions of the homogeneous vector Helmholtz equation. The generating or eigenfunctions, which are solutions of the cylindrical scalar wave equation $\nabla^2\Psi + k_\lambda^2\Psi=0$, with the differential equation in the cylindrical coordinate system

$$\frac{1}{r}\frac{\partial}{\partial r}(r\frac{\partial\Psi}{\partial r}) + \frac{1}{r^2}\frac{\partial^2\Psi}{\partial\phi^2} + \frac{\partial^2\Psi}{\partial\phi^2} + \frac{\partial^2\Psi}{\partial z^2} + K^2\Psi = 0 \tag{5.1}$$

with K, the separation constant and k_λ being an undetermined wave number. Implementation of the method of separation of variables in this system finally results the generating function [29] in the form

$$\Psi_{\substack{ee\\oo}n}(h) = j_n(\lambda r)^{\cos}_{\sin} n\phi^{\cos}_{\sin} hz, \tag{5.2}$$

Here subscripts "e" stands for even and "o" is the odd character of the generating functions. $h = \frac{q\pi}{l}$ are the eigenvalues in the z-direction with $q = 0, 1, 2, ...$ and l is the length of cylinder. $j_n(\lambda r)$ identifies the cylindrical Bessel functions of the order n to represent both outgoing and incoming waves. λ is the continuous eigenvalue. Cylindrical vector wave functions are akin to the Debye potentials.

$$\overline{L}_{\substack{ee\\oo}n\lambda}(h) = \nabla\Psi_{\substack{ee\\oo}n}, \tag{5.3}$$

$$\overline{P}_{\substack{ee\\oo}n\lambda}(h) = \nabla\times[\Psi_{\substack{ee\\oo}n}\hat{z}], \tag{5.4}$$

$$\overline{Q}_{\substack{ee\\oo}n\lambda}(h) = \frac{1}{k_\lambda}\nabla\times\nabla\times[\Psi_{\substack{ee\\oo}n}\hat{z}]. \tag{5.5}$$

Where $\hat{z}$ is the piloting vector.

The complete expressions for the solenoidal (rotational or transverse) functions

are

$$\overline{P}_{\substack{ee\\oo}n\lambda}(h) = \left\{ \begin{array}{c} \mp\frac{n}{r} j_n(\lambda r)^{\sin}_{\cos} n\phi^{\cos}_{\sin} hz\hat{r} \\ -(\frac{\partial j_n(\lambda r)}{\partial r})^{\cos}_{\sin} n\phi^{\cos}_{\sin} hz\hat{\phi} \\ 0 \end{array} \right\} \tag{5.6}$$

$$\overline{Q}_{\substack{ee\\oo}n\lambda}(h) = \left\{ \begin{array}{c} \mp h[\frac{\partial j_n(\lambda r)}{\partial r}]^{\cos}_{\sin} n\phi^{\sin}_{\cos} hz\hat{r} \\ \frac{hn}{r}[j_n(\lambda r)]^{\sin}_{\cos} n\phi^{\sin}_{\cos} hz\hat{\phi} \\ \lambda^2[j_n(\lambda r)]^{\cos}_{\sin} n\phi^{\cos}_{\sin} hz\hat{z} \end{array} \right\} \frac{1}{k_\lambda} \tag{5.7}$$

And the complete expressions for the nonsolenoidal (irrotational or lamellar) functions are

$$\overline{L}_{\substack{ee\\oo}n\lambda}(h) = \left\{ \begin{array}{c} \frac{\partial}{\partial r}[j_n(\lambda r)]^{\cos}_{\sin} n\phi^{\cos}_{\sin} hz\hat{r} \\ \mp\frac{n}{r}[j_n(\lambda r)]^{\sin}_{\cos} n\phi^{\cos}_{\sin} hz\hat{\phi} \\ \mp h[j_n(\lambda r)]^{\cos}_{\sin} n\phi^{\sin}_{\cos} hz\hat{z} \end{array} \right\} \tag{5.8}$$

where $k_\lambda^2 = \lambda^2 + h^2$ and in these vector wave functions one should be careful with the sign of the elements in the matrices when cross-multiplying the terms from "e" to "o" and vice-versa e.g. "sin sin" always remains negative while "cos cos" positive. Also "$-$ cos sin" and "$-$ sin cos" in second elements of matrices in $\overline{P}_{eo}$ and $\overline{P}_{oe}$ respectively. In $\overline{L}_{eo}$ and $\overline{L}_{oe}$ both "cos sin" and "sin cos" are positive in the first element of their respective matrix. For $\overline{Q}_{eo}$, "$-$ sin cos" in second element of matrix, while "$+$ cos sin" in the third element. For $\overline{Q}_{oe}$, "$-$ cos sin" and "$+$ sin cos" in the elements 2 and 3 respectively. "$\mp$" applies the negative to the top line while positive to the bottom line.

Note that in the set of cylindrical vector wave functions only $\overline{P}_{\substack{ee\\oo}n\lambda}$ do not possess the z component. The $\hat{r}$, ϕ and $\hat{z}$ are the cylindrical unit vectors. These functions are defined in the entire space, corresponding to $0 \leq r \leq \infty$, $0 \leq \phi \leq 2\pi$ and $0 < z < l$.

The volume integral of the product of the cylindrical vector wave functions is clearly zero if $n \neq n'$ and $h \neq h'$ because of the orthogonal property of the $\cos n\phi$ and $\sin n\phi$ functions and the Fourier integral relation. The derivation of the orthogonal properties of these vector wave functions were investigated in the previous chapter.

5.3 Formulation of the Problem

Consider the cylinder in Figure 4 of radius "α" concentric along z-axis with length "l" is illuminated by an electromagnetic wave. An electromagnetic field is induced in the system and an electromagnetic wave is scattered by the system.

A time dependence $e^{j\omega t}$ is assumed and suppressed throughout.

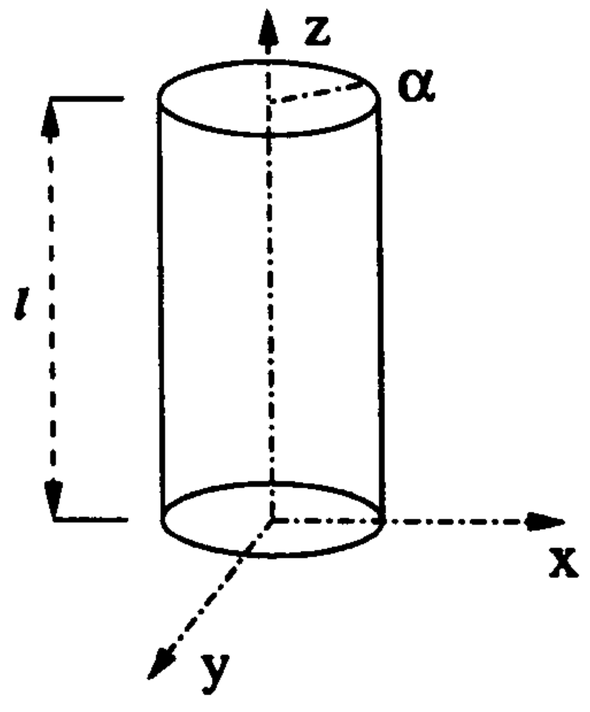

Figure 4: Diagram of a Finite Circular Cylinder

5.3.1 DGF for a finite Length Cylinder of Circular Cross-Section

Because the dyadic $\nabla \times [\overline{\overline{I}}\delta_e(\overline{R} - \overline{R}')]$ is solenoidal, it can be expanded in terms of solenoidal vector wave functions; $\overline{P}_{\substack{ee\\oo}n\lambda}$ and $\overline{Q}_{\substack{ee\\oo}n\lambda}$ defined previously.

Applying the method of (G_m) and according to the Ohm-Rayleigh procedure, an EFE for the source function $\nabla \times [\overline{\overline{I}}\delta_e(\overline{R} - \overline{R}')]$ using the solenoidal vector wave functions can be

$$\nabla \times [\overline{\overline{I}}\delta_e(\overline{R} - \overline{R}')] = \int_0^\infty d\lambda \int_0^l dh \sum_{n=0}^\infty \begin{bmatrix} \overline{Q}_{\substack{eo\\o}n\lambda}(h)\overline{A}_{\substack{eo\\o}n\lambda}(h) \\ \overline{P}_{\substack{ee\\o}n\lambda}(h)\overline{B}_{\substack{ee\\o}n\lambda}(h) \end{bmatrix}, \tag{5.9}$$

where λ and h are continuous eigenvalues and $\overline{A}_{\substack{eo\\o}n\lambda}(h)$ and $\overline{B}_{\substack{ee\\o}n\lambda}(h)$ are two unknown vector functions to be determined. This is a three-dimensional problem with a dyadic singular function, therefore the above equation can be treated as the Fourier transform and the Fourier-Bessel transform or the Hankel transform of

$\nabla\times[\overline{\overline{I}}\delta_e(\overline{R}-\overline{R}')]$. By taking the anterior scalar product of the above equation with $\overline{Q}_{o^{eo}n'\lambda'}(h')$ and integrating the resultant equation through the entire space and as a result of the orthogonal relationships and repeating the same routine with the $\overline{P}_{o^{ee}n'\lambda'}(h')$ we can obtain the EFE, where we have preserved the Fourier integration. The plane of discontinuity for the magnetic DGF is located at $r=r'$. The expression for $(\overline{\overline{G}}_{e1})$ for a finite cylinder of radius "α" concentric with the z-axis can now be written in the form

$$\overline{\overline{G}}_{e1}(\overline{R},\overline{R}')=-\frac{\hat{r}\hat{r}}{k^2}\delta_e(\overline{R}-\overline{R}')+\int_0^l dh\sum_{n=0}^{\infty}C_\lambda \cdot\begin{cases}\left\{\begin{array}{l}[\overline{P}^{(1)}_{o^{eo}\eta_o}(h;\eta_o)\overline{P}'_{o^{eo}\eta_o}(h;\eta_o)]\\ [\overline{Q}^{(1)}_{o^{ee}\eta_o}(h;\eta_o)\overline{Q}'_{o^{ee}\eta_o}(h;\eta_o)]\end{array}\right\}, & r>r',\\ \left\{\begin{array}{l}[\overline{P}_{o^{eo}\eta_o}(h;\eta_o)\overline{P}'^{(1)}_{o^{eo}\eta_o}(h;\eta_o)]\\ [\overline{Q}_{o^{ee}\eta_o}(h;\eta_o)\overline{Q}'^{(1)}_{o^{ee}\eta_o}(h;\eta_o)]\end{array}\right\}, & r<r'.\end{cases} \tag{5.10}$$

where

$$C_\lambda=\frac{i(2-\delta_o^n)}{2l\eta_o^2} \tag{5.11}$$

Coefficient C_λ depends on the value of δ_o^n which is the Kronecker delta functions defined with respect to n, when

$$\delta_o^n=\begin{cases}1, & \text{if } n=o\\ 0, & \text{if } n\neq o\end{cases} \tag{5.12}$$

Here $\hat{r}\hat{r}$ is a dyad (dyadic product of the unit vectors) and $\delta(\overline{R}-\overline{R}')$ is weighted Dirac delta function in three dimensions. This is included explicitly as a correction to the general solenoidal EFE which is valid outside the source point. The dyadic delta function term at the source point in cylindrical coordinates

$$\delta(\overline{R}-\overline{R}')=\frac{1}{r'}\delta(\overline{r}-\overline{r}')\delta(\overline{\phi}-\overline{\phi}')\delta(\overline{z}-\overline{z}') \tag{5.13}$$

Comparing the DGFs for a finite cylinder developed here with those presented by other authors e.g. Tai [19] for an infinite cylinder, one can notice that they are similar in mathematical form but different in the calculations of Ps and Qs and the limits of integration for a finite cylinder.

5.4 Scattering DGF for a Finite Conducting Cylinder of Circular Cross-Section

When a perfectly conducting cylinder of the same size as above is illuminated by an electromagnetic wave, the scattered terms can be written in the form

$$\overline{\overline{G}}_{es}(\overline{R},\overline{R}') = \int_0^l dh \sum_{n=0}^{\infty} C_\lambda \cdot \begin{bmatrix} \alpha_{\substack{e_o\\o}\eta} \overline{P}^{(1)}_{\substack{e_o\\o}\eta}(h;\eta)\overline{P}'^{(1)}_{\substack{e_o\\o}\eta}(h;\eta) \\ \beta_{\substack{e_e\\o}\eta} \overline{Q}^{(1)}_{\substack{e_e\\o}\eta}(h;\eta)\overline{Q}'^{(1)}_{\substack{e_e\\o}\eta}(h;\eta) \end{bmatrix}. \tag{5.14}$$

Applying the principle of scattering superposition, we obtain

$$\overline{\overline{G}}_{E1}(\overline{R},\overline{R}') = \overline{\overline{G}}_{e1}(\overline{R},\overline{R}') + \overline{\overline{G}}_{es}(\overline{R},\overline{R}') \tag{5.15}$$

Where we consider the function for a finite circular cylinder in a region $0 \leq r \leq \infty$. After applying the boundary condition one can determine the unknown coefficients. In order to satisfy the boundary condition at interface $r = \alpha$,

$$\hat{r} \times \left[\overline{P}_{\substack{e_o\\o}\eta}(h;\eta)\overline{P}'^{(1)}_{\substack{e_o\\o}\eta}(h;\eta) + \alpha_{\substack{e_o\\o}\eta}\overline{P}^{(1)}_{\substack{e_o\\o}\eta}(h;\eta)\overline{P}'^{(1)}_{\substack{e_o\\o}\eta}(h;\eta)\right]_{r=\alpha} \tag{5.16}$$

$$\hat{r} \times \left[\overline{Q}_{\substack{e_e\\o}\eta}(h;\eta)\overline{Q}'^{(1)}_{\substack{e_e\\o}\eta}(h;\eta) + \beta_{\substack{e_e\\o}\eta}\overline{Q}^{(1)}_{\substack{e_e\\o}\eta}(h;\eta)\overline{Q}'^{(1)}_{\substack{e_e\\o}\eta}(h;\eta)\right]_{r=\alpha} \tag{5.17}$$

$$\hat{r} \times \left[\overline{P}_{\substack{e_o\\o}\eta}(h;\eta) + \alpha_{\substack{e_o\\o}\eta}\overline{P}^{(1)}_{\substack{e_o\\o}\eta}(h;\eta)\right]_{r=\alpha} = 0 \tag{5.18}$$

$$\hat{r} \times \left[\overline{Q}_{\substack{e_e\\o}\eta}(h;\eta) + \beta_{\substack{e_e\\o}\eta}\overline{Q}^{(1)}_{\substack{e_e\\o}\eta}(h;\eta)\right]_{r=\alpha} = 0 \tag{5.19}$$

substituting for $\overline{P}_{\substack{e_o\\o}\eta}(h;\eta)$ and $\overline{P}^{(1)}_{\substack{e_o\\o}\eta}(h;\eta)$

$$\overline{P}_{\substack{e_o\\o}\eta}(h;\eta) = \nabla\times[j_n(\eta r)^{\cos}_{\sin} n\phi \sin hz\hat{z}], \tag{5.20}$$

$$\overline{P}^{(1)}_{\substack{e_o\\o}\eta}(h;\eta) = \nabla\times[H^{(1)}_n(\eta r)^{\cos}_{\sin} n\phi \sin hz\hat{z}], \tag{5.21}$$

in equation (5.18) produces $\alpha_{{}^{e_o}_{o}\eta} = -\frac{[\partial j_n(\eta\alpha)]/\partial(\eta\alpha)}{[\partial H_n^{(1)}(\eta\alpha)]/\partial(\eta\alpha)}$.

Similarly inserting for $\overline{Q}_{{}^{e_e}_{o}\eta}(h;\eta)$ and $\overline{Q}^{(1)}_{{}^{e_e}_{o}\eta}(h;\eta)$

$$\overline{Q}_{{}^{e_e}_{o}\eta}(h;\eta) = \frac{1}{k}\nabla\times\nabla\times[j_n(\eta r)^{\cos}_{\sin} n\phi \cos hz\hat{z}], \tag{5.22}$$

$$\overline{Q}^{(1)}_{{}^{e_e}_{o}\eta}(h;\eta) = \frac{1}{k}\nabla\times\nabla\times[H_n^{(1)}(\eta r)^{\cos}_{\sin} n\phi \cos hz\hat{z}], \tag{5.23}$$

in equation (5.19) produces $\beta_{{}^{e_e}_{o}\eta} = -\frac{[j_n(\eta\alpha)]}{[H_n^{(1)}(\eta\alpha)]}$.

5.5 Magnetic DGF in the Antenna-Prosthesis Configuration

The principle of duality states that once the electric DGF is obtained, the magnetic DGF is derivable by interchanging the field functions $\overline{P}_{{}^{e_e}_{o_o}} \rightarrow k\overline{Q}_{{}^{e_e}_{o_o}}$ and $\overline{Q}_{{}^{e_e}_{o_o}} \rightarrow k\overline{P}_{{}^{e_e}_{o_o}}$ and omitting the singularity term contribution and vice versa.

On the other hand the corresponding total magnetic DGF at any point in the system can be calculated from $\nabla\times\overline{\overline{G}}_e = \overline{\overline{G}}_m$, bearing in mind the discontinuous nature of magnetic DGF across a point source at $R = R'$ and the Ampère-Maxwell equation relating $\overline{\overline{G}}_e$ and $\overline{\overline{G}}_m$ in the dyadic form i.e.: $\nabla\times\overline{\overline{G}}_m = \overline{\overline{I}}\delta_e(\overline{R}-\overline{R}') + k^2\overline{\overline{G}}_e$.

5.6 Electric and Magnetic Field at any Point in the Configuration

The use of DGF technique allows us to determine the expansion of the electric and magnetic fields in a cylinder/antenna configuration in a direct and elegant manner.

For any current source with current density function $\overline{J}(\overline{R}')$ located outside the cylinder, the electric or magnetic field radiated by such a dipole can be calculated using the formulae,

$$\overline{E}(\overline{R}) = i\omega\mu_o\iiint_V \overline{\overline{G}}_{E1}(\overline{R},\overline{R}')\cdot\overline{J}(\overline{R}')dV' \tag{5.24}$$

$$\overline{H}(\overline{R}) = i\omega\epsilon_o\iiint_V \overline{\overline{G}}_{M1}(\overline{R},\overline{R}')\cdot\overline{J}(\overline{R}')dV'. \tag{5.25}$$

These signify the computation of the E and H-fields in the structure, which states the superposition of the incident field $\overline{E}_i(\overline{R})$ or $\overline{H}_i(\overline{R})$ and the scattered field $\overline{E}_s(\overline{R})$ or $\overline{H}_s(\overline{R})$ is given by

$$\overline{E}(\overline{R}) = \overline{E}_i(\overline{R}) + \overline{E}_s(\overline{R}) \tag{5.26}$$

$$\overline{H}(\overline{R}) = \overline{H}_i(\overline{R}) + \overline{H}_s(\overline{R}). \tag{5.27}$$

5.7 Concluding Remarks

General expressions have been derived in simple form for the finite conducting circular cylinder (medical devices/prostheses) of any size and of very small radius (resonant length). The DGFs are obtained by employing the EFE and the method of scattering superposition.

The results of this chapter could be useful for a further analysis of the problem as a thin wire or an implant such as heart pace-maker embedded in the body and biotelemetry transmitters for medical applications and could easily be expanded so as to handle any scatterer having finite radius and length.

They can be applied to the problems of optical fibers and waveguides for the investigation of inhomogeneities or obstacles inside them or by considering the cylinder as an excitation or scatterer. They can also be of use in the study and design of antennas of high frequency.

The usefulness of the present technique obviously requires comparison with numerical and experimental results. It is envisaged that future work will address this aspect of the problem in more detail.

Chapter 6

Electromagnetic Modeling of Implantable Medical Devices Using Cylindrical DGFs

GSM (global system for mobile communication) and PCS's (personal communication services) can interfere with implantable medical devices/prostheses particularly for systems using TDMA (time-division multiple access) and cause possible malfunction. Also the performance of an antenna is significantly altered by the presence of conducting medical devices/prostheses. Development of a computational algorithm to perform a systematic evaluation of the EM interactions between antennas and biological systems embedded with one or more prostheses is of great importance. The objective of this chapter is to outline an alternative general expression of dyadic Green's function (DGF) for the problem of electromagnetic radiation from a source of excitation in the presence of a finite length "l" of perfectly conducting thin circular cylinder of radius "a" concentric along z-axis of any size as well as of resonant length, which is valid everywhere, including the source region. The whole structure is assumed to be uniform along the propagation direction. The advantage of the proposed analysis is its simplicity and efficiency in computation.

6.1 Introduction

The understanding of the effects of perfect conducting prostheses on the absorbed power distribution within a biological system as an arbitrary placed source point is essential for the modern cellular phones and new implants design. The derivations presented here are motivated by the need to understand the behaviour of antennas near to or embedded in living tissue. Interaction of electromagnetic fields (EMF) with living systems and public concern regarding their allegedly/possible harmful health effects have been of current research interest. These investigations are motivated by two relating factors:

i a need to evaluate the specific absorption rate (SAR) (the rate of RF energy deposition) in the user's body, in order to evaluate potential health effects and compliance with standards, and;

ii the antenna performance in the proximity of the user's body and to develop better antenna designs whose performance is less affected by the biological systems and produce lower SAR.

Several theoretical studies have analyzed these models in Reyhani [28, 29, 31]. This chapter is organized as follows. The complete set of cylindrical vector wave functions are introduced in section 6.2. In section 6.3, we construct the DGF, $\overline{\overline{G}}_{e1}^{\infty}(\overline{R},\overline{R}')$, in terms that constitute the continuous eigenfunction expansion (EFE) in which the eigenfunctions are guided in the preferred r and z-coordinate directions, using the procedures described in Tai [19] or Collin [21]. The procedure required to derive the complete EFE of the general scattering DGF for the infinite circular cylinder, in terms of only the solenoidal eigenfunctions is shown to be a simple and straight-forward general expression and is summarized in section 6.4. The DGF for a semi-infinite cylinder, $\overline{\overline{G}}_{E1}^{s\infty}(\overline{R},\overline{R}')$ is then constructed from the principle of the superposition, where it satisfies the boundary conditions. Section 6.5, presents the final construction of the DGFs expansions. It is in this development that the princi-

pal point of this chapter is identified. Conclusions are then presented in section 6.8 summarizing the important points contained in this work.

6.2 Cylindrical Vector Wave Functions

The vector wave functions are the building blocks of the EFE of various kinds of DGF. They are solutions of the homogeneous vector Helmholtz equation. The generating functions, which are solutions of the cylindrical scalar wave equation $\nabla^2\Psi + k_\lambda^2\Psi=0$, can be written in the form $\Psi_{e_n}(h) = j_n(\lambda r)^{\cos}_{\sin} n\phi e^{ihz}$. k_λ is an undetermined wave number and subscripts "e" stands for even and "o" is the odd character of the generating functions. Where $j_n(\lambda r)$ identifies the cylindrical Bessel functions of the order n to represent both out-going and in-coming waves. λ is the continuous eigenvalue. Cylindrical vector wave functions are akin to the Debye potentials. $\overline{P}_{e_n\lambda}(h) = \nabla\times[\Psi_{e_n}\hat{z}]$ and $\overline{Q}_{e_n\lambda}(h) = \frac{1}{k_\lambda}\nabla\times\nabla\times[\Psi_{e_n}\hat{z}]$. Where $\hat{z}$ is the piloting vector. These functions are defined in the entire space, corresponding to $0 \leq r \leq a$, $0 \leq \phi \leq 2\pi$ and $-\infty < z < \infty$.

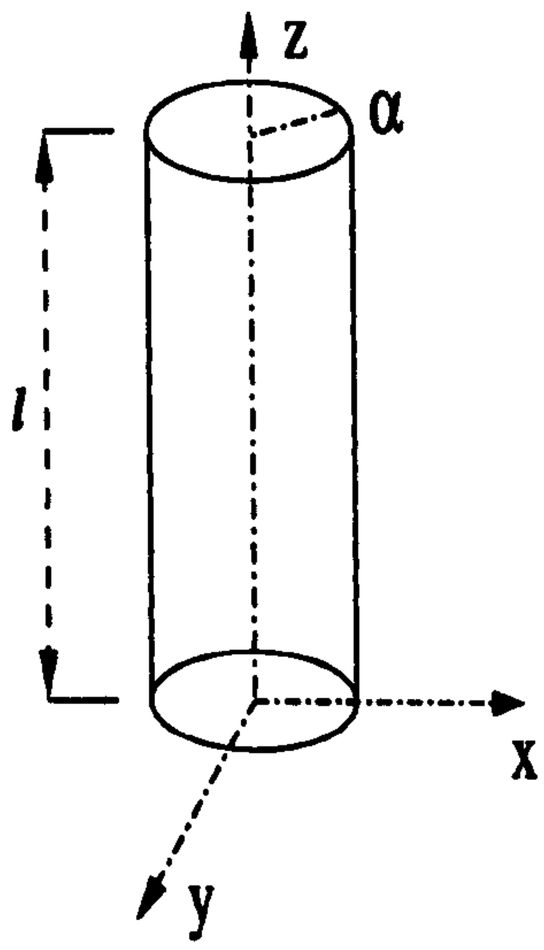

Figure 5: Diagram of a Finite Circular Cylindrical Implant

The orthogonal properties of these vector wave functions have been discussed by Tai [19] and Collin [21].

6.3 DGF for an Infinite Length Cylinder of Circular Cross-Section

Because the dyadic source function $\nabla \times [\overline{\overline{I}}\delta(\overline{R}-\overline{R}')]$ is solenoidal, it can be expanded in terms of solenoidal vector wave functions $P_{\substack{e\\o}n\lambda}$ and $Q_{\substack{e\\o}n\lambda}$. Applying the method of (G_m) and according to the Ohm-Rayleigh procedure, an EFE for the source function

$$\nabla \times [\overline{\overline{I}}\delta(\overline{R}-\overline{R}')] = \int_0^a d\lambda \int_{-\infty}^{\infty} dh \sum_{n=0}^{\infty} \begin{bmatrix} \overline{Q}_{\substack{e\\o}n\lambda}(h)\overline{A}_{\substack{e\\o}n\lambda}(h) \\ \overline{P}_{\substack{e\\o}n\lambda}(h)\overline{B}_{\substack{e\\o}n\lambda}(h) \end{bmatrix}, \tag{6.1}$$

where λ and h are continuous eigenvalues and $\overline{A}_{\substack{e\\o}n\lambda}(h)$ and $\overline{B}_{\substack{e\\o}n\lambda}(h)$ are two unknown vector functions to be determined. This is a three-dimensional problem with a dyadic singular function, therefore the electric DGF for infinite conducting cylinder can be written as

$$\begin{aligned} \overline{\overline{G}}^{\infty}_{e1}(\overline{R},\overline{R}') = -\frac{\hat{z}\hat{z}}{k^2}\delta(\overline{R}-\overline{R}') + \int_0^a d\lambda \sum_{n=0}^{\infty} C_\lambda \\ \cdot \begin{bmatrix} \overline{P}_{\substack{e\\o}n\lambda}(\pm h_1)\overline{P}'_{\substack{e\\o}n\lambda}(\mp h_1) \\ \overline{Q}_{\substack{e\\o}n\lambda}(\pm h_1)\overline{Q}'_{\substack{e\\o}n\lambda}(\mp h_1) \end{bmatrix}, \quad z \gtrless z', \end{aligned} \tag{6.2}$$

$C_\lambda = \frac{i(2-\delta_o^n)}{4\pi\lambda^2 I_\lambda h_1}$ depends on the value of δ_o^n which are the Kronecker delta functions defined with respect to n and I_λ is the normalization factor. Poles of integrand are $h = \pm(k^2-\lambda^2)^{\frac{1}{2}} = \pm h_1$.

6.4 DGF for a Semi-Infinite Length Cylinder of Circular Cross-Section

The scattered terms for cylinder of infinite length is

$$\overline{\overline{G}}_{es}(\overline{R},\overline{R}') = \int_0^a d\lambda \sum_{n=0}^{\infty} C_\lambda \begin{bmatrix} \alpha_{\substack{e\\o}n\lambda}\overline{P}_{\substack{e\\o}n\lambda}(h_1)\overline{P}'_{\substack{e\\o}n\lambda}(h_1) \\ \beta_{\substack{e\\o}n\lambda}\overline{Q}_{\substack{e\\o}n\lambda}(h_1)\overline{Q}'_{\substack{e\\o}n\lambda}(h_1) \end{bmatrix}. \tag{6.3}$$

Applying the principle of scattering superposition,

$$\overline{\overline{G}}^{s\infty}_{E1}(\overline{R},\overline{R}') = \overline{\overline{G}}^{\infty}_{e1}(\overline{R},\overline{R}') + \overline{\overline{G}}_{es}(\overline{R},\overline{R}') \tag{6.4}$$

Where we consider the function for a semi-infinite circular cylinder in region $0 \leq z < \infty$. After applying the boundary condition at interface $z = 0$ one can determine the unknown coefficients.

$$\hat{z} \times [\overline{P}_{\substack{e\\o}n\lambda}(-h_1) + \alpha_{\substack{e\\o}n\lambda}\overline{P}_{\substack{e\\o}n\lambda}(h_1)]_{z=0} = 0 \tag{6.5}$$

$$\hat{z} \times [\overline{Q}_{\substack{e\\o}n\lambda}(-h_1) + \beta_{\substack{e\\o}n\lambda}\overline{Q}_{\substack{e\\o}n\lambda}(h_1)]_{z=0} = 0 \tag{6.6}$$

Equations (6.5) and (6.6) produce $\alpha_{\substack{e\\o}n\lambda} = -1$ and $\beta_{\substack{e\\o}n\lambda} = 1$ respectively. Furthermore, if we introduce vector wave functions

$$\overline{P}_{\substack{e\\o}n\lambda o}(z) = \nabla\times[j_n(\lambda r)^{\cos}_{\sin} n\phi \sin h_1 z\hat{z}], \tag{6.7}$$

$$\overline{Q}_{\substack{e\\o}n\lambda e}(z) = \frac{1}{k}\nabla\times\nabla\times[j_n(\lambda r)^{\cos}_{\sin} n\phi \cos h_1 z\hat{z}]. \tag{6.8}$$

then the expression for electric DGF for semi-infinite cylinder (6.4) can be written in the following compact form:

$$\overline{\overline{G}}^{s\infty}_{E1}(\overline{R},\overline{R}') = -\frac{\hat{z}\hat{z}}{k^2}\delta(\overline{R}-\overline{R}') + \int_0^a d\lambda \sum_{n=0}^{\infty}(-2i)C_\lambda \cdot \left\{ \begin{bmatrix} \overline{P}_{\substack{e\\o}n\lambda}(h_1)\overline{P}'_{\substack{e\\o}n\lambda o}(z') \\ i\overline{Q}_{\substack{e\\o}n\lambda}(h_1)\overline{Q}'_{\substack{e\\o}n\lambda e}(z') \end{bmatrix} \right\} \begin{bmatrix} \overline{P}_{\substack{e\\o}n\lambda o}(z)\overline{P}'_{\substack{e\\o}n\lambda}(h_1) \\ i\overline{Q}_{\substack{e\\o}n\lambda e}(z)\overline{Q}'_{\substack{e\\o}n\lambda}(h_1) \end{bmatrix} z \gtrless z'. \tag{6.9}$$

6.5 DGF for a Finite Length Cylinder of Circular Cross-Section

The electric DGF for a finite cylinder in Figure 5 can now be derived with the aid of equation (6.9) in the form

$$\overline{\overline{G}}^{FL}_{E1}(\overline{R},\overline{R}') = \overline{\overline{G}}^{s\infty}_{E1}(\overline{R},\overline{R}') + \overline{\overline{G}}^{s\infty}_{E1_s}(\overline{R},\overline{R}') \tag{6.10}$$

The scattered representation $\overline{\overline{G}}^{s\infty}_{E1_s}$ can be assumed

$$\overline{\overline{G}}^{s\infty}_{E1_s}(\overline{R},\overline{R}') = \int_0^a d\lambda \sum_{n=0}^{\infty} -2iC_\lambda \begin{bmatrix} A_{\substack{e\\o}n\lambda o}\overline{P}_{\substack{e\\o}n\lambda o}(z)\overline{P}'_{\substack{e\\o}n\lambda o}(z') \\ B_{\substack{e\\o}n\lambda e}\overline{Q}_{\substack{e\\o}n\lambda e}(z)\overline{Q}'_{\substack{e\\o}n\lambda e}(z') \end{bmatrix}, \tag{6.11}$$

The boundary condition must also be fulfilled at $z = l$. This yield, $A_{\substack{e\\o}n\lambda o} = -\frac{e^{ih_1 l}}{\sin h_1 l}$ and $B_{\substack{e\\o}n\lambda e} = -\frac{ie^{ih_1 l}}{\sin h_1 l}$. Substituting into (6.11) and using (6.10) with the aid of new vector wave functions, we finally obtain the following representation for

$$\overline{\overline{G}}^{FL}_{E1}(\overline{R},\overline{R}') = -\frac{\hat{z}\hat{z}}{k^2}\delta(\overline{R}-\overline{R}') + \int_0^a d\lambda \sum_{n=0}^{\infty} \frac{2C_\lambda}{i\sin h_1 l} \cdot \begin{cases} \left\{ \begin{array}{l} \overline{P}_{\substack{e\\o}n\lambda o}(l-z)\overline{P}'_{\substack{e\\o}n\lambda o}(z') \\ -\overline{Q}_{\substack{e\\o}n\lambda e}(l-z)\overline{Q}'_{\substack{e\\o}n\lambda o}(z') \end{array} \right\}, & z > z', \\ \left\{ \begin{array}{l} \overline{P}_{\substack{e\\o}n\lambda o}(z)\overline{P}'_{\substack{e\\o}n\lambda o}(l-z') \\ -\overline{Q}_{\substack{e\\o}n\lambda o}(z)\overline{Q}'_{\substack{e\\o}n\lambda o}(l-z') \end{array} \right\}, & z < z'. \end{cases} \quad (6.12)$$

6.6 Magnetic DGF in the Antenna-Prosthesis Configuration

The principle of duality states that once the electric DGF is obtained, the magnetic DGF is derivable by interchanging the field functions $\overline{P}_{\substack{e\\o}} \to k\overline{Q}_{\substack{e\\o}}$ and $\overline{Q}_{\substack{e\\o}} \to k\overline{P}_{\substack{e\\o}}$ and omitting the singularity term contribution and vice versa.

On the other hand, the corresponding total magnetic DGF at any point in the system can be calculated from $\nabla \times \overline{\overline{G}}_e = \overline{\overline{G}}_m$, bearing in mind the discontinuous nature of magnetic DGF across a point source at $R = R'$ and the Ampère-Maxwell equation relating $\overline{\overline{G}}_e$ and $\overline{\overline{G}}_m$ in the dyadic form i.e.: $\nabla \times \overline{\overline{G}}_m = \overline{\overline{I}}\delta_e(\overline{R}-\overline{R}') + k^2\overline{\overline{G}}_e$.

6.7 Electric and Magnetic Field at any Point in the Configuration

The use of DGF technique allows us to determine the expansion of the electric and magnetic fields in a cylinder/antenna configuration in a direct and elegant manner.

For any current source with current density function $\overline{J}(\overline{R}')$ located outside the cylinder, the electric or magnetic field radiated by such a dipole can be calculated

using the formulae,

$$\overline{E}(\overline{R}) = i\omega\mu_o \iiint_V \overline{\overline{G}}^{FL}_{E1}(\overline{R},\overline{R}') \cdot \overline{J}(\overline{R}')dV' \tag{6.13}$$

$$\overline{H}(\overline{R}) = i\omega\varepsilon_o \iiint_V \overline{\overline{G}}^{FL}_{M1}(\overline{R},\overline{R}') \cdot \overline{J}(\overline{R}')dV'. \tag{6.14}$$

These signify the computation of the E and H-fields in the structure, which states the superposition of the incident field $\overline{E}_i(\overline{R})$ or $\overline{H}_i(\overline{R})$ and the scattered field $\overline{E}_s(\overline{R})$ or $\overline{H}_s(\overline{R})$ is given by

$$\overline{E}(\overline{R}) = \overline{E}_i(\overline{R}) + \overline{E}_s(\overline{R}) \tag{6.15}$$

$$\overline{H}(\overline{R}) = \overline{H}_i(\overline{R}) + \overline{H}_s(\overline{R}). \tag{6.16}$$

6.8 Concluding Remarks

General expressions have been derived in simple form for the finite conducting circular cylinder (medical devices/prostheses) of any size as well as of very small radius (resonant length). The DGFs are obtained by employing the EFE and the method of scattering superposition. The advantage of the proposed analysis is its simplicity and efficiency in computation.

As well as applications mentioned in the previous chapter, this enhancement can also be be of use in the study and design of antennas of high frequency whose performance is less affected by the biological systems and produce lower SAR.

The usefulness of the present technique obviously requires comparison with numerical and experimental results. It is envisaged that a later publication will address this aspect of the problem in more detail.

Chapter 7

Insulated Implantable Medical Device Model Using Electromagnetic Dyadic Green's Function

MODERN wireless telecommunication devices (GSM Mobile system and PCS's) can interfere with implantable medical devices/prostheses and cause possible malfunction. Also the performance of an antenna is significantly altered by the presence of these conducting medical devices/prostheses. Dielectric-coated medical devices are preferable over bare ones for use in a human body. The reason is that the often undesirable contact (hyperthermic/heating effect) between the prostheses and the surrounding tissue is avoided and, more importantly, the radiation efficiency of the antenna can be improved by insulating all or part of the medical devices surface. The principle objective of this chapter is to outline a general expression of dyadic Green's function (DGF) for the problem of electromagnetic radiation from a source of excitation in the presence of a finite length of insulated perfectly conducting circular cylinder of any size as well as of resonant length, which is valid everywhere, including the source region. The whole structure is assumed to be uniform along

the propagation direction. The DGFs are obtained by employing the method of scattering superposition. The advantage of the proposed analysis is its simplicity and efficiency in computation.

7.1 Introduction

Rapid development in PC technology necessitate an efficient near and far-field analytical technique for the radiation performance of cellular phones considering the influence of the implanted user's body. While the EMI in most cases does not generally pose a health risk, it may constitute a considerable annoyance, which may prevent the hearing aid users from using of the new devices. Dielectric-coated medical devices are preferable over bare ones for use in a human body. The reason is that the often undesirable contact (hyperthermic/localized heating effect) between the prostheses and the surrounding tissue is avoided and, more importantly, the radiation efficiency of the antenna can be improved by insulating all or part of the medical devices surface. The EFE of DGFs in EM theory provide a systematic means of constructing and interpreting these dyadics. The DGFs in terms of the Hansen [25] vector wave functions must be carried out carefully in order to ensure that one is dealing with a complete expansion. This chapter is organized as follows. The complete set of cylindrical vector wave functions are introduced in section 7.2.

In section 7.3 we begin to formulate the problem for a finite circular cylinder and in subsection 7.3.1, we set out with the case, in which we construct the DGF, $\overline{\overline{G}}_{e1}(\overline{R}, \overline{R}')$, in terms that constitute the continuous eigenfunction expansion (EFE) in which the eigenfunctions are guided in the preferred r and z-coordinate directions, using the procedures described in Tai [19] or Collin [21]. This expansion also contains an explicit dyadic delta function term which is required for completeness at the source point. It is considered as a correction to the general solenoidal EFE which is valid outside the source point.

Subsection 7.3.3, presents the general scattering DGFs expansions (7.10) in terms of only the solenoidal eigenfunctions (EF). It is in this development that

the principal point of this chapter is identified. Magnetic type DGF discussed in section 7.4, can be found by invoking duality or once the electric field is obtained the magnetic field is derivable by taking the curl of the electric field, and vice versa.

Conclusions are then presented in section 7.6 summarizing the important points contained in this work.

7.2 Vector Wave Functions for a Circular Cylinder of Finite Length

The cylindrical vector wave functions are the building blocks of the EFE of various kinds of DGFs. They are solutions of the homogeneous vector Helmholtz equation. The generating or eigenfunctions, which are solutions of the cylindrical scalar wave equation $\nabla^2\Psi + k_\lambda^2\Psi{=}0$ can be written [29] in the form

$$\Psi_{\substack{e\\o}n}(h) = j_n(\lambda r)^{\cos}_{\sin} n\phi^{\cos}_{\sin} hz, \tag{7.1}$$

Here subscripts "e" stands for even and "o" is the odd character of the generating functions. $h = \frac{q\pi}{l}$ are the eigenvalues in the z-direction with $q = 0, 1, 2, ...$ and l is the length of cylinder.

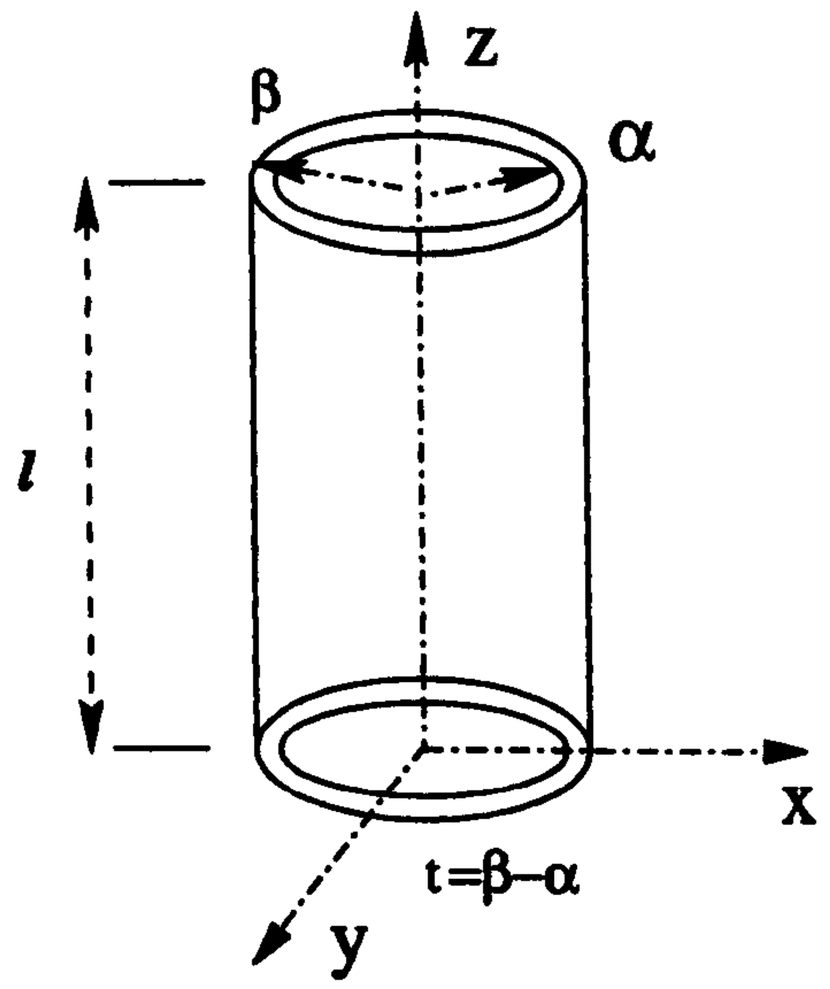

Figure 6: Diagram of a Finite Insulated Circular Implant Model

$j_n(\lambda r)$ identifies the cylindrical Bessel functions of the order n to represent both out-going and in-coming waves. λ is the continuous eigenvalue. Cylindrical vector wave functions are akin to the Debye potentials.

$$\overline{L}_{\substack{ee\\oo}n\lambda}(h) = \nabla \Psi_{\substack{ee\\oo}n} \tag{7.2}$$

$$\overline{P}_{\substack{ee\\oo}n\lambda}(h) = \nabla \times [\Psi_{\substack{ee\\oo}n} \hat{z}] \tag{7.3}$$

$$\overline{Q}_{\substack{ee\\oo}n\lambda}(h) = \frac{1}{k_\lambda} \nabla \times \nabla \times [\Psi_{\substack{ee\\oo}n} \hat{z}]. \tag{7.4}$$

Where $\hat{z}$ is the piloting vector and here $k_\lambda^2 = \lambda^2 + h^2$.

The complete expressions for the solenoidal (rotational or transverse) and the non-solenoidal (irrotational or lamellar) functions are given in Reyhani [28]. These functions are defined in the entire space, corresponding to $0 \leq r \leq \infty$, $0 \leq \phi \leq 2\pi$ and $0 < z < l$.

7.3 Formulation of the Problem

When a conducting cylinder coated by a layer of dielectric of the same length as in Figure 6 is illuminated by an electromagnetic wave, the scattered functions for a source in open space region "0", corresponding to the exterior region of the coated implant will be denoted by $\overline{\overline{G}}_{E1}^{L0o}$ and for interior region is $\overline{\overline{G}}_{E1}^{L1o}$. Region "1" is within the layer $(\alpha \leq r \leq \beta)$ for a conducting implant of radius α with thickness of the layer equal to $t = \beta - \alpha$. The function $\overline{\overline{G}}_{E1}^{L1o}$ must satisfy the Dirichlet boundary condition at $r = \alpha$, the interface of the conducting implant.

A time dependence $e^{j\omega t}$ is assumed and suppressed throughout.

7.3.1 DGF for a Finite Length Cylinder of Circular Cross-Section

Applying the method of (G_m) and according to the Ohm-Rayleigh procedure the expression for $(\overline{\overline{G}}_{e1})$ for a finite cylinder of radius "α" concentric with the z-axis is

given in Reyhani [28] in the form

$$\overline{\overline{G}}_{e1}(\overline{R},\overline{R}') = -\frac{\hat{r}\hat{r}}{k^2}\delta_e(\overline{R}-\overline{R}') + \int_0^l dh \sum_{n=0}^{\infty} C_\lambda$$

$$\cdot \begin{cases} \left\{ \begin{array}{l} [\overline{P}^{(1)}_{\substack{e_o e_o \\ o o}\eta_o}(h;\eta_o)\overline{P}'_{\substack{e_o e_o \\ o o}\eta_o}(h;\eta_o)] \\ [\overline{Q}^{(1)}_{\substack{e_e e_e \\ o o}\eta_o}(h;\eta_o)\overline{Q}'_{\substack{e_e e_e \\ o o}\eta_o}(h;\eta_o)] \end{array} \right\}, & r > r', \\ \left\{ \begin{array}{l} [\overline{P}_{\substack{e_o e_o \\ o o}\eta_o}(h;\eta_o)\overline{P}'^{(1)}_{\substack{e_o e_o \\ o o}\eta_o}(h;\eta_o)] \\ [\overline{Q}_{\substack{e_e e_e \\ o o}\eta_o}(h;\eta_o)\overline{Q}'^{(1)}_{\substack{e_e e_e \\ o o}\eta_o}(h;\eta_o)] \end{array} \right\}, & r < r'. \end{cases} \tag{7.5}$$

where coefficient $C_\lambda = \frac{i(2-\delta_o^n)}{2l\eta_o^2}$.

7.3.2 Scattering DGF for a Coated Implant Model

When a conducting cylinder coated by a layer of dielectric of the same size as above is illuminated by an electromagnetic wave, the scattered functions for a source in open space region "0", corresponding to the exterior region of the coated implant will be denoted by $\overline{\overline{G}}^{10o}_{E1}$ and $\overline{\overline{G}}^{11o}_{E1}$. Region "1" is within the layer ($\alpha \le r \le \beta$) for a conducting implant of radius α with thickness of the layer equal to $t = \beta - \alpha$. the function $\overline{\overline{G}}^{11o}_{E1}$ must satisfy the Dirichlet boundary condition at $r = \alpha$, the interface of the conducting implant.

For a dielectric cylinder, an incident TE mode will excite both a scattered TE and a scattered TM mode.

The Scattered DGF term for the exterior of insulated implant in this case, has the form

$$\overline{\overline{G}}^{10o}_{es}(\overline{R},\overline{R}') = \int_0^l dh \sum_{n=0}^{\infty} C_\lambda$$

$$\cdot \left\{ \begin{array}{l} [A^{10o}_{\substack{e_o e_o \\ o o}\eta_o}\overline{P}^{(1)}_{\substack{e_o e_o \\ o o}\eta_o}(h;\eta_o) + B^{10o}_{\substack{o_o o_o \\ e e}\eta_o}\overline{Q}^{(1)}_{\substack{o_o o_o \\ e e}\eta_o}(h;\eta_o)]\overline{P}'^{(1)}_{\substack{e_o e_o \\ o o}\eta_o}(h;\eta_o) \\ [C^{10o}_{\substack{e_e e_e \\ o o}\eta_o}\overline{Q}^{(1)}_{\substack{e_e e_e \\ o o}\eta_o}(h;\eta_o) + D^{10o}_{\substack{o_e o_e \\ e e}\eta_o}\overline{P}^{(1)}_{\substack{o_e o_e \\ e e}\eta_o}(h;\eta_o)]\overline{Q}'^{(1)}_{\substack{e_e e_e \\ o o}\eta_o}(h;\eta_o) \end{array} \right\}, \tag{7.6}$$

Where $k_o^2 = \omega^2(\mu_o\varepsilon_o)$ and $\eta_o^2 = (k_o^2 - h^2)$.

And for the interior region,

$$\overline{\overline{G}}_{es}^{11o}(\overline{R},\overline{R}') = \int_0^l dh \sum_{n=0}^{\infty} C_\lambda \cdot \left\{ \begin{array}{l} \left[\begin{array}{l} A_{\substack{e^o \\ o^e}\eta_1}^{11o} \overline{P}_{\substack{e^o \\ o^e}\eta_1}^{(1)}(h;\eta_1) + B_{\substack{o^o \\ e^e}\eta_1}^{11o} \overline{Q}_{\substack{o^o \\ e^e}\eta_1}^{(1)}(h;\eta_1) \\ a_{\substack{e^o \\ o^e}\eta_1}^{11o} \overline{P}_{\substack{e^o \\ o^e}\eta_1}(h;\eta_1) + b_{\substack{o^o \\ e^e}\eta_1}^{11o} \overline{Q}_{\substack{o^o \\ e^e}\eta_1}(h;\eta_1) \end{array} \right] \overline{P}'^{(1)}_{\substack{e^o \\ o^e}\eta_o}(h;\eta_o) \\ \\ \left[\begin{array}{l} C_{\substack{e^e \\ o^o}\eta_1}^{11o} \overline{Q}_{\substack{e^e \\ o^o}\eta_1}^{(1)}(h;\eta_1) + D_{\substack{o^e \\ e^o}\eta_1}^{11o} \overline{P}_{\substack{o^e \\ e^o}\eta_1}^{(1)}(h;\eta_1) \\ c_{\substack{e^e \\ o^o}\eta_1}^{11o} \overline{Q}_{\substack{e^e \\ o^o}\eta_1}(h;\eta_1) + d_{\substack{o^e \\ e^o}\eta_1}^{11o} \overline{P}_{\substack{o^e \\ e^o}\eta_1}(h;\eta_1) \end{array} \right] \overline{Q}'^{(1)}_{\substack{e^e \\ o^o}\eta_o}(h;\eta_o) \end{array} \right\}, \quad (7.7)$$

here $k_1^2 = \omega^2(\mu_1\varepsilon_1)$ and $\eta_1^2 = (k_1^2 - h^2)$.

The principle of scattering superposition can be applied to compute the total DGF, in each layer.

DGF for the outer layer

$$\overline{\overline{G}}_{E1}^{10o}(\overline{R},\overline{R}') = \overline{\overline{G}}_{e1}(\overline{R},\overline{R}') + \overline{\overline{G}}_{es}^{10o}(\overline{R},\overline{R}') \quad (7.8)$$

and for the inner layer

$$\overline{\overline{G}}_{E1}^{11o}(\overline{R},\overline{R}') = \overline{\overline{G}}_{es}^{11o}(\overline{R},\overline{R}') \quad (7.9)$$

7.3.3 General Expression of Scattering DGFs for an Electric Dipole in the Presence of a Dielectrically Multi-Layered Coated Implant Model

Observation and analysis of the above expressions for the scattering equations allows an efficient formulation of the general scattering DGF. The Scattered DGF term for the exterior and the interior of a dielectrically multi-layered insulated/coated

cylindrical implant in this case, has the form

$$\overline{\overline{G}}_{es}^{Lfo}(\overline{R},\overline{R}') = \int_0^l dh \sum_{n=0}^{\infty} C_\lambda$$

$$\cdot \left\{ \begin{array}{l} \left\{ \begin{array}{l} \begin{bmatrix} A_{\substack{e^o \\ o^o}\eta_f}^{Lfo}\, \overline{P}_{\substack{e^o \\ o^o}\eta_f}^{(1)}(h;\eta_f) \\ B_{\substack{o^o \\ e^o}\eta_f}^{Lfo}\, \overline{Q}_{\substack{o^o \\ e^o}\eta_f}^{(1)}(h;\eta_f) \end{bmatrix} \\ (1-\delta_f^o) \begin{bmatrix} a_{\substack{e^o \\ o^o}\eta_f}^{Lfo}\, \overline{P}_{\substack{e^o \\ o^o}\eta_f}(h;\eta_f) \\ b_{\substack{o^o \\ e^o}\eta_f}^{Lfo}\, \overline{Q}_{\substack{o^o \\ e^o}\eta_f}(h;\eta_f) \end{bmatrix} \end{array} \right\} \overline{P}'^{(1)}_{\substack{e^o \\ o^o}\eta_o}(h;\eta_o) \\ \left\{ \begin{array}{l} \begin{bmatrix} C_{\substack{e^e \\ o^e}\eta_f}^{Lfo}\, \overline{Q}_{\substack{e^e \\ o^e}\eta_f}^{(1)}(h;\eta_f) \\ D_{\substack{o^e \\ e^e}\eta_f}^{Lfo}\, \overline{P}_{\substack{o^e \\ e^e}\eta_f}^{(1)}(h;\eta_f) \end{bmatrix} \\ (1-\delta_f^o) \begin{bmatrix} c_{\substack{e^e \\ o^e}\eta_f}^{Lfo}\, \overline{Q}_{\substack{e^e \\ o^e}\eta_f}(h;\eta_f) \\ d_{\substack{o^e \\ e^e}\eta_f}^{Lfo}\, \overline{P}_{\substack{o^e \\ e^e}\eta_f}(h;\eta_f) \end{bmatrix} \end{array} \right\} \overline{Q}'^{(1)}_{\substack{e^e \\ o^e}\eta_o}(h;\eta_o) \end{array} \right\} . \tag{7.10}$$

Where $k_f^2 = \omega^2(\mu_f \varepsilon_f)$ and $\eta_f^2 = (k_f^2 - h^2)$.

"L" is the symbol for last inner layer in the implant model. "f" ($f = 0, 1, 2, ..., L$) is the field point or observer layer. Superscript/subscript "o" stands for source point at open space. Subscript "s" is scattering, while its superscript represents the layer at which the source is located. δ_f^o is the Kronecker delta function, where

$$\delta_f^o = \begin{cases} 1, & \text{if } o = f \\ 0, & \text{if } o \neq f \end{cases} . \tag{7.11}$$

$A_{\substack{e^o \\ o^o}\eta_f}^{Lfo}$, $a_{\substack{e^o \\ o^o}\eta_f}^{Lfo}$, $B_{\substack{o^o \\ e^o}\eta_f}^{Lfo}$, $b_{\substack{o^o \\ e^o}\eta_f}^{Lfo}$, $C_{\substack{e^e \\ o^e}\eta_f}^{Lfo}$, $c_{\substack{e^e \\ o^e}\eta_f}^{Lfo}$, $D_{\substack{o^e \\ e^e}\eta_f}^{Lfo}$ and $d_{\substack{o^e \\ e^e}\eta_f}^{Lfo}$ are the amplitude coefficients of scattered DGF to be determined by applying the boundary condition at the

interfaces $r = \alpha_l$ $(l = 1, 2, ..., L)$. These boundary conditions are;

$$\hat{r} \times \overline{\overline{G}}_e^{LLo} = 0 \tag{7.12}$$

$$\hat{r} \times \overline{\overline{G}}_e^{Lfo} = \hat{r} \times \overline{\overline{G}}_e^{L(f+1)o} \tag{7.13}$$

$$\frac{1}{\mu_f}\hat{r} \times \nabla \times \overline{\overline{G}}_e^{Lfo} = \frac{1}{\mu_{(f+1)}}\hat{r} \times \nabla \times \overline{\overline{G}}_e^{L(f+1)o} \tag{7.14}$$

We can now obtain the total DGF by applying the principle of scattering superposition,

$$\overline{\overline{G}}_{E1}^{Lfo}(\overline{R}, \overline{R}') = \overline{\overline{G}}_{e1}(\overline{R}, \overline{R}')\delta_f^o + \overline{\overline{G}}_{es}^{Lfo}(\overline{R}, \overline{R}') \tag{7.15}$$

If our concern is only with the region exterior to the source, then the singular term, which is important only in the source region can be dropped from the expression for the Green's function.

7.4 Magnetic DGF in the Antenna-Prosthesis Configuration

The principle of duality states that once the electric DGF is obtained, the magnetic DGF is derivable by interchanging the field functions $\overline{P}_{oo}^{ee} \rightarrow k\overline{Q}_{oo}^{ee}$ and $\overline{Q}_{oo}^{ee} \rightarrow k\overline{P}_{oo}^{ee}$ and omitting the singularity term contribution and vice versa.

On the other hand, the corresponding total magnetic DGF at any point in the system can be calculated from $\nabla \times \overline{\overline{G}}_e = \overline{\overline{G}}_m$, bearing in mind the discontinuous nature of magnetic DGF across a point source at $R = R'$ and the Ampere-Maxwell equation relating $\overline{\overline{G}}_e$ and $\overline{\overline{G}}_m$ in the dyadic form i.e.: $\nabla \times \overline{\overline{G}}_m = \overline{\overline{I}}\delta_e(\overline{R} - \overline{R}') + k^2\overline{\overline{G}}_e$.

7.5 Electric and Magnetic Field at any Point in the Configuration

The use of DGF technique allows us to determine the expansion of the electric and magnetic fields in a cylinder/antenna configuration in a direct and elegant manner.

For any current source with current density function $\overline{J}(\overline{R}')$ located outside the cylinder, the electric or magnetic field radiated by such a dipole can be calculated using the formulae,

$$\overline{E}^{Lfo}(\overline{R}) = i\omega\mu_f \iiint_V \overline{\overline{G}}_{EJ}^{Lfo}(\overline{R}, \overline{R}') \cdot \overline{J}(\overline{R}')dV' \tag{7.16}$$

$$\overline{H}^{Lfo}(\overline{R}) = i\omega\varepsilon_f \iiint_V \overline{\overline{G}}_{MJ}^{Lfo}(\overline{R}, \overline{R}') \cdot \overline{J}(\overline{R}')dV'. \tag{7.17}$$

7.6 Concluding Remarks

General expressions have been derived in simple form for the finite insulated conducting circular cylinder (insulated medical devices/prostheses) of any size as well as of very small radius (resonant length). The DGFs are obtained by employing the EFE and the method of scattering superposition.

The results of this chapter could be useful for a further analysis of the problem as a thin insulated wire or a dielectric-coated implant such as heart pace-maker embedded in the body and biotelemetry transmitters for medical applications and could easily be expanded so as to handle any scatterer having finite radius and length. They can be applied to problems of optical fibers and waveguides for the investigation of inhomogeneities or obstacles inside them or by considering the cylinder as an excitation or scatterer. They can also be of use in the study and design of antennas of high frequency whose performance is less affected by the biological systems and produce lower SAR.

The usefulness of the present technique obviously requires comparison with numerical and experimental results. It is envisaged that a later publication will address this aspect of the problem in more detail.

Chapter 8

Far Field Electromagnetic Modeling of Implantable Medical Devices Using Cylindrical DGFs

ELECTROMAGNETIC pollution is increasing due to massive increase in both mobile and fixed electronic equipments, whilst at the same time, industry is producing devices with ever increasing clock speeds. Modern wireless telecommunication devices (GSM Mobile system) can interfere with implantable medical devices/prostheses and cause possible malfunction. Also the performance of an antenna is significantly altered by the presence of conducting medical devices/prostheses. Hence the need to consider electromagnetic compatibility (EMC) becomes ever more important. The principle objective of this chapter is to outline a far field general expression of dyadic Green's function (DGF) for the problem of electromagnetic radiation from a source of excitation in the presence of a finite length of perfectly conducting circular cylinder of any size as well as of resonant length, which is valid everywhere, including the source region. The whole structure is assumed to be uniform along the propagation direction. The DGFs are obtained by employing the eigenfunction expansion (EFE) and the method of scattering superposition. The advantage of the proposed analysis is its simplicity and efficiency in computation.

8.1 Introduction

There is an accelerating growth in the use of radio transmission as the demand for mobile communication expands to embrace data as well as speech. As a result, the mutual interference between transmitting devices and active medical prostheses should be calculated. Analytical solutions are useful for calibrating measurement systems and understanding fundamental propagation mechanisms. We represent here implanted medical devices as conducting cylinders which can be embedded in concentric layered dielectrics.

Although electromagnetic scattering by a finite cylinder is a well known canonical problem, published work does not include the effects of arbitrary placed source point. The derivations presented here are motivated by the need to understand the behaviour of antennas/insulated antennas near to or embedded in living tissue. The eigenfunction expansion (EFE) of DGFs in electromagnetic theory provide a systematic means of constructing and interpreting these dyadics. The pioneering work by Tai [19] has set the stage for most of what has been achieved over the last two and a half decades. The expansion of DGFs in terms of the Hansen [25] vector wave functions must be carried out carefully in order to ensure that one is dealing with a complete expansion. Several theoretical studies have utilized DGFs to analyze the implanted head/body antenna models in Reyhani [29] - [31].

This chapter is organized as follows. The complete set of cylindrical vector wave functions are introduced in section 8.2. This material is included here in order to explicitly define notation and to call attention to a few points in connection with these expansions.

In section 8.3 we begin to formulate the problem for a finite circular cylinder and in subsection 8.3.1, we set out with the case, in which we construct the DGF, $\overline{\overline{G}}_{e1}(\overline{R}, \overline{R}')$, in terms that constitute the continuous eigenfunction expansion (EFE) in which the eigenfunctions are guided in the preferred r and z-coordinate directions, using the procedures described in Tai [19] or Collin [21]. This expansion also contains an explicit dyadic delta function term which is required for completeness at the

source point. It is considered as a correction to the general solenoidal EFE which is valid outside the source point.

The procedure required to derive the complete EFE of the scattering DGF for the finite circular cylinder, in terms of only the solenoidal eigenfunctions is shown to be a simple and straight-forward general expression and is summarized in subsection 8.3.2. The DGF for a finite conducting cylinder, $\overline{\overline{G}}_{E1}(\overline{R},\overline{R}')$ can be constructed from the principle of the superposition, where it satisfies the boundary conditions. The far zone field expression of the prosthesis configuration has been developed in subsection 8.3.3.

Magnetic type DGF discussed in section 8.4, can be found by invoking duality or once the electric field is obtained the magnetic field is derivable by taking the curl of the electric field, and vice versa.

Conclusions are then presented in section 8.6 summarizing the important points contained in this work.

8.2 Vector Wave Functions for a Circular Cylinder of Finite Length

The cylindrical vector wave functions are the building blocks of the EFE of various kinds of DGFs. They are solutions of the homogeneous vector Helmholtz equation. The generating or eigenfunctions, which are solutions of the cylindrical scalar wave equation $\nabla^2\Psi + k_\lambda^2\Psi=0$ can be written [29] in the form

$$\Psi_{\substack{e\\o}\eta}(h) = j_n(\lambda r)^{\cos}_{\sin} n\phi^{\cos}_{\sin} hz, \tag{8.1}$$

Here subscripts "e" stands for even and "o" is the odd character of the generating functions. $h = \frac{q\pi}{l}$ are the eigenvalues in the z-direction with $q = 0, 1, 2, ...$ and l is the length of cylinder. $j_n(\lambda r)$ identifies the cylindrical Bessel functions of the order n to represent both out-going and in-coming waves. λ is the continuous eigenvalue. Cylindrical vector wave functions are akin to the Debye potentials. $\overline{P}_{\substack{e\\o}\eta\lambda}(h) =$

$\nabla\times[\Psi_{\substack{ee\\oo}n}\hat{z}]$ and $\overline{Q}_{\substack{ee\\oo}n\lambda}(h) = \frac{1}{k_\lambda}\nabla\times\nabla\times[\Psi_{\substack{ee\\oo}n}\hat{z}]$. Where $\hat{z}$ is the piloting vector and here $k_\lambda^2 = \lambda^2 + h^2$.

The complete expressions for the solenoidal (rotational or transverse) and the nonsolenoidal (irrotational or lamellar) functions are given in Reyhani [28]. These functions are defined in the entire space, corresponding to $0 \leq r \leq \infty$, $0 \leq \phi \leq 2\pi$ and $0 < z < l$.

8.3 Formulation of the Problem

Consider the cylinder in Figure 7 of radius "α" concentric along z-axis with length "l" is illuminated by an electromagnetic wave. An electromagnetic field is induced in the system and an electromagnetic wave is scattered by the system.

A time dependence $e^{j\omega t}$ is assumed and suppressed throughout.

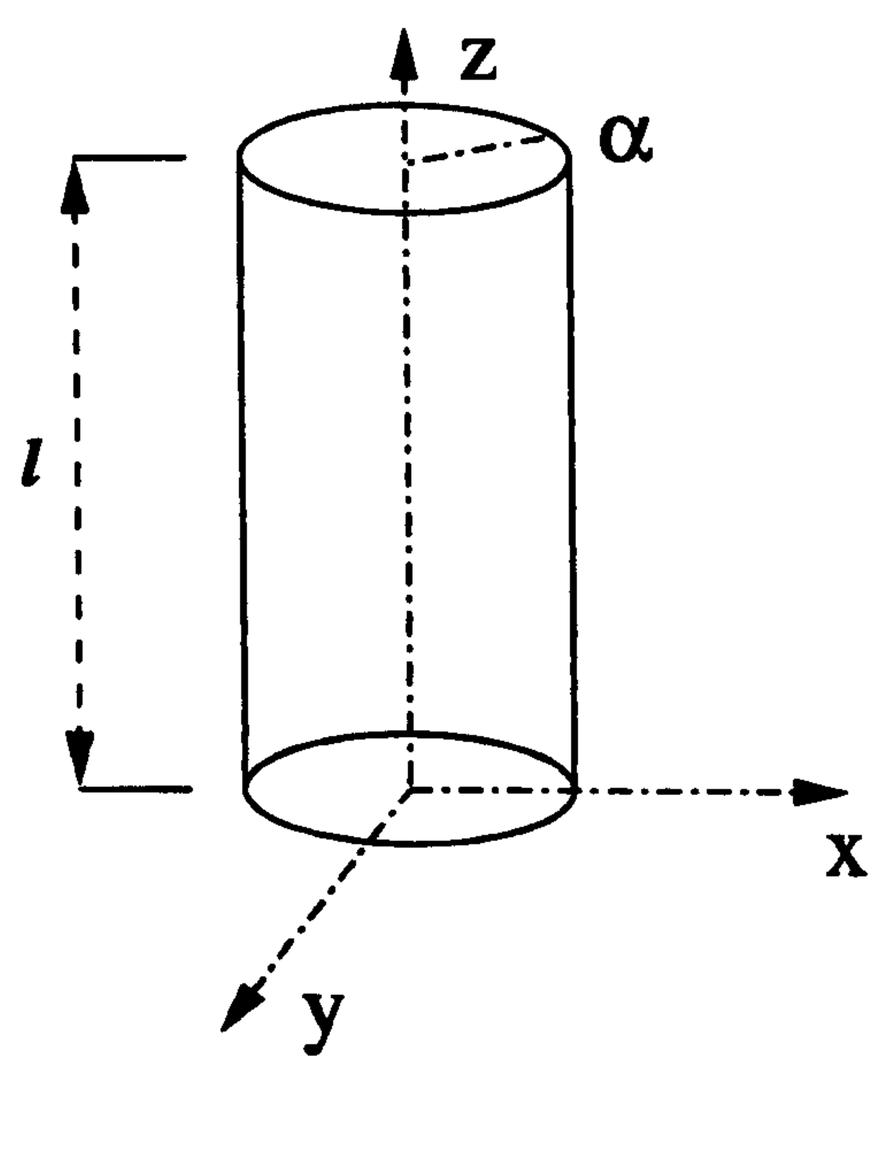

Figure 7: Diagram of a Finite Circular Cylinder

8.3.1 DGF for a Finite Length Cylinder of Circular Cross-Section

Applying the method of (G_m) and according to the Ohm-Rayleigh procedure the expression for $(\overline{\overline{G}}_{e1})$ for a finite cylinder of radius "α" concentric with the z-axis is

given in Reyhani [28] in the form

$$\overline{\overline{G}}_{e1}(\overline{R},\overline{R}') = -\frac{\hat{r}\hat{r}}{k^2}\delta_e(\overline{R}-\overline{R}') + \int_0^l dh \sum_{n=0}^{\infty} C_\lambda$$

$$\cdot \begin{cases} \left\{ \begin{array}{l} [\overline{P}^{(1)}_{\substack{e_o e_o \\ o o}\eta_o}(h;\eta_o)\overline{P}'_{\substack{e_o e_o \\ o o}\eta_o}(h;\eta_o)] \\ [\overline{Q}^{(1)}_{\substack{e_e e_e \\ o o}\eta_o}(h;\eta_o)\overline{Q}'_{\substack{e_e e_e \\ o o}\eta_o}(h;\eta_o)] \end{array} \right\}, & r > r', \\ \left\{ \begin{array}{l} [\overline{P}_{\substack{e_o e_o \\ o o}\eta_o}(h;\eta_o)\overline{P}'^{(1)}_{\substack{e_o e_o \\ o o}\eta_o}(h;\eta_o)] \\ [\overline{Q}_{\substack{e_e e_e \\ o o}\eta_o}(h;\eta_o)\overline{Q}'^{(1)}_{\substack{e_e e_e \\ o o}\eta_o}(h;\eta_o)] \end{array} \right\}, & r < r'. \end{cases} \tag{8.2}$$

where coefficient $C_\lambda = \frac{i(2-\delta_o^n)}{2l\eta_o^2}$.

8.3.2 Scattering DGF for a Finite Conducting Cylinder of Circular Cross-Section

When a perfectly conducting cylinder of the same size as above is illuminated by an electromagnetic wave, the scattered terms can be written in the form

$$\overline{\overline{G}}_{es}(\overline{R},\overline{R}') = \int_0^l dh \sum_{n=0}^{\infty} C_\lambda \cdot \begin{bmatrix} \alpha_{\substack{e_o e_o \\ o o}\eta}\overline{P}^{(1)}_{\substack{e_o e_o \\ o o}\eta}(h;\eta)\overline{P}'^{(1)}_{\substack{e_o e_o \\ o o}\eta}(h;\eta) \\ \beta_{\substack{e_e e_e \\ o o}\eta}\overline{Q}^{(1)}_{\substack{e_e e_e \\ o o}\eta}(h;\eta)\overline{Q}'^{(1)}_{\substack{e_e e_e \\ o o}\eta}(h;\eta) \end{bmatrix}. \tag{8.3}$$

Applying the principle of scattering superposition, we obtain

$$\overline{\overline{G}}_{E1}(\overline{R},\overline{R}') = \overline{\overline{G}}_{e1}(\overline{R},\overline{R}') + \overline{\overline{G}}_{es}(\overline{R},\overline{R}') \tag{8.4}$$

Where we consider the function for a finite circular cylinder in a region $0 \le r \le \infty$. After applying the boundary condition one can determine the unknown coefficients. In order to satisfy the boundary condition at interface $r = \alpha$,

$$\hat{r} \times \left[\overline{P}_{\substack{e_o e_o \\ o o}\eta}(h;\eta)\overline{P}'^{(1)}_{\substack{e_o e_o \\ o o}\eta}(h;\eta) + \alpha_{\substack{e_o e_o \\ o o}\eta}\overline{P}^{(1)}_{\substack{e_o e_o \\ o o}\eta}(h;\eta)\overline{P}'^{(1)}_{\substack{e_o e_o \\ o o}\eta}(h;\eta)\right]_{r=\alpha} \tag{8.5}$$

$$\hat{r} \times \left[\overline{Q}_{\substack{e_e e_e \\ o o}\eta}(h;\eta)\overline{Q}'^{(1)}_{\substack{e_e e_e \\ o o}\eta}(h;\eta) + \beta_{\substack{e_e e_e \\ o o}\eta}\overline{Q}^{(1)}_{\substack{e_e e_e \\ o o}\eta}(h;\eta)\overline{Q}'^{(1)}_{\substack{e_e e_e \\ o o}\eta}(h;\eta)\right]_{r=\alpha} \tag{8.6}$$

$$\hat{r}\times\left[\overline{P}_{\substack{e_o\\o}\eta}(h;\eta)+\alpha_{\substack{e_o\\o}\eta}\overline{P}^{(1)}_{\substack{e_o\\o}\eta}(h;\eta)\right]_{r=\alpha}=0 \tag{8.7}$$

$$\hat{r}\times\left[\overline{Q}_{\substack{e_e\\o}\eta}(h;\eta)+\beta_{\substack{e_e\\o}\eta}\overline{Q}^{(1)}_{\substack{e_e\\o}\eta}(h;\eta)\right]_{r=\alpha}=0 \tag{8.8}$$

substituting for $\overline{P}_{\substack{e_o\\o}\eta}(h;\eta)$ and $\overline{P}^{(1)}_{\substack{e_o\\o}\eta}(h;\eta)$

$$\overline{P}_{\substack{e_o\\o}\eta}(h;\eta)=\nabla\times[j_n(\eta r)^{\cos}_{\sin}n\phi\sin hz\hat{z}], \tag{8.9}$$

$$\overline{P}^{(1)}_{\substack{e_o\\o}\eta}(h;\eta)=\nabla\times[H^{(1)}_n(\eta r)^{\cos}_{\sin}n\phi\sin hz\hat{z}], \tag{8.10}$$

in equation (8.7) produces $\alpha_{\substack{e_o\\o}\eta}=-\frac{[\partial j_n(\eta\alpha)]/\partial(\eta\alpha)}{[\partial H^{(1)}_n(\eta\alpha)]/\partial(\eta\alpha)}$.

Similarly inserting for $\overline{Q}_{\substack{e_e\\o}\eta}(h;\eta)$ and $\overline{Q}^{(1)}_{\substack{e_e\\o}\eta}(h;\eta)$

$$\overline{Q}_{\substack{e_e\\o}\eta}(h;\eta)=\frac{1}{k}\nabla\times\nabla\times[j_n(\eta r)^{\cos}_{\sin}n\phi\cos hz\hat{z}], \tag{8.11}$$

$$\overline{Q}^{(1)}_{\substack{e_e\\o}\eta}(h;\eta)=\frac{1}{k}\nabla\times\nabla\times[H^{(1)}_n(\eta r)^{\cos}_{\sin}n\phi\cos hz\hat{z}], \tag{8.12}$$

in equation (8.8) produces $\beta_{\substack{e_e\\o}\eta}=-\frac{[j_n(\eta\alpha)]}{[H^{(1)}_n(\eta\alpha)]}$.

8.3.3 Far Zone Field Expression of the Prosthesis Configuration

The far field of this medical device in the presence of a source can be computed using the asymptotic expression for $\overline{\overline{G}}_{E1}(\overline{R},\overline{R}')$, utilizing the saddle-point integration method. Assuming $\eta r\gg 1$, the Hankel function in $\overline{P}^{(1)}_{\substack{e_o\\o}\eta}(h;\eta)$ and $\overline{Q}^{(1)}_{\substack{e_e\\o}\eta}(h;\eta)$ can be approximated to its asymptotic expression, Chew [40, chap.1, page 15]

$$H^{(1)}_n(\eta r)\simeq\left(\frac{2}{\pi\eta r}\right)^{\frac{1}{2}}(-i)^{n+\frac{1}{2}}e^{i\eta r} \tag{8.13}$$

$$\overline{P}^{(1)}_{\substack{e_o\\o}\eta}(h;\eta)\simeq(-i)^{n+\frac{3}{2}}\eta\left(\frac{2}{\pi\eta r}\right)e^{i(\eta r+hz)}{}^{\cos}_{\sin}n\phi\sin hz\hat{\phi} \tag{8.14}$$

$$\overline{Q}^{(1)}_{\substack{e_e\\o}\eta}(h;\eta)\simeq(-i)^{n+\frac{1}{2}}\frac{\eta}{k}\left(\frac{2}{\pi\eta r}\right)^{\frac{1}{2}}e^{i(\eta r+hz)}\cdot\left\{\begin{array}{l}{}^{\cos}_{\sin}n\phi\sin hz(-h\hat{r})\\ {}^{\cos}_{\sin}n\phi\cos hz(\eta\hat{z})\end{array}\right\} \tag{8.15}$$

The expression for $\overline{\overline{G}}_{E1}(\overline{R},\overline{R}')$ can be approximated with the functions $\overline{P}^{(1)}_{\substack{eo\\o}\eta}(h;\eta)$ and $\overline{Q}^{(1)}_{\substack{ee\\o}\eta}(h;\eta)$ replaced by (8.14) and (8.15), can be written in the form

$$\overline{\overline{G}}_{E1}(\overline{R},\overline{R}') \simeq \int_0^l dh \sum_{n=0}^{\infty} C_\lambda \frac{2\eta}{(2\pi\eta r)^{\frac{1}{2}}}(-i)^{n+\frac{1}{2}} e^{i(\eta r+hz)} \cdot \left\{ \begin{array}{l} -i^{\cos}_{\sin} n\phi \sin hz\hat{\phi} \begin{bmatrix} \overline{P}'_{\substack{eo\\o}\eta}(h;\eta) \\ \alpha_{\substack{eo\\o}\eta}\overline{P}^{(1)}_{\substack{eo\\o}\eta}(h;\eta) \end{bmatrix} \\ \frac{1}{k}{}^{\cos}_{\sin} n\phi \sin hz(-h\hat{r}) \begin{bmatrix} \overline{Q}'_{\substack{ee\\o}\eta}(h;\eta) \\ \beta_{\substack{ee\\o}\eta}\overline{Q}^{(1)}_{\substack{ee\\o}\eta}(h;\eta) \end{bmatrix} \\ \frac{1}{k}{}^{\cos}_{\sin} n\phi \cos hz(\eta\hat{z}) \begin{bmatrix} \overline{Q}'_{\substack{ee\\o}\eta}(h;\eta) \\ \beta_{\substack{ee\\o}\eta}\overline{Q}^{(1)}_{\substack{ee\\o}\eta}(h;\eta) \end{bmatrix} \end{array} \right\} \tag{8.16}$$

where terms of the order $\geq (\eta r)^{-\frac{3}{2}}$ have been ignored.

8.4 Magnetic DGF in the Antenna-Prosthesis Configuration

The principle of duality states that once the electric DGF is obtained, the magnetic DGF is derivable by interchanging the field functions $\overline{P}_{\substack{ee\\oo}} \rightarrow k\overline{Q}_{\substack{ee\\oo}}$ and $\overline{Q}_{\substack{ee\\oo}} \rightarrow k\overline{P}_{\substack{ee\\oo}}$ and omitting the singularity term contribution and vice versa.

On the other hand, the corresponding total magnetic DGF at any point in the system can be calculated from $\nabla \times \overline{\overline{G}}_e = \overline{\overline{G}}_m$, bearing in mind the discontinuous nature of magnetic DGF across a point source at $R = R'$ and the Ampère-Maxwell equation relating $\overline{\overline{G}}_e$ and $\overline{\overline{G}}_m$ in the dyadic form i.e.:

$$\nabla \times \overline{\overline{G}}_m = \overline{\overline{I}}\delta_e(\overline{R}-\overline{R}') + k^2\overline{\overline{G}}_e. \tag{8.17}$$

8.5 Electric and Magnetic Field at any Point in the Configuration

The use of DGF technique allows us to determine the expansion of the electric and magnetic fields in a cylinder/antenna configuration in a direct and elegant manner.

For any current source with current density function $\overline{J}(\overline{R}')$ located outside the cylinder, the electric or magnetic field radiated by such a dipole can be calculated using the formulae,

$$\overline{E}(\overline{R}) = i\omega\mu_o \iiint_V \overline{\overline{G}}_{E1}(\overline{R},\overline{R}') \cdot \overline{J}(\overline{R}')dV' \tag{8.18}$$

$$\overline{H}(\overline{R}) = i\omega\varepsilon_o \iiint_V \overline{\overline{G}}_{M1}(\overline{R},\overline{R}') \cdot \overline{J}(\overline{R}')dV'. \tag{8.19}$$

These signify the computation of the E and H-fields in the structure, which states the superposition of the incident field $\overline{E}_i(\overline{R})$ or $\overline{H}_i(\overline{R})$ and the scattered field $\overline{E}_s(\overline{R})$ or $\overline{H}_s(\overline{R})$ is given by

$$\overline{E}(\overline{R}) = \overline{E}_i(\overline{R}) + \overline{E}_s(\overline{R}) \tag{8.20}$$

$$\overline{H}(\overline{R}) = \overline{H}_i(\overline{R}) + \overline{H}_s(\overline{R}). \tag{8.21}$$

8.6 Concluding Remarks

General far field expressions have been derived in simple form for the finite conducting circular cylinder (medical devices/prostheses) of any size as well as of very small radius (resonant length). The DGFs are obtained by employing the EFE and the method of scattering superposition.

The results of this chapter could be useful for a further analysis of the problem as a thin wire/insulated wire or an implant/dielectric-coated implant such as heart pace-maker embedded in the body and biotelemetry transmitters for medical applications and could easily be expanded to handle any scatterer having finite radius and length. They can be applied to problems of optical fibers and waveguides for the investigation of inhomogeneities or obstacles inside them or by considering the cylin-

der as an excitation or scatterer. They can also be of use in the study and design of antennas of high frequency whose performance is less affected by the biological systems and produce lower SAR (specific absorption rate, the rate of electromagnetic energy deposition) and as a result contribute to the efficiency of handheld/mobile phones.

Numerical simulation techniques developed for the comprehensive analysis of the human exposure to electromagnetic waves and estimating the SAR may require considerable time and large computer memory for calculation. Analytical methods provide valuable tools in evaluating the interaction between canonical head/body models and antenna sources. The usefulness of the present technique obviously requires comparison with numerical and experimental results. It is envisaged that a later publication will address this aspect of the problem in more detail.

Chapter 9

Implanted Spherical Head Model for Numerical EMC Investigation

PERSONAL communication systems and cellular phones are required to operate satisfactory beside the human body. They are usually hand-held and randomly orientated by the operator. Therefore, their antennas are required to be small in size, light-weight, and sensitive to two perpendicular polarizations. Their radiation patterns should be quasi-isotropic, in all the principal planes, and they should have a wide bandwidth. In this case, the antenna is very close to the user's head during normal use of the handset and there is concern about the level of microwave emissions to which the brain is being exposed. The effect of the human body on the antenna as well as the specific absorption rate (SAR) of the radiation from the antenna by the human body should be as small as possible. Reports have appeared in the media linking the use of mobile telephones with, among other things, headaches, hot spots in the brain and brain cancer. Therefore, caution should be exercised when using modern wireless telecommunication devices around sensitive electromedical equipments used in hospital intensive care units. Mobile telephones can also cause interference in certain other medical devices, such as cardiac pace makers and hearing aids. Key issues to address are the questions of whether mobile phones have a detrimental effect on implants, and how the interaction of the handset with the body can be minimized in order to both alleviate public fears and improve

handset antenna performance and new prosthetic designs.

This work supplements the previous chapters. It aims to extend the results of scattering of electromagnetic waves by a spherical head model in chapter 3 to the scattering of a plane EM wave from a perfectly conducting spherical/cylindrical implant of electrically small radius (of resonant length), embedded eccentrically into a dielectric spherical head model. The method of dyadic Green's function (DGF) for spherical vector wave functions is used. Analytical expressions for the scattered fields of both cylindrical and spherical implants embedded head models are obtained. The whole structure is assumed to be uniform along the propagation direction. It is assumed that the size of the head is much larger than the size and thickness of the implant so that the fringing field can be neglected. The effect of interconnect cross section and the fringing field are not taken into account.

The advantage of the proposed analysis is its simplicity and efficiency in computation.

9.1 Introduction

The march of progress is immutable. Like the rising and setting of the sun, so technology evolves, changing the patterns of our daily lives. The need for higher performance in devices as well as in human functions has been debated for many years. The experimental discipline of neural control relies on the exchange of information between an electronic circuit and a nervous system for the purpose of studying or supplementing a biological function. One of the main objectives of such research is the development of prosthetic devices for replacing defective parts of the human nervous system. The cochlea implant aids hearing, while a similar implant recently stopped the shake in Parkinson's disease sufferers. A computer-memory chip implanted into the optical nerve behind the eye could record a person's every lifetime thought, sensation and visual data could be developed. By combining this information with a record of the person's genes, one could create a person physically, emotionally and spiritually. Similar receptors could gather signals for smell, sound,

taste and touch. Down-loading the experience of an older person can enhance the quality of life of a younger one. This could revolutionize the communication beyond current concepts.

Like a computer with ever larger and larger memory and better and more powerful processor one can enhance the memory capacity and processing power of brain by means of implants. Whence all these implants can be developed as one unit and can also be automatically controlled by remote sensing. The most important feature of this system is the active security and monitoring of both the system and its information contents to be prevented from unauthorized users gaining access to the system.

Of course, these new developments are not going to happen overnight. The proposals won't be set in stone until years to come. But, in the meantime where they comfortably fulfill the need, the contribution of the EM fields must, of course, be considered in antennae, prostheses and equipment design and certification. These can be designed to produce improved EMC performance.

Strong interest in the bio-medical/engineering applications of modeling biological bodies exposed in near as well as in the far-field is to assess the induced and scattered fields. The scattering of EM waves by spherical head and cylindrical torso models have been studied in my previous chapters. In this chapter we have extended these results to the electromagnetic case for a simple implanted head/torso model by a perfect conductor.

This chapter is formatted as follows. The relations between the unit vectors in coordinate systems and the relationship between the spherical and cylindrical coordinates have been pointed out in section 9.2. Vector wave functions are introduced in section 9.3.

In section 9.4 we begin to formulate the problem for an spherical head model embedded with a prosthesis model (finite circular cylinder/sphere).

Subsection 9.4.2, presents the general scattering DGFs expansions (9.25) and (9.26) for the implanted head model problem in terms of only the solenoidal eigenfunctions.

It is in this development that the principal point of this chapter is identified.

Magnetic type DGF can be found by invoking duality or once the electric field is obtained the magnetic field is derivable by taking the curl of the electric field, and vice versa.

Conclusions are then presented in section 9.7 summarizing the important points contained in this work.

9.2 Relations between the Unit Vectors in Coordinate Systems

The spatial variables associated with three commonly used coordinate systems (The Cartesian, x, y, z, Cylindrical, r, ϕ, z, and Spherical, R, θ, ϕ) are shown in Figure 8. It should be pointed out that the same ϕ-variable is used for both the cylindrical and the spherical systems.

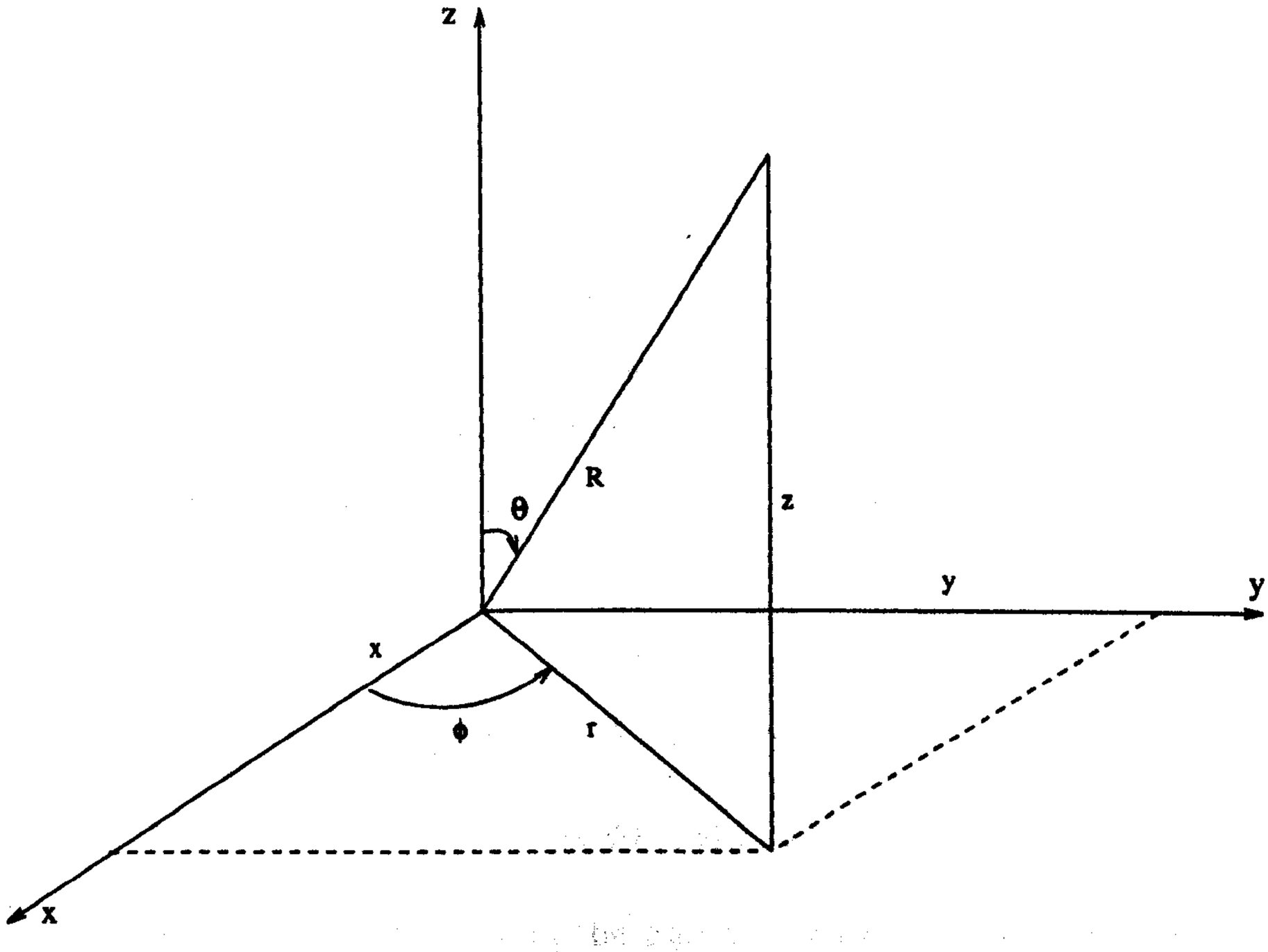

Figure 8: Three Commonly Used Coordinate Systems

From the above diagram one can deduce the following equations between cylin-

drical and spherical, and also with rectangular coordinate systems

$$R^2_{sphere} = x^2 + y^2 + z^2 \tag{9.1}$$

$$r^2_{cylinder} = x^2 + y^2 \tag{9.2}$$

The relationship between the cylindrical coordinates (r, ϕ, z) and the spherical coordinates (R, ϕ, θ) of a point is

$$R^2_{sphere} = r^2_{cylinder} + z^2, \qquad \phi = \phi, \qquad \tan\theta = \frac{r_{cylinder}}{z} \tag{9.3}$$

The relationship between the spherical coordinates (R, ϕ, θ) and the cylindrical coordinates (r, ϕ, z) of a point is

$$r_{cylinder} = R_{sphere}\sin\theta, \qquad \phi = \phi, \qquad z = R_{sphere}\cos\theta \tag{9.4}$$

The relation between these unit vectors are summarized in Table 1 and Table 2.

Unit Vectors	$\hat{\mathbf{x}}$	$\hat{\mathbf{y}}$	$\hat{\mathbf{z}}$
$\hat{\mathbf{r}}$	$+\cos\phi$	$+\sin\phi$	0
$\hat{\phi}$	$-\sin\phi$	$+\cos\phi$	0
$\hat{\mathbf{z}}$	0	0	1

Table 1: Relations between the Unit Vectors in the Rectangular and the Cylindrical Coordinate Systems

To express unit vector $\hat{r}$ in terms of the unit vectors in rectangular system, one uses the coefficients in the first row of Table: 1, which gives

$$\hat{r} = \cos\phi\hat{x} + \sin\phi\hat{y}. \tag{9.5}$$

To express unit vector $\hat{x}$ in terms of the unit vectors in spherical system, one uses the coefficients in the first column of (Table: 2), which gives

$$\hat{x} = \sin\theta\cos\phi\hat{R} + \cos\theta\cos\phi\hat{\theta} - \sin\phi\hat{\phi}. \tag{9.6}$$

Unit Vectors	$\hat{\mathbf{x}}$	$\hat{\mathbf{y}}$	$\hat{\mathbf{z}}$
$\hat{\mathbf{R}}$	$\sin\theta\cos\phi$	$\sin\theta\sin\phi$	$\cos\theta$
$\hat{\theta}$	$\cos\theta\cos\phi$	$\cos\theta\sin\phi$	$-\sin\theta$
$\hat{\phi}$	$-\sin\phi$	$\cos\phi$	0

Table 2: Relations between the Unit Vectors in the Rectangular and the Spherical Coordinate Systems

9.3 Vector Wave Functions for an Implanted Spherical Head Model

The generating function for a finite length cylinder in cylindrical coordinates is represented in chapter 4, by the equation (4.8).

$$\Psi_{\substack{ee\\oo}mn}(h) = j_n(\lambda r)^{\cos}_{\sin} n\phi^{\cos}_{\sin} hz, \tag{9.7}$$

Also the generating function or eigenfunction for an sphere in spherical coordinate system is mentioned in chapter 3, by the equation (3.1).

$$\Psi_{emn}(k) = j_n(kR)P_n^m(\cos\theta)^{\cos}_{\sin} m\phi, \tag{9.8}$$

For an implanted head model the generating function is a combination of generating functions of both head (sphere) and prosthesis (cylinder) together, such as

$$\Psi_{total} = \Psi_{head} + \Psi_{implant\ spherical} \tag{9.9}$$

$\Psi_{implant\ spherical}$ designates the generating function of the prosthesis in spherical coordinate system and in this case

$$\Psi_{total} = \Psi_{emn}(k) + \Psi_{\substack{ee\\oo}mn}(h)_{spherical} \tag{9.10}$$

Where $\Psi_{\substack{ee\\oo}mn}(h)_{spherical}$ represents the eigenfunction for the cylinder but converted to spherical coordinates using equations given in the last section. One thing to remember is the origin of cylinder in this case start from a distance from the coordinate

system. Also bearing in mind that the spherical Bessel function is related to the half-order cylindrical Bessel function

$$j_n(x) = \left(\frac{\pi}{2x}\right)^{\frac{1}{2}} J_{(n+\frac{1}{2})}(x) \tag{9.11}$$

The spherical Hankel function of the first kind, denoted by $h_n^{(1)}(x)$, is also related to the half-order cylindrical Hankel function of the first kind in the same way.

$$h_n^{(1)}(x) = \left(\frac{\pi}{2x}\right)^{\frac{1}{2}} H^{(1)}_{(n+\frac{1}{2})}(x) \tag{9.12}$$

Now the total spherical vector wave functions (denoted by $\overline{L}_{total}$, $\overline{M}_{total}$, and $\overline{N}_{total}$) can be calculated in the same manner as those introduced in chapter 3, in section 3.2 by the equations (3.2), (3.3) and (3.4).

9.4 Formulation of the Problem

When electric fields act on conductive materials, they influence the distribution of electric charges at their surface. Tiny electrical currents exist in the human body due to the chemical reactions that occur as part of the normal bodily functions, even in the absence of external electric fields. For example, nerves relay signals by transmitting electric impulses. Most biochemical reactions from digestion to brain activities go along with the rearrangement of charged particles. Even the heart is electrically active - an activity that ones doctor can trace with the help of an electrocardiogram.

The parameters that influence the antenna-user interaction are

i) to what extent the effect of the human head/body with/without implant on the antenna radiation pattern can be simulated;

ii) how well do SAR's obtained predict those in the body;

iii) how important are the quality and resolution of the model in determination of the body effect on the antenna pattern, total power absorbed in the body (or antenna efficiency in the presence of users).

Interest in such problems arises from their usefulness in the detection of metallic bodies embedded in dielectrics, in the determination of scattering by "impurities" in dielectric structures, etc. Also, scattering data from complex bodies is often used to obtain information about their internal structure (inhomogeneities, nonsymmetries etc.).

Consider an implanted spherical head model as in Figure 9 is illuminated by an electromagnetic wave. An electromagnetic field is induced in the system and an electromagnetic wave is scattered by the system.

A time dependence $e^{j\omega t}$ is assumed and suppressed throughout.

9.4.1 Free Space DGF for an Electric Dipole in Unbounded Medium

The electric and magnetic field intensities of an incident electromagnetic wave traveling due to an electric dipole located at R' in an infinite homogeneous space without the presence of an scatterer (obstacle) can be computed in spherical coordinates based on derivations in chapter 3.

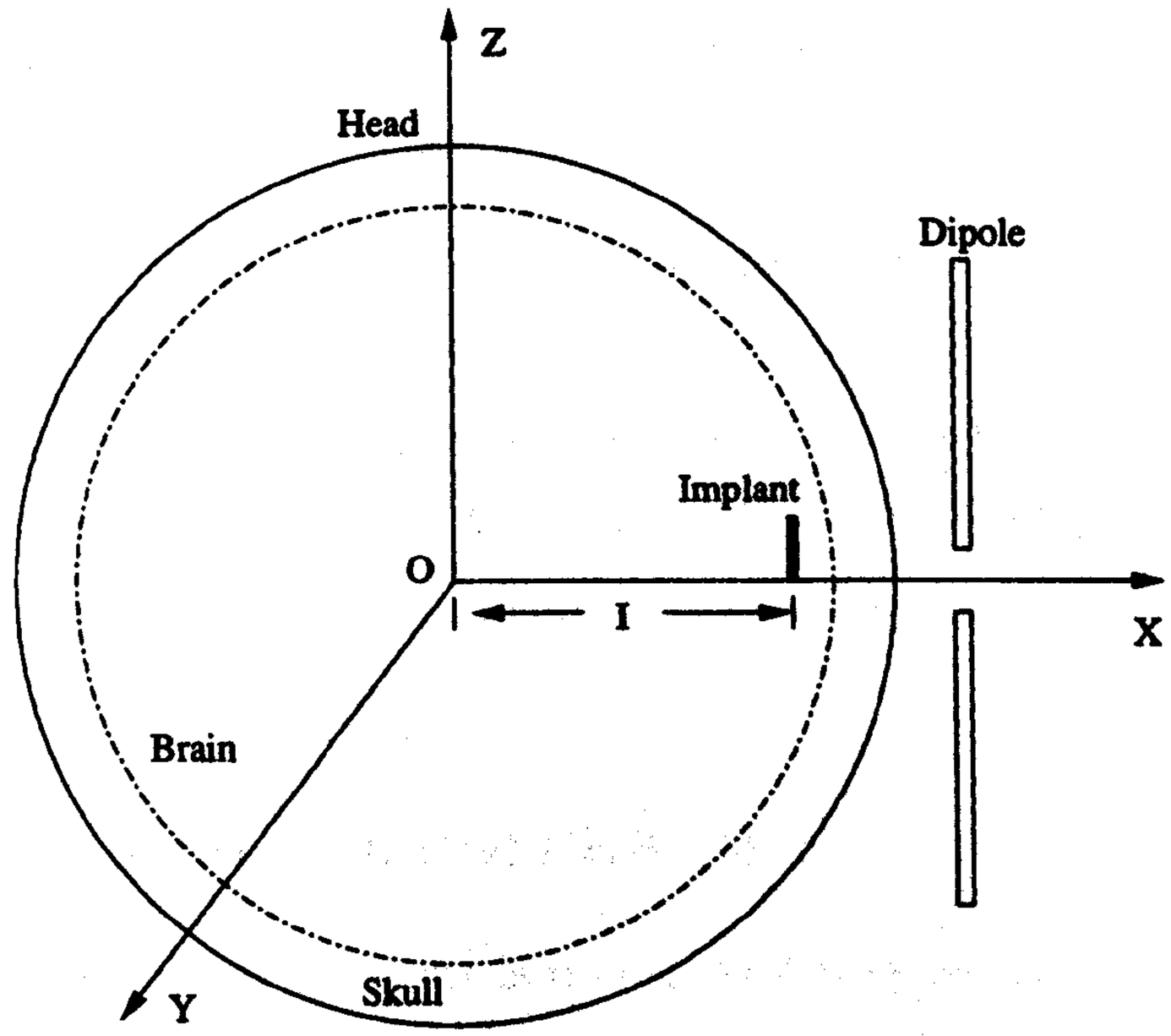

Figure 9: Diagram of an Implanted Head radiated by a Dipole

$$\overline{\overline{G}}^{00o}_{eo}(\overline{R},\overline{R}') = -\frac{\hat{R}\hat{R}}{k_o^2}\delta(\overline{R}-\overline{R}') + \frac{ik_o}{4\pi}\sum_{n=1}^{\infty}\sum_{m=0}^{n} C_{mn}$$
$$\cdot\begin{cases} \left\{ \begin{array}{l} [\overline{M}^{(1)}_{\substack{e\\o}mn}(k_o)\overline{M}'_{\substack{e\\o}mn}(k_o)] \\ [\overline{N}^{(1)}_{\substack{e\\o}mn}(k_o)\overline{N}'_{\substack{e\\o}mn}(k_o)] \end{array} \right\}, & R > R', \\ \left\{ \begin{array}{l} [\overline{M}_{\substack{e\\o}mn}(k_o)\overline{M}'^{(1)}_{\substack{e\\o}mn}(k_o)] \\ [\overline{N}_{\substack{e\\o}mn}(k_o)\overline{N}'^{(1)}_{\substack{e\\o}mn}(k_o)] \end{array} \right\}, & R < R'. \end{cases} \tag{9.13}$$

As before in chapter 3,

$$C_{mn} = (2-\delta_o^m)\frac{2n+1}{n(n+1)}\frac{(n-m)!}{(n+m)!} \tag{9.14}$$

Again coefficient C_{mn} depends on the value of m and n, where δ_o^m is the Kronecker delta functions, when

$$\delta = \begin{cases} 1, & \text{if } m = o, \\ 0, & \text{if } m \neq o \end{cases}. \tag{9.15}$$

9.4.2 Scattering DGFs for an Electric Dipole in the Presence of an Implanted Spherical Head Model

The scattering from composite bodies can give information for their internal composition. Thus, by observing their scattered field one can detect inner inhomogeneities, nonsymmetries, etc. In this chapter the medium is assumed to be isotropic, linear, nondispersive and stationary. We now use the DGF for an unbounded medium in terms of spherical vector wave functions to construct one for an implanted spherical head model.

DGF for a Single-layer Spherical Head Model

This can be considered as the contribution of the reflections and transmissions of a single layer sphere of radius α_1 centered at O, superimposed in an unbounded homogeneous medium with the radiation source located outside the sphere at R'. The

medium is characterized by (μ_o, ε_o), and material properties of sphere is represented by $(\mu_{hl}, \varepsilon_{hl})$, where subscripts "$o$" and "$h$" stand for unbounded (open) space and head, respectively.

The scattered DGF term for the exterior of head model in this case has the form

$$\overline{\overline{G}}^{10o}_{es}(\overline{R},\overline{R}') = \frac{ik_o}{4\pi}\sum_{n=1}^{\infty}\sum_{m=0}^{n} C_{mn}\cdot\begin{bmatrix} A^{10o}_{e_oM}\overline{M}^{(1)}_{e_omn}(k_o)\overline{M}'^{(1)}_{e_omn}(k_o) \\ A^{10o}_{e_oN}\overline{N}^{(1)}_{e_omn}(k_o)\overline{N}'^{(1)}_{e_omn}(k_o)\end{bmatrix}, \tag{9.16}$$

It is apparent that the presence of the inner conducting prosthesis, with very small dimensions, slightly perturb, the intensity of the scattered field and for the interior region, the total scattering DGF comprises of the DGF of the inner head as well as the scattering from the prosthesis i.e.

$$\left(\overline{\overline{G}}^{11o}_{es}(\overline{R},\overline{R}')\right)_{total} = \left(\overline{\overline{G}}^{11o}_{es}(\overline{R},\overline{R}')\right)_{head} + \left(\overline{\overline{G}}_{es}(\overline{R},\overline{R}')\right)_{implant} \tag{9.17}$$

Where

$$\left(\overline{\overline{G}}^{11o}_{es}(\overline{R},\overline{R}')\right)_{head} = \frac{ik_o}{4\pi}\sum_{n=1}^{\infty}\sum_{m=0}^{n} C_{mn}\cdot\begin{bmatrix} B^{11o}_{e_oM}\overline{M}_{e_omn}(k_1)\overline{M}'^{(1)}_{e_omn}(k_o) \\ B^{11o}_{e_oN}\overline{N}_{e_omn}(k_1)\overline{N}'^{(1)}_{e_omn}(k_o)\end{bmatrix}. \tag{9.18}$$

The scattered terms for a perfectly conducting cylindrical implant model (presented in chapter 5, (5.14)) can be written in the form

$$\left(\overline{\overline{G}}_{es}(\overline{R},\overline{R}')\right)_{implant} = \int_0^l dh\sum_{n=0}^{\infty} C_\lambda\cdot\begin{bmatrix} \alpha_{e_oe_o\eta}\overline{P}^{(1)}_{e_oe_o\eta}(h;\eta)\overline{P}'^{(1)}_{e_oe_o\eta}(h;\eta) \\ \beta_{e_oe_e\eta}\overline{Q}^{(1)}_{e_oe_e\eta}(h;\eta)\overline{Q}'^{(1)}_{e_oe_e\eta}(h;\eta)\end{bmatrix}. \tag{9.19}$$

Here, the coefficients are

$$\alpha_{e_oe_o\eta} = -\frac{[\partial j_n(\eta\alpha)]/\partial(\eta\alpha)}{[\partial H^{(1)}_n(\eta\alpha)]/\partial(\eta\alpha)}, \tag{9.20}$$

$$\beta_{e_oe_e\eta} = -\frac{[j_n(\eta\alpha)]}{[H^{(1)}_n(\eta\alpha)]}. \tag{9.21}$$

On the other hand, the scattered terms for a perfectly conducting spherical implant model is stated in chapter 3, (9.22) presented in the form

$$\left(\overline{\overline{G}}_{es}(\overline{R},\overline{R}')\right)_{implant} = \frac{ik_o}{4\pi}\sum_{n=1}^{\infty}\sum_{m=0}^{n} C_{mn}\cdot\begin{bmatrix} \alpha_{e_oM}\overline{M}^{(1)}_{e_omn}(k_o)\overline{M}'^{(1)}_{e_omn}(k_o) \\ \beta_{e_oN}\overline{N}^{(1)}_{e_omn}(k_o)\overline{N}'^{(1)}_{e_omn}(k_o)\end{bmatrix}, \tag{9.22}$$

Where the coefficients are

$$\alpha_{e_o M} = -\frac{[j_n(k_o\alpha)]}{[h_n^{(1)}(k_o\alpha)]}, \tag{9.23}$$

$$\beta_{e_o N} = -\frac{\partial[(k_o\alpha)j_n(k_o\alpha)]/\partial(k_o\alpha)}{\partial[(k_o\alpha)h_n^{(1)}(k_o\alpha)]/\partial(k_o\alpha)}. \tag{9.24}$$

Where the wave number in any medium is $k_f^2 = \omega^2(\mu_f\varepsilon_f)$ and $\eta_f^2 = (k_f^2 - h^2)$.

The principle of scattering superposition can now be applied to compute the total DGF exterior or interior of the obstacle,

$$\overline{\overline{G}}_{E1}^{10o}(\overline{R},\overline{R}') = \overline{\overline{G}}_{eo}(\overline{R},\overline{R}') + \overline{\overline{G}}_{es}^{10o}(\overline{R},\overline{R}') \tag{9.25}$$

$$\overline{\overline{G}}_{E1}^{11o}(\overline{R},\overline{R}') = \left(\overline{\overline{G}}_{es}^{11o}(\overline{R},\overline{R}')\right)_{total}. \tag{9.26}$$

The criteria for computation of fields for the implanted head model can be extended to the implanted torso model utilizing the equivalent equations given in chapter 4. This approach is more general, in that it can be easily extended to consider fields at any layer in the head/torso model.

As before if our concern is only with the region exterior to the source, then the singular term, which is important only in the source region, can be dropped from the expression for the Green's function.

In the present chapter full use of the solenoidal and nonsolenoidal functions in different directions are made. These are represented in sections A.1 and A.2 of Appendix A.

9.5 Magnetic DGF in a Configuration with an Embedded Prosthesis

The principle of duality states that once the electric DGF is obtained, the magnetic DGF is derivable by interchanging the field functions $\overline{P}_{\substack{e\\o}o} \rightarrow k\overline{Q}_{\substack{e\\o}o}$ and $\overline{Q}_{\substack{e\\o}o} \rightarrow k\overline{P}_{\substack{e\\o}o}$ for cylindrical form and interchanging the field functions $\overline{M}_{\substack{e\\o}mn} \rightarrow k\overline{N}_{\substack{e\\o}mn}$ and $\overline{N}_{\substack{e\\o}mn} \rightarrow k\overline{M}_{\substack{e\\o}mn}$ in spherical form, and in either cases omitting the singularity term contribution and vice versa.

On the other hand, the corresponding total magnetic DGF at any point in the system can be calculated from $\nabla \times \overline{\overline{G}}_e = \overline{\overline{G}}_m$, bearing in mind the discontinuous nature of magnetic DGF across a point source at $R = R'$ and the Ampere-Maxwell equation relating $\overline{\overline{G}}_e$ and $\overline{\overline{G}}_m$ in the dyadic form i.e.: $\nabla \times \overline{\overline{G}}_m = \overline{\overline{I}}\delta_e(\overline{R} - \overline{R}') + k^2\overline{\overline{G}}_e$.

$$\overline{\overline{G}}_{M1}^{10o}(\overline{R}, \overline{R}') = \overline{\overline{G}}_{mo}(\overline{R}, \overline{R}') + \overline{\overline{G}}_{ms}^{10o}(\overline{R}, \overline{R}') \tag{9.27}$$

$$\overline{\overline{G}}_{M1}^{11o}(\overline{R}, \overline{R}') = \left(\overline{\overline{G}}_{ms}^{11o}(\overline{R}, \overline{R}')\right)_{total} \tag{9.28}$$

9.6 Electric and Magnetic Field at any Point in the Configuration

The DGF method allows us to determine the expansion of the electric and magnetic fields in a configuration directly. For any current source with current density function $\overline{J}(\overline{R}')$ located outside the cylinder, the electric or magnetic field radiated by such a dipole can be calculated using the formulae,

$$\overline{E}^{Lfo}(\overline{R}) = i\omega\mu_f \iiint_V \overline{\overline{G}}_{E1}^{Lfo}(\overline{R}, \overline{R}') \cdot \overline{J}(\overline{R}')dV' \tag{9.29}$$

$$\overline{H}^{Lfo}(\overline{R}) = i\omega\varepsilon_f \iiint_V \overline{\overline{G}}_{M1}^{Lfo}(\overline{R}, \overline{R}') \cdot \overline{J}(\overline{R}')dV'. \tag{9.30}$$

The equivalent conduction and polarization current in the conductor can be represented by $\overline{J}_{eq}(\overline{R}') = \Delta\sigma(\overline{R}')\overline{E}(\overline{R}')$ where it serves as the distributed volume source with $\Delta\sigma(\overline{R}') = \sigma(\overline{R}') - \sigma_f - i\omega(\varepsilon(\overline{R}') - \varepsilon_f)$. The quantities $\varepsilon(\overline{R}')$ and $\sigma(\overline{R}')$ are the permitivity and conductivity, respectively in the cross section of the conductor. ε_f and σ_f are the background permittivity and conductivity respectively, in layer (f) and V denotes the volume occupied by the source. The well known Born approximation is characterized by assuming $\overline{E}(\overline{R}') \approx \overline{E}_{eo}^{00o}(\overline{R}')$ inside the integral which yields a direct but approximate solution for $\overline{E}^{Lfo}(\overline{R})$. This solution is linear in the inhomogeneity, which implies that it neglects multibounce interactions from the scatterer.

For a vertical dipole with current moment $\overline{c} = c\hat{z}$ pointed in the z-direction and located at $R' = b$, $\theta' = 0$, $\phi = 0$, i.e., $\overline{R}' = (b, 0, 0)$ using equations (2.41) and (3.76)

we let

$$\overline{J}(\overline{R}') = c\frac{1}{b^2 \sin\theta'}\delta(R'-b)\delta(\theta'-0)\delta(\phi'-0)\hat{z} \tag{9.31}$$

$$\overline{c} = c\hat{z} = c(\hat{R}\cos\theta - \hat{\theta}\sin\theta) = \iiint_V \overline{J}(\overline{R}')dV' \tag{9.32}$$

but

$$\iiint_V \delta(\overline{R}-\overline{R}')dV = 1 \tag{9.33}$$

Therefore the fields (9.29) and (9.30) produced by this dipole in the presence of the head model with radius equal to a are given by

$$\overline{E}^{Lfo}(\overline{R}) = i\omega\mu_f c\overline{\overline{G}}^{Lfo}_{EI}(\overline{R},\overline{R}')\cdot\hat{z} \tag{9.34}$$

$$\overline{H}^{Lfo}(\overline{R}) = i\omega\varepsilon_f c\overline{\overline{G}}^{Lfo}_{MI}(\overline{R},\overline{R}')\cdot\hat{z}. \tag{9.35}$$

substitution for $\hat{z}$ in above equations in terms of spherical unit vectors presents

$$\overline{E}^{Lfo}(\overline{R}) = i\omega\mu_f c\overline{\overline{G}}^{Lfo}_{EI}(\overline{R},\overline{R}')\cdot(\hat{R}\cos\theta - \hat{\theta}\sin\theta) \tag{9.36}$$

$$\overline{H}^{Lfo}(\overline{R}) = i\omega\varepsilon_f c\overline{\overline{G}}^{Lfo}_{MI}(\overline{R},\overline{R}')\cdot(\hat{R}\cos\theta - \hat{\theta}\sin\theta). \tag{9.37}$$

When the current element is confined to a filament of length ℓ and of constant amplitude I as in a Hertzian dipole then $c = I\ell$.

In general the field in any layer can be found using

$$\overline{E}^{Lfo}(\overline{R}) = \delta^o_f\overline{E}^{00o}_{eo}(\overline{R}) + \overline{E}^{Lfo}_{es}(\overline{R}) + \sum_1^{IM}\delta^{fI}_f\overline{E}^{Imp\_Shape}_{fI}(\overline{R}) \tag{9.38}$$

$$\overline{H}^{Lfo}(\overline{R}) = \delta^o_f\overline{H}^{00o}_{eo}(\overline{R}) + \overline{H}^{Lfo}_{es}(\overline{R}) + \sum_1^{IM}\delta^{fI}_f\overline{H}^{Imp\_Shape}_{fI}(\overline{R}) \tag{9.39}$$

Here IM is the number of implants and fI stand for the layer where the implant is located.

Where δ^{fI}_f is the Kronecker delta functions, when

$$\delta = \begin{cases} 1, & \text{if } f = fI, \\ 0, & \text{if } f \neq fI \end{cases}. \tag{9.40}$$

9.7 Concluding Remarks

The DGF technique was applied to derive the general electromagnetic representation for a simple prosthesis model eccentrically implanted in an spherical human head model (in simple form for the single-layered homogeneous lossy dielectric sphere embedded by a circular cylinder of finite length) in order to evaluate deterioration of the handset antennas performance and obtain the rates of RF energy deposition (SAR). The representation may be used to optimize mobile handset antennas design which radiate less into body tissue, ascertain potential health hazards, and compliance with standards legislation. The DGFs are obtained by employing the EFE and the method of scattering superposition.

This method can be employed in other areas since scattering from complex bodies can be used for detecting possible internal inhomogeneities and nonsymmetries. By observing the field scattered by a body on which radiation is impinging, it is possible to obtain information about its internal structure, (and in case of inhomogeneities in human body, its effect on the behaviour of nerve excitation elicited by magnetic simulation) investigation of cells and of biological bodies, remote sensing techniques and detection of imperfections inside optical waveguides and lenses and straightforward examples.

The outcome of this investigation will be improvements in the electronic circuitry of the implantable medical devices (New prosthetic designs) such as Cochlea implant planted in head, Cardiac (heart) pace-maker embedded in the body and biotelemetry transmitters for medical applications and could easily be expanded so as to handle any scatterer having finite radius and length. They can also be applied to problems of identification of buried unexploded ordnance (UXO) and optical fibers and waveguides for the investigation of inhomogeneities or obstacles inside them. Electromagnetic assessment and antenna design relating to the health implications of mobile phones is another aspect of this work. The problem of detecting known buried objects and estimating their location from electromagnetic field measurements is relevant in many technological areas such as demining, buried

waste clean up, excavation planning, and archaeological investigations.

From the theme of this research, one can use technology to transmit, receive and collect data, turn that data into information, and use that information to increase our knowledge of how that data can be utilized to its maximum (if we could store more data in ourselves).

Digital information is becoming more pervasive in our lives. Memory devices such as hard disk technology is set to move down in size and up in capacity offering designers of such systems a huge increase on current memory (disk) capacity. By applying our technologies to pack lots of information into something as small as the microimplant, we can help people keep in touch with their information more conveniently wherever they go.

I am sure that the microimplants will form the basis of new technology, arguing that such large capacity storage devices in such a small package will allow us to begin developing very small devices that in the past may have been impossible. The microimplants will allow data to be transferred between different hardware devices as well as human species. Information from anybody/device could quite easily be transferred to another person(s) as well as various devices by simply down loading information. Another boon is that additional information and data could be kept on separate storage devices and then accessed when they are needed.

Chapter 10

Numerical Computations and Results

POSSIBLE adverse effects of EM fields on the human body and especially on the nervous system and the brain/implanted head are of increasing concern, particularly with reference to mobile transceivers held close to the head/torso.

Spherical head model, while not accurate, provides easy and reasonably effective means for the estimation of the "worst case SAR" either through modeling or experiment. This thesis is complete only if there are substantial numerical results presented with it. The purpose of this work was to develop a model that will describe the field distributions inside a biological entity. The model was delivered based on a new approach based on a solution of DGF in spherical and cylindrical coordinates. Numerical results from analytical expressions are to be computed for the problem of spherical head model and implanted head/body and then compared with the results from the same models using the EMU/FDTD Electromagnetic simulator developed by FDTD research group at the Department of Electronic and Computer Engineering at Brunel University.

A critical evaluation of the process/method is discussed. The results presented here show that this method correlates well with other techniques.

The complete expressions used for solenoidal and nonsolenoidal functions in different directions are represented in sections A.1 and A.2 of Appendix A.

10.1 Introduction

Research on this subject goes back to at least three decades. At that time, numerous investigations have been conducted with mainly experimental approach [83] - [85]. Theoretical studies based on analytical methods and simple models of the human body commenced later. Amemiya and Uebayshi [86], have derived closed form formula for homogeneous sphere irradiated by a half-wavelength dipole antenna. They modeled the human head as a lossy dielectric sphere and then calculated the power deposition inside the sphere by using the theoretical study. With the advances in the computer technology, another approach based on computer simulation (Computational Electromagnetics) and as a result, using more sophisticated models were attainable.

Various numerical techniques have been used, amongst which, method of moments (MoM), [17], the method of Multiple Multipole expansion (MMP), [87], and Finite Difference Time Domain (FDTD), [88], should be noted. Regarding the geometric complexity and heterogeneity of dielectric properties inherent in the biological objects, the method of FDTD seems to be very effective and the most relevant method of analyzing this problem. This technique is well established in the field upto now. It has its advantages and disadvantages, trade-offs, some of which are discussed in chapter 1 and some will be discussed in "Further research" in chapter 12.

In 1991, Dimbylow [89], used the FDTD method to calculate SAR distribution in a realistic heterogeneous model of the head for plane wave exposure from 600 MHz to 3 GHz. His concerns in this report were an enhanced absorption due to resonance in the head, hot spots in the brain, and in higher frequencies the increasingly superficial absorption of power particularly in the eyes. He then considered the calculations of the SAR for a dipole closely coupled to the head at 600 MHz and 1.9 GHz in another paper [90]. In this paper, he calculated energy absorption in the eye using a detailed model of the eye including four tissue types and arrived at the SAR as a function of distance between the electromagnetic source and the eye surface. Toftgard et al. [91], analyzed this problem using a homogeneous spherical model of the head, a

block model of the head and a box model of the radio-handset at the frequencies of 914 MHz and 1890 MHz. Based on their findings half of the power is deposited in the hand and head, most of which, (96%) is deposited in the head and just (4%) is absorbed in the hand.

In 1994 Martens [92, 93], conducted similar investigations at 900 MHz, using an MRI (Magnetic Resonance Imaging) based model of the head, for a monopole mounted on a box. He reported an absorbed power ratio of about 50%, in [92], and 15%, in [93].

Jensen et al., [2] - [5], investigated the problem of the interaction at 900 MHz, using an MRI based model of the head including five tissue layers and considering four models of antennas and reported 48-68% of the total power absorption in the head and hand.

Hombach and colleagues [94], conducted a different study at 900 MHz using realistic models of the head with various shapes and different sizes and models of the internal anatomy. They observed an independence of the SAR properties from the size and the shape of models. In a more recent paper [95], based on the same methodology at 1800 MHz, used a dipole antenna and a realistic model of the head. They concluded that a homogeneous representation of the head is suitable for assessing the worst case SAR in the head if appropriate parameters are chosen.

Gandhi et al., [96], worked on the same problem, at 835 MHz and 1.5 GHz. He used a $\lambda/4$ and a $3\lambda/8$ monopole antennas, with realistic MRI based models with the resolutions down to 1 mm. They too calculated the SAR distribution in the head and observed that using homogeneous models of the head leads to gross overestimations in the results of the SAR calculations.

Okoniewsky and Stuchly [97], investigated another study at 915 MHz using various boxes, spherical and realistic head models to consider the effects of the head, hand and ear. They reported that the hand holding the handset absorbs a significant proportion of the antenna power output, an amount which can be considerably decreased by modifying the geometry of the handset metal box.

10.2 Numerical Implementation and Validation

The problem of electromagnetic scattering from a spherical scatterer is considered. The approach is based on the model technique presented in chapter 3, conjecturing that the features of the scatterer can be determined from the near scattered field via DGFs. An expansion in spherical wave functions for the scattered field based on the development of formulation by Tai [19, 20].

With the help of the DGF expressions (3.62) and (3.63) in chapter 3, for the head model problem of a sphere of 10 *cm* radius illustrated in Figure 1 consisting of brain and skull with constitutive parameters given in Table 3 illuminated by a dipole of a length 0.4 wavelengths with a non-zero feed gap width. Frequencies representative of personal communications systems (900 and 1800 MHz) were considered. The center of dipole is symmetrically positioned with respect to the head and 1.5 *cm* away from it.

Material	Density [g cm^{-3}]	Relative permitivity	Conductivity [mho/m]
Skull @ 900MHz	1.20	17	0.25
Skull @ 1800MHz	1.20	16	0.43
Brain @ 900MHz	1.05	43	0.83
Brain @ 1800MHz	1.05	41	1.14

Table 3: Constitutive parameters

Due to the high non-uniformity of the SAR distribution induced by a cellular mobile phone within the head, the *peak* SAR is the relevant parameter to assess the risk caused by these devices.

The specific absorption rate (SAR), is calculated from:

$$SAR = \frac{\sigma E^2}{\rho} \tag{10.1}$$

where E is the RMS magnitude of the electric field, σ the conductivity, ρ the mass density of the head giving SAR in power per unit mass. The SAR is calculated on the lines through the center of the homogeneous (brain) head in x-, y-, and in the z-directions as shown in Figure 10, Figure 11 and Figure 12 respectively. The SAR decreases exponentially with distance from dipole. The DGF theory agrees closely with the FDTD algorithm down to low levels. The peak SAR of 15.1 W/Kg from the DGF method is comparable with the 15.4 W/Kg calculated by the FDTD method, normalized to one watt input power. The FDTD method with Mur second order boundary condition was applied to this problem where the computational domain of 30 cm in each dimension with grid cells of 2.5 mm and time increment approximately 4.76 ps were used.

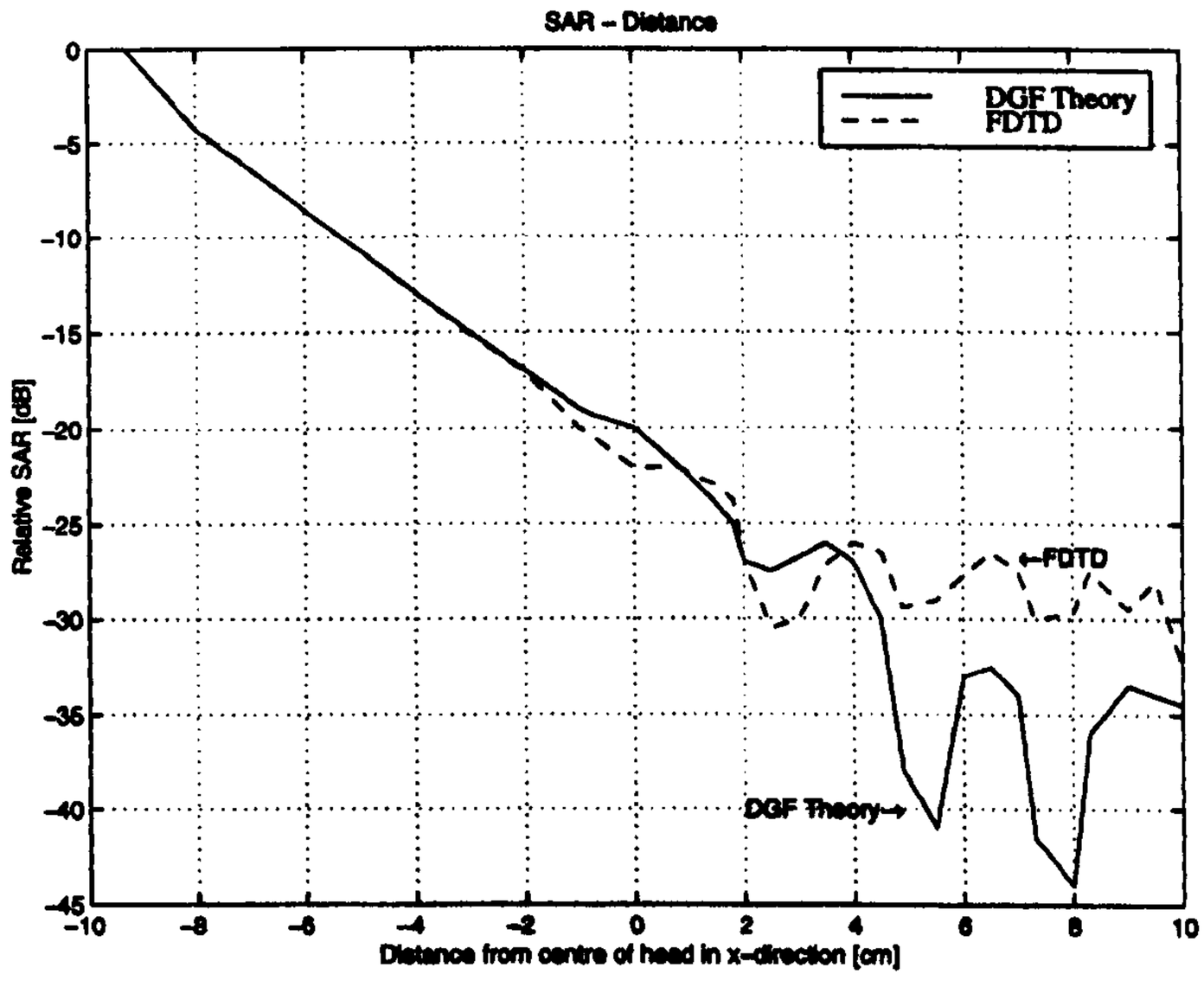

Figure 10: Specific Absorption Rates in the x-direction

In Figure 10, comparison of DGF and FDTD results with a homogeneous spherical head model at 900 MHz, (the relative SAR in the model as a function of the distance "d" between the center of the head model and the antenna point source in the x-direction) is shown. Since the total electric field approximately decays expo-

nentially inside the head, peak SAR will occur where the conductivity of the tissue is higher.

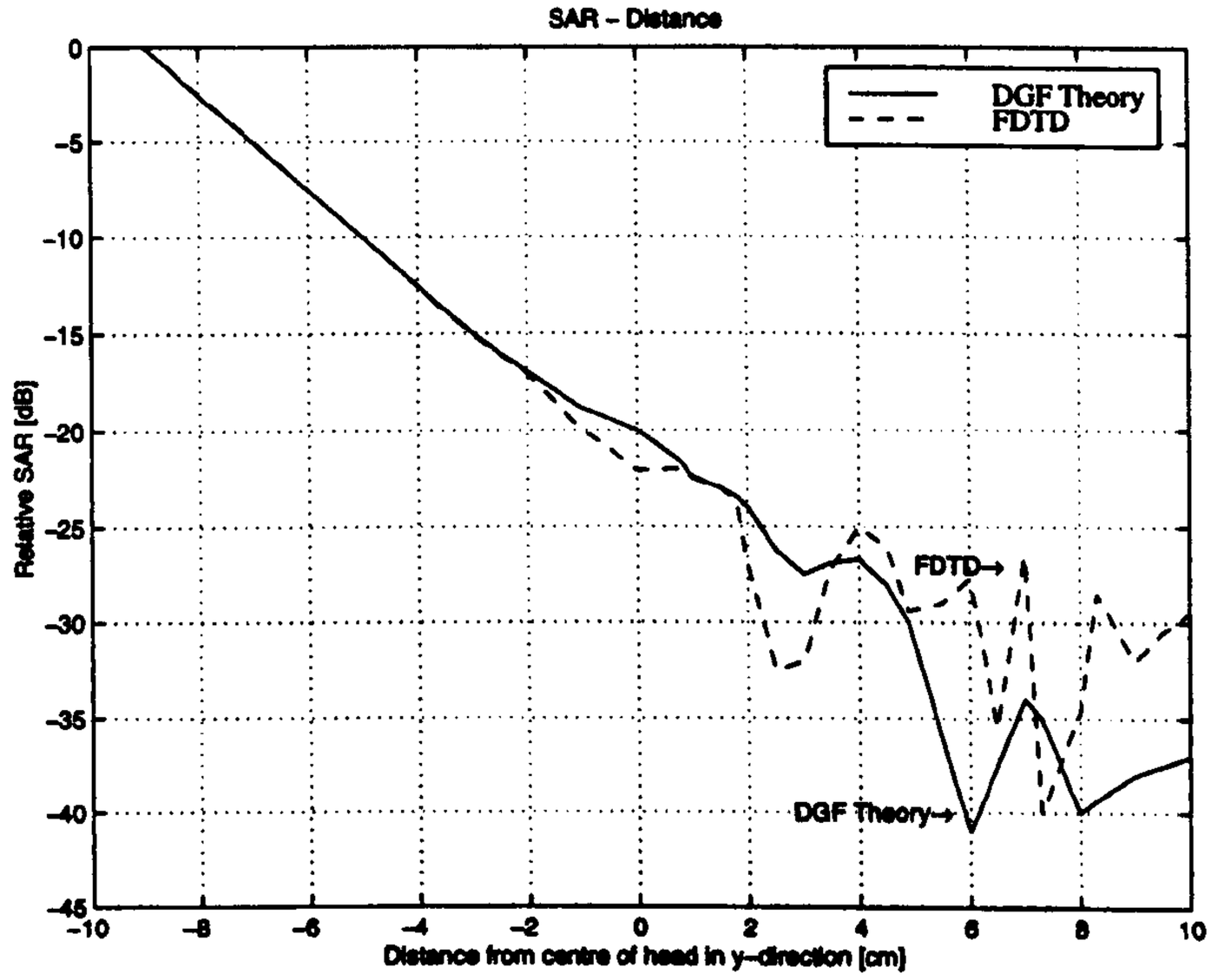

Figure 11: Specific Absorption Rates in the y-direction

Figure 11 like Figure 10, shows the relative SAR in the model as a function of the distance "d" between the centre of the head model and the antenna point source but in the y-direction for both DGF and FDTD.

Again, Figure 12, shows the relative SAR in the model as a function of the distance "d" between the center of the head model and the antenna point source in the z-direction for DGF as well as FDTD technique.

Mobile telephone handsets generate substantial field levels close to the antenna and since the antenna is close to the head of the telephone user it is of interest to measure the power density and electric field in the region of the head and thereby close to the transmitting antenna.

The total electric field distributions ($20\log|E|$) inside the two head configurations are compared in Figure 13 when the power delivered by the antenna is set at 1 Watt. The distance is measured from the center of the head. The field distribution

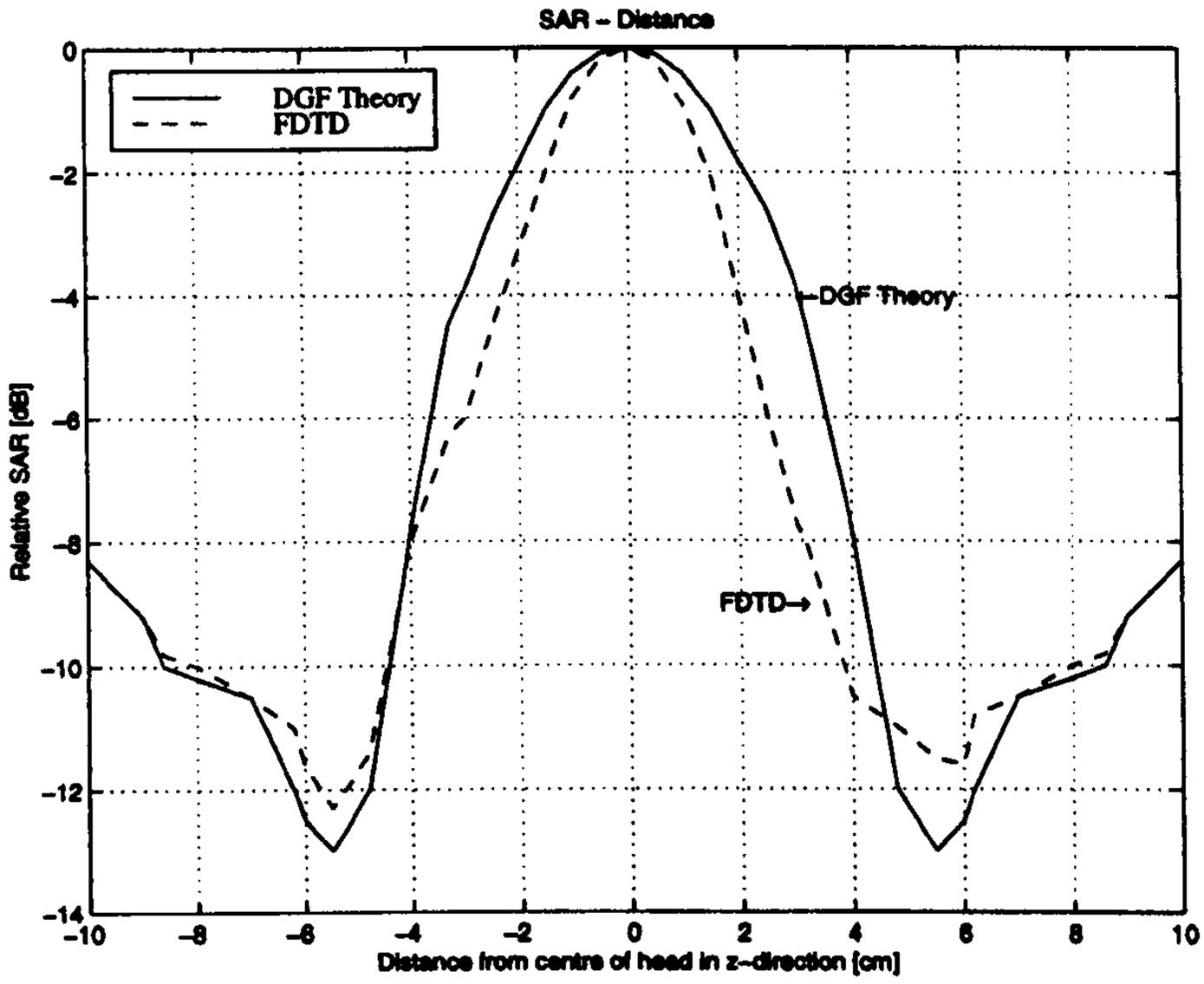

Figure 12: Specific Absorption Rates in the z-direction

of the two layered and homogeneous heads are similar. This shows that the field near the surface of the head agrees very well for the two heads. From this, one can suggest that this spherical head model can be used for a reasonable estimate of the *peak* electric field or the *peak* SAR in the head.

Since the electric field near the surface of the head for these two configurations are similar, a simple homogeneous spherical head model can be sufficient to estimate a reasonable value of *peak* SAR for a variety of antennas.

The radiated power can be calculated by integrating the real part of the normal component of the Poynting vector over a closed surface S around the antenna and the head:

$$P_{rad} = \frac{1}{2} Re \left\{ \iint_S E \times H^* \cdot \hat{n} \, dS \right\}, \tag{10.2}$$

where $\hat{n}$ is a unit vector perpendicular to the surface S and pointing outward of the volume.

The absorbed power is determined by integrating the absorbed power density

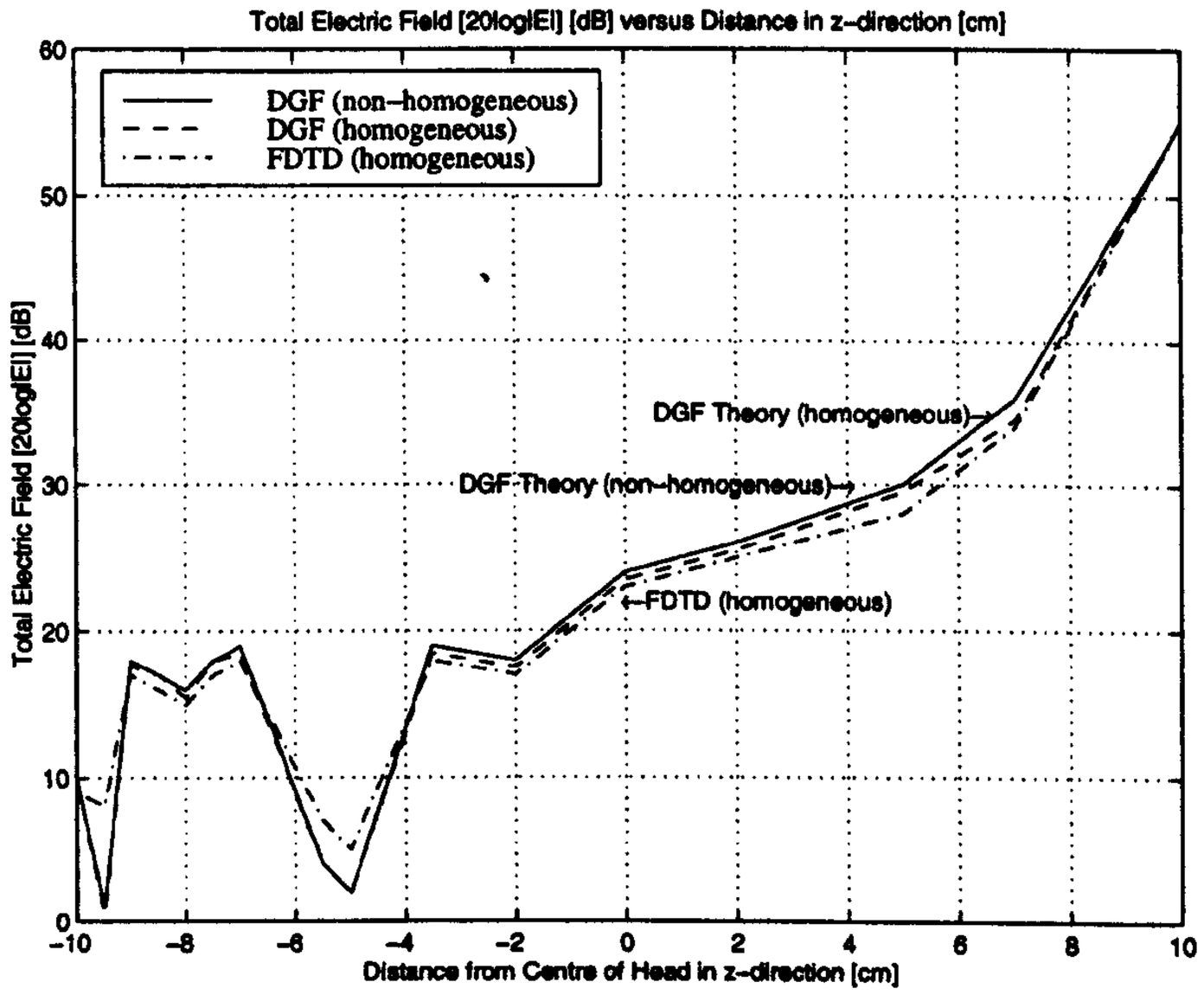

Figure 13: Total Electric Field versus Distance in the z-direction

over the volume V of the head:

$$P_{abs} = \frac{1}{2}\iiint_V \sigma(r)\,|E(r)|^2\,dV \tag{10.3}$$

with $\sigma(r)$ the conductivity (in Siemens per meter) of the different tissues in the head and $E(r)$ the electric field (in volts per meter) inside the head.

The formula for calculating the efficiency is as follows:

$$\text{Efficiency} = \frac{P_{in} - P_{abs}}{P_{abs}} \tag{10.4}$$

Figure 14 shows the power absorption as a function of distance inside the non- and homogeneous spherical head model. The power delivered by antenna is at 1 W, and the operating frequency of the antenna is 900 MHz. As one can notice, significant amount of power has been absorbed in the head, when the antenna is in close proximity to the head (about 50% at a distance of 2 cm from the head and less than 10% for a distance as far as 10 cm from the head). Therefore, the total power absorption in the head is dependent upon the proximity between the head and the antenna.

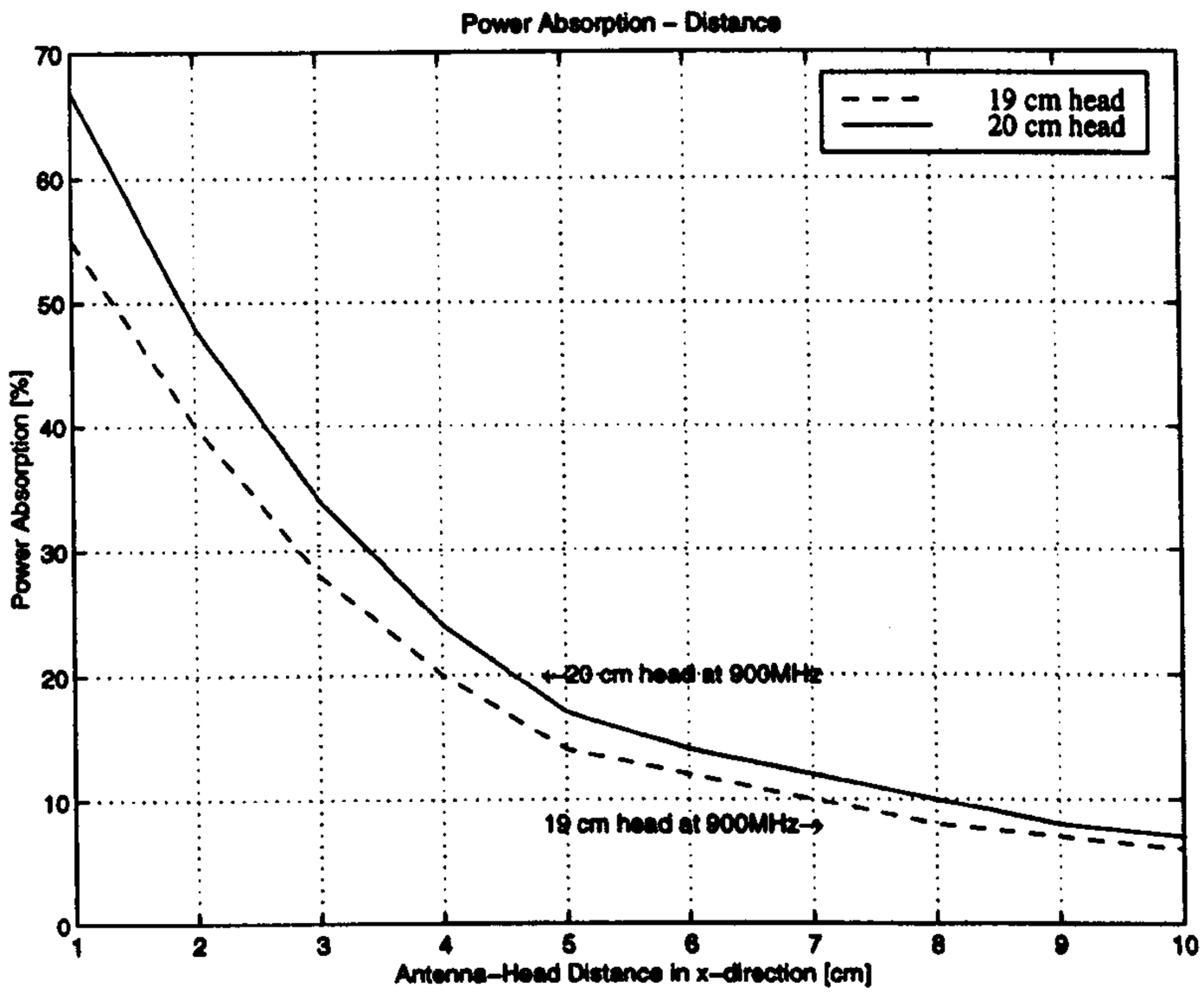

Figure 14: Power Absorption versus Distance inside the layered Head

Considering the power absorbed in the head our study indicates that at a distance of 15 mm, more than 36% of the input power is absorbed in the head, which corresponds to a radiation efficiency around 64%. These values are in a very good agreement with similar results reported by Gandhi, [96], using MRI based model of the head.

The intent of this chapter is not to describe any possible measurement technique, but to prove the derivation of the underlying physical relations in terms of the mathematical formulation employed to express the scattered field. In other words, in the problem of scattering, the mathematical formulation definitely dictates the development of a most suitable measurement technique.

This study clearly demonstrates the merits of the DGF scattering model technique developed in this thesis, and it shows that the technique is convenient method for a numerical solution of this type of problems.

In a rapidly growing market for mobile telephones, besides the public biological concerns in cellular mobile communication systems, and manufacturers and antenna

designers great demand to know the deterioration of the antenna performance, there is also some concerns of effect of EM fields on implants (prostheses) and increase in SAR in human head arising from implantation. The current safety limits do not take into account the possible effect of hot spots arising from conducting implants (prostheses) resonant at personal communication frequencies. The expected implant effects and interaction in a real human head which consists of many different tissues has to be investigated and made clear.

We have adopted the configuration in Figure 9 from chapter 9. The DGF expressions (9.25) and (9.26), also expressions (9.27) and (9.28) are used for the implanted head model problem of a sphere of 10 *cm* radius consisting of brain and skull with constitutive parameters given in table 3 illuminated by a dipole of a length 0.4 wavelengths with a non-zero feed gap width. The implant is modeled by a perfect conducting cylinder. The length of this cylindrical implant is considered up to 3 *cm* with a radius of 0.5 *cm*. Frequency 900 MHz was considered. In this case once again, the center of the dipole is symmetrically placed with respect to the head and 1.5 *cm* away from it. Owing to polarization, the increase in local SAR is greatest when the implant is parallel to the radiating dipole.

In this section, the effect of perfect conductor implant on the absorbed power distribution within a human head is studied numerically using a lossy dielectric sphere containing conducting implant excited by the near field of a dipole antenna. The implant of resonant dimensions within a homogeneous dielectric lossy sphere can enhance local values of SAR considerably.

Figure 15 shows the relative power absorption as a function of implant length inside the homogeneous spherical head model at a distance of 1 *cm* from the head surface facing the antenna. It is observed that the length of implant blocks the penetration of the incident wave further into the head model, so that the total power absorbed is reduced.

Figure 16 shows the relative power absorption as a function of implant distance from the edge of the spherical head model facing the dipole for an implant of length

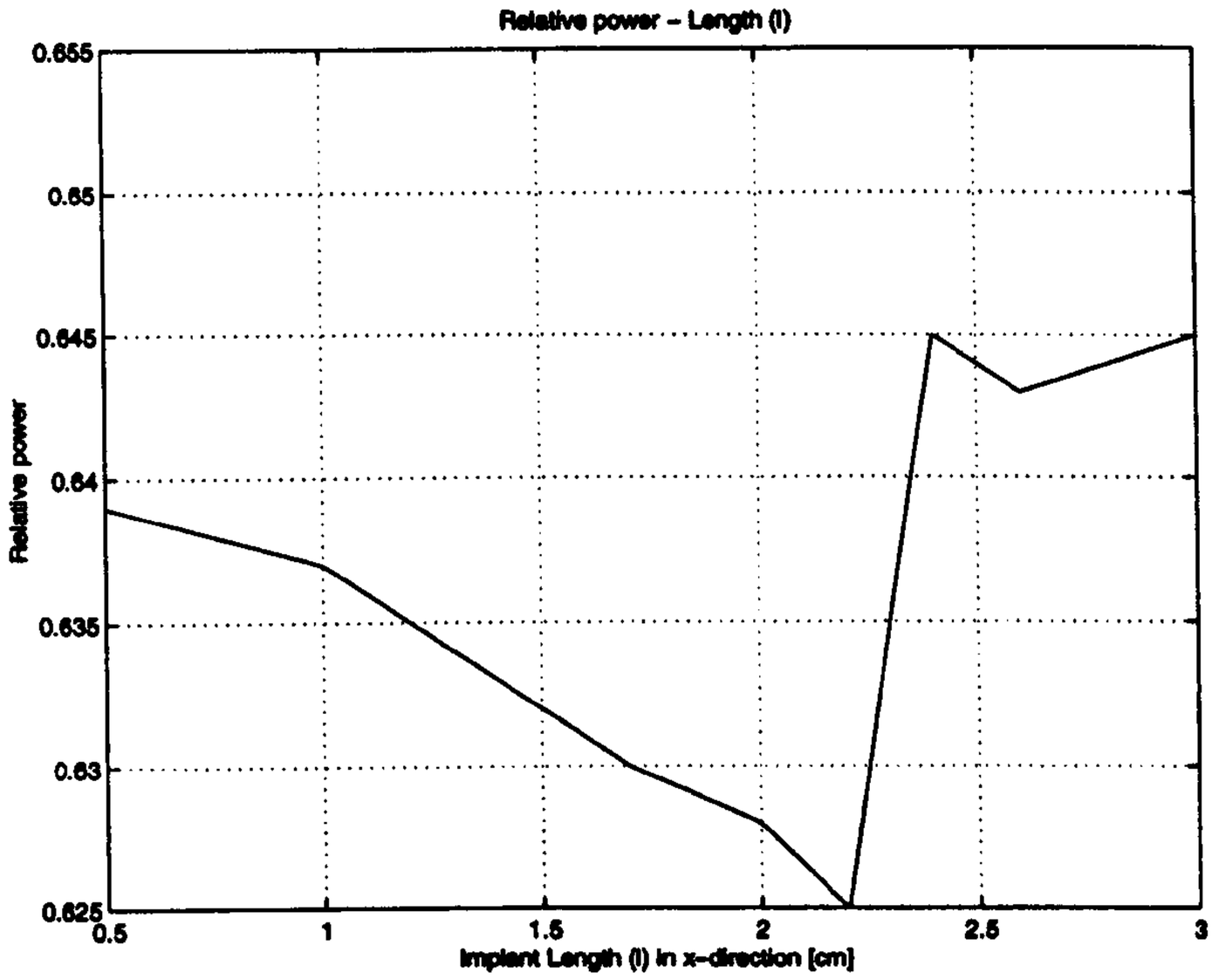

Figure 15: Relative Absorbed Power - Implant Length (l) in x-direction

2 *cm*. It is noticed that the presence of an implant changes the total relative absorbed power by less than 5% with respect to that absorbed by the head model in its absence.

The maximum power deposition (measured in Specific Absorption Rate of RF energy, or SAR) allowed by the FCC (US Federal Communications Commission) is 1.6 W/Kg in 1 g of head tissue from exposure to cellular telephone radiation.

The ICNIRP (International Commission on Non-Ionizing Radiation Protection) located in Geneva guidelines stipulate a maximum SAR of 2 W/Kg in any 10 g of tissue in the head.

In Figure 17, the SAR as a function of implant length at 1 *cm* from the head surface facing the antenna inside the homogeneous spherical head model for radiated power of 0.25 W is shown.

From this, one can observe that the damping of the traveling wave as it traverses the sphere causes the maximum SAR at the implant to decrease with distance b. Also an increase in local SAR can be seen for implant to be very close to the surface

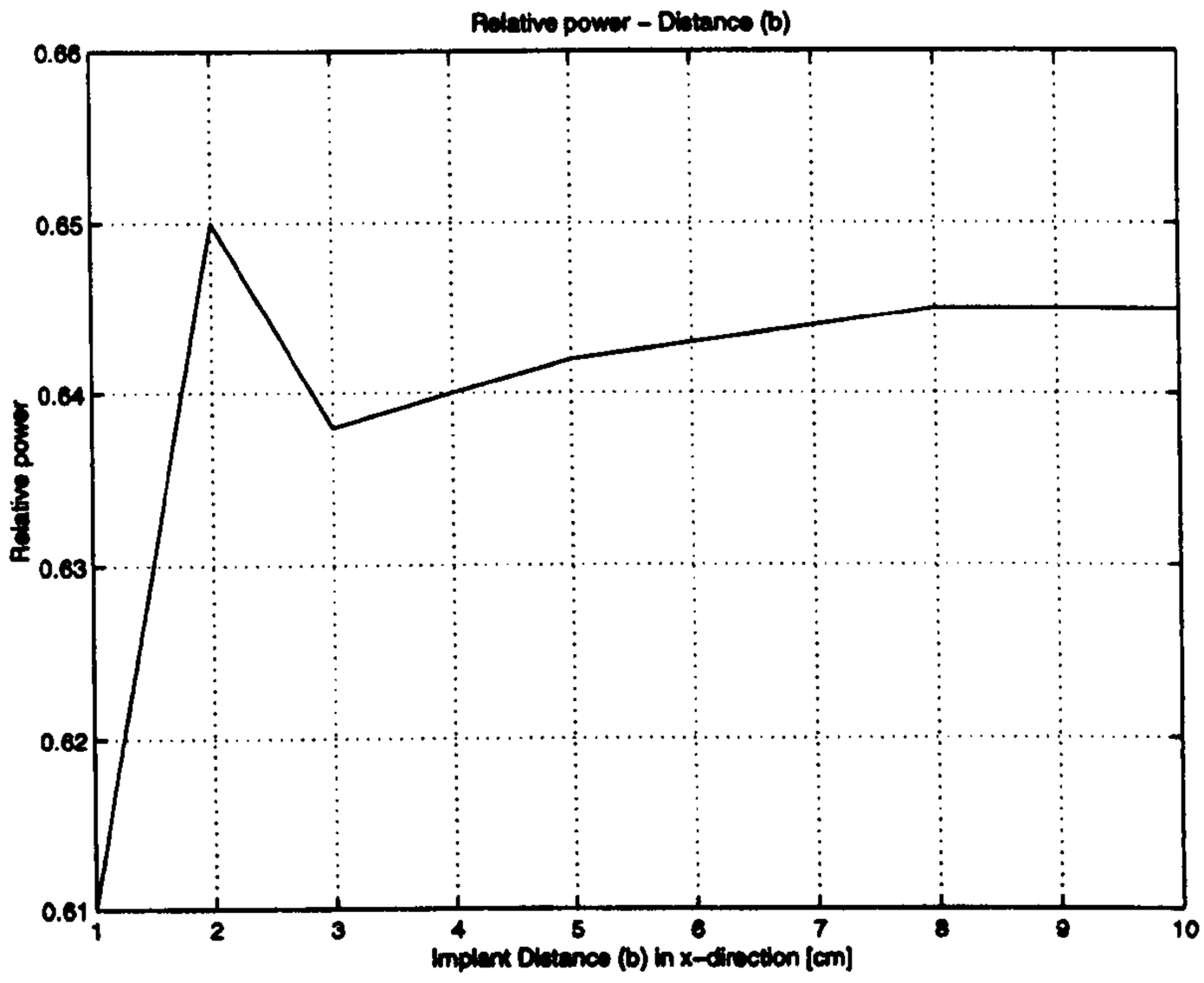

Figure 16: Relative Absorbed Power - Distance (b) in x-direction

of the head model.

Figure 18 like 17, shows the maximum SAR in the model as function of the implant distance "*b*" from the edge of the spherical head model facing the dipole for an implant of length 2 *cm*.

All values are normalized to an antenna radiation power of 1 *W*.

10.3 Concluding Remarks

Mobile telephones have transformed the telecommunications industry. These devices can be used to make telephone calls from almost anywhere. But reports have appeared in the media linking the use of mobile telephones with, among other things, headaches, hot spots in the brain and brain cancer. At the same time, radio frequency (RF) fields are known to produce heating and the induction of electrical currents. The effect of perfect conductor implants on the absorbed power distribution within a human head is studied theoretically using a lossy dielectric sphere containing conducting prosthesis excited by the near field of a dipole antenna rep-

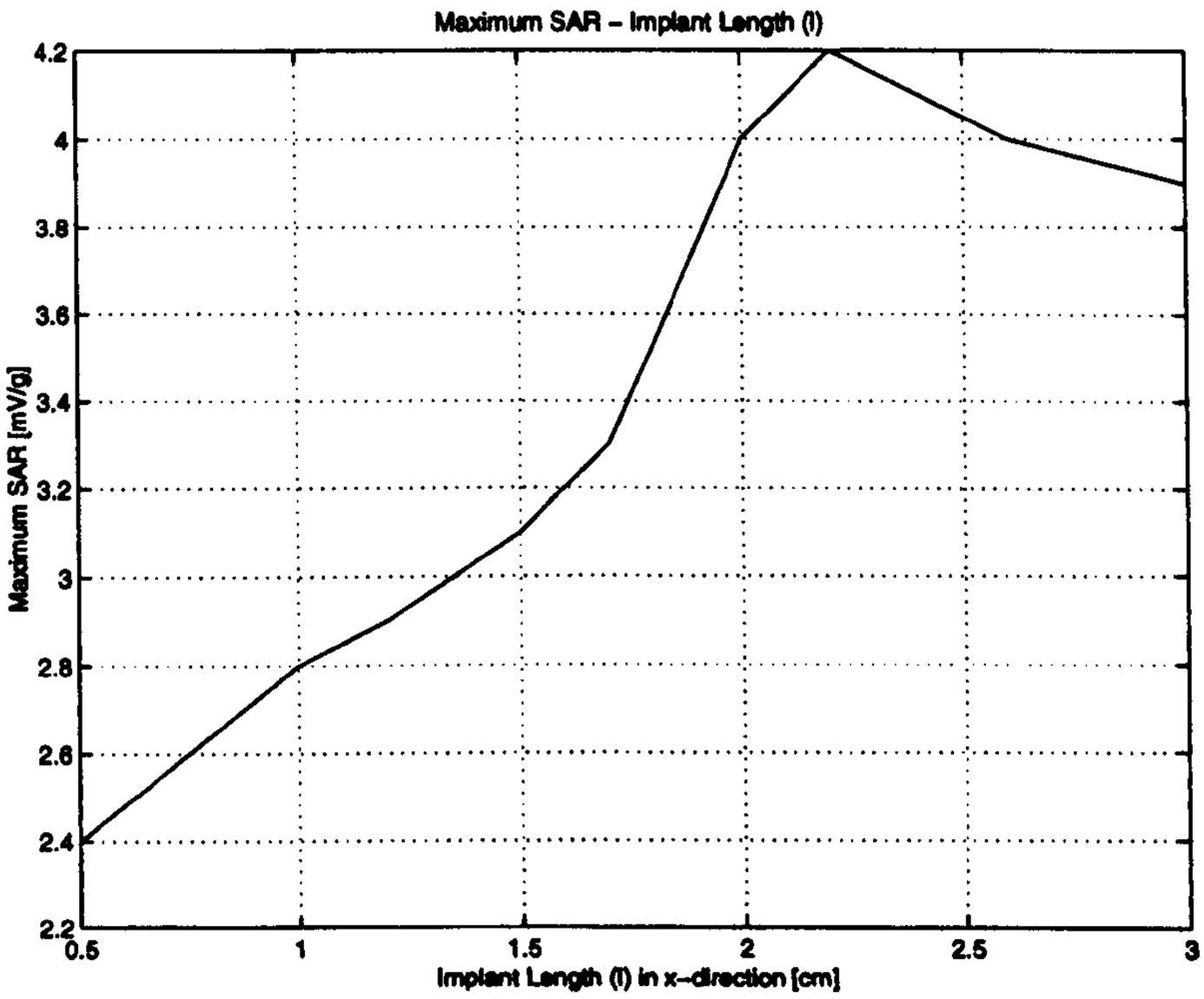

Figure 17: Maximum SAR - Implant Length (l) in x-direction

resenting a mobile phone.

The validity of the proposed solution is verified for the unimplanted spherical head by comparing the resulting values of the scattered field with those based on the FDTD method. The effect of implant within spherical head has been investigated and presented for plane wave incidence.

Examination of our analytical solution indicates that a perfectly conducting implant of resonant length within a homogeneous lossy dielectric spherical head give rise to an increase in local SAR considerably and the average SAR over 1g could be doubled by the conductor. The maximum increase in local SAR happens when the implant is parallel to the source. The average SAR over 10g can be increased approximately by 4 per cent.

In a real human head which consists of many different tissues, the expected implant effect has to be made clear. One also should consider the effect of resonance. The prosthesis should be modeled by other types of shapes as well as materials such as an infinitely thin disc and non-circular arbitrary inhomogeneities.

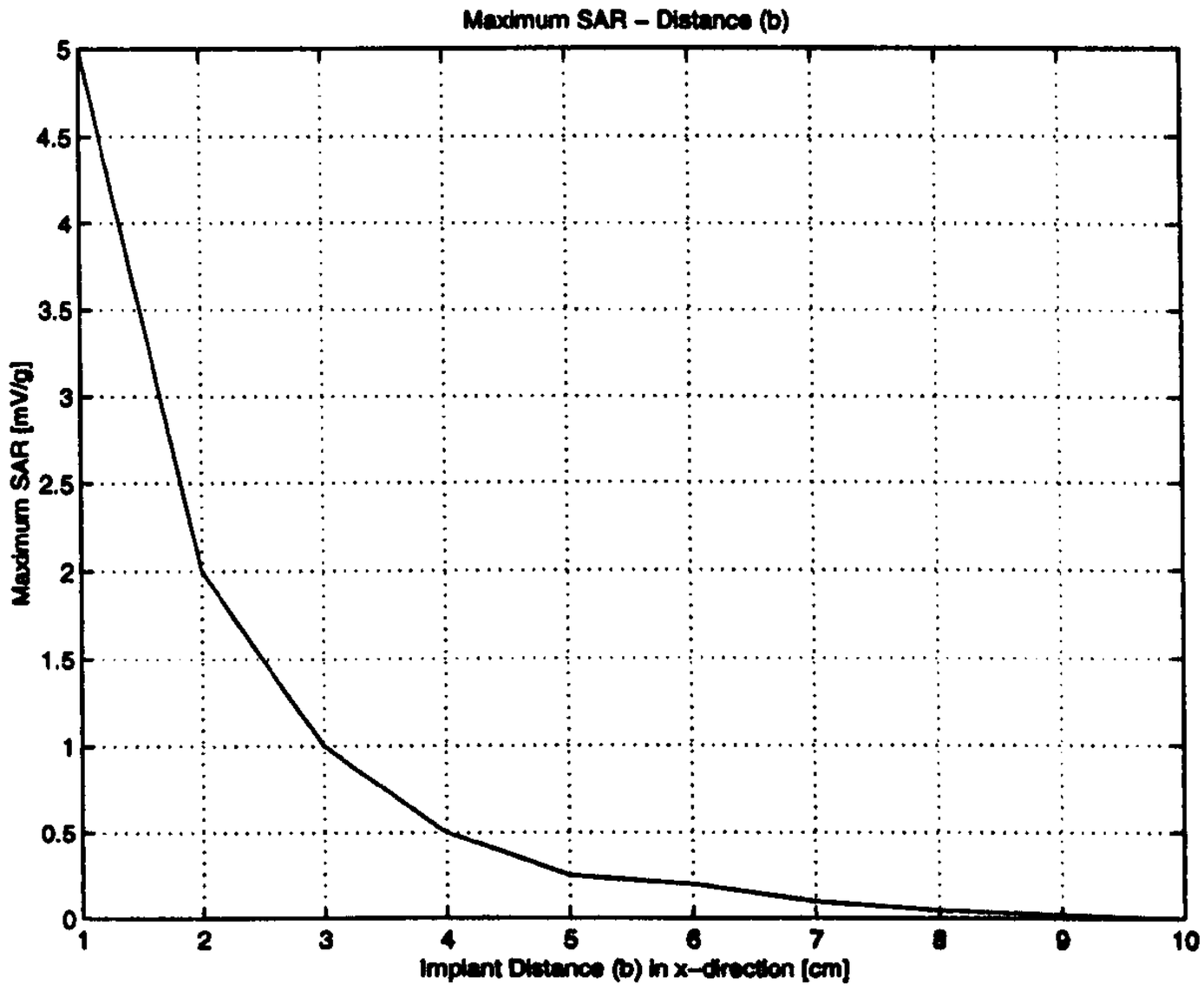

Figure 18: Maximum SAR - Distance (b) in x-direction

The travelling wave as it traverses the sphere causes the maximum SAR at the element to decrease with distance b. A resonant implant very near the sphere surface can rise to a very marked increase in local SAR. The implant prevents the incident wave to penetrate into the head, so that total power absorbed by the head is reduced.

Sample numerical results are presented to illustrate the versatility of the method. Good agreement is observed between the numerical results based on the proposed method and the FDTD method. The results for these specific cases agree with those given by other authors such as Gandhi, [96], showing the validity of our DGF representation. This provides a valuable check on all previous formulae and results of this work.

Numerical computations can be used to show that valuable information can be obtained about the inner structure of a body observing the field scattered from it.

The advantage of the proposed analysis is the simplicity and efficiency in computation.

Chapter 11

Conclusions

The major conclusions of this thesis based on the research carried out are drawn within this chapter. It contains a summary of the findings and results of this dissertation. It also brings together the various results obtained in the preceding chapters of this thesis and analyses the conclusions reached at each stage of the research investigation. Finally ideas which could help future research on the subject are suggested.

Analytical techniques were in vogue before computers became available. Hence, many complicated problems can be formulated using this technique.

In electromagnetic theory, many scalar wave concepts cannot simply be extended to the vector wave case. Even though most problems can be solved without the use of dyadic Green's functions, the symbolic simplicity with which they could be used to express relationships makes the formulations of many problems simpler and more compact. Moreover, it is easier to conceptualize many problems with the dyadic Green's functions e.g. the dyadic Green's functions in layered media which are discussed in chapters 3 and 4.

A straightforward application of numerical methods to many wave and field problems involve using intensive computation and extensive computer time, may saturate the resources. A combination of numerical and analytical methods, however, can generate computer codes that are many times more efficient.

11.1 Critical Appraisal of Research/DGF Method

Reviewing the research and the results obtained, show that, although this method is exact and can be used for validation of models in numerical techniques, the method is cumbersome because the fields for every points has to be evaluated/calculated or the equations for max field derived e.g to find the max field.

The technique also lacks visualization therefore hybridization is surely the answer i.e., improve the technique by considering the capability of other methods in order to construct a realistic DGF model.

Although a wide variety of techniques are currently being applied to compute electromagnetic fields from a source radiation on biological systems, this work presents a new approach to the study of biological systems which can employ FEM, MoM and FDTD techniques to generate results. Its salient characteristics is that of the saving in memory and CPU computational time and speed.

11.2 Concluding Remarks

Technological progress in the broadest sense of the word has always been associated with various hazards and risks, both perceived and real. The industrial, commercial and household application of electromagnetic fields (EMF) is no exception.

Throughout the world, the general public is concerned that exposure to EMF from such sources as high voltage power lines, radars, mobile telephones and their base stations could lead to adverse health consequences, especially in children. As a result, the construction of new power lines and mobile telephone networks has met with considerable opposition in some countries. Therefore research such as this is necessary and economically the cheapest way of evaluating these hazards.

In chapter 3, a theoretical analysis of antenna/layered head configuration is demonstrated. An improved general multilayered homogeneous lossy dielectric spherical head/antenna model of DGF for numerical EMC investigation has been proposed and compared with the models by various authors. This study enables one to assess

the influence of the presence of a close-by biological head upon the operating characteristics of a mobile phone, antennas input impedance, SAR values inside the head, the power absorbed, the total radiated power, the thermal emission, the induced current on a scatterer, novel antenna design, the electric and magnetic near-/far-fields patterns, and also other situations.

In this chapter we have also drawn attention to the fact that the singular behaviour of the eigenfunction expansion (EFE) of the DGF is incorrectly formulated in some authors' related works. This is significant because this expansion is used in the numerical calculation of the electric field in the source region.

Furthermore, by defining a symmetry operator the required memory for efficient numerical computations using the method of moments can be reduced drastically by formulating a new compact general expression. The validity of general model is verified by the DGF of the specific models, which agrees with other authors' study. Further work is in hand to find a reduced general formulation for electromagnetic DGF in spherically multilayered media by utilizing the technique presented in this chapter.

The results of this study could be useful for a further analysis of the problem. Both GSM (global system for mobile communication) and PCS (personal communication services) pose potential problems with regard to interactions with the human body and implanted medical devices. Interaction/interference-free antennas design is useful and, increasingly, is becoming necessary. Since anything that conducts can be considered as an antenna and two antennas interact with each other, the interaction problem could potentially be solved by using the mobile phone (handset transceiver) user (human body) as an antenna and transmitting at frequency levels (for example, noise) unharmful to humans. This would make possible the design of antenna-less PCS, receiving/transmitting signals only in close proximity to biological antennas (users).

In chapter 4, we have derived general electromagnetic representations for a human torso model (in simple form for the multilayered homogeneous lossy dielectric

circular cylinder of finite length) in order to evaluate deterioration of the antennas performance and obtain the rates of RF energy deposition (SAR), the power absorbed, the total power radiated, the thermal emission and the current induced on a scatterer. The representations may be used to optimize antenna design, ascertain potential health hazards, and compliance with standards legislation.

Scattering from complex bodies is often used for detecting possible internal inhomogeneities and non-symmetries. By observing the field scattered by a body on which radiation is impinging it is possible to obtain information about its internal structure. Investigation of cells and of biological bodies, remote sensing techniques and detection of imperfections inside optical waveguides and lenses are straightforward examples.

In chapter 5, general expressions have been derived in simple form for the finite conducting circular cylinder (medical devices/prostheses) of any size as well as of very small radius (resonant length).

The usefulness of the present technique obviously requires comparison with numerical and experimental results. It is envisaged that future work will address this aspect of the problem in more detail.

In chapter 6, alternative general expressions have been developed in simple form for the medical devices/prostheses (finite conducting circular cylinder) of any size as well as of resonant length. The advantage of the proposed analysis is its simplicity and efficiency in computation.

In chapter 7, simple general expressions have been derived for the finite insulated conducting circular cylinder (insulated medical devices/prostheses) of any size as well as of very small radius (resonant length).

In chapter 8, general far field expressions have been derived in simple form for the finite conducting circular cylinder (medical devices/prostheses) of any size as well as of very small radius (resonant length). The DGFs are obtained by employing the EFE and the method of scattering superposition.

In chapter 9 the DGF technique was applied to derive the general electromag-

netic representation for a prosthesis eccentrically implanted in a human head model (in simple form for the multi-layered homogeneous lossy dielectric sphere embedded by a circular cylinder of finite length) in order to evaluate deterioration of the handset antennas performance and obtain the rates of RF energy deposition (SAR). The representation may be used to optimize mobile handset antennas design which radiate less into body tissue, ascertain potential health hazards, and compliance with standards legislation. The DGFs are obtained by employing the EFE and the method of scattering superposition.

The outcome of this investigation will provide a platform for improvements in the electronic circuitry of the implantable medical devices (new prosthetic designs) such as cochlea implant planted in the head, cardiac (heart) pace-maker embedded in the body and biotelemetry transmitters for medical applications and could easily be expanded so as to handle any scatterer having finite radius and length. They can also be applied to problems of identification of buried unexploded ordnance (UXO) and optical fibers and waveguides for the investigation of inhomogeneities or obstacles inside them.

Throughout the thesis in the above chapters, the DGFs are obtained by employing the EFE and the method of scattering superposition.

The results of these chapters could be useful for a further analysis of the problem as a thin wire/insulated wire or an implant/dielectric-coated implant such as heart pace-maker embedded in the body and biotelemetry transmitters for medical applications and could easily be expanded so as to handle any scatterer having finite radius and length. They can be applied to problems of optical fibers and waveguides for the investigation of inhomogeneities or obstacles inside them or by considering the cylinder as an excitation or scatterer. They can also be of use in the study and design of antennas of high frequency whose performance is less affected by the biological systems and produce lower SAR (specific absorption rate, the rate of electromagnetic energy deposition) and as a result contribute to the efficiency of handheld/mobile phones.

In chapter 10 the effect of perfect conductor implants on the absorbed power distribution within a human head is studied theoretically using a lossy dielectric sphere containing conducting prosthesis excited by the near field of a dipole antenna representing a mobile phone.

The validity of the proposed solution is verified for the unimplanted spherical head by comparing the resulting values of the scattered field with those based on the FDTD method. The effect of implant within spherical head has been investigated and presented for plane wave incidence.

Examination of our analytical solution indicate that a perfectly conducting implant of resonant length within a homogeneous lossy dielectric spherical head give rise to a considerable increase in local SAR and the average SAR over 1g could be doubled by the conductor. The maximum increase in local SAR happens when the implant is parallel to the source. The average SAR over 10g can be increased by approximately 4 per cent.

In a real human head which consists of many different tissues, the expected implant effect has to be made clear. One should also consider the effect of resonance. The prosthesis should be modeled by other types of shapes as well as materials such as an infinitely thin disc and non-circular arbitrary inhomogeneities.

The traveling wave as it traverses the sphere causes the maximum SAR at the element to decrease with distance b. A resonant implant very near the sphere surface can rise to a very marked increase in local SAR. The implant prevents the incident wave penetrating into the head, so that total power absorbed by the head is reduced.

Sample numerical results are presented to illustrate the versatility of the method. Good agreement is observed between the numerical results based on the proposed method and the FDTD method. The results for these specific cases agree with those given by other authors such as Gandhi, [96], showing the validity of our DGF representation.

Numerical computations can be used to show that valuable information can be obtained about the inner structure of a body observing the field scattered from it.

The method used in this thesis can be of great interest in the analysis of the electromagnetic wave propagation in layered media in underwater communications, geophysical explorations, radio propagation in forests, agricultural applications, etc.

This study enables one to assess the influence of the operating characteristics as well as the presence of a closeby source (mobile phone) upon the operating characteristics of an electronic tag or implant in a layered biological head, antennas input impedance, SAR values inside the implant, the power absorbed, the total radiated power, the thermal emission, the induced current on a scatterer, novel antenna design, the electric and magnetic near-/far-fields patterns, and also other situations.

Electronic tagging can be regarded as a more permanent form of identification than a smart card. Information on the holder can be read into a computer system. In a simple example, when a smart card or tag is presented, and the individual is recognized, machinery such as a light or a door can operate if the system passes that individual's status.

An even more permanent arrangement is for an individual to be implanted with silicon chip circuitry, which gives out a unique code, identifying the individual concerned. The potential of this technology is enormous. For example it is quite possible for an implant to replace an Access, Visa or bankers card. There is very little danger in losing an implant or having it stolen. Security in banking would therefore be higher.

An implant could carry huge amounts of data on an individual, such as National Insurance number and blood type, with this data being updated and added to where necessary. It could contain information on any medical problems, qualifications, prior convictions and even speeding fines. It would be difficult to lie or cover up such information.

Within businesses, individuals with implants could be clocked in and out of their office automatically. It would be known, at all times exactly where an individual was within a building and whom they were with. They could therefore be contacted for a message or an urgent meeting. An implant could also be extremely useful as far

as vehicle (car) security is concerned. Unless a vehicle (car) recognized the unique signal from its owner it would remain disabled.

But all of this smacks of Big Brother. With an implant, a machine will know where an individual is in a building, at all times. An individual might not even be able to pay a visit to the toilet without a machine knowing about it.

Numerical simulation techniques developed for the comprehensive analysis of the human exposure to electromagnetic waves and estimating the SAR may require considerable time and large computer memory for calculation. Analytical methods provide valuable tools in evaluating the interaction between canonical head/body models and antenna sources.

Chapter 12

Further Work

HOWEVER , in view of the encouraging results of this study the present section addresses different areas of future work which have emerged during the study for this dissertation. These areas can be summarized as follows;

- Investigation of new type of EM simulators based on real life simulation making use of alternative algorithms in particular hybridization of numerical methods with the help of DGFs.
- Another avenue for further work is to investigate the redesign of sources (mobile communications) with respect to biological systems with EM hazard mitigation in mind.

12.1 Performance Improvement

In electromagnetic theory, many scalar wave concepts cannot simply be extended to the vector wave case. Even though most problems can be solved without the use of dyadic Green's functions, the symbolic simplicity with which they could be used to express relationships makes the formulations of many problems simpler and more compact. Moreover, it is easier to conceptualize many problems with dyadic Green's functions.

A straightforward application of numerical methods to many wave and field problems involve using intensive computation and extensive computer time, may

saturate the resources. A combination of numerical and analytical methods, however, can generate computer codes that are many times more efficient, and allow the analysis of larger or extremely smaller EM scattering and coupling problems with reduced unwanted reflections.

12.1.1 Hybridization of MoM-FDTD Hybrid with the DGF Method

Wide-spread use of personal communication (PC) systems necessitates better understanding of EM interactions between various types of antennas and the human body especially in GHz bandwidths or higher. There is a need to solve problems which extend beyond the scope of workstation technology in bioelectromagnetic modeling as well as aerospace design. The recent improvements towards the understanding of EM interactions in PCs have been achieved by popular numerical computations employing various methodologies such as FDTD method [1] - [18], method of moments (MoM) [1] and others. Although MoM is excellent for modeling perfect conductors and FDTD very suitable for simulation of dielectrics these techniques have their disadvantages. Both of these techniques owing to present computer memory and processors computation time have limitations in dealing with the effects of very thin layers (e.g. skin of about 1 mm thick) and high or even extremely higher operating frequencies (e.g. 30-300 GHz). They are also limited in their ability to handle scatterers whose characteristic dimensions are greater than a few wavelengths.

The problem of EM scattering from large bodies is of great practical interest. Indications are that modeling of a finely discretized large object with a very high frequency source may lead to problems when using numerical techniques. This is because large finely discretized models have a large number of cells requiring certain amount of memory allocation and a finite computation time. This results in a burden on computational resources. Therefore EEM (Eigenfunction Expansion), an efficient exact modular technique that uses DGFs can be used to critically investigate these problems especially the effects on very thin layers (e.g. skin), large objects and extremely high frequencies without the limitations/drawbacks of com-

puter resources. This technique allows to compute the fields for a variety of antennas or antenna arrays very cheaply in terms of hardware as well as software in a modular fashion. But this method lacks the visualization capability.

It appears that a large number of benefits are possible from the hybridization. Therefore these popular numerical techniques can be hybridized by EEM to implement the EM problems (head/body-antenna interactions) in personal communications more accurately, efficiently and increased confidence in the final developed model. One technique of hybridization is to truncate the computational volume by enclosing some sort of absorbing boundary condition utilizing DGF around the source and another surrounding radiated specimen and then using a second or even third computational method such as FDTD for computation of fields inside these boundary conditions. The boundaries can be placed close to the contours of source and specimen in this approach to save computer memory and computational time. Another method is to do exactly the opposite of the former technique.

12.1.2 The Development of an Antenna-less PCSs

Both GSM (global system for mobile communication) and PCS (personal communication services) pose potential problems with regard to interactions with the human body and implanted medical devices. Interaction/interference-free antennas design is useful and, increasingly, is becoming necessary.

Since anything that conducts can be considered as an antenna and two antennas interact with each other, the interaction problem could potentially be solved by using the mobile phone (handset transceiver) user (human body) as an antenna and transmitting at frequency levels (for example, noise) unharmful to humans. This would make possible the design of antenna-less PCS, receiving/transmitting signals only in close proximity to biological antennas (users).

Wireless personal communication is a rapidly expanding sector, particularly in the field of cellular mobile phones and wireless local area networks (WLAN's).

In an indoor WLAN system, the user of the mobile terminal can find himself

in close proximity to the radiating antenna. It is, therefore, important to consider possible health hazards due to this type of exposure. As the adverse effects of the electromagnetic (EM) fields are of thermal nature, particularly with reference to the eye, we have to try to somehow decrease these health hazards.

Indoor applications of wireless of local area networks (WLAN's) were introduced in the early 80's to reduce the installation and relocation costs of conventional wired local area networks (LAN's) and to allow the mobility of connected elements in the work space. The existing applications of WLAN's are unlicensed spread-spectrum systems operating the industrial, scientific and medical (ISM) frequencies around 2.45 and 5.8 GHz, and licensed cellular systems operating at 18-19 GHz. More recent WLAN's projects contemplate the use of millimeter-wave frequencies (30 and 60 GHz). In fact, in this frequency region, wide bands are still available from spectrum regular agencies, and the signal is more confined within rooms or buildings, thereby the possibility of frequency reuse and the privacy of communications.

To transmit data, wireless LAN systems use a direct antenna placed at a mobile personal terminal (computer, telephone, camera, etc.) and a wide beam antenna placed at a fixed site (the base station) usually located at the room ceiling or high on a vertical wall. In this arrangement, the user can find himself in close proximity to the radiating mobile antenna, where the electromagnetic (EM) field assumes its highest values. In particular, the user is exposed to an EM field made of the wave directly coming from the radiating antenna and waves produced by reflection and scattering from objects present in the area. As a consequence, it is important to consider the possible health hazard due to such systems and, in particular, to define the EM field values that are safe for human beings.

With reference to the kind of applications under consideration, the frequency range around 2.45 GHz has already been sufficiently investigated due to its extensive use in ISM applications. In this proposal, therefore we specifically focus our attention on the whole interaction of fields.

Over 6 GHz, the correlation between the power-flux density of the incident field

and the specific absorption rate (SAR) (the rate of RF energy deposition) inside the exposed body has been obtained.

In this frequency range, the eyes seems to be one of the most hazardously exposed organs. In fact, the absorption takes place mainly in the skin, and the eye, at least when eyelids are open, is not protected by a skin layer. The eye is an organ particularly sensitive to heating because of the lack of blood flowing into it, and it is subject to thermal damage (lens cataract) even in the presence of weak heating.

At frequencies around 2.45 GHz, the EM radiation penetrates sufficiently deep (starting in the eye so that part of the eye most at risk is its inner region). However, when moving toward higher frequencies (6-30 GHz range), the EM radiation has a smaller penetration depth and therefore, a greater power deposition takes place directly which becomes another hazardously exposed tissue. Unfortunately thermal sensitivity has not been extensively investigated.

On the basis of these facts we have to change our attitude to design of new technology.

As concerns the experimental studies because of the difficulty in performing experiments directly on the humans. Investigators could work on other biological systems e.g. Another type of study, involving animals/insects, is more closely related to real life situations. These studies provide evidence that is more directly relevant to establishing safe exposure levels in humans and often employ several different field levels to investigate dose-response relationships.

12.2 EM Modeling of Moving/Rotating/Bouncing/Spinning Scatterers

Over the past decade, the ability to simulate EM phenomena in a computer has developed considerably. The increase in readily available computing power and speed, coupled with improvements in modeling software now provides the modeler with much greater detail in the analysis of EM structures. Despite all this progress there are no simulators to model/simulate moving, rotating, bouncing, spinning (or

a combination of these) objects. Further work should also address this realistic improvement. This requires;

12.3 Electromagnetic DGF Modeling of Moving Spherical Scatterers

The analysis of the interaction of electromagnetic (EM) fields with moving charged bodies is one of the classic problems in the theory of electromagnetics. The study of moving bodies is relevant to many areas of engineering where the electromagnetic effects induced by motion have to be modeled for device(s) or system(s). The effects on submarines as well as on the body of airplanes and radar scattering objects such as missiles, charged particles moving in a Colimeter, or movement of cells in blood may be presented by multilayered, spherical model in three dimensions. The theme of this investigation can also be focused on the electric activity of nerve and muscle and extracellular electric and magnetic fields that they generate Malmivuo [82]. Also on account of the recent progress in mobile telecommunications systems in the high frequency range, the human body is increasingly exposed to electromagnetic fields. Therefore, the analytical solutions/numerical simulation of the power absorbed in human tissue becomes extremely important in order to meet safety requirements. A typical example is the strong interaction between the near field of an antenna of a hand held transceiver and the sensitive organs on the moving head, such as the eyes.

One could suggest an analytical description based upon Maxwell-Minkowski's relations of an electromagnetic dyadic Green's function (DGFs) for a uniformly moving (multilayered homogeneous lossy dielectric) spherical scatterer model in an isotropic, homogeneous, linear and non-dispersive medium in all directions which is valid everywhere, including the source region bearing in mind the computational efficiency and economy in terms of speed, time and memory. The scatterer could be assumed as a charged particle, cell, ion, human head or even a bullet moving with a constant velocity in the x-direction. In this study we can assume the object to be

rigid, so that all portions of the material may be considered to be moving with the same velocity.

12.4 Electromagnetic DGF for a Moving Human Torso Model

Antenna-body interaction is of interest with the use of biotelemetry transmitters for medical applications. Short range telemeters being developed for medical applications increasingly operate at UHF, taking advantage of greater spectrum availability and reduced levels of synthetic noise. Power dissipation in the body and impedance mismatches induced by effects of proximity presents system losses, so the risk of signal drop-out in the link is increased. The most important operational parameters for a closed-coupled antenna-body interaction for biotelemetry are its antenna efficiency and radiation pattern in the azimuthal plane.

Moreover, the relations between electrodynamics of moving media formulations and Minkowski's classical work which was based upon the special theory of relativity were reviewed by Tai in his articles [98] - [100]. On this basis as suggested in the previous section, one aims to express a mathematical model based upon Maxwell-Minkowski's relations of dyadic Green's function (DGF) for the problem of electromagnetic radiation from a source of excitation in the presence of a uniformly moving human torso model (multi-layered homogeneous lossy dielectric circular cylinder of finite length) as well as any part of the body assuming the shape of a cylinder in an isotropic, homogeneous, linear and non-dispersive medium in all directions. The whole structure is assumed to be uniform along the propagation direction and the object to be rigid, so that all portions of the material may be considered to be moving with the same velocity.

12.5 Various Research Ideas

There is considerable room for future investigation, both theoretical and experimental, of various sources in the presence of biological systems. Using the method of

DGFs, together with scattering superposition, exact expressions could be formulated for the radiation from biological systems. Numerical results could then be easily obtained with the help of a computer since only the calculations of the scattering coefficients would need to be modified. The radiation pattern of the source could also be evaluated.

It would be interesting to construct the model of a whole biological systems e.g., human person and measure its performance.

Finally a great number of further recommendations for future work are suggested;

1. Dyadic Green's Function in a Finite Cylindrically Multilayered Chiral Media.

2. Radiation From a Wrist-Mounted, Motion/Pulse-Activated Mobile Phone on the Wrist.

3. Radiation From a Wrist-Mounted, Motion/Pulse-Activated antenna-less Mobile Phone on the Wrist.

4. Radiation From Sources in the Presence of a Moving Biological System (Head /Body).

5. Dyadic Green's Function for a Moving Finite Cylindrically Multilayered Chiral Media.

6. Dyadic Green's Function for a Moving Finite Cylindrically Multilayered Media in uniform translation motion.

7. Dyadic Green's Function for a Moving Spherically Multilayered Media in uniform translation motion.

8. Particles with Spin in an Electromagnetic Field using Dyadic Green's Function.

9. Effect of Electromagnetic Radiation on Particles at Point of Impact using Dyadic Green's Function.

10. Effect of Electromagnetic Radiation on Rotating Particles/Bodies under Gravitational Influence using Dyadic Green's Function.

11. Electromagnetic Modeling of Moving Spherical Head Using Dyadic Green's Function.

12. Electromagnetic Dyadic Green's Function for a Moving Human Torso Model.

13. Electromagnetic Modeling of Moving Spherical Head Using a Hybrid MoM/DGF /FDTD.

14. Electromagnetic Hybrid MoM/DGF/FDTD for a Moving Human Torso Model.

15. Microwave Thermal Emission from a Spherical Stratified Medium with Non-uniform Temperature Distribution.

16. Microwave Thermal Emission from a Cylindrical Stratified Medium with Non-uniform Temperature Distribution.

17. Microwave Thermal Emission from an Implanted Spherical Stratified Head Model Medium with Non-uniform Temperature Distribution.

18. Microwave Thermal Emission from an Implanted Cylindrical Stratified Body Model Medium with Non-uniform Temperature Distribution.

19. Electromagnetic Dyadic Green's Function in an Implanted Cylindrically Multilayered Body Model Media.

20. Electromagnetic Dyadic Green's Function in an Implanted Spherically Multilayered Head Model Media.

21. Microwave Thermal Emission from an Implanted Spherical Stratified Head Model in a Moving Medium with Non-uniform Temperature Distribution.

22. Microwave Thermal Emission from an Implanted Cylindrical Stratified Body Model in a Moving Medium with Non-uniform Temperature Distribution.

23. Electromagnetic FDTD's Function in an Implanted Cylindrically Multilayered Body Model Media.

24. Electromagnetic FDTD's Function in an Implanted Spherically Multilayered Body Model Media.

25. Electromagnetic FDTD's Function in a Whole Multilayered Person Model Media.

26. Electromagnetic FDTD's Function in an Implanted Whole Multilayered Person Model Media.

27. Electromagnetic Dyadic Green's Function in a Whole Multilayered Person Model Media.

28. Electromagnetic Dyadic Green's Function in an Implanted Whole Multilayered Person Model Media.

29. Electromagnetic Dyadic Green's Function of a Small Cylindrical/Spherical Implant Embedded into a Dielectric Single/Multi-Layered Spherical Head Model Media.

30. Electromagnetic Dyadic Green's Function of a Small Cylindrical/Spherical Implant Embedded into a Dielectric Single/Multi-Layered Cylindrical Body Model Media.

31. Electromagnetic FDTD's Function of a Small Cylindrical/Spherical Implant Embedded into a Dielectric Single/Multi-Layered Spherical Head Model Media.

32. Electromagnetic FDTD's Function of a Small Cylindrical/Spherical Implant Embedded into a Dielectric Single/Multi-Layered Cylindrical Body Model Media.

33. Electromagnetic FDTD's Function of a Small Helical Implant Embedded into a Dielectric Single/Multi-Layered Spherical Head Model Media.

34. Electromagnetic FDTD's Function of a Small Helical Implant Embedded into a Dielectric Single/Multi-Layered Cylindrical Body Model Media.

35. Electromagnetic Dyadic Green's Function of a Small Helical Implant Embedded into a Dielectric Single/Multi-Layered Spherical Head Model Media.

36. Electromagnetic Dyadic Green's Function of a Small Helical Implant Embedded into a Dielectric Single/Multi-Layered Cylindrical Body Model Media.

37. Electromagnetic Fields Induced Inside an Implanted Multi-Layered Arbitrarily Shaped Head Model in a Moving Medium with Non-uniform Temperature Distribution.

38. Electromagnetic Fields Induced Inside an Implanted Multi-Layered Arbitrarily Shaped Head Model.

39. Fast Algorithm for Electromagnetic Fields induced Inside an Implanted Multi-Layered Arbitrarily Shaped Head Model.

40. Performance of Various Mobile Communication Antennas in a Conducting Structure using EEM.

41. Electromagnetic Fields from an Electrosurgical Device that Interferes with other Medical Devices using EEM for Numerical EMC Investigation.

42. Fast Algorithm for Electromagnetic Scattering by Implanted Conducting Prostheses of Large Size using EEM.

43. The Effect of Shape, Size and Material of Different Antennas on Biological Systems.

Different areas for future work have been raised, many more exist, and they should be considered.

Appendix A

Vector Wave Functions and Their Mutual Relationships

A.1 Spherical Vector Wave Functions

The spherical vector wave functions are the building blocks of the EFE of various kinds of spherical DGF. They are solutions of the homogeneous vector equations. The generating functions, which are solutions of the spherical scalar wave equation $\nabla^2\Psi + k^2\Psi=0$, can be written in the form

$$\Psi_{emn}(k) = j_n(kR)F_n^m(\cos\theta)^{\cos}_{\sin}m\phi, \tag{A.1}$$

Here k is an undetermined wave number determined by the boundary conditions and x is the piloting vector. Subscripts "e" stands for even and "o" is odd character of the generating functions. Where $F_n^m(\cos\theta)$ identifies the Associated Legendre functions of the first kind with order (n, m) and $j_n(kR)$ denotes the spherical Bessel functions of the order n to represent both out-going and in-coming waves.

The solenoidal vector wave functions needed to construct $\overline{\overline{G}}_e^{Lfo}$ and $\overline{\overline{G}}_m^{Lfo}$ are solutions of the following homogeneous differential equation

$$\nabla\times\left[\nabla\times\left(\overline{\Psi}\right)\right] - k^2\overline{\Psi} = 0 \tag{A.2}$$

Spherical vector wave functions are akin to the Debye potentials. $\overline{M}_{emn}(k) = \frac{1}{k}\nabla\times[\Psi_{emn}\hat{x}]$ and $\overline{N}_{emn}(k) = \frac{1}{k}\nabla\times[\overline{M}_{emn}(k)] = \frac{1}{k^2}\nabla\times(\nabla\times\Psi_{emn}\hat{x}) = \frac{1}{k^2}\nabla\times\nabla\times[\Psi_{emn}\hat{x}]$. These

functions are defined in the entire space, corresponding to $0 \leq R \leq \infty$, $0 \leq \phi \leq 2\pi$ and $0 \leq \theta \leq \pi$. The orthogonal properties of these vector wave functions have been discussed by Tai [19].

The complete expressions for the solenoidal (rotational or transverse) functions in the $\hat{R}$-direction for stationary scatterer are given by Tai [19]:

$$\begin{aligned}\overline{M}^{(R)}_{\substack{e\\o}mn}(k) &= \nabla\times[\Psi_{\substack{e\\o}mn}\hat{R}] \\ &= \left\{\begin{array}{c} 0 \\ \mp\frac{m}{\sin\theta}j_n(kR)F_n^m(\cos\theta)^{\sin}_{\cos}m\phi\hat{\theta} \\ -j_n(kR)(\frac{\partial F_n^m(\cos\theta)}{\partial\theta})^{\cos}_{\sin}m\phi\hat{\phi} \end{array}\right\},\end{aligned} \tag{A.3}$$

and

$$\begin{aligned}\overline{N}^{(R)}_{\substack{e\\o}mn}(k) &= \frac{1}{k}\nabla\times\nabla\times[\Psi_{\substack{e\\o}mn}\hat{R}] \\ &= \left\{\begin{array}{c} \frac{n(n+1)}{kR}j_n(kR)F_n^m(\cos\theta)^{\cos}_{\sin}m\phi\hat{R} \\ \frac{1}{kR}\frac{\partial}{\partial R}[Rj_n(kR)](\frac{\partial F_n^m(\cos\theta)}{\partial\theta})^{\cos}_{\sin}m\phi\hat{\theta} \\ \frac{1}{kR}\frac{\partial}{\partial R}[Rj_n(kR)][\mp\frac{m}{\sin\theta}F_n^m(\cos\theta)^{\sin}_{\cos}m\phi\hat{\phi}] \end{array}\right\},\end{aligned} \tag{A.4}$$

where $\overline{M}^{(R)}_{\substack{e\\o}mn}(k)$ and $\overline{N}^{(R)}_{\substack{e\\o}mn}(k)$ are the even or odd spherical vector wave functions.

These functions can also be derived in terms of other directions such as x;

$$\begin{aligned}\overline{M}^{(x)}_{emn}(k) &= \frac{1}{k}\nabla\times[\Psi_{emn}\hat{x}] \\ &= \frac{1}{k}\nabla\times\left[\Psi_{emn}\left(\sin\theta\cos\phi\hat{R}+\cos\theta\cos\phi\hat{\theta}-\sin\phi\hat{\phi}\right)\right] \\ &= \frac{1}{kR}\left\{\begin{array}{l} \frac{-1}{\sin\theta}\left[\frac{\partial}{\partial\theta}(\sin\theta\sin\phi\Psi_{emn})+\frac{\partial}{\partial\phi}(\cos\theta\cos\phi\Psi_{emn})\right]\hat{R} \\ +\left[\frac{1}{\sin\theta}\frac{\partial}{\partial\phi}(\sin\theta\cos\phi\Psi_{emn})+\frac{\partial}{\partial R}(R\sin\phi\Psi_{emn})\right]\hat{\theta} \\ +\left[\frac{\partial}{\partial R}(R\cos\theta\cos\phi\Psi_{emn})-\frac{\partial}{\partial\theta}(\sin\theta\cos\phi\Psi_{emn})\right]\hat{\phi} \end{array}\right\}\end{aligned} \tag{A.5}$$

The relationship to the $\overline{M}^{(R)}_{\substack{e\\ omn}}(k)$ and $\overline{N}^{(R)}_{\substack{e\\ omn}}(k)$ functions;

$$\begin{aligned}
\overline{M}^{(x)}_{\substack{e\\ omn}}(k) &= \frac{1}{k}\nabla\times[\Psi_{\substack{e\\ omn}}\hat{x}] \\
&= \frac{1}{k}\nabla\times\left[\Psi_{\substack{e\\ omn}}\left(\sin\theta\cos\phi\hat{R}+\cos\theta\cos\phi\hat{\theta}-\sin\phi\hat{\phi}\right)\right] \\
&= \pm\frac{1}{2n(n+1)}\left[\overline{N}^{(R)}_{\substack{o\\ e}(m+1)n}(k)+(n+m)(n-m+1)\overline{N}^{(R)}_{\substack{o\\ e}(m-1)n}(k)\right] \\
&+\frac{1}{2(n+1)(2n+1)}\left[\overline{M}^{(R)}_{\substack{o\\ e}(m+1)(n+1)}(k)-(n-m+1)(n-m+2)\overline{M}^{(R)}_{\substack{o\\ e}(m-1)(n+1)}(k)\right] \\
&-\frac{1}{2n(2n+1)}\left[\overline{M}^{(R)}_{\substack{o\\ e}(m+1)(n-1)}(k)-(n+m-1)(n+m)\overline{M}^{(R)}_{\substack{o\\ e}(m-1)(n-1)}(k)\right]
\end{aligned} \tag{A.6}$$

$$\begin{aligned}
\overline{N}^{(x)}_{\substack{e\\ omn}}(k) &= \frac{1}{k^2}\nabla\times\nabla\times[\Psi_{\substack{e\\ omn}}\hat{x}] \\
&= \frac{1}{k^2}\nabla\times\nabla\times\left[\Psi_{\substack{e\\ omn}}\left(\sin\theta\cos\phi\hat{R}+\cos\theta\cos\phi\hat{\theta}-\sin\phi\hat{\phi}\right)\right] \\
&= \pm\frac{1}{2n(n+1)}\left[\overline{M}^{(R)}_{\substack{o\\ e}(m+1)n}(k)+(n+m)(n-m+1)\overline{M}^{(R)}_{\substack{o\\ e}(m-1)n}(k)\right] \\
&+\frac{1}{2(n+1)(2n+1)}\left[\overline{N}^{(R)}_{\substack{o\\ e}(m+1)(n+1)}(k)-(n-m+1)(n-m+2)\overline{N}^{(R)}_{\substack{o\\ e}(m-1)(n+1)}(k)\right] \\
&-\frac{1}{2n(2n+1)}\left[\overline{N}^{(R)}_{\substack{o\\ e}(m+1)(n-1)}(k)-(n+m-1)(n+m)\overline{N}^{(R)}_{\substack{o\\ e}(m-1)(n-1)}(k)\right]
\end{aligned} \tag{A.7}$$

The additional constant $\frac{1}{k}$ which included in these functions makes them of the same dimension as that of $\overline{M}^{(R)}_{\substack{e\\ omn}}(k)$ or $\overline{N}^{(R)}_{\substack{e\\ omn}}(k)$ defined by (A.3) and (A.4).

$$\begin{aligned}
\overline{M}^{(y)}_{\substack{e\\ omn}}(k) &= \frac{1}{k}\nabla\times[\Psi_{\substack{e\\ omn}}\hat{y}] \\
&= \frac{1}{k}\nabla\times\left[\Psi_{\substack{e\\ omn}}\left(\sin\theta\sin\phi\hat{R}+\cos\theta\sin\phi\hat{\theta}+\cos\phi\hat{\phi}\right)\right] \\
&= -\frac{1}{2n(n+1)}\left[\overline{N}^{(R)}_{\substack{e\\ o}(m+1)n}(k)-(n+m)(n-m+1)\overline{N}^{(R)}_{\substack{e\\ o}(m-1)n}(k)\right] \\
&\pm\frac{1}{2(n+1)(2n+1)}\left[\overline{M}^{(R)}_{\substack{e\\ o}(m+1)(n+1)}(k)+(n-m+1)(n-m+2)\overline{M}^{(R)}_{\substack{e\\ o}(m-1)(n+1)}(k)\right] \\
&\mp\frac{1}{2n(2n+1)}\left[\overline{M}^{(R)}_{\substack{e\\ o}(m+1)(n-1)}(k)+(n+m-1)(n+m)\overline{M}^{(R)}_{\substack{e\\ o}(m-1)(n-1)}(k)\right]
\end{aligned} \tag{A.8}$$

$$
\begin{aligned}
\overline{N}^{(y)}_{\substack{e\\ o}mn}(k) &= \frac{1}{k^2}\nabla\times\nabla\times[\Psi_{\substack{e\\ o}mn}\hat{y}] \\
&= \frac{1}{k^2}\nabla\times\nabla\times\Big[\Psi_{\substack{e\\ o}mn}\left(\sin\theta\sin\phi\hat{R}+\cos\theta\sin\phi\hat{\theta}+\cos\phi\hat{\phi}\right)\Big] \\
&= -\frac{1}{2n(n+1)}\left[\overline{M}^{(R)}_{\substack{o\\ e}(m+1)n}(k)-(n+m)(n-m+1)\overline{M}^{(R)}_{\substack{o\\ e}(m-1)n}(k)\right] \\
&\pm\frac{1}{2(n+1)(2n+1)}\left[\overline{N}^{(R)}_{\substack{e\\ o}(m+1)(n+1)}(k)+(n-m+1)(n-m+2)\overline{N}^{(R)}_{\substack{e\\ o}(m-1)(n+1)}(k)\right] \\
&\mp\frac{1}{2n(2n+1)}\left[\overline{N}^{(R)}_{\substack{e\\ o}(m+1)(n-1)}(k)+(n+m-1)(n+m)\overline{N}^{(R)}_{\substack{e\\ o}(m-1)(n-1)}(k)\right]
\end{aligned}
\tag{A.9}
$$

$$
\begin{aligned}
\overline{M}^{(z)}_{\substack{e\\ o}mn}(k) &= \frac{1}{k}\nabla\times[\Psi_{\substack{e\\ o}mn}\hat{z}] \\
&= \frac{1}{k}\nabla\times\Big[\Psi_{\substack{e\\ o}mn}\left(\cos\theta\hat{R}-\sin\theta\hat{\theta}\right)\Big] \\
&= \mp\frac{m}{n(n+1)}\left[\overline{N}^{(R)}_{\substack{e\\ o}mn}(k)\right] \\
&+\frac{1}{(2n+1)}\left[\frac{n-m+1}{n+1}\overline{M}^{(R)}_{\substack{e\\ o}m(n+1)}(k)+\frac{(n+m)}{n}\overline{M}^{(R)}_{\substack{e\\ o}m(n-1)}(k)\right]
\end{aligned}
\tag{A.10}
$$

$$
\begin{aligned}
\overline{N}^{(z)}_{\substack{e\\ o}mn}(k) &= \frac{1}{k^2}\nabla\times\nabla\times[\Psi_{\substack{e\\ o}mn}\hat{z}] \\
&= \frac{1}{k^2}\nabla\times\nabla\times\Big[\Psi_{\substack{e\\ o}mn}\left(\cos\theta\hat{R}-\sin\theta\hat{\theta}\right)\Big] \\
&= \mp\frac{m}{n(n+1)}\left[\overline{M}^{(R)}_{\substack{e\\ o}mn}(k)\right] \\
&+\frac{1}{(2n+1)}\left[\frac{n-m+1}{n+1}\overline{N}^{(R)}_{\substack{e\\ o}m(n+1)}(k)+\frac{(n+m)}{n}\overline{N}^{(R)}_{\substack{e\\ o}m(n-1)}(k)\right]
\end{aligned}
\tag{A.11}
$$

A.2 Vector Wave Functions for a Circular Cylinder of Finite Length

The cylindrical vector wave functions are the building blocks of the EFE of various kinds of cylindrical DGF. They are denoted by $\overline{L}_{\substack{ee\\ oo}n\lambda}$, $\overline{P}_{\substack{ee\\ oo}n\lambda}$ and $\overline{Q}_{\substack{ee\\ oo}n\lambda}$, that are solutions of the homogeneous vector Helmholtz equation. The generating or Eigenfunctions, which are solutions of the cylindrical scalar wave equation $\nabla^2\Psi+\kappa_\lambda^2\Psi=0$,

with the differential equation in the cylindrical coordinate system

$$\frac{1}{r}\frac{\partial}{\partial r}(r\frac{\partial \Psi}{\partial r}) + \frac{1}{r^2}\frac{\partial^2 \Psi}{\partial \phi^2} + \frac{\partial^2 \Psi}{\partial \phi^2} + \frac{\partial^2 \Psi}{\partial z^2} + K^2\Psi = 0 \tag{A.12}$$

with K, the separation constant and κ_λ being an undetermined wave number. Implementation of the method of separation of variables in this system finally results the generating function in Reyhani [28] in the form

$$\Psi_{\substack{ee\\oo}n}(h) = j_n(\lambda r)^{\cos}_{\sin} n\phi^{\cos}_{\sin} hz, \tag{A.13}$$

Here subscripts "e" stands for even and "o" is odd character of the generating functions. $h = \frac{q\pi}{l}$ are the eigenvalues in the z-direction with $q = 0, 1, 2, ...$ and l is the length of cylinder (fig. 2). $j_n(\lambda r)$ identifies the cylindrical Bessel functions of the order n to represent both out-going and in-coming waves. λ is the continuous eigen-value.

The solenoidal vector wave functions needed to construct $\overline{\overline{G}}_e^{Lfo}$ and $\overline{\overline{G}}_m^{Lfo}$ are solutions of the following homogeneous differential equation

$$\nabla \times [\nabla \times (\overline{\Psi})] - \kappa_\lambda^2 \overline{\Psi} = 0 \tag{A.14}$$

Cylindrical vector wave functions are akin to the Debye potentials.

$$\overline{P}^{(x)}_{\substack{ee\\oo}n\lambda}(h) = \nabla \times [\Psi_{\substack{ee\\oo}n}\hat{x}] \tag{A.15}$$

$$\overline{Q}^{(x)}_{\substack{ee\\oo}n\lambda}(h) = \frac{1}{\kappa_\lambda}\nabla \times (\nabla \times \Psi_{\substack{ee\\oo}n}\hat{x}) = \frac{1}{\kappa_\lambda}\nabla \times \nabla \times [\Psi_{\substack{ee\\oo}n}\hat{x}] \tag{A.16}$$

Where $\hat{x}$ is the piloting vector.

The complete expressions for the solenoidal (rotational or transverse) functions in the $\hat{z}$-direction for stationary scatterer are given by Reyhani [28, 29]:

$$\overline{P}^{(z)}_{\substack{ee\\oo}n\lambda}(h) = \left\{ \begin{array}{c} \mp\frac{n}{r} j_n(\lambda r)^{\sin}_{\cos} n\phi^{\cos}_{\sin} hz\hat{r} \\ -(\frac{\partial j_n(\lambda r)}{\partial r})^{\cos}_{\sin} n\phi^{\cos}_{\sin} hz\hat{\phi} \\ 0 \end{array} \right\} \tag{A.17}$$

$$\overline{Q}^{(z)}_{\substack{ee\\oo}n\lambda}(h) = \left\{ \begin{array}{c} \mp h[\frac{\partial j_n(\lambda r)}{\partial r}]^{\cos}_{\sin} n\phi^{\sin}_{\cos} hz\hat{r} \\ \frac{hn}{r}[j_n(\lambda r)]^{\sin}_{\cos} n\phi^{\sin}_{\cos} hz\hat{\phi} \\ \lambda^2[j_n(\lambda r)]^{\cos}_{\sin} n\phi^{\cos}_{\sin} hz\hat{z} \end{array} \right\} \frac{1}{\kappa_\lambda} \tag{A.18}$$

where $\overline{P}^{(z)}_{\substack{ee\\oo}n\lambda}(h)$ and $\overline{Q}^{(z)}_{\substack{ee\\oo}n\lambda}(h)$ are the even or odd cylindrical vector wave functions.

Here $\kappa^2_\lambda = \lambda^2 + h^2$, and in these vector wave functions one should be careful with the sign of the elements in the matrices when cross-multiplying the terms from "e" to "o" and vice-versa e.g. "sin sin" always remains negative while "cos cos" positive. Also "$-$ cos sin" and "$-$ sin cos" in second elements of matrices in $\overline{P}_{eo}$ and $\overline{P}_{oe}$ respectively. In $\overline{L}_{eo}$ and $\overline{L}_{oe}$ both "cos sin" and "sin cos" are positive in the first element of their respective matrix. For $\overline{Q}_{eo}$, "$-$ sin cos" in second element of matrix, while "$+$ cos sin" in the third element. For $\overline{Q}_{oe}$, "$-$ cos sin" and "$+$ sin cos" in the elements 2 and 3 respectively. "$\mp$" applies the negative to the top line while positive to the bottom line.

Note that in the set of cylindrical vector wave functions only $\overline{P}_{\substack{ee\\oo}n\lambda}$ do not possess the z component. The $\hat{r}$, $\hat{\phi}$ and $\hat{z}$ are the cylindrical unit vectors. These functions are defined in the entire space, corresponding to $0 \leq r \leq \infty$, $0 \leq \phi \leq 2\pi$ and $0 < z < l$.

The volume integral of the product of the cylindrical vector wave functions is clearly zero if $n \neq n'$ and $h \neq h'$ because of the orthogonal property of the $\cos n\phi$ and $\sin n\phi$ functions and the Fourier integral relation. The derivation of the orthogonal properties of these vector wave functions have been presented in chapter 4 and also in Reyhani [28, 29] and are very similar to those for infinite circular cylinder discussed by Tai [19].

These functions can also be derived in terms of other directions such as x;

$$\begin{aligned}\overline{P}^{(x)}_{\substack{ee\\oo}n\lambda}(h) &= \nabla\times[\Psi_{\substack{ee\\oo}n}\hat{x}] \\ &= \nabla\times\left\{\Psi_{\substack{ee\\oo}n}\begin{bmatrix}\cos\phi\hat{r}\\ -\sin\phi\hat{\phi}\\ 0\end{bmatrix}\right\}\end{aligned} \tag{A.19}$$

The relationship to the $\overline{P}^{(z)}_{\substack{ee\\oo}n\lambda}(h)$ and $\overline{Q}^{(z)}_{\substack{ee\\oo}n\lambda}(h)$ functions;

$$\begin{aligned}\overline{P}^{(x)}_{\substack{ee\\oo}n\lambda}(h) &= \nabla\times[\Psi_{\substack{ee\\oo}n}(h)\hat{x}] \\ &= -\frac{h}{2\lambda}\begin{bmatrix}\overline{P}^{(z)}_{\substack{ee\\oo}(n+1)\lambda}(h)\\ -\overline{P}^{(z)}_{\substack{ee\\oo}(n-1)\lambda}(h)\end{bmatrix} \pm \frac{\kappa_\lambda}{2\lambda}\begin{bmatrix}\overline{Q}^{(z)}_{\substack{oo\\ee}(n+1)\lambda}(h)\\ \overline{Q}^{(z)}_{\substack{oo\\ee}(n+1)\lambda}(h)\end{bmatrix}\end{aligned} \tag{A.20}$$

$$\begin{aligned}\overline{Q}^{(x)}_{\substack{ee\\oo}n\lambda}(h) &= \frac{1}{\kappa_\lambda}\nabla\times\nabla\times[\Psi_{\substack{ee\\oo}n}(h)\hat{x}] \\ &= -\frac{h}{2\lambda}\begin{bmatrix}\overline{Q}^{(z)}_{\substack{ee\\oo}(n+1)\lambda}(h)\\ -\overline{Q}^{(z)}_{\substack{ee\\oo}(n-1)\lambda}(h)\end{bmatrix} \pm \frac{\kappa_\lambda}{2\lambda}\begin{bmatrix}\overline{P}^{(z)}_{\substack{oo\\ee}(n+1)\lambda}(h)\\ \overline{P}^{(z)}_{\substack{oo\\ee}(n+1)\lambda}(h)\end{bmatrix}\end{aligned} \tag{A.21}$$

Appendix B

Electromagnetic Fields due to Electric and Magnetic Current Distributions using Dyadic Green's Functions

THE convenience of introducing non-physical magnetic current sources into electromagnetic analysis has long been recognized. Thus we can exploit symmetry of the field structure when both electric and magnetic sources are present. Integral solutions of electromagnetic vector wave equations arising from electric and magnetic current sources are presented. The basic philosophy of this appendix then lies in the choice of a particular set of basic functions (dependent on the nature of the problem) which are valid everywhere, including the source region. The method of analysis involves the derivation of dyadic Green's functions of both electric and magnetic type by employing the principle of scattering superposition. We shall assume that one can expand the DGFs for other geometries in a similar manner. Furthermore, we have also made an attempt to compare these solutions with the formulations of previous related studies.

B.1 Introduction

The dyadic Green's function (DGF) was introduced by Schwinger in the early 1940's, and has become a powerful and important tool for evaluation of fields and solving boundary-value problems. Its properties has been extensively discussed by Tai [20] - [19], Collin [21], Samii [22], Yaghjian [24] and others. This technique allows the formulation of various canonical electromagnetic problems in a systematic manner and to enable many special cases to be treated as one general problem. If the current source in these problems has a number of specific distribution, we have to consider each distribution as special cases. for example, excitation by a transversal electric dipole or a longitudinal or a magnetic dipole. The DGF, which relates the current source and the field is singular in the source region. Although opinions in the literature are not seriously divided, this appendix reviews a number of references commencing with early contributors such as Yaghjian [24] and [27] - [66] in order to highlight some of the difficulties that were encountered in constructing the correct DGF, especially in the source region.

The format of this appendix is as follows. Section B.2 presents the integral solutions of electromagnetic vector wave equations for fields due to the electric and magnetic current sources. Two methods for determining the electric and magnetic fields generated by both current sources located inside a finite volume are presented; one based on Tai's utilization of second vector dynamic Green's theorem [19] and the other employing the method of potentials using the Hertzian (Debye) potentials $\overline{\overline{\Pi}}_e(\overline{R})$ and $\overline{\overline{\Pi}}_m(\overline{R})$. Our objective is to present a more complete formulation than previously reported.

The complete set of rectangular vector wave functions are introduced in section B.3.

In section B.4, we consider the unbounded case, in which the point source radiates with no interface present and construct the corresponding DGF, $\overline{\overline{G}}_{e_{mo}}(\overline{R}, \overline{R}')$, in terms of an integral over the spectra of plane waves that constitute the continuous eigenfunction expansion in which the eigenfunctions are guided in the preferred

R-coordinate direction. These expansions also contain an explicit dyadic delta function term, which is required for completeness, at the source point. It is considered as a correction to the general solenoidal eigenfunction expansion which is valid outside the source point. In this section, we also express the complete Eigen-function expansion of the scattering DGF for the media, in terms of only the solenoidal eigenfunctions. These are simple and straight-forward expressions. The DGFs for complex media, $\overline{\overline{G}}_{em}^{(fs)}(\overline{R},\overline{R}')$ can then be constructed from the principle of the superposition, which involves the sum of the fields of a source in free space (or the free space Green's function $\overline{\overline{G}}_{em_o}(\overline{R},\overline{R}')$) and secondly, the fields scattered by the media $\overline{\overline{G}}_{em_s}^{(Lfs)}(\overline{R},\overline{R}')$.

Section B.5 discusses the discrepancies involved in other authors' corresponding formulations and some remedies are proposed.

Conclusions are then presented in section B.6 summarizing the important points contained in this work.

B.2 Derivation of Electromagnetic Fields due to Electric and Magnetic Current Distributions using Dyadic Green's Functions

The derivation of a general relation for $(\overline{E}_f)$ and $(\overline{H}_f)$ for the case of two types of current sources such as $\overline{J}_e$ and $\overline{J}_m$ radiating in an isotropic, homogeneous medium is quite simple and may be usefully applied to various problems of propagation in media.

Here, the time-harmonic convention of $e^{-i\omega t}$ is used. Consider electric $(\overline{E}_e)$ and magnetic $(\overline{H}_e)$ vectors to be generated by an electric current described by the current density vector $\overline{J}_e$. The vectors $\overline{E}_e$ and $\overline{H}_e$ are then the solutions of Maxwell's equations, (B.1) and (B.2).

$$\nabla \times \overline{E}_e(\overline{R}) = i\omega\mu_o \overline{H}_e(\overline{R}) \tag{B.1}$$

$$\nabla \times \overline{H}_e(\overline{R}) = \overline{J}_e(\overline{R}) - i\omega\epsilon_o\overline{E}_e(\overline{R}) \tag{B.2}$$

Similarly $\overline{E}_m$ and $\overline{H}_m$ are generated by a non-physical magnetic current density vector $\overline{J}_m$

$$\nabla \times \overline{E}_m(\overline{R}) = i\omega\mu_o\overline{H}_m(\overline{R}) - \overline{J}_m(\overline{R}) \tag{B.3}$$

$$\nabla \times \overline{H}_m(\overline{R}) = -i\omega\epsilon_o\overline{E}_m(\overline{R}) \tag{B.4}$$

The use of the magnetic current density vector ensures symmetric Maxwell's equations. It is sometimes necessary to calculate the electromagnetic fields due to both electric and equivalent magnetic current sources.

Assuming $\overline{H}_e + \overline{H}_m = \overline{H}_f$ and $\overline{E}_e + \overline{E}_m = \overline{E}_f$. Therefore Maxwell's equations with a magnetic current density $\overline{J}_m$ could be written as

$$\nabla \times \overline{E}_f(\overline{R}) = i\omega\mu_f\overline{H}_f(\overline{R}) - \overline{J}_m(\overline{R}) \tag{B.5}$$

$$\nabla \times \overline{H}_f(\overline{R}) = \overline{J}_e(\overline{R}) - i\omega\epsilon_f\overline{E}_f(\overline{R}). \tag{B.6}$$

Since electromagnetic fields are vector fields, the general wave equation is a vector wave equation. For an homogeneous isotropic medium, the general form of the vector wave equation is given by:

$$\nabla\times\nabla\times\overline{E}_f - k_f^2\overline{E}_f = (i\omega\mu_f\overline{J}_e - \nabla\times\overline{J}_m)\delta_f^s \tag{B.7}$$

$$\nabla\times\nabla\times\overline{H}_f - k_f^2\overline{H}_f = (i\omega\epsilon_f\overline{J}_m + \nabla\times\overline{J}_e)\delta_f^s \tag{B.8}$$

The above equations follow directly from duality principle. To obtain the electromagnetic fields due to these electric and magnetic current distributions, one first constructs $\overline{\overline{G}}_e^{fs}(\overline{R},\overline{R}')$ and $\overline{\overline{G}}_m^{fs}(\overline{R},\overline{R}')$, the electric and magnetic dyadic Green's functions respectively [19] and [21]. These two DGFs are the solutions of the following dyadic differential equations (taking into account the discontinuous nature of magnetic or electric DGF with respect to electric or magnetic dipole respectively at $z = z'$ i.e., $\nabla\times\overline{\overline{I}}\delta_{e,m}(\overline{R}-\overline{R}') = 0$ and in case of cavities the source term $\overline{J}_{e,m} = 0$ on the surface):

$$\nabla\times\nabla\times\overline{\overline{G}}_{e,m}^{(fs)}(\overline{R},\overline{R}') - k_f^2\overline{\overline{G}}_{e,m}^{(fs)}(\overline{R},\overline{R}') = i\omega\vartheta\overline{\overline{I}}\delta_{e,m}(\overline{R}-\overline{R}')\delta_f^s \tag{B.9}$$

Where ϑ represents ε or μ in the electric or magnetic DGF equations respectively. Here a unit current density at $\overline{R}'$ in the direction of e or m has the space form $\delta_{\substack{e\\m}}(\overline{R}-\overline{R}')$. This requires that both DGFs satisfy the non-solenoidal condition $\nabla \cdot \overline{\overline{G}}^{fs}_{\substack{e\\m}}(\overline{R},\overline{R}') \neq 0$ because

$$\nabla \cdot \overline{E} = \frac{\overline{\rho}_e}{\varepsilon} = \frac{\nabla \cdot \overline{J}_e}{i\omega\varepsilon} \tag{B.10}$$

and

$$\nabla \cdot \overline{H} = \frac{\overline{\rho}_m}{\mu} = \frac{\nabla \cdot \overline{J}_m}{i\omega\mu} \tag{B.11}$$

To find the integral solutions for the vector wave equations (B.7) we can either apply the second vector dyadic Green's theorem or method of potential [19];

B.2.1 Method (1)

Using the second vector dyadic Green's theorem, namely;

$$\begin{aligned}\iiint_V [\overline{P}\cdot\nabla\times\nabla\times\overline{\overline{Q}} - (\nabla\times\nabla\times\overline{P})\cdot\overline{\overline{Q}}]dV \\ = -\oiint_S n\cdot[\overline{P}\times\nabla\times\overline{\overline{Q}} + (\nabla\times\overline{P})\times\overline{\overline{Q}}]dS\end{aligned} \tag{B.12}$$

Where V is the entire volume enclosed by surface S. By letting $\overline{P} = \overline{E}(\overline{R})$, $\overline{\overline{Q}} = \overline{\overline{G}}_e(\overline{R},\overline{R}')$ and assuming $\overline{S}_e(\overline{R}) = i\omega\mu_f\overline{J}_e(\overline{R}) - \nabla\times\overline{J}_m(\overline{R})$ corresponds to a source of finite extent, and in view of (B.7) and (B.9) we obtain

$$\begin{aligned}\iiint_V \left\{ \begin{array}{c} [k^2\overline{E}(\overline{R}) + \overline{S}_e(\overline{R})]\cdot\overline{\overline{G}}_e(\overline{R},\overline{R}') \\ -\overline{E}(\overline{R})\cdot[k^2\overline{\overline{G}}_e(\overline{R},\overline{R}') + i\omega\epsilon\overline{\overline{I}}\delta_e(\overline{R}-\overline{R}')] \end{array} \right\} dV \\ = \oiint_S n\cdot\left\{ \begin{array}{c} \overline{E}(\overline{R})\times\nabla\times\overline{\overline{G}}_e(\overline{R},\overline{R}') \\ [\nabla\times\overline{E}(\overline{R})]\times\overline{\overline{G}}_e(\overline{R},\overline{R}') \end{array} \right\} dS\end{aligned} \tag{B.13}$$

Two of the terms in the volume integral of the above equation cancel each other,

and using the integral property of a delta function

$$\iiint_V \overline{E}(\overline{R}) \cdot i\omega\epsilon\overline{\overline{I}}\delta_e(\overline{R}-\overline{R}')dV = i\omega\epsilon\iiint_V \overline{E}(\overline{R})\delta_e(\overline{R}-\overline{R}')dV = i\omega\epsilon\overline{E}(\overline{R}') \tag{B.14}$$

Hence

$$i\omega\epsilon\overline{E}(\overline{R}') - \iiint_V \left\{\overline{S}_e(\overline{R})\cdot\overline{\overline{G}}_e(\overline{R},\overline{R}')\right\}dV = -\oiint_S n\cdot\left\{\begin{array}{c}\overline{E}(\overline{R})\times\nabla\times\overline{\overline{G}}_e(\overline{R},\overline{R}') \\ [\nabla\times\overline{E}(\overline{R})]\times\overline{\overline{G}}_e(\overline{R},\overline{R}')\end{array}\right\}dS \tag{B.15}$$

for a Maxwellian field such as (B.5), and because of the dyadic identity

$$\overline{a}\cdot(\overline{b}\times\overline{\overline{c}}) = \overline{b}\cdot(\overline{a}\times\overline{\overline{c}}) = (\overline{a}\times\overline{b})\cdot\overline{\overline{c}} \tag{B.16}$$

the surface integral in (B.5) can be changed to an alternative form,

$$i\omega\epsilon\overline{E}(\overline{R}') - \iiint_V \left\{\overline{S}_e(\overline{R})\cdot\overline{\overline{G}}_e(\overline{R},\overline{R}')\right\}dV = -\oiint_S \left\{\begin{array}{c}[i\omega\mu_f\overline{H}_f(\overline{R}) - \overline{J}_m(\overline{R})]\cdot[\hat{n}\times\overline{\overline{G}}_e(\overline{R},\overline{R}')] \\ -[\hat{n}\times\overline{E}(\overline{R})]\cdot\nabla\times\overline{\overline{G}}_e(\overline{R},\overline{R}')\end{array}\right\}dS \tag{B.17}$$

$\overline{R}'$ is now the position vector of the field point and $\overline{R}$ that of a source point. In the absence of a scattering body, the surface integrals are absent and the DGFs, $\overline{\overline{G}}_e^{fs}(\overline{R},\overline{R}')$ and $\overline{\overline{G}}_m^{fs}(\overline{R},\overline{R}')$ therein correspond to $\overline{\overline{G}}_{eo}(\overline{R},\overline{R}')$ and $\overline{\overline{G}}_{mo}(\overline{R},\overline{R}')$, the electric and magnetic type DGF respectively. If the region is bounded interiorly by a surface S_d and exteriorly by a surface S_∞ at infinity. At S_∞, $\overline{E}(\overline{R})$ and $\overline{H}(\overline{R})$ satisfy the Sommerfeld radiation condition at $\overline{R}\to\infty$, i.e.

$$\lim_{R\to\infty}\left\{R[\nabla\times\overline{E}(\overline{R}) - ik\hat{R}\times\overline{E}(\overline{R})]\right\} = 0 \tag{B.18}$$

and

$$\lim_{R\to\infty}\left\{R[\nabla\times\overline{H}(\overline{R}) - ik\hat{R}\times\overline{H}(\overline{R})]\right\} = 0 \tag{B.19}$$

and the dyadic form of Sommerfeld radiation condition

$$\lim_{R\to\infty}\left\{[\nabla\times\overline{\overline{G}}_e^{fs}(\overline{R},\overline{R}')-ik\hat{R}\times\overline{\overline{G}}_e^{fs}(\overline{R},\overline{R}')]\right\}=0 \tag{B.20}$$

As a result of the radiation condition, the surface integrals in (B.17) evaluated at S_∞ are zero. The only contribution is from S_d, which in case of electric DGF should satisfy the dyadic Dirichlet condition on S_d, i.e. $\hat{n}\times\overline{\overline{G}}_e^{fs}(\overline{R},\overline{R}')=0$ and for a perfectly conducting body then $\hat{n}\times\overline{E}(\overline{R})=0$, whence the surface integral on S_d vanishes completely. By interchanging $\overline{R}$ and $\overline{R}'$ in the above expressions and making use of symmetrical properties of DGFs

$$\overline{E}(\overline{R})=\frac{1}{i\omega\varepsilon}\iiint_V\left\{\overline{\overline{G}}_e(\overline{R},\overline{R}')\cdot\overline{S}_e(\overline{R}')\right\}dV' \tag{B.21}$$

substituting for $\overline{S}_e(\overline{R}')$, we can obtain;

$$\begin{aligned}\overline{E}(\overline{R})=&\frac{1}{i\omega\varepsilon}\iiint_V\left\{\overline{\overline{G}}_e(\overline{R},\overline{R}')\cdot[i\omega\mu_f\overline{J}_e(\overline{R}')]\right\}dV'\\&-\frac{1}{i\omega\varepsilon}\iiint_V\left\{\overline{\overline{G}}_e(\overline{R},\overline{R}')\cdot[\nabla'\times\overline{J}_m(\overline{R}')]\right\}dV'\end{aligned} \tag{B.22}$$

Once $\overline{E}(\overline{R}')$ is known, one can readily find the companion equation for $\overline{H}(\overline{R}')$ using the appropriate Maxwell's equations.

By letting $\overline{P}=\overline{H}(\overline{R})$, $\overline{\overline{Q}}=\overline{\overline{G}}_m(\overline{R},\overline{R}')$ and assuming $\overline{S}_m(\overline{R})=i\omega\varepsilon_f\overline{J}_m(\overline{R})+\nabla\times\overline{J}_e(\overline{R})$ corresponds to a source of finite extent, and in view of (B.8) and (B.9) we obtain

$$\begin{aligned}\overline{H}(\overline{R})=&\frac{1}{i\omega\mu}\iiint_V\left\{\overline{\overline{G}}_m(\overline{R},\overline{R}')\cdot[i\omega\varepsilon_f\overline{J}_m(\overline{R}')]\right\}dV'\\&+\frac{1}{i\omega\mu}\iiint_V\left\{\overline{\overline{G}}_m(\overline{R},\overline{R}')\cdot[\nabla'\times\overline{J}_e(\overline{R}')]\right\}dV'\end{aligned} \tag{B.23}$$

Where the prime on the dels denote differentiation with respect to the primed co-ordinate $\overline{R}'$ of the source point.

B.2.2 Method (2)

The electromagnetic field also can be obtained from a superposition of $T.M$ and $T.E$ modes which are derived from electric and magnetic Hertz vectors. The total

field consists of the field due to $\overline{J}_e$ and the field due to $\overline{J}_m$.

$$\overline{E} = \overline{E}_e + \overline{E}_m \tag{B.24}$$

$$\overline{H} = \overline{H}_e + \overline{H}_m \tag{B.25}$$

The fields excited by prescribed current sources may be expressed by applying the method of potential using the Hertzian (Debye) potentials $\overline{\prod}_e(\overline{R})$ and $\overline{\prod}_m(\overline{R})$ i.e.

$$\overline{E} = i\omega(\overline{\overline{I}} + \frac{1}{k^2}\nabla\nabla)\overline{\prod}_e - \frac{1}{\varepsilon_f}\nabla \times \overline{\prod}_m \tag{B.26}$$

$$\overline{H} = i\omega(\overline{\overline{I}} + \frac{1}{k^2}\nabla\nabla)\overline{\prod}_m + \frac{1}{\mu_f}\nabla \times \overline{\prod}_e \tag{B.27}$$

Where

$$\overline{\prod}_e(\overline{R}) = \mu_f \iiint_V G_e^s(\overline{R}, \overline{R}')\overline{J}_e(\overline{R}')dV' \tag{B.28}$$

$$\overline{\prod}_m(\overline{R}) = \varepsilon_f \iiint_V G_m^s(\overline{R}, \overline{R}')\overline{J}_m(\overline{R}')dV' \tag{B.29}$$

$G_{e\ m}^s$ represent the single source scalar Green function for either electric or magnetic type for a three dimensional scalar wave equation. Substituting $\overline{\prod}_e(\overline{R})$ and $\overline{\prod}_m(\overline{R})$ in (B.26) and (B.27) and using DGF in terms of scalar Green function

$$\overline{\overline{G}}_{e\ m}^{fs}(\overline{R}, \overline{R}') = (\overline{\overline{I}} + \frac{1}{k^2}\nabla\nabla)G_{e\ m}^s(\overline{R}, \overline{R}') \tag{B.30}$$

Then equation (B.26) becomes

$$\begin{aligned}\overline{E}(\overline{R}) = i\omega\mu_f \iiint_V \left\{\overline{\overline{G}}_e^{fs}(\overline{R}, \overline{R}') \cdot \overline{J}_e(\overline{R}')\right\} dV' \\ - \iiint \left\{\nabla \times [G_m^s(\overline{R}, \overline{R}') \cdot \overline{J}_m(\overline{R}')]\right\} dV'\end{aligned} \tag{B.31}$$

making use of the identity and taking into consideration the integration over the prime quantities e.g. source point $\overline{R}'$

$$\nabla \times (a\overline{b}) = a\nabla \times \overline{b} - \overline{b} \times (\nabla a) \tag{B.32}$$

$$\nabla \times (a\overline{\overline{b}}) = a\nabla \times \overline{\overline{b}} + (\nabla a) \times \overline{\overline{b}} \tag{B.33}$$

$$\overline{E}_f(\overline{R}) = i\omega\mu_f \iiint_V \left\{ \overline{\overline{G}}_e^{fs}(\overline{R},\overline{R}') \cdot \overline{J}_e(\overline{R}') \right\} dV' - \iiint_V \left\{ \nabla \times G_m^s(\overline{R},\overline{R}') \cdot \overline{J}_m(\overline{R}') \right\} dV' \tag{B.34}$$

where

$$\nabla \times \overline{\overline{G}}_{em}^{fs}(\overline{R},\overline{R}') = \nabla \times [\overline{\overline{I}} G_{em}^{s}(\overline{R},\overline{R}')] \tag{B.35}$$

then

$$\overline{E}_f(\overline{R}) = i\omega\mu_f \iiint_V \left\{ \overline{\overline{G}}_e^{fs}(\overline{R},\overline{R}') \cdot \overline{J}_e(\overline{R}') \right\} dV' - \iiint_V \left\{ \nabla \times \overline{\overline{G}}_m^{fs}(\overline{R},\overline{R}') \cdot \overline{J}_m(\overline{R}') \right\} dV' \tag{B.36}$$

and applying either the duality principle or again the same procedure as before we can obtain

$$\overline{H}_f(\overline{R}) = i\omega\varepsilon_f \iiint_V \left\{ \overline{\overline{G}}_m^{fs}(\overline{R},\overline{R}') \cdot \overline{J}_m(\overline{R}') \right\} dV' + \iiint_V \left\{ \nabla \times G_e^s(\overline{R},\overline{R}') \cdot \overline{J}_e(\overline{R}') \right\} dV' \tag{B.37}$$

$$\overline{H}_f(\overline{R}) = i\omega\varepsilon_f \iiint_V \left\{ \overline{\overline{G}}_m^{fs}(\overline{R},\overline{R}') \cdot \overline{J}_m(\overline{R}') \right\} dV' + \iiint_V \left\{ \nabla \times \overline{\overline{G}}_e^{fs}(\overline{R},\overline{R}') \cdot \overline{J}_e(\overline{R}') \right\} dV' \tag{B.38}$$

We have to take into consideration that the differential (∇) operators are with respect to observation point $\overline{R}$, while the integral is with respect to the source point $\overline{R}'$ in (B.31) to (B.38). For $\overline{E}(\overline{R})$ and $\overline{H}(\overline{R})$ to be identical with those in previous method respectively, their second integral term should be identical in each case.

B.3 Rectangular Vector Wave Functions

The vector wave functions was introduced by Hansen [25] are the building blocks of the eigenfunction expansions of various kinds of DGF. They are denoted by $\overline{L}_{emn}$,

$\overline{M}_{\substack{e\\o}mn}$ and $\overline{N}_{\substack{e\\o}mn}$, that are solutions of the homogeneous vector Helmholtz equation. The generating or eigenfunctions, which are solutions of the scalar wave equation $\nabla^2\Psi + k^2\Psi=0$, can be written in the form

$$\Psi_{\substack{e\\o}mn}(h) = \begin{pmatrix} C_x C_y \\ S_x S_y \end{pmatrix} e^{ihz}, \tag{B.39}$$

where

$$S_x = \sin k_x x, \qquad C_x = \cos k_x x \tag{B.40}$$

$$S_y = \sin k_y y, \qquad C_y = \cos k_y y \tag{B.41}$$

and here constants k_x and k_y have the following characteristic values,

$$k_x = \frac{m\pi}{a}, \qquad m = 0, 1, \ldots \tag{B.42}$$

$$k_y = \frac{n\pi}{b}, \qquad n = 0, 1, \ldots \tag{B.43}$$

The cut-off wave number of a rectangular waveguide k_c is related to k_x and k_y by

$$k_c^2 = k_x^2 + k_y^2$$

and the arbitrary constant k is then related to

$$k^2 = k_c^2 + h^2.$$

Here k is an undetermined wave number and z is the piloting vector. Subscripts "e" stands for even and "o" is odd character of the generating functions.

The complete expressions for the solenoidal or rotational or transverse functions are given by Tai [19]

$$\overline{M}_{\substack{e\\o}mn}(h) = \nabla\times[\Psi_{\substack{e\\o}mn}(h)\overline{z}], \tag{B.44}$$

$$\overline{N}_{\substack{e\\o}mn}(h) = \frac{1}{k}\nabla\times\nabla\times[\Psi_{\substack{e\\o}mn}(h)\overline{z}]. \tag{B.45}$$

And the complete expressions for the non-solenoidal or irrotational or lamellar functions are given again by Tai [19]

$$\overline{L}_{\substack{e\\o}mn}(h) = \nabla[\Psi_{\substack{e\\o}mn}(h)]. \tag{B.46}$$

It should be pointed out that the odd functions with m or $n = 0$ are null modes.

To satisfy the symmetrical properties of DGF one should consider the relations as follow;

$$\overline{N}_{emn}(h) = \frac{1}{k}\nabla\times\overline{M}_{emn}(h), \tag{B.47}$$

$$\overline{M}_{emn}(h) = \frac{1}{k}\nabla\times\overline{N}_{emn}(h). \tag{B.48}$$

Green's functions for bounded regions are usually given in the form of modal expansions. Modal series are unsuitable for use in numerical algorithms which require the computation of the field inside the source region. In this case, the Green's function must be computed at points $\overline{z}'$ close to $\overline{z}$, where the convergence of the series is very poor due to the singularity of $\overline{\overline{G}}_{e_m}(\overline{R},\overline{R}')$ at point source $z = z'$. This drawback can be avoided by using expressions where a diverging term, expressed in closed form, is extracted from the modal expansion of $\overline{\overline{G}}_{e_m}(\overline{R},\overline{R}')$, so that the remaining series represents a function finite at point source $z = z'$ Bressan [26].

The orthogonal properties of these vector wave functions have been discussed by Tai [20], [19]. If only the electric current source is used, $\overline{L}_{emn}$ functions are not required to derive the eigenfunction expansion of the magnetic DGF that are solenoidal and satisfy the vector wave equation, but to find the eigenfunction expansion of the electric DGF then the $\overline{L}_{emn}$ functions are also necessary, because $\overline{\overline{G}}_e^{Lfo}(\overline{R},\overline{R}')$ unlike $\overline{\overline{G}}_m^{Lfo}(\overline{R},\overline{R}')$, the dyadic Green's functions of electric and magnetic type respectively is a non-solenoidal dyadic function. But in the case of both, an electric as well as a magnetic source, both electric and magnetic DGF's expressions contain the singularity terms.

The method for deriving the magnetic/electric DGF given in the following section for rectangular configurations used the Ohm-Rayleigh (G_e) procedure. However, there exist several alternative derivations which will not be discussed further.

B.4 General Representation of Dyadic Green's Function

Before we develop the analysis of electromagnetic wave propagation in the scattering medium, it is convenient to examine the media firstly with no scatterer, and then secondly with scatterer in position.

B.4.1 Free Space DGFs for Electric and Magnetic Dipoles in unbounded medium

The electric and magnetic fields due to electric and magnetic dipoles located at z' in an infinite homogeneous space without the presence of an scatterer (obstacle) can be computed in rectangular co-ordinates. There are various methods that can be utilized to achieve this using equation (B.9).

$$\nabla \times \nabla \times \overline{\overline{G}}_{e_m}^{(fs)}(\overline{R}, \overline{R}') - k_f^2 \overline{\overline{G}}_{e_m}^{(fs)}(\overline{R}, \overline{R}') = i\omega\vartheta \overline{\overline{I}} \delta_{e_m}(\overline{R} - \overline{R}') \delta_f^s$$

A fundamental problem in electromagnetic theory is to calculate the field at source point. It arises in the evaluation of the antenna impedance, the power radiation, the induced current on a scatterer, and other situations. A DGF is highly singular. Inside the source region the field is not solenoidal so the $\overline{L}_{e_{mn}}$ functions must also be included. The singular behaviour of the DGF at the source point caused considerable difficulty in the early development of the theory. Many authors examined this elusive singular nature of DGF [20] - [66]. Collin [39] has elegantly shown that, "a relatively straight-forward analysis using the complete set of eigenfunctions described by Tai led to the discovery that there was a sub-spectrum of zero frequency or "static-like" modes that were part of the spectrum of the transverse eigenfunctions (the N functions of Hansen). These zero frequency modes cancel the longitudinal mode spectrum outside the source region. Inside the source region the cancellation is not complete but the non-cancellating part can be expressed as a delta function contribution".

A symbolic way to represent a point source of excitation is the use of weighted Dirac's three-dimensional delta function expressed in Cartesian co-ordinates if R' is (x', y', z'); thus

$$\delta(\overline{R} - \overline{R}') = \delta(\overline{x} - \overline{x}')\delta(\overline{y} - \overline{y}')\delta(\overline{z} - \overline{z}') \tag{B.49}$$

Tai [19] pointed that the method of expressing the point source dyadics only in terms of the transverse (divergenceless) vector functions $\overline{M}_{\substack{e\\o}mn}$ and $\overline{N}_{\substack{e\\o}mn}$ can lead to a contradiction: the left hand side of the vector wave equation is solenoidal, but the right hand side is not. A remedy for this dilemma, is by including the longitudinal wave functions. In the case of electromagnetic sources $\overline{\overline{G}}_{\substack{e\\m}}(\overline{R}, \overline{R}')$ is a non-solenoidal dyadic function because

$$\nabla \cdot \overline{\overline{G}}_{\substack{e\\m}}(\overline{R}, \overline{R}') = \frac{1}{i\omega\vartheta}\nabla\delta_{\substack{e\\m}}(\overline{R} - \overline{R}') \tag{B.50}$$

which are not zero except for $\overline{R} \neq \overline{R}'$. The expansion of the electric and magnetic fields require both the transverse and longitudinal vector eigenfunctions and hence the DGFs must also have both sets of eigenfunctions in their expansions Tai [19], Samii [22].

$$\overline{\overline{G}}_{\substack{e\\m}o}(\overline{R}, \overline{R}') = \frac{\hat{z}\hat{z}}{i\omega\vartheta}\delta_{\substack{e\\m}}(\overline{R} - \overline{R}') + PV_{\delta_{\substack{e\\m}}}\overline{\overline{G}}_{\substack{e\\m}o}(\overline{R}, \overline{R}') \tag{B.51}$$

The vector wave function $\overline{M}_{omn}(h)$ represents the electric field of the TE_{mn} mode while $\overline{N}_{omn}(h)$ represents that of TM_{mn} mode. On the other hand $\overline{M}_{omn}(h)$ and $\overline{N}_{omn}(h)$ are the proper functions to represent the H-field in a rectangular waveguide. Having expressed the DGF for an unbounded medium in terms of rectangular vector wave functions, we may now use that result to construct one for a rectangular waveguide or cavity.

$$\overline{\overline{G}}_{\substack{e1\\e2}o}(\overline{R},\overline{R}') = \frac{\hat{z}\hat{z}}{i\omega\mu}\delta_{\substack{e1\\e2}}(\overline{R}-\overline{R}') + (i\omega\epsilon)\frac{i}{ab}\sum_{n=0}^{\infty}\sum_{m=0}^{\infty}C_{mn} \cdot \left\{ \begin{array}{l} [\overline{M}_{\substack{e\\o}mn}(\pm\gamma)\overline{M}'_{\substack{e\\o}mn}(\mp\gamma)] \\ [\overline{N}_{\substack{o\\e}mn}(\pm\gamma)\overline{N}'_{\substack{o\\e}mn}(\mp\gamma)] \end{array} \right\}, \quad z \gtrless z', \tag{B.52}$$

$$\overline{\overline{G}}_{\substack{m2\\m1}o}(\overline{R},\overline{R}') = \frac{\hat{z}\hat{z}}{i\omega\epsilon}\delta_{\substack{m2\\m1}}(\overline{R}-\overline{R}') + \frac{ik}{ab}\sum_{n=0}^{\infty}\sum_{m=0}^{\infty}C_{mn} \cdot \left\{ \begin{array}{l} [\overline{N}_{\substack{e\\o}mn}(\pm\gamma)\overline{M}'_{\substack{e\\o}mn}(\mp\gamma)] \\ [\overline{M}_{\substack{o\\e}mn}(\pm\gamma)\overline{N}'_{\substack{o\\e}mn}(\mp\gamma)] \end{array} \right\}, \quad z \gtrless z', \tag{B.53}$$

Where the prime on the vector wave functions indicates that, functions are defined with respect to the co-ordinates of the position vector $\overline{R}'$, co-ordinates (x', y', z'). $\hat{z}\hat{z}$ is a dyad (dyadic product of the unit vectors), here the dyadic delta function term at the source point is included explicitly as a correction to the general solenoidal eigenfunction expansion which is valid outside the source point.

$$C_{mn} = \frac{(2-\delta_o^{m,n})}{\gamma k_c^2} \tag{B.54}$$

Coefficient C_{mn} depends on the value of m and n where $\delta_o^{m,n}$ is the Kronecker delta functions, when

$$\delta = \begin{cases} 1, & \text{if } m \text{ or } n = o \\ 0, & \text{if } m \text{ and } n \neq o \end{cases}. \tag{B.55}$$

Note that the equations (B.52) and (B.53) satisfy the dyadic form of Maxwell's equations i.e.,

$$\nabla \times \overline{\overline{G}}_{\substack{e\\m}}(\overline{R},\overline{R}') = \pm i\omega\vartheta\overline{\overline{G}}_{\substack{m\\e}}(\overline{R},\overline{R}') \mp \overline{\overline{I}}\delta_{\substack{m\\e}}(\overline{R}-\overline{R}') \tag{B.56}$$

and are used in E and H-field formulations (B.22) and (B.23) of method 1 (B.2.1). They result in approximate solutions in E and H-field formulations (B.36) and (B.38) of method 2 (B.2.2).

Exact DGFs to satisfy E and H-field formulations (B.36) and (B.38) of method 2 (B.2.2) based on the presence of one dipole in the system only and the principle of superposition of fields are presented below:

$$\overline{\overline{G}}_{\substack{e1\\e2}o}(\overline{R},\overline{R}') = -\frac{\hat{z}\hat{z}}{k^2}\delta_{\substack{e1\\e2}}(\overline{R}-\overline{R}') + \frac{i}{ab}\sum_{n=0}^{\infty}\sum_{m=0}^{\infty} C_{mn} \cdot \begin{Bmatrix} [\overline{M}_{\substack{e\\o}mn}(\pm\gamma)\overline{M}'_{\substack{e\\o}mn}(\mp\gamma)] \\ [\overline{N}_{\substack{o\\e}mn}(\pm\gamma)\overline{N}'_{\substack{o\\e}mn}(\mp\gamma)] \end{Bmatrix}, \quad z \gtrless z', \tag{B.57}$$

$$\overline{\overline{G}}_{\substack{m1\\m2}o}(\overline{R},\overline{R}') = -\frac{\hat{z}\hat{z}}{k^2}\delta_{\substack{m1\\m2}}(\overline{R}-\overline{R}') + \frac{i}{ab}\sum_{n=0}^{\infty}\sum_{m=0}^{\infty} C_{mn} \cdot \begin{Bmatrix} [\overline{M}_{\substack{e\\o}mn}(\pm\gamma)\overline{M}'_{\substack{e\\o}mn}(\mp\gamma)] \\ [\overline{N}_{\substack{o\\e}mn}(\pm\gamma)\overline{N}'_{\substack{o\\e}mn}(\mp\gamma)] \end{Bmatrix}, \quad z \gtrless z', \tag{B.58}$$

B.4.2 General Expression of Scattering DGFs

Observation and analysis of the above expressions allows the formulation of the general scattering DGF for the media taking the reflected waves into consideration:

$$\overline{\overline{G}}^{Lfs}_{\substack{e1\\e2}s}(\overline{R},\overline{R}') = (i\omega\epsilon)\frac{i}{ab}\sum_{n=0}^{\infty}\sum_{m=0}^{\infty} C_{mn} \cdot \begin{Bmatrix} \overline{M}_{\substack{e\\o}mn}(\gamma_f)\begin{bmatrix} A^{(fs)TE}_{\substack{e\\o}mn}\overline{M}'_{\substack{e\\o}mn}(\gamma_s) \\ (1-\delta^L_s)B^{(fs)TE}_{\substack{e\\o}mn}\overline{M}'_{\substack{e\\o}mn}(-\gamma_s)\end{bmatrix} \\ \overline{N}_{\substack{o\\e}mn}(\gamma_f)\begin{bmatrix} A^{(fs)TM}_{\substack{e\\o}mn}\overline{N}'_{\substack{o\\e}mn}(\gamma_s) \\ (1-\delta^L_s)B^{(fs)TM}_{\substack{e\\o}mn}\overline{N}'_{\substack{o\\e}mn}(-\gamma_s)\end{bmatrix} \end{Bmatrix} \cdot \begin{Bmatrix} (1-\delta^L_f)\overline{M}_{\substack{e\\o}mn}(-\gamma_f)\begin{bmatrix} A'^{(fs)TE}_{\substack{e\\o}mn}\overline{M}'_{\substack{e\\o}mn}(\gamma_s) \\ (1-\delta^L_s)B'^{(fs)TE}_{\substack{e\\o}mn}\overline{M}'_{\substack{e\\o}mn}(-\gamma_s)\end{bmatrix} \\ (1-\delta^L_f)\overline{N}_{\substack{o\\e}mn}(-\gamma_f)\begin{bmatrix} A'^{(fs)TM}_{\substack{e\\o}mn}\overline{N}'_{\substack{o\\e}mn}(\gamma_s) \\ (1-\delta^L_s)B'^{(fs)TM}_{\substack{e\\o}mn}\overline{N}'_{\substack{o\\e}mn}(-\gamma_s)\end{bmatrix} \end{Bmatrix}. \tag{B.59}$$

In a corresponding manner, we can expand the magnetic DGF as follows:

$$\overline{\overline{G}}^{Lfs}_{m2\,m1\,s}(\overline{R},\overline{R}') = \frac{ik}{ab}\sum_{n=0}^{\infty}\sum_{m=0}^{\infty} C_{mn} \cdot \left\{ \begin{array}{c} \overline{N}_{\substack{e\\o}mn}(\gamma_f)\begin{bmatrix} A^{(fs)TE}_{\substack{e\\o}mn}\overline{M}'_{\substack{e\\o}mn}(\gamma_s) \\ (1-\delta^L_s)B^{(fs)TE}_{\substack{e\\o}mn}\overline{M}'_{\substack{o\\e}mn}(-\gamma_s)\end{bmatrix} \\ \overline{M}_{\substack{o\\e}mn}(\gamma_f)\begin{bmatrix} A^{(fs)TM}_{\substack{e\\o}mn}\overline{N}'_{\substack{e\\e}mn}(\gamma_s) \\ (1-\delta^L_s)B^{(fs)TM}_{\substack{e\\o}mn}\overline{N}'_{\substack{o\\e}mn}(-\gamma_s)\end{bmatrix} \\ (1-\delta^L_f)\overline{N}_{\substack{e\\o}mn}(-\gamma_f)\begin{bmatrix} A'^{(fs)TE}_{\substack{e\\o}mn}\overline{M}'_{\substack{e\\o}mn}(\gamma_s) \\ (1-\delta^L_s)B'^{(fs)TE}_{\substack{e\\o}mn}\overline{M}'_{\substack{e\\o}mn}(-\gamma_s)\end{bmatrix} \\ (1-\delta^L_f)\overline{M}_{\substack{o\\e}mn}(-\gamma_f)\begin{bmatrix} A'^{(fs)TM}_{\substack{e\\o}mn}\overline{N}'_{\substack{e\\e}mn}(\gamma_s) \\ (1-\delta^L_s)B'^{(fs)TM}_{\substack{e\\o}mn}\overline{N}'_{\substack{o\\e}mn}(-\gamma_s)\end{bmatrix} \end{array} \right\}. \tag{B.60}$$

$A^{(fs)TE,TM}_{\substack{e\\o}mn}$, $A'^{(fs)TE,TM}_{\substack{e\\o}mn}$, $B^{(fs)TE,TM}_{\substack{e\\o}mn}$ and $B'^{(fs)TE,TM}_{\substack{e\\o}mn}$ are the amplitude coefficients of scattered DGF to be calculated by applying the boundary condition at the surface of the waveguide. These boundary conditions are:

$$\hat{n}\times\overline{\overline{G}}^{(b)}_{\substack{e\\m}}(\overline{R},\overline{R}') = 0 \tag{B.61}$$

$$\hat{n}\times\nabla\times\overline{\overline{G}}^{(b)}_{\substack{e\\m}}(\overline{R},\overline{R}') = 0 \tag{B.62}$$

and at the interfaces $z = z_l$ where $(l = 1, 2, ..., L-2)$

$$\hat{z}\times\overline{\overline{G}}^{(b)}_{\substack{e\\m}}(\overline{R},\overline{R}') = \hat{z}\times\overline{\overline{G}}^{[(l+1)s]}_{\substack{e\\m}}(\overline{R},\overline{R}') \tag{B.63}$$

and

$$\frac{1}{\vartheta_f}\hat{z}\times\nabla\times\overline{\overline{G}}^{(b)}_{\substack{e\\m}}(\overline{R},\overline{R}') = \frac{1}{\vartheta_{(f+1)}}\hat{z}\times\nabla\times\overline{\overline{G}}^{[(l+1)s]}_{\substack{e\\m}}(\overline{R},\overline{R}') \tag{B.64}$$

"L" is the symbol for last inner layer in the media. "f" is the field point or observer layer. Superscript/subscript "s" stands for source point at open space while subscript "s" is scattering.

δ_f^L and δ_f^o are the Kronecker delta functions, where

$$\delta = \begin{cases} 1, & \text{if } L = o \\ 0, & \text{if } L \neq o \end{cases}. \tag{B.65}$$

The scattering DGF for magnetic as well as electric type formulations for method 2 (B.2.2) can be presented as follows:

$$\begin{aligned} \overline{\overline{G}}^{Lfs}_{\substack{e1\\e2}s}(\overline{R},\overline{R}') = \overline{\overline{G}}^{Lfs}_{\substack{m1\\m2}s}(\overline{R},\overline{R}') = \frac{i}{ab}\sum_{n=0}^{\infty}\sum_{m=0}^{\infty} C_{mn} \\ \cdot \begin{Bmatrix} \overline{M}_{\substack{e\\o}mn}(\gamma_f)\begin{bmatrix} A^{(fs)TE}_{\substack{e\\o}mn}\overline{M}'_{\substack{e\\o}mn}(\gamma_s) \\ (1-\delta_s^L)B^{(fs)TE}_{\substack{e\\o}mn}\overline{M}'_{\substack{e\\o}mn}(-\gamma_s)\end{bmatrix} \\ \overline{N}_{\substack{o\\e}mn}(\gamma_f)\begin{bmatrix} A^{(fs)TM}_{\substack{o\\e}mn}\overline{N}'_{\substack{o\\e}mn}(\gamma_s) \\ (1-\delta_s^L)B^{(fs)TM}_{\substack{o\\e}mn}\overline{N}'_{\substack{o\\e}mn}(-\gamma_s)\end{bmatrix} \\ (1-\delta_f^L)\overline{M}_{\substack{e\\o}mn}(-\gamma_f)\begin{bmatrix} A'^{(fs)TE}_{\substack{e\\o}mn}\overline{M}'_{\substack{e\\o}mn}(\gamma_s) \\ (1-\delta_s^L)B'^{(fs)TE}_{\substack{e\\o}mn}\overline{M}'_{\substack{e\\o}mn}(-\gamma_s)\end{bmatrix} \\ (1-\delta_f^L)\overline{N}_{\substack{o\\e}mn}(-\gamma_f)\begin{bmatrix} A'^{(fs)TM}_{\substack{e\\o}mn}\overline{N}'_{\substack{o\\e}mn}(\gamma_s) \\ (1-\delta_s^L)B'^{(fs)TM}_{\substack{e\\o}mn}\overline{N}'_{\substack{o\\e}mn}(-\gamma_s)\end{bmatrix} \end{Bmatrix}. \end{aligned} \tag{B.66}$$

For more details on evaluation of coefficients the readers are referred to Cavalcante et al [35] and Li et al [36] - [37].

The principle of scattering superposition can be applied to construct the DGFs i.e.

$$\overline{\overline{G}}^{(fs)}_{\substack{e\\m}}(\overline{R},\overline{R}') = \overline{\overline{G}}_{\substack{e\\m}o}(\overline{R},\overline{R}')\delta_f^s + \overline{\overline{G}}^{(Lfs)}_{\substack{e\\m}s}(\overline{R},\overline{R}'). \tag{B.67}$$

B.5 Discussions and Comparison of General Representation of DGFs with Other Authors' Related Works

Since understanding the properties of the singularity is essential to the use of the DGF in numerical analyses, it is highly desirable to resolve and clarify the apparent incongruities. Samii [22] stated that "Care must be exercised in defining the derivatives in the sense of distribution and in using the correct completeness relation in order to compute the correct DGF". Proper handling of the electric DGF in the source region is essential when using it in numerical analyses involving dielectric scatterer. The difficulty arises in the computation of the "self-cell" or self-coupling matrix element that must be generated when using the method of moments.

Yaghjian [24] explained the difference in the delta function terms between Tai et al. [52] and Samii [22] caused by their different choices of the principal volume and emphasized the need to include in $\overline{\overline{G}}_e(\overline{R},\overline{R}')$ the shape of the principal volume involved. Yaghjian [24] and Lee et al. [56] outlined proofs to show that singularity associated with the electric DGF in a bounded region is exactly the same as that for the free space.

Wang [60] has also attempted to clarify some of the apparent discrepancies in the literature regarding the singular behaviour of $\overline{\overline{G}}_e(\overline{R},\overline{R}')$ and seeking a unified and consistent view on this important subject.

According to the homogeneous vector Helmholtz decomposition theorem and its manifestation in field theory, a general E-field can be decomposed into an irrotational (lamellar) and a rotational (solenoidal) component:

$$E = E_{irr} + E_{rot}. \tag{B.68}$$

The E_{irr} describes current source's near field, the field lines for which emanate from and terminate on the dipole electrodes while the E_{rot} approximately describes the far field, the field lines for which neither touch nor encompass the dipole. Also

in Ampere's law

$$\nabla \times H = J, \tag{B.69}$$

where $J = J_c + J_d$, and here the displacement current density J_d can be decomposed in an irrotational component $J_{d_{irr}}$ and a rotational component $J_{d_{rot}} \cdot J_c$ is the conduction-current density. $J_{d_{irr}}$ represents the quasistatic displacement-current density completing J_c to form a closed current loop, thereby satisfying the continuity law $\nabla \cdot (J_c + J_{d_{irr}}) = 0$. The $J_{d_{rot}}$ represents the far field. Hence the true current density of the non-stationary case consists of three components

$$J = J_c + J_{d_{irr}} + J_{d_{rot}}, \tag{B.70}$$

where $J_c + J_{d_{irr}}$ represent the quasistaic true current density corresponding to the applied excitation. The total displacement-current density $J_d = J_{d_{irr}} + J_{d_{rot}}$, consists of $J_{d_{irr}}$, driven by the applied voltage and $J_{d_{rot}}$ existing isolated from the applied voltage source, so that $J_{d_{rot}}$ remains in existent also after disconnecting the voltage source [71].

In numerical codes, based on the method of moments, the integration domain is limited to the conductor surfaces, hence the integration of the quasistatic displacement current density $J_{d_{irr}}$ is excluded.

Our purpose here is to bring to light the importance of characteristics of delta function term in source region. These comparisons may prove valuable in estimating the effect of delta term.

In this section, we are observing a few different discrepancies in other authors' works in comparison to ours, taking into account to what was mentioned above.

B.5.1 The Electric and Magnetic Field Representations

Kisliuk [101] presented two methods for evaluating E and H-fields. The first is based on vector analysis and the second utilized Hertz potentials method. The comparison of our formulations with Kisliuk's show that the format of all equations

in both methods is very similar except for the factor terms $(\overline{\overline{I}}+\frac{1}{k^2}\nabla'\nabla')$ in method 1 (B.2.1) and $(\overline{\overline{I}}+\frac{1}{k^2}\nabla\nabla)$ which has been introduced due to the choice of Green dyads for z_e and z_m in Hertzian potentials of second method. I believe the proper choice of Hertzian (Debye) potentials were to use scalar Green functions for electric as well as magnetic wave equations as in (B.26) to (B.29) resulting in equations that Li [102], [80] and Daniel [103] have already used in evaluation of fields.

B.5.2 The Isolated Singular Term in $\overline{\overline{G}}_{e,m}(\overline{R},\overline{R}')$ in the Form of Delta Term $\frac{\hat{z}\hat{z}}{i\omega\vartheta}\delta_{e,m}(\overline{R}-\overline{R}')$

Li et al in section III of [102] has categorically stated, "in deriving the DGFs at the source regions, as mentioned by Rahmat-Samii [22], care must be exercised. At the source regions, singularities exist and therefore need to be taken into account in the representation of DGFs. In fact, a delta function can be used to express the singularity term". Again in the same section undoubtedly he expounded, "the unbounded electromagnetic types of DGFs $\overline{\overline{G}}_{e,m\,o}(\overline{r},\overline{r}')$ consisting of the singularity and the principal value is according to the Sommerfeld radiation conditions". He has then included this delta term into the free space equations for both the electric as well as the magnetic DGFs.

But in section II (fundamental problem) in an earlier [80] but very similar paper to the above mentioned [102] Li stated "it is noticed that the electric Green dyads of the first and second kinds have a singularity contributed by the source in the source region. However, the magnetic Green dyads of the first and second kinds do not have because the singularity term is canceled by the derivatives of the delta function and the unit step function at the source point.".

Comparison between DGFs in [102] and [80] shows that [102] contains singularity term but [80] has not while $\overline{\overline{G}}_{e2}(\overline{R},\overline{R}')$ in [80] is equal to $\overline{\overline{G}}_{m}(\overline{R},\overline{R}')$ in [102].

In comparison with our DGF representations our first and second kind electric DGFs are the same as those in [80], but our first and second kind magnetic DGFs contain singularity delta term as in magnetic DGF representation in [102]. On the

other hand we have also specified the direction of our current densities, such as $\overline{\overline{I}}\delta_{\substack{e\\m}}(\overline{R}-\overline{R}')$.

B.5.3 The Electric and Magnetic DGFs Representations

Li et al in the introduction of [102] has absolutely stated unconditionally that "Since the magnetic type of dyadic Green's function can not be converted directly from the electric type by simple and conventional substitutions [39], both the electric and the magnetic types of the dyadic Green's functions are derived in that paper". Besides, in section III of the same paper [102] he has again explicitly stated "this paper presents both the electric and magnetic types of DGFs for the rectangular cavities and waveguides. To present both electric and magnetic types in the $\frac{e}{m}$ format requires no extra space, but gives readers a straightforward expression to work with". Also in [80] he mentioned that "the magnetic Green dyads of the second kind derived here is compared with those reported in the literature and the corresponding correctness of the solutions discussed". Firstly these statements are totally contradictory. Secondly these above mentioned equations are not derived but expressed in [102]. Thirdly the equations (B.52), (B.53), (B.59) and (B.60) in our communication are direct approach representations of DGFs in unbounded media with $\overline{\overline{G}}^{(Lfs)}_{\substack{e1_s\\e2_s}}$ and $\overline{\overline{G}}^{(Lfs)}_{\substack{m2_s\\m1_s}}$ are used in determination of E and H-fields of method 1 (B.2.1), while $\overline{\overline{G}}^{(Lfs)}_{\substack{e1\\e2_o}}$, $\overline{\overline{G}}^{(Lfs)}_{\substack{m2\\m1_o}}$ and $\overline{\overline{G}}^{(Lfs)}_{\substack{e1_s\\e2_s}} = \overline{\overline{G}}^{(Lfs)}_{\substack{m1_s\\m2_s}}$ in (B.57), (B.58) and (B.66) are compared with the corresponding equations in Li [102] and [80]. We can easily notice that in [80] Li has presented both electric and magnetic DGFs of the first and second kind while in [102] he has only considered electric field of first and attributed the second kind to the magnetic DGF in [102].

B.5.4 The Range for z and z'

In Li's [102] expression for free space electric DGF, the range $z \geq z'$ is also inaccurate because when $z = z'$ the operational property Delta $\delta(\overline{z}-\overline{z}') = \infty$, i.e. impulse occurs at $z = z'$ as a result of which free space electric DGF also becomes infinite.

Therefore, correct ranges are $z > z'$ and $z < z'$ and the operational property that Delta $\delta(\overline{z} - \overline{z}') = 0$ for $z \neq z'$ and for any vector function $F(R')$ that is continuous at $z = z'$:

$$\iiint_V F(\overline{R})\delta(\overline{R} - \overline{R}')dV = \begin{cases} F(\overline{R}'), & R' \text{ in V}, \\ 0, & R' \text{ not in V} \end{cases} \tag{B.71}$$

and

$$\int_{R-\alpha}^{R+\alpha} \delta(R - R')dR' = 1 \tag{B.72}$$

where the product of delta functions is used to represent a unit source.

Li et al [37] and one of their references Cavalcante et al [35] also suffers from this problem respectively by assuming $z \geq z'$ and $z \leq z'$ for the DGF in free space.

B.6 Concluding Remarks

A theoretical analysis of electromagnetic fields generated by a given distribution of electric and magnetic currents located inside a finite volume are defined using dyadic Green's functions. It is seen that the DGFs in unbounded space, both consist of the singularity and the principal value terms according to the Sommerfeld radiation conditions and the dyadic form of Maxwell's equations. The eigenfunction expansions of the DGFs for waveguides and cavities can be obtained by employing the method of scattering superposition. Consequently it should be emphasized that one expects a similar situation will exist for other geometries.

In this communication we have also drawn attention to the fact that the singular behaviour of the eigenfunction expansion of the DGF is incorrectly formulated in some authors' related works. This is significant because this expansion is used in the numerical calculation of the electromagnetic fields in the source region. Also the DGFs in some related efforts are in contradiction to the dyadic form of Maxwell's equations. The technique proposed here, overcomes the above mentioned difficulties.

Appendix C

Selected Publications

C.1 Publications List

C.1.1 Journal Papers

1. S. M. S. Reyhani and R. J. Glover, "Electromagnetic Dyadic Green's Function for a Multilayered Homogeneous Lossy Dielectric Spherical Head Model for Numerical EMC Investigation", Journal of Electromagnetics Vol. 20, no.2, pp. 141-153, March-April 2000. ETRMDV: 20(2)(2000), ISSN: 0272-6343.

2. S. M. S. Reyhani and R. J. Glover, "Electromagnetic Dyadic Green's Function for a Multilayered Homogeneous Human Torso Model for Numerical EMC Investigation", submitted to Journal of Electromagnetics for Publication.

3. S. M. S. Reyhani and R. J. Glover, "Electromagnetic Dyadic Green's Function Modeling of a Moving Human Torso", submitted to IEEE Transactions on Antennas and Propagation for Publication.

4. S. M. S. Reyhani and R. J. Glover, "Electromagnetic Modeling of Moving Spherical Head Using Dyadic Green's Function", submitted to IEEE Transactions on Microwave Theory and Technique for Publication.

C.1.2 Book Chapters

S. M. S. Reyhani and R. J. Glover, "Electromagnetic Dyadic Green's Function of an Implantable Medical Device Model for Numerical EMC Investigation", In "Recent Advances in Signal Processing and Communications", Edited by Nikos E. Mastorakis. World Scientific and Engineering Society Press, pp. 224-227, July 1999. ISBN:960-8052-03-3.

This chapter is 1 of 66 selected for publication from a total of over 1100 papers.

C.1.3 Invited Conference Papers

1. S. M. S. Reyhani and R. J. Glover, "Models of Antenna-Head Interactions by Electromagnetic Green's Dyadic Function", proceedings of the 2nd WSES International Conference on Mathematics and Computers in Biology and Chemistry (MCBC 2001) (Engineering in Biosciences and Biotechnologies) Skiathos, Greece, Ref-186, 26-30 Sept. 2001.

2. S. M. S. Reyhani, "Electromagnetic Dyadic Green's Function for a Moving Human Torso Model", proceedings of the 2nd WSES International Conference on Mathematics and Computers in Biology and Chemistry (MCBC 2001) (Engineering in Biosciences and Biotechnologies) Skiathos, Greece, Ref-182, 26-30 Sept. 2001.

C.1.4 Conference Papers

1. S. M. S. Reyhani and R. J. Glover, "Far Field Electromagnetic Modeling of Implantable Medical Devices Using Cylindrical DGFs", proceedings of the International Conference on EMC (EMC York 2000) University of York, UK: pp. 1B3, 10-11 July 2000.

2. S. M. S. Reyhani and R. J. Glover, "Insulated Implantable Medical Device Model

Using Electromagnetic Dyadic Green's Function", proceedings of the AP2000 Millennium Conference on Antennas and Propagation (AP2000/IEEE, IEE, ICAP, JINA & EUREL), Davos, Switzerland, paper no. p1566 9-14 April 2000.

3. S. M. S. Reyhani and R. J. Glover, "Electromagnetic Modeling of Implantable Medical Devices Using Cylindrical DGFs", proceedings of the 7th International Symposium on Recent Advances in Microwave Technology ISRAMT 99/IEEE, Malaga, Spain, proceedings, pp.456-460, 13-17 Dec. 1999.

4. S. M. S. Reyhani and R. J. Glover, "Electromagnetic Dyadic Green's Function for a Human Torso Model for Numerical EMC Investigation", proceedings of the 11th International Conference on EMC (IEE EMC York 99) University of York, UK: pp. 21-25, Publication No.464, 12-13 July 1999.

5. S. M. S. Reyhani and R. J. Glover, "Electromagnetic Dyadic Green's Function of an Implantable Medical Device Model for Numerical EMC Investigation", proceedings of the 3rd IMACS/IEEE International Multiconference on: Circuits, Systems, Communications and Computers (CSCC'99) (IMACS/IEEE CSCC'99), Athens, Greece, pp. 1311-1314, 4-8 July 1999.

C.1.5 Colloquia Papers

1. S. M. S. Reyhani and R. J. Glover, "Electromagnetic Modeling of Spherical Head Using Dyadic Green's Function", proceedings of the IEE Colloquium: On Electromagnetic Assessment and Antenna Design relating to the Health Implications of Mobile Phones, Savoy Place, London, U.K, pp. 8/1-8/5, 28 June 1999.

Glossary

abs	Absolute Values
ABC	Absorption Boundary Condition
CEM	Computational Electromagnetics
CPU	Central Processing Unit
del	Delivered
3D	Three Dimensions
DGF	Dyadic Green's Function
EFE	Eigen-Function expansion
EM	Electromagnetic
EMC	Electromagnetic Compatibility
EMI	Electromagnetic Interference
FDTD	Finite-Difference Time-Domain
FFT	Fast Fourier Transform
FT	Fourier Transform
GHz	Giga Hertz (10^9Hz)
GSM	Global System for Mobile Communication
inc	Incident
irr	Irrotational
ISM	Industrial, Scientific and Medical
LAN	Local Area Network
max	Maximum
min	Minimum

MHz	Mega Hertz (10^6Hz)
MoM	Method of Moments
MRI	Magnetic Resonant Imaging
NMR	Nuclear Magnetic Resonance
PC	Personal Communication
PCS	Personal Communication Services
rad	Radiated
rot	Rotational
RF	Radio Frequency
scat	Scatter
SA	Specific Absorption
SAR	Specific Absorption Rate
tan	Tangential
tot	Total
TDMA	Time-Division Multiple Access
TLM	Transmission Line Method
UXO	Unexploded Ordnance
WLAN	Wireless Local Area Network

References

[1] R. F. Harrington, "Field Computation by Moment Methods". Macmillan, New York, 1968.

[2] M. A. Jensen and Y. Rahmat-Samii, "FD-TD Analysis of PIFA Diversity Antennas on a Hand-held Transceiver Unit". IEEE Antennas and Propagat. Soc. Int. Symposium, Volume-2, pp. 814-817, Ann Arbor, MI, June 1993.

[3] M. A. Jensen and Y. Rahmat-Samii, "The Electromagnetic Interaction between Biological Tissue and Antennas on a Transceiver Handset". IEEE Antennas and Propagat. Soc. Int. Symposium, Volume-1, pp. 367-369, Seattle, WA, June 1994.

[4] M. A. Jensen and Y. Rahmat-Samii, "Performance Analysis of Antennas for Hand-held Transceivers using FD-TD". IEEE Trans. Antennas Propagat., Vol. AP-42, no.8, pp. 1106-1113, 1994.

[5] M. A. Jensen and Y. Rahmat-Samii, "EM Interaction of Handset Antennas and a Human in Personal Communications". Proc. of the IEEE, Vol. 83, no.1, pp. 7-17, Jan. 1995.

[6] K. M. Chen and B. S. Guru, "Internal EM Field and Absorbed Power Density in Human Torsos Induced by 1-500 MHz EM Waves". IEEE Trans. Microwave Theory and Tech., Vol. MTT-25, no.9, pp. 746-755, 1977.

[7] M. J. Hagman, O. P. Gandhi and C. H. Durney, "Numerical Calculation

of Electromagnetic Energy Deposition for a Realistic Model of Man". IEEE Trans. Microwave Theory and Tech., Vol. MTT-27, no.9, pp. 804-809, 1979.

[8] M. J. Hagman and O. P. Gandhi, "Numerical Calculation of Electromagnetic Energy Deposition in Man with Grounding and Reflector Effects". Radio Science, Vol. 14, no.6(S), pp. 23-29, 1979.

[9] M. J. Hagman, O. P. Gandhi, J. A. D'Andrea and I. Chatterjee, "Head Resonance: Numerical Solutions and Experimentatal Results". IEEE Trans. Microwave Theory and Tech., Vol. MTT-27, no.9, pp. 809-813, Sepetember 1979.

[10] D. T. Borup and O. P. Gandhi, "Fast-Fourier-Transform Method for Calculation of SAR Distributions in Finely Discretized Inhomogeneous Models of Biological Bodies". IEEE Trans. Microwave Theory Tech., Vol. MTT-32, no.8, pp. 355-360, 1984.

[11] K. S. Yee, "Numerical Solution of Initial Boundary Value Problems Involving Maxwell's Equations in Isotropic Media". IEEE Trans. Antennas and Propagat., Vol. AP-14, no.4, pp. 302-307, May 1966.

[12] A. Taflove and M. E. Brodwin, "Numerical Solution of Steady-State Electromagnetic Scattering Problems Using the Time-Dependent Maxwell's Equations". IEEE Trans. Microwave Theory Tech., Vol. MTT-23, no.8, pp. 623-630, 1975.

[13] A. Taflove, "Application of the Finite-Difference Time-Domain Method to Sinusoidal Steady-State Electromagnetic-Penetration Problems". IEEE Trans. Electromagn. Compat., Vol. EMC-22, no.2, pp. 191-202, 1980.

[14] A. Taflove and K. R. Umashankar, "Radar Cross Section of General Three-Dimensional Scatterers". IEEE Trans. Electromagn. Compat., Vol. EMC-25, no.2, pp. 433-440, 1983.

[15] R. Holland, L. Simpson and K. S. Kunz "Finite-Difference Analysis of EMP Coupling to Lossy Dielectric Structures", IEEE Trans. Electromagn. Compat., Vol. EMC-22, no.3, pp. 203-209, 1980.

[16] K. S. Kunz and K. M. Lee "A Three-Dimensional Finite-Difference Solution of the External Response of an Aircraft to a Complex Transient EM Environment: Part 1- The Method and its Implementation". IEEE Trans. Electromagn. Compat., Vol. EMC-20, no.2, pp. 328-333, 1978.

[17] D. M. Sullivan, D. T. Borup, and O. P. Gandhi, "Use of the Finite-Difference Time-Domain Method in Calculating EM Absorption in Human Tissues". IEEE Trans. Biomed. Eng., Vol. BME-34, no.2, pp. 148-157, 1987.

[18] D. M. Sullivan, O. P. Gandhi, and A. Taflove, "Use of the Finite-difference Time-Domain Method in Calculating EM Absorption in Man Models". IEEE Trans. Biomed. Eng., Vol. BME-35, no.3, pp. 179-186, 1988.

[19] C. T. Tai, "Dyadic Green Functions in Electromagnetic Theory". IEEE Press, series on Electromagnetic waves, New York, Second Edition, 1994.

[20] C. T. Tai, "Dyadic Green Functions in Electromagnetic Theory". Scranton, Intext Educational Publishers, New York, First Edition, 1971.

[21] R. E. Collin, "Field Theory of Guided Waves". IEEE Press, New York, Second Edition, 1991.

[22] Y. Rahmat-Samii, "On the Question of Computation of the Dyadic Green's Functions at the Source Region in Wave-guides and Cavities". IEEE Trans. Microwave Theory Tech., Vol. MTT-23, pp. 762-765, Sept. 1975.

[23] A. D. Yaghjian, "A Direct Approach to the Derivation of Electric Dyadic Green's Functions". in AP-S Int. Symp. Dig. (Univ. Mass.), pp. 71-73, Tues. October 12, 1976.

[24] A. D. Yaghjian, "Electric Dyadic Green's Functions in the Source Region". Proc. IEEE, Vol. 68, no.2, pp. 248-263, Feb. 1980.

[25] W. W. Hansen, "A New Type of Expansion in Radiation Problems". Phys. review, Vol. 47, pp. 139-143, 1935.

[26] M. Bressan and G. Conciauro, "Singularity Extraction from the Electric Green's Function for a Spherical Resonator". IEEE Trans. Microwave Theory Tech., Vol. MTT-33, no.5, pp. 407-414, May 1985.

[27] J. A. Kong, "Electromagnetic Wave Theory". Wiley-Interscience Publication, New York, Second Edition, 1990.

[28] S. M. S. Reyhani and R. J. Glover, "Electromagnetic Dyadic Green's Function of an Implantable Medical Device Model for Numerical EMC Investigation", In "Recent Advances in Signal Processing and Communications" Edited by Nikos E. Mastorakis. World Scientific and Engineering Society Press, pp. 224-227, July 1999. ISBN:960-8052-03-3.

[29] S. M. S. Reyhani and R. J. Glover, "Electromagnetic Dyadic Green's Function for a Human Torso Model for Numerical EMC Investigation", proceedings of the 11th International Conference on EMC (IEE EMC York 99) University of York, UK: pp. 21-25, Publication No.464, 12-13 July 1999.

[30] S. M. S. Reyhani and R. J. Glover, "Electromagnetic Modeling of Implantable Medical Devices Using Cylindrical DGFs", proceedings of the 7th International Symposium on Recent Advances in Microwave Technology ISRAMT 99/IEEE, Malaga, Spain, proceedings, pp.456-460, 13-17 Dec. 1999.

[31] S. M. S. Reyhani and R. J. Glover, "Electromagnetic Dyadic Green's Function for a Multi-layered Homogeneous Lossy Dielectric Spherical Head Model for Numerical EMC Investigation", Journal of Electromagnetics Vol. 20, no.2, pp. 141-153, March-April 2000. ETRMDV: 20(2)(2000), ISSN: 0272-6343.

[32] S. M. S. Reyhani and R. J. Glover, "Insulated Implantable Medical Device Model Using Electromagnetic Dyadic Green's Function", proceedings of the AP2000 Millennium Conference on Antennas and Propagation (AP2000/IEEE, IEE, ICAP, JINA & EUREL), Davos, Switzerland: paper no. p1566, 9-14 April 2000.

[33] S. M. S. Reyhani and R. J. Glover, "Far Field Electromagnetic Modeling of Implantable Medical Devices Using Cylindrical DGFs", proceedings of the International Conference on EMC (EMC York 2000) University of York, UK: pp. 1B3, 10-11 July 2000.

[34] J. J. Bowman, T. B. A. Senior and P. L. E. Uslenghi, "Electromagnetic and Acoustic Scattering by Simple Shapes". Wiley- Interscience, New York, 1969.

[35] G. P. S. Cavalcante, D. A. Rogers and A. J. Giardola, "Analysis of Electromagnetic Wave Propagation in Multi-layered Media using Dyadic Green's Functions". Radio Science, Vol. 17, no.3, pp. 503-508, May-June 1982.

[36] L. W. Li, P. S. Kooi, M. S. Leong and T. S. Yeo, "Electromagnetic Dyadic Green's Function in Spherically Multilayered Media". IEEE Trans. Microwave Theory Tech., Vol. MTT-42, no.12, pp. 2302-2310, Dec. 1994.

[37] L. W. Li, J. A. Bennett and P. L. Dyson, "Some Method for Solving the Coefficients of Dyadic Green's Function in Isotropic Stratified Media". Int. J. Electronics, Vol. 70, no.4, pp. 803-814, 1991.

[38] S. M. S. Reyhani and R. J. Glover, "Exploiting the Symmetry of the Principle Terms in DGF Formulation", technical report, TR-FDTD695, Department of Electronic and Computer Engineering, Brunel University, UK 1997.

[39] R. E. Collin, "Dyadic Green's Function Expansions in Spherical Co-ordinates". Electromagnetics, Vol. 6, pp. 183-207, 1986.

[40] W. C. Chew, "Waves and Fields in Inhomogeneous Media". New York, Van Nostrand, 1990.

[41] K. Kurokawa, "The Expansions of Electromagnetic Fields in Cavities". IRE Trans. Microwave Theory Tech., Vol. MTT-6, no.2, pp. 178-187, April 1958.

[42] J. Van Bladel, "Some Remarks on Green's Dyadic for Infinite Space". IRE Trans. Antennas Propagat., Vol. AP-9, pp. 563-566, Nov. 1961.

[43] J. G. Fikioris, "Electromagnetic Field Inside a Current-Carrying Region". J. Math. Physics, Vol. -6, no.11, pp. 1617-1620, Nov. 1965.

[44] J. Grzesik, "Comment on the Singularities of the Tensor Green's Function". Proc. IEEE (Letters), Vol. 54, pp. 1967, Dec. 1966.

[45] I. Sugai and J. Grzesik, "Further Comment on the Singularities of the Tensor Green's Function". Proc. IEEE (Letters), Vol. 55, no.9, pp. 1624-1626, Sept. 1967.

[46] C. T. Tai, "On the Eigenfunction Expansion of Dyadic Green's Functions". Proc. IEEE, Vol. 61, pp. 480-481, April 1973.

[47] R. E. Collin, "On the Incompleteness of E and H Modes in Waveguides". Can. J. Physics, Vol. 51, pp. 1135-1140, June 1973.

[48] P. Rozenfeld, "The Electromagnetic Theory of Three-Dimensional Inhomogeneous Lenses and the Dyadic Green Functions for Cavities". Ph.D. Dissertation, Dept. of Electrical Engineering, The University of Michigan, Ann Arbor, Michigan, 1974.

[49] A. Q. Howard Jr., "On the Longitudinal Component of the Green's Function Dyadic". Proc. IEEE, Vol. 62, pp. 1704-1705, Dec. 1974.

[50] C. M. Butler, "Evaluation of Potential Integral at Singularity of Exact Kernel in Thin-Wire Calculations". IEEE Trans. Antennas Propagat., Vol. AP-23, pp. 293-295, Mar. 1975.

[51] F. M. Tesche and A. R. Neureuther, "The Analysis of Monopole Antennas Located on a Spherical Vehicle: Part 1, Theory". IEEE Trans. Electromagn. Compat., Vol. EMC-18, no.1, pp. 2-8, Feb. 1976.

[52] C. T. Tai and P. Rozenfeld, "Different Representations of Dyadic Green's Functions for a Rectangular Cavity". IEEE Trans. Microwave Theory Tech., Vol. MTT-25, pp. 597-601, Sept. 1976.

[53] K. M. Chen, "A Simple Physical Picture of Tensor Green's Function in Source Region". Proc. IEEE, Vol. 65, pp. 1202-1204, Aug. 1977.

[54] A. Q. Howard and D. B. Seidel, "Singularity Extraction in Kernel Functions in a Closed Region Problem". Radio Science, Vol. 13, no.3, pp. 425-429, May-June 1978.

[55] A. D. Yaghjian, "Mathematical Properties and Physical Interpretation of the Source Dyadic of Electric Dyadic Green's Functions". in ISAP Summaries of Papers (Sendai, Japan), pp. 371-372, Aug. 1978.

[56] S. W. Lee, J. Boersma, C. L. Law and G. A. Deschamps, "Singularity in Green's Function and its Numerical Evaluation". IEEE Trans. Antennas Propagat., Vol. AP-28, no.3 pp. 311-317, May 1980.

[57] C. T. Tai, "Comments on Electric Dyadic Green's Functions in the Source region". Proc. IEEE (Letters), Vol. 69, no.2, pp. 282-285, Feb. 1981.

[58] C. T. Tai, "Equivalent Layers of Surface Charge, Current Sheet, and Polarisation in the Eigen-function Expansions of Green's Functions in Electromagnetic Theory". IEEE Trans. Antennas Propagat., Vol. AP-29, no.5, pp. 733-739, Sept. 1981.

[59] A. D. Yaghjian, "A Delta-Distribution Derivation of the Electric Field in the Source Region". Electromagnetics, no.2, pp. 161-167, 1982.

[60] J. J. H. Wang, "A Unified and Consistent View on the Singularities of the Electric Dyadic Green's Function in the Source Region". IEEE Trans. Antennas Propagat., Vol. AP-30, no.3, pp. 463-468, May 1982.

[61] W. A. Johnson, A. Q. Howard and D. G. Dudley, "On the Irrotational Component of the Electric Green's Dyadic". Radio Science, Vol. 14, no.6, pp. 961-967, Nov.-Dec. 1982.

[62] M. Kisliuk, "Comments on "A Unified and Consistent View on the Singularities of the Electric Dyadic Green's Function in the Source Region". IEEE Trans. Antennas Propagat., Vol. AP-31, no.2, pp. 346-347, Mar. 1983.

[63] P. H. Pathak, "On the Eigen-function Expansion of Electromagnetic Dyadic Green's Functions". IEEE Trans. Antennas Propagat., Vol. AP-31, no.6, pp. 837-846, Nov. 1983.

[64] C. T. Tai, "Dyadic Green Functions for a Rectangular Wave-guide filled with two Dielectrics". J. Electromagnetic Waves and Appl., Vol.2, no.3/4, pp. 245-253, 1988.

[65] A. D. Yaghjian, T. B. Hansen and A. J. Devaney, "Minimum Source Region for a given Far-Field Pattern". IEEE Trans. Antennas Propagat., Vol. AP-45, no.5, pp. 911-912, May 1997.

[66] D. H. S. Cheng, "On the Formulation of the Dyadic Green's Function in a Layered Medium". Electromagnetics Vol. 6, no.2, pp. 171-182, 1986.

[67] H. -O. Ruoss and F. M. Landstorfer, "Electromagnetic Dyadic Green's Function for a Layered Homogeneous Lossy Dielectric Sphere as Head Model for Numerical EMC Investigation". Electron. Lett., Vol.32, no. 21, pp. 1935-1937, Oct. 1996.

[68] C. M. Butler and T. L. Keshavamurthy, "Analysis of a Wire Antenna in the Presence of a Sphere". IEEE Trans. Electromagn. Compat., Vol. EMC-22, no.2, pp. 113-118, May 1980.

[69] D. S. Jones, "Accoustic and Electromagnetic Waves". Oxford University Press, New York, 1986.

[70] D. S. Jones, "The Theory of Electromagnetism". Pergamon Press, MacMillian, New York, 1964.

[71] A. Schwab, C. Fuchs and P. Kistenmacher, "Semantics of the Irrotational Component of the Magnetic Vector Potential, A". IEEE Antennas Propagat. Magazine, Vol. AP-39, no.1, pp. 46-51, Feb. 1997.

[72] L. W. Li, "Dyadic Green's Function of Inhomogeneous Ionospheric Waveguide". J. Electromagn. Waves and Applic., Vol. 6, no.1, pp. 53-70, 1992.

[73] C. F. Bohren, "Light Scattering by Optically Active Sphere". Chemical Physics Letters, Vol. 29, no.3, pp. 458-462, 1 Dec. 1974.

[74] N. Engheta and M. W. Kowarz, "Antenna Radiation in the Presence of a Chiral Sphere". J. Applied Physics, Vol. 67, no.2, pp. 639-647, Jan. 1990.

[75] J. S. Bagby and D. P. Nyquist, "Dyadic Green's Function for Integral Electronic and Optical Circuits". IEEE Trans. Microwave Theory Tech., Vol. MTT-35, no.2, pp. 206-210, Feb. 1987.

[76] M. S. Viola and D. P. Nyquist, "An Observation on the Sommerfeld-Integral Representation of the Electric Dyadic Green's Function for Layered Media". IEEE Trans. Microwave Theory Tech., Vol. MTT-36, no.8, pp. 1289-1292, Aug. 1988.

[77] L. Pearson and Wilson, "On the Spectral Expansion of the Electric and Magnetic Dyadic Green's Functions in Cylindrical Co-ordinates". Radio Sci., Vol. 18, pp. 166-174, 1983.

[78] C. F. Stubenrauch, "Radiation from Source in the Presence of a Moving Dielectric Column". Ph.D. Dissertation, Dept. of Electrical Engineering, The University of Michigan, Ann Arbor, Michigan, 1972.

[79] L. W. Li, P. S. Kooi, M. S. Leong, and T. S. Yeo, "A General Expression of Dyadic Green's Functions in radially multilayered chiral media". IEEE Trans. Antennas Propagat., Vol. AP-43, no.3, pp. 232-238, Mar. 1995.

[80] L. W. Li, P. S. Kooi, M. S. Leong, T. S. Yeo and S. L. Ho, "On the Eigenfunction Expansion of Electromagnetic Dyadic Green's Functions in Rectangular Cavities and Waveguides". IEEE Trans. Microwave Theory Tech., Vol. MTT-43, no.3, pp. 700-702, Mar. 1995.

[81] Zhonggui Xiang and Yilong Lu, "Electromagnetic Dyadic Green's Function in Cylindrically Multilayered Media". IEEE Trans. Microwave Theory Tech., Vol. MTT-44, no.4, pp. 614-621, April 1996.

[82] Jaakko Malmivuo and Robert Plonsey, "Bioelectromagnetism: Principles and Applications of Bioelectric and Biomagnetic Fields, Oxford University Press, New York, Oxford, 1995.

[83] L. Chatterjee, Y. Gu and O. P. Gandhi, "Quantification of Electromagnetic Absorption in Humans from Body-Mounted Communication Transceivers". IEEE Trans. Veh. Technol., Vol. VT-34, no.2, pp. 55-62, 1985.

[84] R. F. Cleveland and T. W. Athey, "Specific Absorption Rate (SAR) in Models of the Human Head Exposed to Hand-Held UHF Portable Radios". Bioelectromagnetics, Vol. 10, pp. 173-186, 1989.

[85] Q. Balzano, O. Garay and T. J. Manning, Jr., "Electromagnetic Energy Exposure of Simulated Users of Portable Cellular Telephones". IEEE Trans. Veh. Technol., Vol. VT-44, no.3, pp. 390-403, 1995.

[86] Y. Amemiya, and S. Uebayashi, "The Distribution of Absorbed Power inside a Sphere Simulating Human Head in the Near Field of a $\lambda/2$ Dipole Antenna". Trans. IECE Japan, Vol. J66-B, no.9, pp. 1115-1122, Nov. 1983.

[87] N. Kuster, "Multiple Multipole Method for Simulating EM Problems Involving Biological Bodies". IEEE Trans. Biol. Eng., Vol. 40, no.7, pp. 611-620, July 1993.

[88] K. S. Kunz and R. J. Lubbers, "The Finite Difference Time Domain Method for Electromagnetics". CRC Press, 1993.

[89] P. J. Dimbylow and O. P. Gandhi, "Finite-Difference Time-Domain Calculations of SAR in a Realistic Heterogeneous Model of the Head for Plane-Wave Exposure from 600 MHz to 3 GHz". Phys. Med. Biol., Vol. 36, no.8, pp. 1075-1089, 1991.

[90] P. J. Dimbylow, "FDTD Calculations of the SAR for a Dipole Closely Coupled to the Head at 900 MHz and 1.9 GHz". Phys. Med. Biol., Vol. 38, pp. 361-368, 1991.

[91] J. Toftgard, H. Hornsleth and B. Anderson, "Effects on Portable Antennas of the Presence of a Person". IEEE Trans. Antennas Propagat., Vol. AP-41, no.6, pp. 739-746, June 1993.

[92] I. Martens "Electromagnetic Field Calculations for Wireless Telephone". The Radio Science Bulletin no.271, pp. 9-11, Dec. 1994.

[93] I. Martens, J. De. Moerloose and D. De. Zutter, "Calculation of the Electromagnetic Fields Induced in the Head of an Operator of a Cordless Telephone". Radio Science, Vol. 30, no.1, pp. 283-290, Jan.-Feb. 1995.

[94] V. Hombach, k. Meier, E. K. Burkhardt and N. Kuster, "The Dependence of EM Energy Absorption upon Human-Head Modeling at 900 MHz". IEEE Trans. Microwave Theory Tech., Vol. MTT-44, no.10, pp. 1865-1873, Oct. 1996.

[95] k. Meier, V. Hombach, R. Kastle, R. Yew-Sio Tay and N. Kuster, "The Dependence of Electromagnetic Energy Absorption upon Human-Head Modeling at 1800 MHz". IEEE Trans. Microwave Theory Tech., Vol. MTT-45, no.11, pp. 2058-2062, Nov. 1997.

[96] O. P. Gandhi, G. Lazzi, and M. F. Cynthia, "Electromagnetic Absorption in the Human Head and for Mobile Telephone at 835 and 1900 MHz". IEEE Trans. Microwave Theory Tech., Vol. MTT-44, no.10, pp. 1884-1897, Oct. 1996.

[97] M. Okoniewsky and M. A. Stuchly, "A Study of the Handset Antenna and Human Body Interaction". IEEE Trans. Microwave Theory Tech., Vol. MTT-44, no.10, pp. 1855-1864, Oct. 1996.

[98] C. T. Tai, "The Dyadic Green Function for a Moving Isotropic Medium". IEEE Trans. Antennas Propagat., Vol. AP-13, pp. 322-323, Mar. 1965.

[99] C. T. Tai, "Huygen's Principle in a Moving Isotropic, Homogeneous, and Linear Medium". Applied Optics, Vol. 4, No. 10, pp. 1347-1349, Oct. 1965.

[100] C. T. Tai, "A Study of Electrodynamics of Moving Media". IEEE Proc., Vol. 52, pp. 685-689, June 1964.

[101] M. Kisliuk, "The Dyadic Green's Functions for Cylindrical Waveguides and Cavities". IEEE Trans. Microwave Theory Tech., Vol. MTT-28, no.8, pp. 894-898, Aug. 1980.

[102] L. W. Li, P. S. Kooi, M. S. Leong, T. S. Yeo and S. L. Ho, "Input Impedance of a Probe-Excited Semi-Infinite Rectangular Waveguide with Arbitrary Mul-

tilayered Loads: Part I — Dyadic Green's Functions". IEEE Trans. Microwave Theory Tech., Vol. MTT-43, no.7, pp. 1559-1566, July 1995.

[103] V. G. Daniele and M. Orefice, "Dyadic Green's Functions in Bounded Media". IEEE Antennas Propagat. Magazine, Vol. AP-32, no.2, pp. 193-196, Feb. 1984.

Index

Electromagnetics, 20:141–153, 2000

0272-6343/00 $12.00 + .00

Electromagnetic Dyadic Green's Function for a Multilayered Homogeneous Lossy Dielectric Spherical Head Model for Numerical EMC Investigation

S. M. S. REYHANI
R. J. GLOVER

Department of Electrical and Electronic Engineering
Brunel University
Uxbridge, Middlesex, England

The principle objectives of our research are twofold. We outline an exact general expression of dyadic Green's function (DGF) for the problem of electromagnetic radiation from a source of excitation in the presence of a layered spherical dielectric head model, which is valid everywhere, including the source region. The medium is assumed to be homogeneous, isotropic, linear, nondispersive, and stationary. The DGFs are obtained by employing the method of scattering superposition. Second, a compact alternative general representation is developed to determine the electric- and magnetic-type DGFs, giving clarity as well as more efficient and economical computation in terms of speed, time, and memory.

Keywords electromagnetic compatibility, head model, antenna, dipole, mobile phone, dyadic Green's function

Introduction

The objective of modeling biological bodies exposed in the near as well as in the far field is to assess the induced and scattered fields. However, near-field exposure is of considerably higher complexity because:

1. the field distribution is extremely nonuniform in the vicinity of the source as well as inside the body;
2. in many cases, the interaction of the scattered field on the source is not small enough to be negligible.

The dyadic Green's function (DGF) was introduced by Schwinger in the early 1940s and has been extensively discussed by Tai [1, 2], Collin [3], Rahmat-Samii [4], Yaghjian [5, 6], and others. This technique was presented mainly to formulate various canonical electromagnetic problems in a systematic manner and to enable many special cases to be treated as one general problem. If the current source in these problems has some specific distributions, we have to consider these distribu-

Received 20 October 1998; accepted 15 March 1999.
Address correspondence to S. M. S. Reyhani, 301F Howell Building, Dept. of Electrical and Electronic Engineering, Brunel University, Uxbridge, Middlesex, UB8 3PH, UK. E-mail: Sayed.Salehi-Reyhani@brunel.ac.uk

tions as special cases, for example, excitation by a transversal electric dipole or a longitudinal or a magnetic dipole. The DGF, which relates the current source and the field, is singular in the source region.

The format of this paper is as follows. The complete set of spherical vector wave functions are introduced in section 2.

In section 3, we start with the unbounded case, in which the point source radiates with no interface present, and construct the corresponding DGF, $\bar{\bar{G}}_{eo}^{00o}(\bar{R}, \bar{R}')$, in terms of an integral over the spectra of plane waves that constitute the continuous eigenfunction expansion (EFE) in which the eigenfunctions are guided in preferred R-coordinate direction, using the procedures described in Tai [2] or Collin [3]. This expansion also contains an explicit dyadic delta function term which is required for completeness at the source point. It is considered as a correction to the general solenoidal EFE, which is valid outside the source point.

The procedure required to derive the complete EFE of the general scattering DGF for the multilayered media in terms of only the solenoidal eigenfunctions is shown to be a simple and straightforward general expression. The DGF for the multilayered media $\bar{\bar{G}}_e^{Lfo}(\bar{R}, \bar{R}')$, is then constructed from the principle of the superposition, which involves the sum of the fields of, first, the source in free space (or the free-space Green's function $\bar{\bar{G}}_{eo}^{00o}(\bar{R}, \bar{R}')$ and, second, the fields scattered by the layered media $\bar{\bar{G}}_{es}^{Lfo}(\bar{R}, \bar{R}')$. A radically new and generic method for deriving the scattering formulae is described in this section, giving an idea of the computational burden involved in the general method described in this paper. This represents one of the main contributions of this study. Magnetic-type DGF can be found by invoking duality. Once the electric field is obtained the magnetic field is derivable by taking the curl of the electric field, and vice versa.

Conclusions are then presented in section 4, which summarizes the important points contained in this work, and finally, a short bibliography is provided for further research.

Spherical Hansen Vector Wave Functions

The spherical vector wave functions that were introduced by Hansen [7] are the building blocks of the EFE of various kinds of DGF. They are denoted by $\bar{L}_{emn}$, $\bar{M}_{emn}$, and $\bar{N}_{emn}$, which are solutions of the homogeneous vector Helmholtz equation. The generating functions or eigenfunctions, which are solutions of the spherical scalar wave equation $\nabla^2\Psi + k^2\Psi = 0$, can be written in the form

$$\Psi_{emn}(k) = j_n(kR)P_n^m(\cos\theta)\begin{matrix}\cos\\ \sin\end{matrix} m\phi, \tag{1}$$

Here k is an undetermined wave number and R is the piloting radial vector. Subscript "e" stands for even, and "o" is an odd character of the generating functions.

$P_n^m(\cos\theta)$ identifies the associated Legendre functions of the first kind with order (n, m), and $j_n(kR)$ denotes the spherical Bessel functions of the order n to represent both outgoing and incoming waves. Spherical vector wave functions are akin to the Debye potentials:

$$\bar{L}_{emn}(k) = \nabla\Psi_{emn}, \tag{2}$$

$$\bar{\bar{M}}_{e_{omn}}(k) = \nabla \times \left[\Psi_{e_{omn}} \bar{R}\right], \tag{3}$$

$$\bar{\bar{N}}_{e_{omn}}(k) = \frac{1}{k}\nabla \times \nabla \times \left[\Psi_{e_{omn}} \bar{R}\right], \tag{4}$$

To satisfy the symmetrical properties of DGF,

$$\bar{\bar{N}}_{e_{omn}}(k) = \frac{1}{k}\nabla \times \bar{\bar{M}}_{e_{omn}}(k), \tag{5}$$

$$\bar{\bar{M}}_{e_{omn}}(k) = \frac{1}{k}\nabla \times \bar{\bar{N}}_{e_{omn}}(k). \tag{6}$$

Green's functions for bounded regions are usually given in the form of modal expansions. Modal series unsuitable for use in numerical algorithms which require the computation of the electric field inside the source region. In this case, the Green's function must be computed at points $\bar{R}'$ close to $\bar{R}$, where the convergence of the series is very poor due to the singularity of $\bar{\bar{G}}_e(\bar{R}, \bar{R}')$ at point source $R = R'$. This drawback can be avoided by using expressions where a diverging term, expressed in closed form, is extracted from the modal expansion of $\bar{\bar{G}}_e(\bar{R}, \bar{R}')$, so that the remaining series represents a function finite at point source $R = R'$; see Bressan and Conciauro [8].

The complete expressions for the solenoidal or rotational or transverse functions are given by Collin [3]:

$$\bar{\bar{M}}_{e_{omn}}(k) = \begin{Bmatrix} 0 \\ \mp \dfrac{m}{\sin\theta} j_n(kR) P_n^m(\cos\theta)^{\sin}_{\cos} m\phi\hat{\theta} \\ -j_n(kR)\left(\dfrac{\partial P_n^m(\cos\theta)}{\partial\theta}\right)^{\cos}_{\sin} m\phi\hat{\phi} \end{Bmatrix}, \tag{7}$$

$$\bar{\bar{N}}_{e_{omn}}(k) = \begin{Bmatrix} \dfrac{n(n+1)}{kR} j_n(kR) P_n^m(\cos\theta)^{\cos}_{\sin} m\phi\hat{R} \\ \dfrac{1}{kR}\dfrac{\partial}{\partial R}[Rj_n(kR)]\left(\dfrac{\partial P_n^m(\cos\theta)}{\partial\theta}\right)^{\cos}_{\sin} m\phi\hat{\theta} \\ \dfrac{1}{kR}\dfrac{\partial}{\partial R}[Rj_n(kR)]\left[\mp \dfrac{m}{\sin\theta} P_n^m(\cos\theta)^{\sin}_{\cos} m\phi\hat{\phi}\right] \end{Bmatrix}, \tag{8}$$

And the complete expressions for the nonsolenoidal or irrotational or lamellar functions are given by Collin [3]:

$$\bar{L}_{e_{omn}}(k) = \begin{Bmatrix} \dfrac{\partial}{\partial R} j_n(kR) P_n^m(\cos\theta)^{\cos}_{\sin} m\phi\hat{R} \\ \left(\dfrac{j_n(kR)}{R}\dfrac{\partial P_n^m(\cos\theta)}{\partial\theta}\right)^{\cos}_{\sin} m\phi\hat{\theta} \\ \mp \dfrac{mj_n(kR)}{R\sin\theta} P_n^m(\cos\theta)^{\sin}_{\cos} m\phi\hat{\phi} \end{Bmatrix}. \tag{9}$$

Note that in the set of spherical vector wave functions, only $\bar{M}_{emn}$ do not possess the radial component. m and n are the eigenvalues associated with the ϕ and θ coordinates, respectively, when for problems involving spheres, they are integers. The $\hat{R}$, $\hat{\theta}$, and $\hat{\phi}$ are the spherical unit vectors.

The orthogonal properties of these vector wave functions have been discussed by Tai [1, 2] and Collin [3]. $\bar{L}_{emn}$ functions are not required to derive the eigenfunction expansion of the magnetic DGF that are solenoidal and satisfy the vector wave equation, but to find the EFE of the electric DGF, the $\bar{L}_{emn}$ functions are also necessary, because $\bar{\bar{G}}_e^{Lfo}(\bar{R}, \bar{R}')$, unlike $\bar{\bar{G}}_m^{Lfo}(\bar{R}, \bar{R}')$, the dyadic Green's functions of electric- and magnetic-type, respectively, is a nonsolenoidal dyadic function.

The method for deriving the magnetic/electric DGF given in the following section for spherical configurations uses the Ohm–Rayleigh (G_m) procedure. However, there exist several alternative derivations, which will not be discussed further.

General Representation of DGF

Before we develop the analysis of electromagnetic wave propagation in the multilayered head model, it is convenient to examine the media first with no scatterer and then with one-, two-, three-, and four-layer head models.

Free Space DGF for an Electric Dipole in Unbounded Medium

The electric and magnetic fields due to an electric dipole located at R' in an infinite homogeneous space without the presence of a scatterer (obstacle) can be computed in spherical coordinates. There are various methods that can be utilized to achieve this. The expansion of the electric field requires both the transverse and longitudinal vector eigenfunctions, and hence the DGF must also have both sets of eigenfunctions in its expansion [2]:

$$\bar{\bar{G}}_{eo}^{00o}(\bar{R}, \bar{R}') = \frac{-\hat{R}\hat{R}}{k_o^2}\delta(\bar{R} - \bar{R}') + \frac{ik_o}{4\pi}\sum_{n=1}^{\infty}\sum_{m=0}^{n} C_{mn} \cdot \begin{cases} \begin{Bmatrix} [\bar{M}_{emn}^{(1)}(k_o)\bar{M}_{emn}'(k_o)] \\ [\bar{N}_{emn}^{(1)}(k_o)\bar{N}_{emn}'(k_o)] \end{Bmatrix}, & R > R', \\ \begin{Bmatrix} [\bar{M}_{emn}(k_o)\bar{M}_{emn}'^{(1)}(k_o)] \\ [\bar{N}_{emn}(k_o)\bar{N}_{emn}'^{(1)}(k_o)] \end{Bmatrix}, & R < R'. \end{cases} \tag{10}$$

Here the first term presents the singularity term specifying inside the source region and the second term outside the source region.

Where the prime on the vector wave functions indicates that functions are defined with respect to the coordinates of the position vector $\bar{R}'$, coordinates (R', θ', ϕ'). The superscript "1" in $\bar{M}_{emn}^{(1)}(k_o)$, $\bar{N}_{emn}^{(1)}(k_o)$, $\bar{M}_{emn}'^{(1)}(k_o)$, and $\bar{N}_{emn}'^{(1)}(k_o)$ is present to indicate the substitution of the spherical Hankel function of the first kind (spherical Bessel functions of the third kind) $h_n(kR)$ for $j_n(kR)$ in the

generating function $\Psi_{e_{mn}}(k)$. It is important to note the singularity of the Hankel function at the origin. $\hat{R}\hat{R}$ is a dyad (dyadic product of the unit vectors) [9]:

$$\hat{R}\hat{R} = \left(\frac{\hat{x}x}{R} + \frac{\hat{y}y}{R} + \frac{\hat{z}z}{R}\right)\left(\frac{\hat{x}x}{R} + \frac{\hat{y}y}{R} + \frac{\hat{z}z}{R}\right), \tag{11}$$

and $\delta(\bar{R} - \bar{R}')$ is the weighted Dirac delta function in three dimensions. Subscripts o and e stand for unbounded (open) space and electric component, respectively.

The dyadic delta function term at the source point is included explicitly as a correction to the general solenoidal EFE which is valid outside the source point.

$$C_{mn} = (2 - \delta_o^m)\frac{2n+1}{n(n+1)}\frac{(n-m)!}{(n+m)!}. \tag{12}$$

Coefficient C_{mn} depends on the values of m and n, where δ_o^m is the Kronecker delta functions, when

$$\delta = \begin{cases} 1, & \text{if } m = o, \\ 0, & \text{if } m \neq o \end{cases}. \tag{13}$$

Scattering DGFs for an Electric Dipole in the Presence of a Spherical Head Model

When a biological system is illuminated by an electromagnetic wave, an electromagnetic field is induced inside the system and an electromagnetic wave is scattered externally by the system. Since the biological system is an irregularly shaped heterogeneous imperfectly conducting medium with frequency-dependent permittivity and conductivity, the distribution of the internal electromagnetic field and the scattered electromagnetic wave will depend on the body's physiological parameters and geometry, as well as the frequency and polarization of the incident wave. The mathematical complexity of the problem has led researchers to investigate simple models. Several theoretical studies have analyzed these models (Reyhani and Glover [10, 11]). In this paper the medium is assumed to be homogeneous, isotropic, linear, nondispersive, and stationary.

Having expressed the DGF for an unbounded medium in terms of spherical vector wave functions, we may now use that result to construct one for a spherical head model.

DGF for a single-layer spherical head model. This can be considered as the contribution of the reflections and transmissions of a single-layer sphere of radius α_1 centered at O, superimposed in an unbounded homogeneous medium with the radiation source located outside the sphere at R'. The medium is characterized by (μ_o, ϵ_o), and material properties of the sphere are represented by $(\mu_{h1}, \epsilon_{h1})$, where subscripts o and h stand for unbounded (open) space and head, respectively.

The scattered DGF terms for this case were examined by [2]:

$$\bar{\bar{G}}_{es}^{10o}(\bar{R}, \bar{R}') = \frac{ik_o}{4\pi}\sum_{n=1}^{\infty}\sum_{m=0}^{n} C_{mn} \cdot \begin{bmatrix} A_{eM}^{10o}\bar{M}_{emn}^{(1)}(k_o)\bar{M}_{emn}^{\prime(1)}(k_o) \\ A_{eN}^{10o}\bar{N}_{emn}^{(1)}(k_o)\bar{N}_{emn}^{\prime(1)}(k_o) \end{bmatrix}, \tag{14}$$

$$\bar{\bar{G}}_{es}^{11o}(\bar{R},\bar{R}') = \frac{ik_o}{4\pi}\sum_{n=1}^{\infty}\sum_{m=0}^{n} C_{mn}\cdot\begin{bmatrix} B_{eM}^{11o}\bar{M}_{emn}(k_1)\bar{M}_{emn}^{\prime(1)}(k_o) \\ B_{eN}^{11o}\bar{N}_{emn}(k_1)\bar{N}_{emn}^{\prime(1)}(k_o)\end{bmatrix}. \tag{15}$$

Where the first number of triple superscripts signifies the last inner layer in the model and the second number identifies the region where the function is defined, that is the observation or field point, and the third number corresponds to the location of the source, i.e., the source point, which in this case is denoted by the letter o. Subscripts M and N attribute the coefficients to the excitation functions.

The choice of $\bar{M}_{emn}^{(1)}$ and $\bar{N}_{emn}^{(1)}$ as the field functions in $\bar{\bar{G}}_{es}^{10o}(\bar{R},\bar{R}')$ is dictated by the radiation condition that the scattered field must consist of outgoing waves, and the choice of $\bar{M}_{emn}^{\prime(1)}$ and $\bar{N}_{emn}^{\prime(1)}$ as the excitation functions is guided by the expression for $\bar{\bar{G}}_{eo}^{00o}(\bar{R},\bar{R}')$ and the boundary condition that at $R = \alpha_1$, $\bar{\bar{G}}_{e}^{Lfo}(\bar{R},\bar{R}')$ must satisfy the Dirichlet boundary condition, which can be satisfied only if the excitation functions are the same as that of $\bar{\bar{G}}_{eo}^{00o}(\bar{R},\bar{R}')$ for $R < R'$.

The field functions for $\bar{\bar{G}}_{es}^{11o}(\bar{R},\bar{R}')$ are so chosen because they are the solutions for the vector wave equation in region 1, and they must be finite like that of $\bar{\bar{G}}_{eo}^{00o}(\bar{R},\bar{R}')$ for $R < R'$.

Also, the expanded version of a typical combination is [12, p. 380]:

$$A_{eM}^{10o}\bar{M}_{emn}^{(1)}(k_o)\bar{M}_{emn}^{\prime(1)}(k_o) = \begin{Bmatrix} A_{eM}^{10o}\bar{M}_{emn}^{(1)}(k_o)\bar{M}_{emn}^{\prime(1)}(k_o) \\ A_{eM}^{10o}\bar{M}_{emn}^{(1)}(k_o)\bar{M}_{emn}^{\prime(1)}(k_o)\end{Bmatrix}. \tag{16}$$

Double-layer spherical head model. We consider two concentric spheres centered at O, superimposed by an unbounded homogeneous medium with the current distribution source located outside the sphere at R'. The medium is characterized by (μ_o, ϵ_o), and material properties of the outer sphere are represented by $(\mu_{h1}, \epsilon_{h1})$ and those of the inner sphere by $(\mu_{h2}, \epsilon_{h2})$. The radii of outer to inner spheres are α_1 and α_2, respectively.

In this case the scattered DGF terms can be shown by

$$\bar{\bar{G}}_{es}^{20o}(\bar{R},\bar{R}') = \frac{ik_o}{4\pi}\sum_{n=1}^{\infty}\sum_{m=0}^{n} C_{mn}\cdot\begin{bmatrix} A_{eM}^{20o}\bar{M}_{emn}^{(1)}(k_o)\bar{M}_{emn}^{\prime(1)}(k_o) \\ A_{eN}^{20o}\bar{N}_{emn}^{(1)}(k_o)\bar{N}_{emn}^{\prime(1)}(k_o)\end{bmatrix}, \tag{17}$$

$$\bar{\bar{G}}_{es}^{21o}(\bar{R},\bar{R}') = \frac{ik_o}{4\pi}\sum_{n=1}^{\infty}\sum_{m=0}^{n} C_{mn}\cdot\begin{Bmatrix} B_{eM}^{21o}\bar{M}_{emn}^{(1)}(k_1)\bar{M}_{emn}^{\prime(1)}(k_o) \\ B_{eN}^{21o}\bar{N}_{emn}^{(1)}(k_1)\bar{N}_{emn}^{\prime(1)}(k_o) \\ C_{eM}^{21o}\bar{M}_{emn}(k_1)\bar{M}_{emn}^{\prime(1)}(k_o) \\ C_{eN}^{21o}\bar{N}_{emn}(k_1)\bar{N}_{emn}^{\prime(1)}(k_o)\end{Bmatrix}, \tag{18}$$

$$\bar{\bar{G}}_{es}^{22o}(\bar{R},\bar{R}') = \frac{ik_o}{4\pi}\sum_{n=1}^{\infty}\sum_{m=0}^{n} C_{mn}\cdot\begin{bmatrix} D_{eM}^{22o}\bar{M}_{emn}(k_2)\bar{M}_{emn}^{\prime(1)}(k_o) \\ D_{eN}^{22o}\bar{N}_{emn}(k_2)\bar{N}_{emn}^{\prime(1)}(k_o)\end{bmatrix}. \tag{19}$$

The choice of the field and excitation functions in $\bar{\bar{G}}_{es}^{21o}(\bar{R},\bar{R}')$ are governed by the fact that the electromagnetic fields consist of radial wave-modes propagating

outwards and inwards. Therefore,

$$\bar{\bar{G}}_{es}^{21o} = \alpha \cdot \bar{\bar{G}}_{es}^{20o} + \dot{\beta} \cdot \bar{\bar{G}}_{es}^{22o}. \tag{20}$$

Trilayer spherical head model. In this case three concentric spheres centered at O, superimposed by an unbounded homogeneous medium with the radiation source located outside the sphere at R' are considered. The material properties of the outer to inner spheres are represented by $(\mu_{h1}, \epsilon_{h1})$, $(\mu_{h2}, \epsilon_{h2})$, and $(\mu_{h3}, \epsilon_{h3})$, respectively. The radii of outer to inner spheres are α_1, α_2, and α_3, respectively.

The scattered DGF terms for $\bar{\bar{G}}_{es}^{30o}$ and $\bar{\bar{G}}_{es}^{31o}$ are the same as those in the last section, and the rest can be expressed by

$$\bar{\bar{G}}_{es}^{32o}(\bar{R}, \bar{R}') = \frac{ik_o}{4\pi} \sum_{n=1}^{\infty} \sum_{m=0}^{n} C_{mn} \cdot \begin{Bmatrix} D_{eM}^{32o} \bar{M}_{emn}^{(1)}(k_2) \bar{M}_{emn}^{\prime(1)}(k_o) \\ D_{eN}^{32o} \bar{N}_{emn}^{(1)}(k_2) \bar{N}_{emn}^{\prime(1)}(k_o) \\ E_{eM}^{32o} \bar{M}_{emn}(k_2) \bar{M}_{emn}^{\prime(1)}(k_o) \\ E_{eN}^{32o} \bar{N}_{emn}(k_2) \bar{N}_{emn}^{\prime(1)}(k_o) \end{Bmatrix}, \tag{21}$$

and for the inner layer,

$$\bar{\bar{G}}_{es}^{33o}(\bar{R}, \bar{R}') = \frac{ik_o}{4\pi} \sum_{n=1}^{\infty} \sum_{m=0}^{n} C_{mn} \cdot \begin{bmatrix} F_{eM}^{33o} \bar{M}_{emn}(k_3) \bar{M}_{emn}^{\prime(1)}(k_o) \\ F_{eN}^{33o} \bar{N}_{emn}(k_3) \bar{N}_{emn}^{\prime(1)}(k_o) \end{bmatrix}. \tag{22}$$

Quad-layer spherical head model. Similarly, the case of four concentric spheres centered at O, superimposed by an unbounded homogeneous medium with the dipole source of radiation located outside the sphere at R', is considered. The material properties of the outer to inner spheres are, respectively, represented by $(\mu_{h1}, \epsilon_{h1})$, $(\mu_{h2}, \epsilon_{h2})$, $(\mu_{h3}, \epsilon_{h3})$, and $(\mu_{h4}, \epsilon_{h4})$. The radii of outer to inner spheres are α_1, α_2, α_3, and α_4 respectively.

The scattered DGF terms for $\bar{\bar{G}}_{es}^{40o}$, $\bar{\bar{G}}_{es}^{41o}$, and $\bar{\bar{G}}_{es}^{42o}$ are the same as those in the previous section and the rest can be presented by

$$\bar{\bar{G}}_{es}^{43o}(\bar{R}, \bar{R}') = \frac{ik_o}{4\pi} \sum_{n=1}^{\infty} \sum_{m=0}^{n} C_{mn} \cdot \begin{Bmatrix} F_{eM}^{43o} \bar{M}_{emn}^{(1)}(k_3) \bar{M}_{emn}^{\prime(1)}(k_o) \\ F_{eN}^{43o} \bar{N}_{emn}^{(1)}(k_3) \bar{N}_{emn}^{\prime(1)}(k_o) \\ G_{eM}^{43o} \bar{M}_{emn}(k_3) \bar{M}_{emn}^{\prime(1)}(k_o) \\ G_{eN}^{43o} \bar{N}_{emn}(k_3) \bar{N}_{emn}^{\prime(1)}(k_o) \end{Bmatrix}. \tag{23}$$

The final inner layer gives

$$\bar{\bar{G}}_{es}^{44o}(\bar{R}, \bar{R}') = \frac{ik_o}{4\pi} \sum_{n=1}^{\infty} \sum_{m=0}^{n} C_{mn} \cdot \begin{bmatrix} H_{eM}^{44o} \bar{M}_{emn}(k_4) \bar{M}_{emn}^{\prime(1)}(k_o) \\ H_{eN}^{44o} \bar{N}_{emn}(k_4) \bar{N}_{emn}^{\prime(1)}(k_o) \end{bmatrix}. \tag{24}$$

General Expression of Scattering DGFs for an Electric Dipole in the Presence of a Multilayered Spherical Head Model

Observation and analysis of the above expressions for the scattering equations allows an efficient formulation of the general scattering DGF for a multilayer spherical head as:

$$\bar{\bar{G}}_{es}^{Lfo}(\bar{R},\bar{R}') = \frac{ik_o}{4\pi}\sum_{n=1}^{\infty}\sum_{m=0}^{n} C_{mn}\cdot\begin{Bmatrix} A_{eM}^{Lfo}\left(1-\delta_f^L\right)\bar{M}_{emn}^{(1)}(k_f)\bar{M}_{emn}^{\prime(1)}(k_o) \\ A_{eN}^{Lfo}\left(1-\delta_f^L\right)\bar{N}_{emn}^{(1)}(k_f)\bar{N}_{emn}^{\prime(1)}(k_o) \\ B_{eM}^{Lfo}(1-\delta_f^o)\bar{M}_{emn}(k_f)\bar{M}_{emn}^{\prime(1)}(k_o) \\ B_{eN}^{Lfo}(1-\delta_f^o)\bar{N}_{emn}(k_f)\bar{N}_{emn}^{\prime(1)}(k_o) \end{Bmatrix}. \quad (25)$$

L is the symbol for last inner layer in the head; f is the field point or observer layer. Superscript/subscript o stands for source point at the open space, while subscript s is scattering.

δ_f^L and δ_f^o are the Kronecker delta functions, where

$$\delta = \begin{cases} 1, & \text{if } L/o = f, \\ 0, & \text{if } L/o \neq f. \end{cases} \quad (26)$$

A_{eM}^{Lfo}, A_{eN}^{Lfo}, B_{eM}^{Lfo}, and B_{eN}^{Lfo} are the amplitude coefficients of scattered DGF to be calculated by applying the boundary condition at the surface ($f = 0, 1, 2, \ldots, L$) of the sphere. These boundary conditions are

$$\hat{R}\times\bar{\bar{G}}_e^{Lfo} = \hat{R}\times\bar{\bar{G}}_e^{L(f+1)o} \quad (27)$$

and

$$\frac{1}{\mu_f}\hat{R}\times\nabla\times\bar{\bar{G}}_e^{Lfo} = \frac{1}{\mu_{(f+1)}}\hat{R}\times\nabla\times\bar{\bar{G}}_e^{L(f+1)o}. \quad (28)$$

For more details on the evaluation of coefficients, readers are referred to Cavalcante, Rogers, and Giardola [13] and Li et al. [14], [15].

A Novel General Expression of Scattering DGFs for an Electric Dipole in the Presence of a Multilayered Spherical Head Model

It is a well-known fact that integral equation methods can solve unbounded problems very effectively. They are often referred to as exact techniques, because they guarantee convergence for sufficiently dense discretizations. However, they have the disadvantage of being difficult to implement for complex objects and generally result in the use of full matrices, whose treatment requires a large amount of memory and CPU time. The computational difficulties can be surmounted by a more convenient and compact general equation. General formula-

tions for scattering DGFs can be expressed by introducing the $\overline{\odot}$ operator, which exploits the symmetry of the principle terms in the DGF expansion to give a general formulation applicable to a wide range of geometrical configurations [16] when one can significantly reduce the number of field samples needed for the field calculation. As shown below,

$$\overline{\overline{G}}_{es}^{Lfo}(\bar{R},\bar{R}') = \frac{ik_o}{4\pi}\sum_{n=1}^{\infty}\sum_{m=0}^{n} C_{mn}\begin{bmatrix} A_{eM}^{Lfo}\,\overline{\odot}_{es_M}^{Lfo} \\ A_{eN}^{Lfo}\,\overline{\odot}_{es_N}^{Lfo} \end{bmatrix}. \tag{29}$$

We give a direct and conceptually simple algorithm whose chief benefit is great computational efficiency. Where

$$\overline{\odot}_{es_M}^{L0o} = 0 \quad \text{for } L = 0$$

(this means that there is only infinite open space in the absence of a scattering body) and

$$\overline{\odot}_{es_M}^{L0o} = \overline{M}_{emn}^{(1)}(k_f)\overline{M}_{emn}^{\prime(1)}(k_o) \quad \text{for } f = 0 \text{ and } L > 0,$$

$$\overline{\odot}_{es_M}^{Lfo} = \begin{bmatrix} \alpha\overline{M}_{emn}^{(1)}(k_f)\overline{M}_{emn}^{\prime(1)}(k_o) \\ \beta\overline{M}_{omn}^{(1)}(k_f)\overline{M}_{omn}^{\prime(1)}(k_o) \end{bmatrix} \quad \text{for } f \neq 0 \text{ or } L,$$

and

$$\overline{\odot}_{es_M}^{LLo} = \overline{M}_{emn}(k_f)\overline{M}_{emn}^{\prime(1)}(k_o) \quad \text{for } f = L,$$

$\overline{\odot}_{es_N}^{Lfo}$ can be calculated from the same procedure as for $\overline{\odot}_{es_M}^{Lfo}$.

Electric DGF in the Antenna-Head Configuration

The electric DGF in the system can be computed by means of the method of scattering superposition expressed as the sum of incident (free-space) DGF and another contribution to account for the field scattered by layered media (secondary DGF); i.e.,

$$\overline{\overline{G}}_e^{Lfo}(\bar{R},\bar{R}') = \overline{\overline{G}}_{eo}^{00o}(\bar{R},\bar{R}')\delta_f^o + \overline{\overline{G}}_{es}^{Lfo}(\bar{R},\bar{R}'), \tag{30}$$

and substituting in the above equation yields the electric DGF in the system

$$\overline{\overline{G}}_e^{Lfo}(\bar{R},\bar{R}') = -\frac{\hat{R}\hat{R}}{k_o^2}\delta(\bar{R}-\bar{R}')\delta_f^o + \frac{ik_o}{4\pi}\sum_{n=1}^{\infty}\sum_{m=0}^{n} C_{mn}$$

$$\times \begin{Bmatrix} \begin{pmatrix} \left[\bar{M}^{(1)}_{emn}(k_o)\bar{M}'_{emn}(k_o)\right]\delta^o_f \\ \left[\bar{N}^{(1)}_{emn}(k_o)\bar{N}'_{emn}(k_o)\right]\delta^o_f \\ A^{Lfo}_{eM}\left(1-\delta^L_f\right)\bar{M}^{(1)}_{emn}(k_f)\bar{M}'^{(1)}_{emn}(k_o) \\ A^{Lfo}_{eN}\left(1-\delta^L_f\right)\bar{N}^{(1)}_{emn}(k_f)\bar{N}'^{(1)}_{emn}(k_o) \\ B^{Lfo}_{eM}(1-\delta^o_f)\bar{M}_{emn}(k_f)\bar{M}'^{(1)}_{emn}(k_o) \\ B^{Lfo}_{eN}(1-\delta^o_f)\bar{N}_{emn}(k_f)\bar{N}'^{(1)}_{emn}(k_o) \end{pmatrix}, & R > R', \\ \begin{pmatrix} \left[\bar{M}_{emn}(k_o)\bar{M}'^{(1)}_{emn}(k_o)\right]\delta^o_f \\ \left[\bar{N}_{emn}(k_o)\bar{N}'^{(1)}_{emn}(k_o)\right]\delta^o_f \\ A^{Lfo}_{eM}\left(1-\delta^L_f\right)\bar{M}^{(1)}_{emn}(k_f)\bar{M}'^{(1)}_{emn}(k_o) \\ A^{Lfo}_{eN}\left(1-\delta^L_f\right)\bar{N}^{(1)}_{emn}(k_f)\bar{N}'^{(1)}_{emn}(k_o) \\ B^{Lfo}_{eM}(1-\delta^o_f)\bar{M}_{emn}(k_f)\bar{M}'^{(1)}_{emn}(k_o) \\ B^{Lfo}_{eN}(1-\delta^o_f)\bar{N}_{emn}(k_f)\bar{N}'^{(1)}_{emn}(k_o) \end{pmatrix}, & R < R'. \end{Bmatrix} \tag{31}$$

using the novel general method

$$\bar{\bar{G}}^{Lfo}_e(\bar{R},\bar{R}') = -\frac{\hat{R}\hat{R}}{k_o^2}\delta(\bar{R}-\bar{R}')\delta^o_f + \frac{ik_o}{4\pi}\sum_{n=1}^{\infty}\sum_{m=0}^{n} C_{mn}$$

$$\times \begin{Bmatrix} \begin{pmatrix} \left[\bar{M}^{(1)}_{emn}(k_o)\bar{M}'_{emn}(k_o)\right]\delta^o_f \\ \left[\bar{N}^{(1)}_{emn}(k_o)\bar{N}'_{emn}(k_o)\right]\delta^o_f \\ A^{Lfo}_{eM}\,\bar{\odot}^{Lfo}_{emn} \\ A^{Lfo}_{eN}\,\bar{\odot}^{Lfo}_{emn} \end{pmatrix}, & R > R', \\ \begin{pmatrix} \left[\bar{M}_{emn}(k_o)\bar{M}'^{(1)}_{emn}(k_o)\right]\delta^o_f \\ \left[\bar{N}_{emn}(k_o)\bar{N}'^{(1)}_{emn}(k_o)\right]\delta^o_f \\ A^{Lfo}_{eM}\,\bar{\odot}^{Lfo}_{emn} \\ A^{Lfo}_{eN}\,\bar{\odot}^{Lfo}_{emn} \end{pmatrix}, & R < R'. \end{Bmatrix} \tag{32}$$

If our concern is only with the region exterior to the source, then the singular term, which is important only in the source region, can be dropped from the expression for the Green's function.

Magnetic DGF in the Antenna-Head Configuration

The principle of duality states that once the electric DGF is obtained, the magnetic DGF is derivable by interchanging the field functions $\bar{M}_{emn} \rightarrow k\bar{N}_{emn}$ and $\bar{N}_{emn} \rightarrow k\bar{M}_{emn}$ and omitting the singularity term contribution and vice versa.

On the other hand, the corresponding total magnetic DGF at any point in the system can be calculated from $\nabla \times \bar{\bar{G}}_e^{Lfo} = \bar{\bar{G}}_m^{Lfo}$, bearing in mind the discontinuous nature of magnetic DGF across a point source at $R = R'$ and the Ampere–Maxwell equation relating $\bar{\bar{G}}_e^{Lfo}$ and $\bar{\bar{G}}_m^{Lfo}$ in the dyadic form; i.e., $\nabla \times \bar{\bar{G}}_m^{Lfo} = \bar{\bar{I}}\delta(\bar{R} - \bar{R}') + k^2 \bar{\bar{G}}_e^{Lfo}$,

$$\bar{\bar{G}}_m^{Lfo}(\bar{R}, \bar{R}') = +\frac{ik_o^2}{4\pi} \sum_{n=1}^{\infty} \sum_{m=0}^{n} C_{mn}$$

$$\times \begin{cases} \begin{pmatrix} \left[\bar{N}_{emn}^{(1)}(k_o)\bar{M}_{emn}'(k_o)\right]\delta_f^o \\ \left[\bar{M}_{emn}^{(1)}(k_o)\bar{N}_{emn}'(k_o)\right]\delta_f^o \\ A_{eM}^{Lfo}\left(1-\delta_f^L\right)\bar{N}_{emn}^{(1)}(k_f)\bar{M}_{emn}^{\prime(1)}(k_o) \\ A_{eN}^{Lfo}\left(1-\delta_f^L\right)\bar{M}_{emn}^{(1)}(k_f)\bar{N}_{emn}^{\prime(1)}(k_o) \\ B_{eM}^{Lfo}(1-\delta_f^o)\bar{N}_{emn}(k_f)\bar{M}_{emn}^{\prime(1)}(k_o) \\ B_{eN}^{Lfo}(1-\delta_f^o)\bar{M}_{emn}(k_f)\bar{N}_{emn}^{\prime(1)}(k_o) \end{pmatrix}, & R > R', \\ \begin{pmatrix} \left[\bar{N}_{emn}(k_o)\bar{M}_{emn}^{\prime(1)}(k_o)\right]\delta_f^o \\ \left[\bar{M}_{emn}(k_o)\bar{N}_{emn}^{\prime(1)}(k_o)\right]\delta_f^o \\ A_{eM}^{Lfo}\left(1-\delta_f^L\right)\bar{N}_{emn}^{(1)}(k_f)\bar{M}_{emn}^{\prime(1)}(k_o) \\ A_{eN}^{Lfo}\left(1-\delta_f^L\right)\bar{M}_{emn}^{(1)}(k_f)\bar{N}_{emn}^{\prime(1)}(k_o) \\ B_{eM}^{Lfo}(1-\delta_f^o)\bar{N}_{emn}(k_f)\bar{M}_{emn}^{\prime(1)}(k_o) \\ B_{eN}^{Lfo}(1-\delta_f^o)\bar{M}_{emn}(k_f)\bar{N}_{emn}^{\prime(1)}(k_o) \end{pmatrix}, & R < R'. \end{cases} \tag{33}$$

Notice that the magnetic DGF does not contain the singularity term because this term is canceled by the derivatives of the delta function and the unit function at the source point. The above equations can be used to accommodate any number of layers in the model system.

Electric and Magnetic Field at Any Point in the Antenna-Head Configuration

The use of the DGF technique allows us to determine the expansion of the electric and magnetic fields in a head/antenna configuration in a direct and elegant manner.

For any current source with current density function $\bar{J}(\bar{R}')$ located outside the head, the electric or magnetic field radiated by such a dipole can be calculated using the formulae

$$\bar{E}^{Lfo}(\bar{R}) = i\omega\mu_f \iiint_V \bar{\bar{G}}_{e1}^{Lfo}(\bar{R}, \bar{R}') \cdot \bar{J}(\bar{R}')dV', \tag{34}$$

$$\bar{H}^{Lfo}(\bar{R}) = i\omega\epsilon_f \iiint_V \bar{\bar{G}}_{m1}^{Lfo}(\bar{R}, \bar{R}') \cdot \bar{J}(\bar{R}')dV'. \tag{35}$$

These signify the computation of the E- and H-fields in the structure, which states that the superposition of the incident field $\bar{E}_i(\bar{R})$ or $\bar{H}_i(\bar{R})$ and the scattered field $\bar{E}_s(\bar{R})$ or $\bar{H}_s(\bar{R})$ is given by

$$\bar{E}^{Lfo}(\bar{R}) = \bar{E}_i^{00o}(\bar{R})\delta_f^o + \bar{E}_s^{Lfo}(\bar{R}), \tag{36}$$

$$\bar{H}^{Lfo}(\bar{R}) = \bar{H}_i^{00o}(\bar{R})\delta_f^o + \bar{H}_s^{Lfo}(\bar{R}). \tag{37}$$

Concluding Remarks

A theoretical analysis of antenna/layered-head configuration is demonstrated. An improved general multilayered homogeneous lossy dielectric spherical head/antenna model of DGF for numerical Electromagnetic Compatibility (EMC) investigation has been proposed and compared with the models by various authors. The DGFs are obtained by employing the method of scattering superposition. This study enables one to assess the influence of the presence of a close-by biological head upon the operating characteristics of a mobile phone, input impedance, Specific Absorbtion Rate (SAR) values inside the head, the power absorbed, the total radiated power, the thermal emission, the induced current on a scatterer, novel antenna design, the electric and magnetic near or far fields patterns, and other situations.

Furthermore, by defining a symmetry operator, the required memory for efficient numerical computations using the method of moments can be reduced drastically by formulating a new compact general expression. The validity of the general model is verified by the DGF of the specific models, which agrees with other authors' studies. Further work is at hand to find a reduced general formulation for electromagnetic DGF in spherically multilayered media by utilizing the technique presented in this paper. Details of this extension will be given in a forthcoming paper.

References

[1] C. T. Tai, *Dyadic Green Functions in Electromagnetic Theory*, 1st ed. (New York: Scranton Intext Educational Publishers, 1971).

[2] C. T. Tai, *Dyadic Green Functions in Electromagnetic Theory*, 2nd ed. (New York: IEEE Press, 1994).

[3] R. E. Collin, *Field Theory of Guided Waves*, 2nd ed. (New York: IEEE Press, 1991).

[4] Y. Rahmat-Samii, *On the Question of Computation of the Dyadic Green's Functions at the Source Region in Wave-Guides and Cavities. IEEE Trans. Microwave Theory Tech.* MTT-23 (1975): 762–765.

[5] A. D. Yaghjian, "A Direct Approach to the Derivation of Electric Dyadic Green's Functions," in AP-S Int. Symp. Dig. (Univ. Mass.), 1976, 71–73.

[6] A. D. Yaghjian, "Electric Dyadic Green's Functions in the Source Region," *Proc. IEEE* 68, no. 2 (1980): 248–263.

[7] W. W. Hansen, "A New Type of Expansion in Radiation Problems," *Phys. Rev.* 47 (1935): 139–143.

[8] M. Bressan and G. Conciauro, "Singularity Extraction from the Electric Green's Function for a Spherical Resonator," *IEEE Trans. Microwave Theory Tech.* MTT-33, no. 5 (1985): 407–414.

[9] J. A. Kong, *Electromagnetic Wave Theory*, 2nd ed. (New York: Wiley-Interscience Publication, 1990).

[10] S. M. S. Reyhani and R. J. Glover, "Electromagnetic Dyadic Green's Function of an Implantable Medical Device Model for Numerical EMC Investigation," in third IMACS/IEEE International Multiconference on Circuits, Systems, Communications and Computers (CSCC'99), Athens, Greece, 1999: 1311–1314.

[11] S. M. S. Reyhani and R. J. Glover, "Electromagnetic Dyadic Green's Function for a Human Torso Model for Numerical EMC Investigation," in 11th International Conference on EMC (IEE EMC York 99), University of York, UK 1999: 21–25.

[12] J. J. Bowman, T. B. A. Senior, and P. L. E. Uslenghi, *Electromagnetic and Acoustic Scattering by Simple Shapes* (New York: Wiley-Interscience, 1969).

[13] G. P. S. Cavalcante, D. A. Rogers, and A. J. Giardola, "Analysis of Electromagnctic Wave Propagation in Multi-layered Media using Dyadic Green's Functions," *Radio Sci.* 17, no. 3 (1982): 503–508.

[14] L. W. Li, P. S. Kooi, M. S. Leong, and T. S. Yeo, "Electromagnetic Dyadic Green's Function in Spherically Multilayered Media," *IEEE Trans. Microwave Theory Tech.* MTT-42, no. 12 (1994): 2302–2310.

[15] L. W. Li, J. A. Bennett, and P. L. Dyson, "Some Method for Solving the Coefficients of Dyadic Green's Function in Isotropic Stratified Media," *Int. J. Electronics* 70, no. 4 (1991): 803–814.

[16] S. M. S. Reyhani and R. J. Glover, "Exploiting the Symmetry of the Principle Terms in DGF Formulation," technical report. TR-FOTD695, Department of Electrical Engineering, Brunel University, UK 1997.

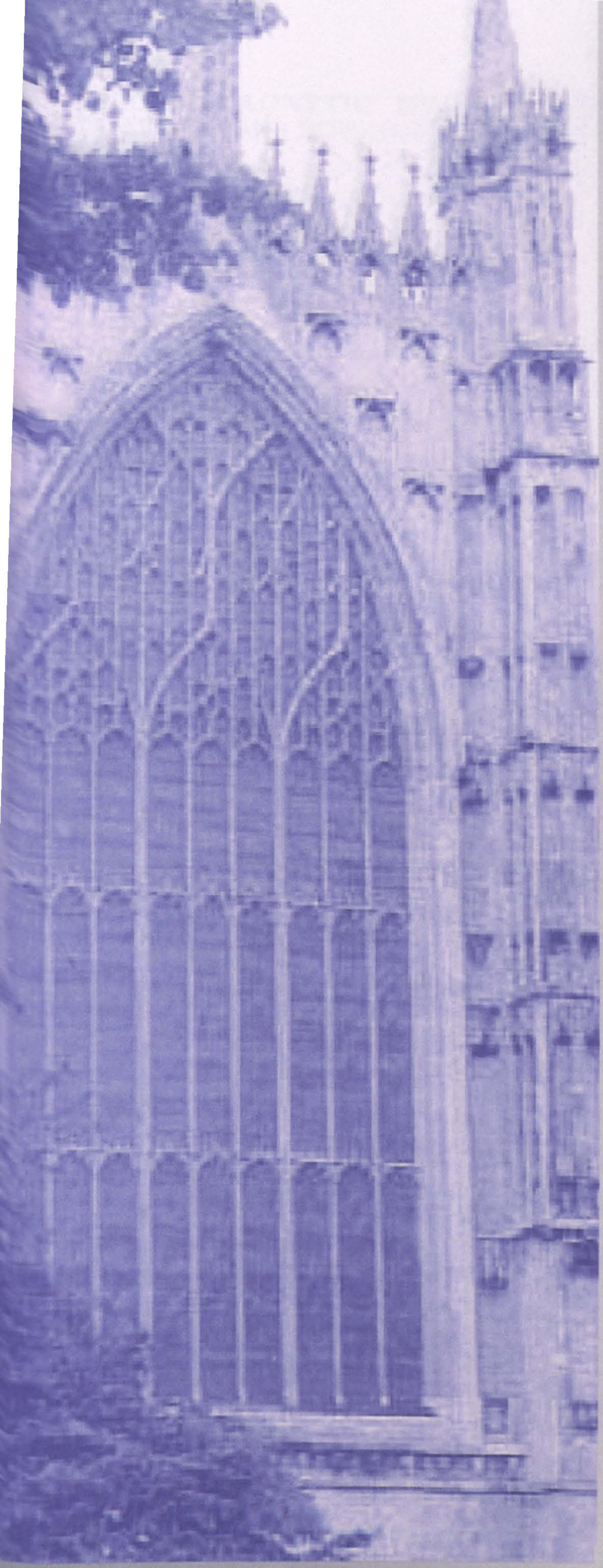

IEE

emc York '99

'Publication Number 464'

York ELECTROMAGNETICS

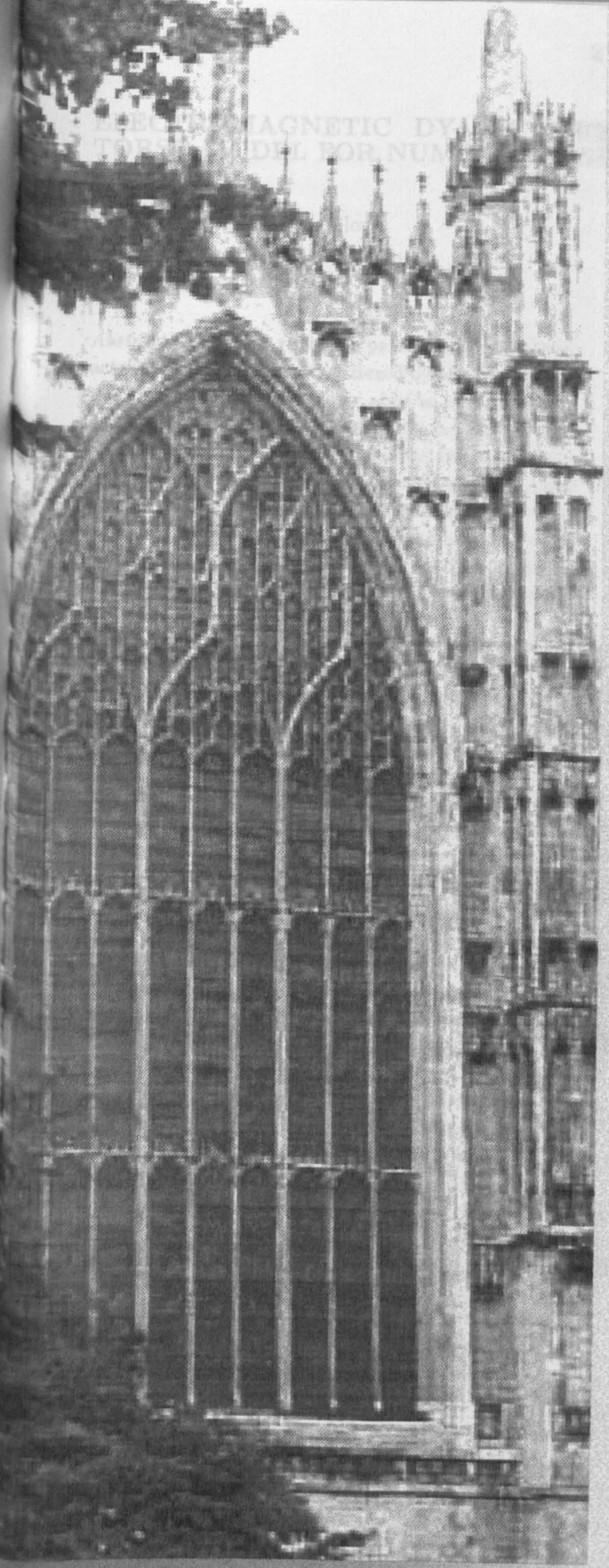

IEE

emc York '99

'Publication Number 464'

York ELECTROMAGNETICS

ELECTROMAGNETIC DYADIC GREEN'S FUNCTION FOR A HUMAN TORSO MODEL FOR NUMERICAL EMC INVESTIGATION

S.M.S. Reyhani and R.J. Glover
Brunel University, United Kingdom

Abstract:—Antenna radiation pattern and other characteristics are significantly altered by the presence of the human body. This paper aims to express a general representation of dyadic Green's function (DGF) for the problem of electromagnetic radiation from a source of excitation in the presence of a human torso model (multi-layered homogeneous lossy dielectric circular cylinder of finite length) as well as any part of the body assuming the shape of a cylinder. The whole structure is assumed to be uniform along the propagation direction.

Keywords:—Electromagnetic, Human Torso, Circular Cylinder, Antenna, Dipole, Dyadic Green's function.

1 INTRODUCTION

Antenna-body interaction is of interest with the use of chest-mounted 418 MHz biotelemetry transmitters for medical applications. Short range telemeters being developed for medical applications increasingly operate at UHF, taking advantage of greater spectrum availability and reduced levels of synthetic noise. Transmitting devices built for the patient-end of the radio link are invariably battery powered so must be lightweight and compact to ensure user comfort. Such physical limitations on packaging mean that even built-in antennas at UHF are electrically small, with correspondingly low efficiencies. Further problems arise as the telemeter is usually worn next to the skin at chest or abdominal level, so the transmitting antenna is in close proximity to the body tissue. Power dissipation in the body and impedance mismatches induced by effects of proximity presents additional system losses, so the risk of signal drop-out in the link is increased. The most important operational parameters for a closed-coupled antenna-body interaction for biotelemetry are its antenna efficiency and radiation pattern in the azimuthal plane.

This paper is organised as follows. The complete set of finite cylindrical vector wave functions are introduced in section 2.

In section 3 we begin to formulate the problem for a finite circular cylinder and in subsection 3.1, we set out with the case, in which we construct the DGF, $\overline{\overline{G}}_{e1}(\overline{R},\overline{R}')$, in terms that constitute the continuous Eigen-function expansion (EFE) in which the Eigen-functions are guided in preferred r and z-coordinate directions, using the procedures described in Tai (1) or Collin (2). This expansion also contains an explicit dyadic delta function term which is required for completeness at the source point. It is considered as a correction to the general solenoidal EFE which is valid outside the source point.

Subsection 3.2, presents the general scattering DGFs expansions (13) in terms of only the solenoidal Eigen-functions. It is in this development that the principal point of this paper is identified.

Magnetic type DGF can be found by invoking duality or once the electric field is obtained the magnetic field is derivable by taking the curl of the electric field, and vice versa.

Conclusions are then presented in section 6 summarising the important points contained in this work and finally a short bibliography is provided for further research.

2 VECTOR WAVE FUNCTION FOR A CIRCULAR CYLINDER OF FINITE LENGTH

The cylindrical vector wave functions are the building blocks of the EFE of various kinds of DGF. They are

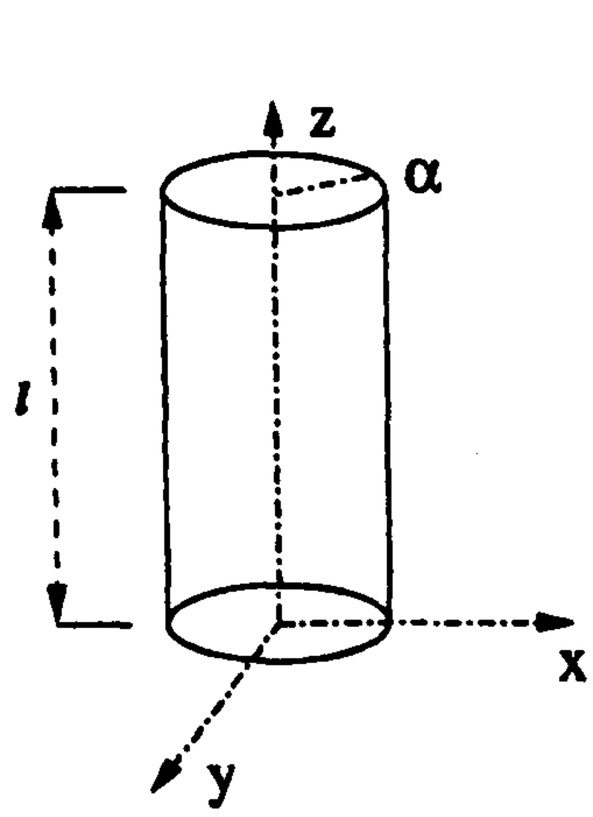

Fig. 1. Diagram of a Finite Cylindrical Human Torso

denoted by $\overline{L}_{\substack{e\\o}n\lambda}$, $\overline{P}_{\substack{e\\o}n\lambda}$ and $\overline{Q}_{\substack{e\\o}n\lambda}$, that are solutions of the homogeneous vector Helmholtz equation. The generating or Eigen-functions, which are solutions of the cylindrical scalar wave equation $\nabla^2\Psi + k_\lambda^2\Psi=0$, with the differential equation in the cylindrical coordinate system

$$\frac{1}{r}\frac{\partial}{\partial r}(r\frac{\partial\Psi}{\partial r}) + \frac{1}{r^2}\frac{\partial^2\Psi}{\partial\phi^2} + \frac{\partial^2\Psi}{\partial\phi^2} + \frac{\partial^2\Psi}{\partial z^2} + K^2\Psi = 0 \tag{1}$$

with K, the separation constant and k_λ being an undetermined wave number. Implementation of the method of separation of variables in this system finally results the generating function in Reyhani (3) in the form

$$\Psi_{\substack{e\\o}n}(h) = j_n(\lambda r)^{\cos}_{\sin} n\phi^{\cos}_{\sin} hz, \tag{2}$$

Here subscripts "e" stands for even and "o" is odd character of the generating functions. $h = \frac{q\pi}{l}$ are the eigenvalues in the z-direction with $q = 0, 1, 2, ...$ and l is the length of cylinder. $j_n(\lambda r)$ identifies the cylindrical Bessel functions of the order n to represent both out-going and in-coming waves. λ is the continuous eigen-value. Cylindrical vector wave functions are akin to the Debye potentials.

$$\overline{L}_{\substack{e\\o}n\lambda}(h) = \nabla\Psi_{\substack{e\\o}n}, \tag{3}$$

$$\overline{P}_{\substack{e\\o}n\lambda}(h) = \nabla\times[\Psi_{\substack{e\\o}n}\hat{z}], \tag{4}$$

$$\overline{Q}_{\substack{e\\o}n\lambda}(h) = \frac{1}{k_\lambda}\nabla\times\nabla\times[\Psi_{\substack{e\\o}n}\hat{z}]. \tag{5}$$

Where $\hat{z}$ is the piloting vector.

The complete expressions for the solenoidal (rotational or transverse) functions are

$$\overline{P}_{\substack{e\\o}n\lambda}(h) = \begin{Bmatrix} \mp\frac{n}{r}j_n(\lambda r)^{\sin}_{\cos} n\phi^{\cos}_{\sin} hz\hat{r} \\ -(\frac{\partial j_n(\lambda r)}{\partial r})^{\cos}_{\sin} n\phi^{\cos}_{\sin} hz\hat{\phi} \\ 0 \end{Bmatrix} \tag{6}$$

$$\overline{Q}_{\substack{e\\o}n\lambda}(h) = \begin{Bmatrix} \mp h[\frac{\partial j_n(\lambda r)}{\partial r}]^{\cos}_{\sin} n\phi^{\sin}_{\cos} hz\hat{r} \\ \frac{hn}{r}[j_n(\lambda r)]^{\sin}_{\cos} n\phi^{\sin}_{\cos} hz\hat{\phi} \\ \lambda^2[j_n(\lambda r)]^{\cos}_{\sin} n\phi^{\cos}_{\sin} hz\hat{z} \end{Bmatrix} \frac{1}{k_\lambda} \tag{7}$$

And the complete expressions for the non-solenoidal (irrotational or lamellar) functions are

$$\overline{L}_{\substack{e\\o}n\lambda}(h) = \begin{Bmatrix} \frac{\partial}{\partial r}[j_n(\lambda r)]^{\cos}_{\sin} n\phi^{\cos}_{\sin} hz\hat{r} \\ \mp\frac{n}{r}[j_n(\lambda r)]^{\sin}_{\cos} n\phi^{\cos}_{\sin} hz\hat{\phi} \\ \mp h[j_n(\lambda r)]^{\cos}_{\sin} n\phi^{\sin}_{\cos} hz\hat{z} \end{Bmatrix} \tag{8}$$

where $k_\lambda^2 = \lambda^2 + h^2$ and in these vector wave functions one should be careful with the sign of the elements in the matrices when cross-multiplying the terms from "e" to "o" and vice-versa e.g. "sin sin" always remains negative while "cos cos" positive. Also "$-$ cos sin" and "$-$ sin cos" in second elements of matrices in $\overline{P}_{\substack{e\\o}}$ and $\overline{P}_{\substack{e\\o}}$ respectively. In $\overline{L}_{\substack{e\\o}}$ and $\overline{L}_{\substack{e\\o}}$ both "cos sin" and "sin cos" are positive in the first element of their respective matrix. For $\overline{Q}_{\substack{e\\o}}$, "$-$ sin cos" in second element of matrix, while "+ cos sin" in the third element. For $\overline{Q}_{\substack{e\\o}}$, "$-$ cos sin" and "+ sin cos" in the elements 2 and 3 respectively. "$\mp$" applies the negative to the top line while positive to the bottom line.

Note that in the set of cylindrical vector wave functions only $\overline{P}_{\substack{e\\o}n\lambda}$ do not possess the z component. The $\hat{r}$, $\hat{\phi}$ and $\hat{z}$ are the cylindrical unit vectors. These functions are defined in the entire space, corresponding to $0 \le r \le \infty$, $0 \le \phi \le 2\pi$ and $0 < z < l$.

The volume integral of the product of the cylindrical vector wave functions is clearly zero if $n \neq n'$ and $h \neq h'$ because of the orthogonal property of the $\cos n\phi$ and $\sin n\phi$ functions and the Fourier integral relation. The derivation of the orthogonal properties of these vector wave functions are very similar to those for infinite circular cylinder discussed by Tai (1) and Collin (2).

3 FORMULATION OF THE PROBLEM

Consider a cylinder (fig. 1) of radius "α" concentric along z-axis with length "l" is illuminated by an electromagnetic wave. An electromagnetic field is induced inside the system and an electromagnetic wave is scattered by the system.

A time dependence $e^{j\omega t}$ is assumed and suppressed throughout.

3.1 DGF for a finite Length Cylinder of Circular Cross-Section

Because the dyadic $\nabla\times[\bar{\bar{I}}\delta_e(\overline{R}-\overline{R}')]$ is solenoidal, it can be expanded in terms of solenoidal vector wave functions; $\overline{P}_{\substack{e\\o}n\lambda}$ and $\overline{Q}_{\substack{e\\o}n\lambda}$ defined previously.

Applying the method of (G_m) and according to the Ohm-Rayleigh procedure, an EFE for the source function $\nabla\times[\bar{\bar{I}}\delta_e(\overline{R}-\overline{R}')]$ using the solenoidal vector wave functions can be

$$\nabla\times[\bar{\bar{I}}\delta_e(\overline{R}-\overline{R}')] = \int_0^\infty d\lambda \int_0^l dh \sum_{n=0}^{\infty} \cdot \begin{bmatrix} \overline{Q}_{\substack{e\\o}n\lambda}(h)\overline{A}_{\substack{e\\o}n\lambda}(h) \\ \overline{P}_{\substack{e\\o}n\lambda}(h)\overline{B}_{\substack{e\\o}n\lambda}(h) \end{bmatrix}, \tag{9}$$

where λ and h are continuous eigen-values and $\overline{A}_{\substack{e\\o}n\lambda}(h)$ and $\overline{B}_{\substack{e\\o}n\lambda}(h)$ are two unknown vector functions to be determined. This is a three-dimensional problem with a dyadic singular function, therefore the

above equation can be treated as the Fourier transform and the Fourier-Bessel transform or the Hankel transform of $\nabla\times[\overline{\overline{I}}\delta_e(\overline{R}-\overline{R}')]$. By taking the anterior scalar product of the above equation with $\overline{Q}_{\substack{\cdot\\ o}}^{\cdot\circ}{}_{n'\lambda'}(h')$ and integrating the resultant equation through the entire space and as a result of the orthogonal relationships and repeating the same routine with the $\overline{P}_{\substack{\cdot\\ o}}^{\cdot\circ}{}_{n'\lambda'}(h')$ we can obtain the EFE, where we have preserved the Fourier integration. The plane of discontinuity for the magnetic DGF is located at $r=r'$. The expression for $(\overline{\overline{G}}_{e1})$ for a finite cylinder of radius "α" concentric with the z-axis can now be written in the form

$$\overline{\overline{G}}_{e1}(\overline{R},\overline{R}') = -\frac{\hat{r}\hat{r}}{k^2}\delta_e(\overline{R}-\overline{R}') + \int_0^l dh \sum_{n=0}^{\infty} C_\lambda \cdot \begin{cases} \left\{ \begin{bmatrix} \overline{P}^{(1)}_{\substack{\cdot\\ o}}{}^{\cdot\circ}{}_{\eta_o}(h;\eta_o)\overline{P}'_{\substack{\cdot\\ o}}{}^{\cdot\circ}{}_{\eta_o}(h;\eta_o) \end{bmatrix} \\ \begin{bmatrix} \overline{Q}^{(1)}_{\substack{\cdot\\ o}}{}^{\cdot\circ}{}_{\eta_o}(h;\eta_o)\overline{Q}'_{\substack{\cdot\\ o}}{}^{\cdot\circ}{}_{\eta_o}(h;\eta_o) \end{bmatrix} \end{cases}, & r>r', \\ \left\{ \begin{bmatrix} \overline{P}_{\substack{\cdot\\ o}}{}^{\cdot\circ}{}_{\eta_o}(h;\eta_o)\overline{P}'^{(1)}_{\substack{\cdot\\ o}}{}^{\cdot\circ}{}_{\eta_o}(h;\eta_o) \end{bmatrix} \\ \begin{bmatrix} \overline{Q}_{\substack{\cdot\\ o}}{}^{\cdot\circ}{}_{\eta_o}(h;\eta_o)\overline{Q}'^{(1)}_{\substack{\cdot\\ o}}{}^{\cdot\circ}{}_{\eta_o}(h;\eta_o) \end{bmatrix} \end{cases}, & r<r'. \end{cases} \tag{10}$$

where

$$C_\lambda = \frac{i(2-\delta_o^n)}{2l\eta_o^2} \tag{11}$$

Coefficient C_λ depends on the value of δ_o^n which is the Kronecker delta functions defined with respect to n, when

$$\delta_o^n = \begin{cases} 1, & \text{if } n=o \\ 0, & \text{if } n\neq o \end{cases} \tag{12}$$

Comparing the DGFs for a finite cylinder developed here with those presented by other authors e.g. Tai (1) for an infinite cylinder, one can notice that they are similar in mathematical form but different in the calculations of Ps and Qs and the limits of integration for a finite cylinder.

3.2 General Expression of Scattering DGFs for an Electric Dipole in the Presence of a Multi-Layered Cylindrical Torso Model

When a biological system is illuminated by an electromagnetic wave, an electromagnetic field is induced inside the system and an electromagnetic wave is scattered externally by the system. Since the biological system is an irregularly shaped heterogeneous imperfectly conducting medium with frequency dependent permittivity and conductivity, the distribution of the internal electromagnetic field and the scattered electromagnetic wave will depend on the body's physiological parameters and geometry, as well as the frequency and polarisation of the incident wave. The mathematical complexity of the problem has led researchers to investigate simple models. In this paper the medium is assumed to be homogeneous, isotropic, linear, non-dispersive and stationary. An efficient formulation of the general scattering DGF for a multilayer cylindrical torso (fig. 2) as:

$$\overline{\overline{G}}_{es}^{Lfo}(\overline{R},\overline{R}') = \int_0^l dh \sum_{n=0}^{\infty} C_\lambda \cdot \begin{cases} \left\{ \begin{bmatrix} (1-\delta_f^L)\begin{bmatrix} A^{Lfo}_{\substack{\cdot\\ o}}{}^{\cdot\circ}{}_{\eta_f}\overline{P}^{(1)}_{\substack{\cdot\\ o}}{}^{\cdot\circ}{}_{\eta_f}(h;\eta_f) \\ B^{Lfo}_{\substack{\cdot\\ o}}{}^{\cdot\circ}{}_{\eta_f}\overline{Q}^{(1)}_{\substack{\cdot\\ o}}{}^{\cdot\circ}{}_{\eta_f}(h;\eta_f) \end{bmatrix} \\ (1-\delta_f^o)\begin{bmatrix} a^{Lfo}_{\substack{\cdot\\ o}}{}^{\cdot\circ}{}_{\eta_f}\overline{P}_{\substack{\cdot\\ o}}{}^{\cdot\circ}{}_{\eta_f}(h;\eta_f) \\ b^{Lfo}_{\substack{\cdot\\ o}}{}^{\cdot\circ}{}_{\eta_f}\overline{Q}_{\substack{\cdot\\ o}}{}^{\cdot\circ}{}_{\eta_f}(h;\eta_f) \end{bmatrix} \end{bmatrix} \overline{P}'^{(1)}_{\substack{\cdot\\ o}}{}^{\cdot\circ}{}_{\eta_o}(h;\eta_o) \\ \begin{bmatrix} (1-\delta_f^L)\begin{bmatrix} C^{Lfo}_{\substack{\cdot\\ o}}{}^{\cdot\circ}{}_{\eta_f}\overline{Q}^{(1)}_{\substack{\cdot\\ o}}{}^{\cdot\circ}{}_{\eta_f}(h;\eta_f) \\ D^{Lfo}_{\substack{\cdot\\ o}}{}^{\cdot\circ}{}_{\eta_f}\overline{P}^{(1)}_{\substack{\cdot\\ o}}{}^{\cdot\circ}{}_{\eta_f}(h;\eta_f) \end{bmatrix} \\ (1-\delta_f^o)\begin{bmatrix} c^{Lfo}_{\substack{\cdot\\ o}}{}^{\cdot\circ}{}_{\eta_f}\overline{Q}_{\substack{\cdot\\ o}}{}^{\cdot\circ}{}_{\eta_f}(h;\eta_f) \\ d^{Lfo}_{\substack{\cdot\\ o}}{}^{\cdot\circ}{}_{\eta_f}\overline{P}_{\substack{\cdot\\ o}}{}^{\cdot\circ}{}_{\eta_f}(h;\eta_f) \end{bmatrix} \end{bmatrix} \overline{Q}'^{(1)}_{\substack{\cdot\\ o}}{}^{\cdot\circ}{}_{\eta_o}(h;\eta_o) \end{cases}. \tag{13}$$

Where $k_f^2=\omega^2(\mu_f\varepsilon_f)$ and $\eta_f^2=(k_f^2-h^2)$.
For the general case, when the current source is located in different layers of the media, one obtains a different expression of DGF.

$$\overline{\overline{G}}_{es}^{Lfoo}(\overline{R},\overline{R}') = \int_0^l dh \sum_{n=0}^{\infty} C_\lambda \cdot \begin{cases} \left\{ \begin{bmatrix} (1-\delta_f^L)\begin{bmatrix} A^{Lfo}_{\substack{\cdot\\ o}}{}^{\cdot\circ}{}_{\eta_f}\overline{P}^{(1)}_{\substack{\cdot\\ o}}{}^{\cdot\circ}{}_{\eta_f}(h;\eta_f) \\ B^{Lfo}_{\substack{\cdot\\ o}}{}^{\cdot\circ}{}_{\eta_f}\overline{Q}^{(1)}_{\substack{\cdot\\ o}}{}^{\cdot\circ}{}_{\eta_f}(h;\eta_f) \end{bmatrix} \\ (1-\delta_f^o)\begin{bmatrix} a^{Lfo}_{\substack{\cdot\\ o}}{}^{\cdot\circ}{}_{\eta_f}\overline{P}_{\substack{\cdot\\ o}}{}^{\cdot\circ}{}_{\eta_f}(h;\eta_f) \\ b^{Lfo}_{\substack{\cdot\\ o}}{}^{\cdot\circ}{}_{\eta_f}\overline{Q}_{\substack{\cdot\\ o}}{}^{\cdot\circ}{}_{\eta_f}(h;\eta_f) \end{bmatrix} \end{bmatrix} \begin{bmatrix} (1-\delta_s^L)\overline{P}'^{(1)}_{\substack{\cdot\\ o}}{}^{\cdot\circ}{}_{\eta_s}(h;\eta_s) \\ (1-\delta_s^o)\overline{P}'_{\substack{\cdot\\ o}}{}^{\cdot\circ}{}_{\eta_s}(h;\eta_s) \end{bmatrix} \\ \begin{bmatrix} (1-\delta_f^L)\begin{bmatrix} C^{Lfo}_{\substack{\cdot\\ o}}{}^{\cdot\circ}{}_{\eta_f}\overline{Q}^{(1)}_{\substack{\cdot\\ o}}{}^{\cdot\circ}{}_{\eta_f}(h;\eta_f) \\ D^{Lfo}_{\substack{\cdot\\ o}}{}^{\cdot\circ}{}_{\eta_f}\overline{P}^{(1)}_{\substack{\cdot\\ o}}{}^{\cdot\circ}{}_{\eta_f}(h;\eta_f) \end{bmatrix} \\ (1-\delta_f^o)\begin{bmatrix} c^{Lfo}_{\substack{\cdot\\ o}}{}^{\cdot\circ}{}_{\eta_f}\overline{Q}_{\substack{\cdot\\ o}}{}^{\cdot\circ}{}_{\eta_f}(h;\eta_f) \\ d^{Lfo}_{\substack{\cdot\\ o}}{}^{\cdot\circ}{}_{\eta_f}\overline{P}_{\substack{\cdot\\ o}}{}^{\cdot\circ}{}_{\eta_f}(h;\eta_f) \end{bmatrix} \end{bmatrix} \begin{bmatrix} (1-\delta_s^L)\overline{Q}'^{(1)}_{\substack{\cdot\\ o}}{}^{\cdot\circ}{}_{\eta_s}(h;\eta_s) \\ (1-\delta_s^o)\overline{Q}'_{\substack{\cdot\\ o}}{}^{\cdot\circ}{}_{\eta_s}(h;\eta_s) \end{bmatrix} \end{cases}. \tag{14}$$

"L" is the symbol for last inner layer in the torso. "f" ($f=0,1,2,.....,L$) is the field point or observer layer.

Superscript/subscript "o" stands for source point at open space. Subscript "s" is scattering, while its superscript represents the layer at which the source is located. δ_f^L and δ_f^o are the Kronecker delta functions, where

$$\delta = \begin{cases} 1, & \text{if } L = o \\ 0, & \text{if } L \neq o \end{cases}. \tag{15}$$

$A_{\bullet\bullet\eta_f}^{Lfo}$, $a_{\bullet\bullet\eta_f}^{Lfo}$, $B_{\bullet\bullet\eta_f}^{Lfo}$, $b_{\bullet\bullet\eta_f}^{Lfo}$, $C_{\bullet\bullet\eta_f}^{Lfo}$, $c_{\bullet\bullet\eta_f}^{Lfo}$, $D_{\bullet\bullet\eta_f}^{Lfo}$ and $d_{\bullet\bullet\eta_f}^{Lfo}$ are the amplitude coefficients of scattered DGF to be determined by applying the boundary condition at the interfaces $r = \alpha_l$ $(l = 1, 2, ..., L)$. These boundary conditions are;

$$\hat{r} \times \overline{\overline{G}}_e^{Lfo} = \hat{r} \times \overline{\overline{G}}_e^{L(f+1)o} \tag{16}$$

and

$$\frac{1}{\mu_f} \hat{r} \times \nabla \times \overline{\overline{G}}_e^{Lfo} = \frac{1}{\mu_{(f+1)}} \hat{r} \times \nabla \times \overline{\overline{G}}_e^{L(f+1)o} \tag{17}$$

All the local reflection coefficients are given by

$$R_{Pf}^{E,H} = \frac{1}{N_\nu} \left(\vartheta_{f+1} \eta_f H_{ff} H'_{f+1,f} - \vartheta_f \eta_{f+1} H_{f+1,f} H'_{ff} \right) \tag{18}$$

$$R_{Ff}^{E,H} = \frac{1}{N_\nu} \left(\vartheta_{f+1} \eta_f j_{ff} j'_{f+1,f} - \vartheta_f \eta_{f+1} j_{f+1,f} j'_{ff} \right) \tag{19}$$

And for the local transmission coefficients,

$$T_{Pf}^{E,H} = \frac{-2i\vartheta_f \eta_{f+1}}{(\pi \eta_f r_f) N_\nu} \tag{20}$$

$$T_{Ff}^{E,H} = \frac{-2i\vartheta_{f+1} \eta_f}{(\pi \eta_{f+1} r_f) N_\nu} \tag{21}$$

Where we have assumed the following abbreviations.

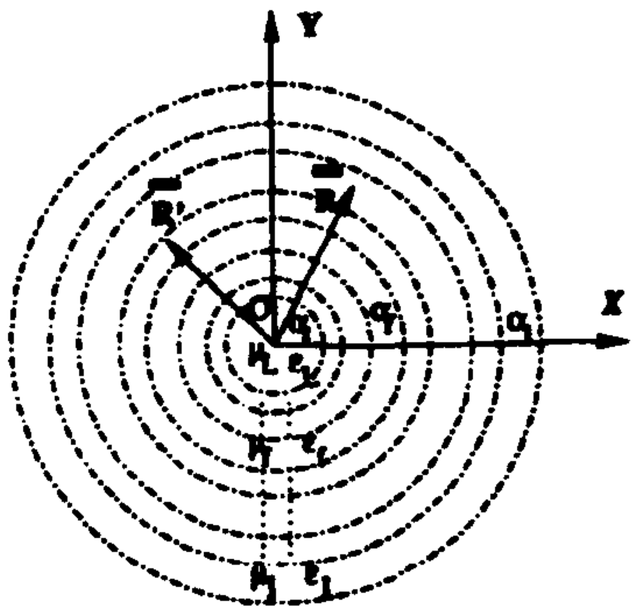

Fig. 2. Cross Section of a Human Torso Model

$$j_n = j_n(\eta_f \alpha_l), \qquad j'_n = j'_n(\eta_f \alpha_l)$$
$$H_n = H_n^{(1)}(\eta_f \alpha_l), \qquad H'_n = H_n^{'(1)}(\eta_f \alpha_l)$$

The superscripts E and H in the above equations denote TM and TE waves, whereas the subscripts P and F define the centripetal and centrifugal reflection or transmission respectively. Here

$$N_\nu = \vartheta_{f+1} \eta_f H_{f+1,f} j'_{ff} - \vartheta_f \eta_{f+1} j_{ff} H'_{f+1,f} \tag{22}$$

Besides ϑ represents ϵ or μ in the E (TM) or H (TE) mode representations respectively. In the above, the Wronskian of the cylindrical Hankel functions is

$$\frac{2i}{\pi x} = j_{ff} H'_{f+1,f} - H_{f+1,f} j'_{ff}. \tag{23}$$

If the source is located outside the cylindrical body for axial symmetry $n = 0$, the scattering DGF is given by

i) For the case of two layered media the coefficients are

$$A_{\bullet\bullet\eta_\nu}^{10o} = R_{F1}^H, \qquad C_{\bullet\bullet\eta_\nu}^{10o} = R_{F1}^E$$
$$a_{\bullet\bullet\eta_1}^{10o} = T_{F1}^H, \qquad c_{\bullet\bullet\eta_1}^{10o} = T_{F1}^E$$

Where $R_{F1}^{E,H}$ and $T_{F1}^{E,H}$ can be obtained from (19) and (21) by letting $f = 1$.

ii) For the case of three layered media the coefficients are

$$c_{\bullet\bullet\eta_2}^{22o} = \frac{T_{P2}^E T_{P1}^E}{1 - R_{F1}^E R_{P2}^E}, \qquad c_{\bullet\bullet\eta_1}^{21o} = \frac{T_{P2}^E}{(1 - R_{F1}^E R_{P2}^E)^2}$$
$$a_{\bullet\bullet\eta_2}^{22o} = \frac{T_{P2}^H T_{P1}^H}{1 - R_{F1}^H R_{P2}^H}, \qquad a_{\bullet\bullet\eta_1}^{21o} = \frac{T_{P2}^H}{(1 - R_{F1}^H R_{P2}^H)^2}$$
$$C_{\bullet\bullet\eta_1}^{21o} = \frac{R_{F1}^E T_{P2}^E}{(1 - R_{F1}^E R_{P2}^E)^2}, \qquad C_{\bullet\bullet\eta_\nu}^{20o} = R_{F2}^E + \frac{R_{F1}^E T_{F2}^E T_{P2}^E}{1 - R_{F1}^E R_{P2}^E}$$
$$A_{\bullet\bullet\eta_1}^{21o} = \frac{R_{F1}^H T_{P2}^H}{(1 - R_{F1}^H R_{P2}^H)^2}, \qquad A_{\bullet\bullet\eta_\nu}^{20o} = R_{F2}^H + \frac{R_{F1}^H T_{F2}^H T_{P2}^H}{1 - R_{F1}^H R_{P2}^H}$$

Where $R_{F1}^{E,H}$, $R_{P2}^{E,H}$ and $T_{F2}^{E,H}$, $T_{P1}^{E,H}$ and $T_{P2}^{E,H}$ can be obtained from (18) to (21) by letting $f = 1$.

The results for these specific cases agree with those given by other authors Xiang and Lu (4), showing the validity of our DGF representation.

We can obtain the total DGF by applying the principle of scattering superposition,

$$\overline{\overline{G}}_{E1}(\overline{R}, \overline{R}') = \overline{\overline{G}}_{e1}(\overline{R}, \overline{R}') + \overline{\overline{G}}_{es}^{Lfo}(\overline{R}, \overline{R}') \tag{24}$$

4 MAGNETIC DGF IN THE ANTENNA-TORSO CONFIGURATION

The principle of duality states that once the electric DGF is obtained, the magnetic DGF is derivable by interchanging the field functions $\overline{P}_{\bullet\bullet} \rightarrow k\overline{Q}_{\bullet\bullet}$ and $\overline{Q}_{\bullet\bullet} \rightarrow k\overline{P}_{\bullet\bullet}$ and omitting the singularity term contribution and vice versa.

On the other hand the corresponding total magnetic DGF at any point in the system can be calculated

from $\nabla\times\overline{\overline{G}}_e = \overline{\overline{G}}_m$, bearing in mind the discontinuous nature of magnetic DGF across a point source at $R = R'$ and the Ampere-Maxwell equation relating $\overline{\overline{G}}_e$ and $\overline{\overline{G}}_m$ in the dyadic form i.e.: $\nabla\times\overline{\overline{G}}_m = \overline{\overline{I}}\delta(\overline{R}-\overline{R}') + k^2\overline{\overline{G}}_e$.

5 ELECTRIC AND MAGNETIC FIELD AT ANY POINT IN THE CONFIGURATION

The use of DGF technique allows us to determine the expansion of the electric and magnetic fields in a body (cylinder)/antenna configuration in a direct and elegant manner.

For any current source with current density function $\overline{J}(\overline{R}')$ located outside the body, the electric or magnetic field radiated by such a dipole can be evaluated using the formulae,

$$\overline{E}^{Lfo}(\overline{R}) = i\omega\mu_f \iiint_V \overline{\overline{G}}_{E1}^{Lfo}(\overline{R},\overline{R}')\cdot\overline{J}(\overline{R}')dV' \qquad (25)$$

$$\overline{H}^{Lfo}(\overline{R}) = i\omega\epsilon_f \iiint_V \overline{\overline{G}}_{M1}^{Lfo}(\overline{R},\overline{R}')\cdot\overline{J}(\overline{R}')dV'. \qquad (26)$$

6 CONCLUDING REMARKS

We have derived general electromagnetic representations for a human torso model (in simple form for the multi-layered homogeneous lossy dielectric circular cylinder of finite length) in order to evaluate deterioration of the antennas performance and obtain the rates of RF energy deposition (SAR). The representations may be used to optimise antenna design, ascertain potential health hazards, and compliance with standards legislation. The DGFs are obtained by employing the EFE and the method of scattering superposition.

The results of this paper could be useful for a further analysis of the problem of an implant such as heart pace-maker embedded in the body and biotelemetry transmitters for medical applications and could easily be expanded so as to handle any scatterer having finite radius and length. They can also be applied to problems of optical fibers and waveguides for the investigation of inhomogeneities or obstacles inside them or by considering the cylinder as an excitation or scatterer.

REFERENCES

1. Tai C. T., Second Edition, 1994, "Dyadic Green Functions in Electromagnetic Theory", IEEE Press, series on Electromagnetic waves, New York.

2. Collin R. E., Second Edition, 1991, "Field Theory of Guided Waves", IEEE Press, New York.

3. Reyhani S. M. S and Glover R. J., 4-8 July 1999, "Electromagnetic Dyadic Green's Function of an Implantable Medical Device Model for Numerical EMC Investigation", to be presented at 3rd IMACS/IEEE International Multiconference on: Circuits, Systems, Communications and Computers (CSCC'99) (IMACS/IEEE CSCC'99), Athens, Greece.

4. Xiang Z and Lu Y, April 1996, "Electromagnetic Dyadic Green's Function in Cylindrically Multilayered Media", IEEE Trans. Microwave Theory Tech, Vol.MTT-44, no.4, pp. 614-621.

Recent Advances in Signal Processing and Communications

Dedicated to the Father of Fuzzy Logic: LOTFI A. ZADEH

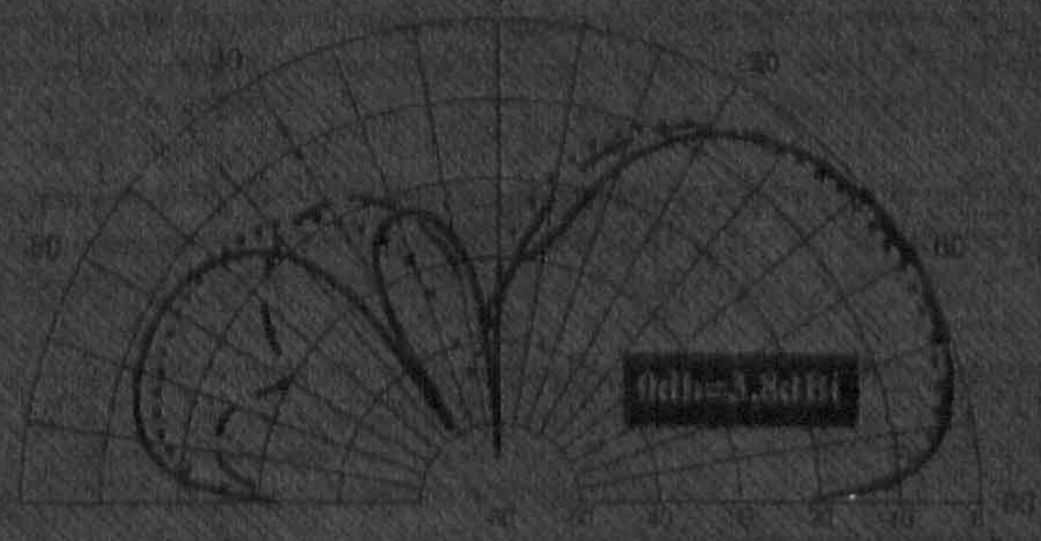

Nikos E. Mastorakis
(Editor)

WSEAS Press
Engineering Society

224

Electromagnetic Dyadic Green's Function of an Implantable Medical Device Model for Numerical EMC Investigation

S.M.S. REYHANI AND R.J. GLOVER
FDTD Research Group
Dept. of Elect. & Electronic Eng.,
Brunel University,
Uxbridge, Middlesex, UB8 3PH.
UNITED KINGDOM.
E-mail: Sayed.Salehi-Reyhani@brunel.ac.uk

Abstract: - Modern wireless telecommunication devices (GSM Mobile system) can interfere with implantable medical devices/prostheses and cause possible malfunction. Also the performance of an antenna is significantly altered by the presence of conducting medical devices/prostheses. The principle objective of this paper is to outline a general expression of dyadic Green's function (DGF) for the problem of electromagnetic radiation from a source of excitation in the presence of a finite length of perfectly conducting circular cylinder of any size as well as of resonant length, which is valid everywhere, including the source region. The whole structure is assumed to be uniform along the propagation direction. The DGFs are obtained by employing the method of scattering superposition.

Key-Words: - Electromagnetic, Circular Cylinder, Implants, Antenna, Dipole, Dyadic Green's function.

1 Introduction

Although electromagnetic scattering by a finite cylinder is a well known cannonical problem, published work does not include the effects of arbitrary placed source point. The derivations presented here are motivated by the need to understand the behaviour of antennas near to or embedded in living tissue. The Eigen-function expansion (EFE) of DGFs in electromagnetic theory provide a systematic means of constructing and interpreting these dyadics. The pioneering work by Tai [1] has set the stage for most of what has been achieved over the last two and a half decades. The expansion of DGFs in terms of the Hansen [2] vector wave functions must be carried out carefully in order to ensure that one is dealing with a complete expansion.

This paper is organized as follows. The complete set of cylindrical vector wave functions are introduced in section 2. This material is included here in order to explicitly define notation and to call attention to a few points in connection with these expansions.

In section 3 we begin to formulate the problem for a finite circular cylinder and in subsection 3.1, we set out with the case, in which we construct the DGF, $\overline{\overline{G}}_{e1}(\overline{R},\overline{R}')$, in terms that constitute the continuous Eigen-function expansion (EFE) in which the Eigen-functions are guided in preferred r and z-coordinate directions, using the procedures described in Tai [3] or Collin [4]. This expansion also contains an explicit dyadic delta function term which is required for completeness at the source point. It is considered as a correction to the general solenoidal EFE which is valid outside the source point.

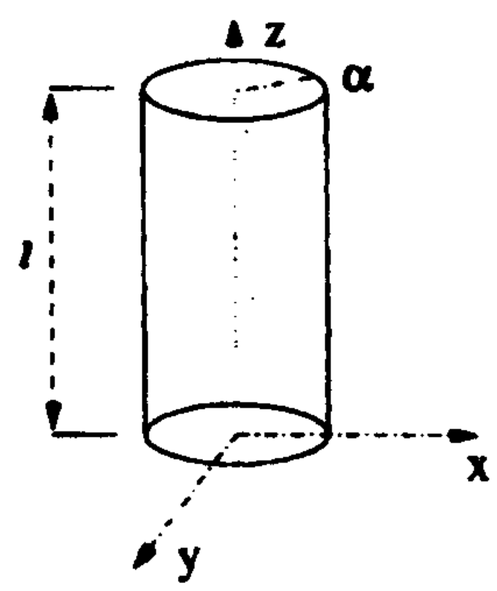

Fig. 1. Diagram of a Finite Circular Cylinder

The procedure required to derive the complete EFE of the scattering DGF for the finite circular cylinder, in terms of only the solenoidal Eigen-functions is shown to be a simple and straight-forward general expression and is summarized in section 4. The DGF for a finite conducting cylinder, $\overline{\overline{G}}_{g1}(\overline{R},\overline{R}')$ can be constructed from the principle of the superpo-

sition, where it satisfies the boundary conditions.

Magnetic type DGF discussed in section 5, can be found by invoking duality or once the electric field is obtained the magnetic field is derivable by taking the curl of the electric field, and vice versa.

Conclusions are then presented in section 7 summarizing the important points contained in this work and finally a short bibliography is provided for further research.

2 Vector Wave Functions for a Circular Cylinder of Finite Length

The cylindrical vector wave functions are the building blocks of the EFE of various kinds of DGF. They are denoted by $\overline{L}_{\substack{e\\o}n\lambda}$, $\overline{P}_{\substack{e\\o}n\lambda}$ and $\overline{Q}_{\substack{e\\o}n\lambda}$, that are solutions of the homogeneous vector Helmholtz equation. The generating or Eigen-functions, which are solutions of the cylindrical scalar wave equation $\nabla^2\Psi + k_\lambda^2\Psi=0$, with the differential equation in the cylindrical coordinate system

$$\frac{1}{r}\frac{\partial}{\partial r}(r\frac{\partial\Psi}{\partial r}) + \frac{1}{r^2}\frac{\partial^2\Psi}{\partial\phi^2} + \frac{\partial^2\Psi}{\partial\phi^2} + \frac{\partial^2\Psi}{\partial z^2} + K^2\Psi = 0 \tag{1}$$

with K, the separation constant and k_λ being an undetermined wave number. Implementation of the method of separation of variables in this system finally results the generating function [5] in the form

$$\Psi_{\substack{e\\o}n}(h) = j_n(\lambda r)^{\cos}_{\sin} n\phi^{\cos}_{\sin} hz, \tag{2}$$

Here subscripts "e" stands for even and "o" is odd character of the generating functions. $h = \frac{q\pi}{l}$ are the eigenvalues in the z-direction with $q = 0, 1, 2, ...$ and l is the length of cylinder. $j_n(\lambda r)$ identifies the cylindrical Bessel functions of the order n to represent both out-going and in-coming waves. λ is the continuous eigen-value. Cylindrical vector wave functions are akin to the Debye potentials.

$$\overline{L}_{\substack{e\\o}n\lambda}(h) = \nabla\Psi_{\substack{e\\o}n}, \tag{3}$$

$$\overline{P}_{\substack{e\\o}n\lambda}(h) = \nabla\times[\Psi_{\substack{e\\o}n}\hat{z}], \tag{4}$$

$$\overline{Q}_{\substack{e\\o}n\lambda}(h) = \frac{1}{k_\lambda}\nabla\times\nabla\times[\Psi_{\substack{e\\o}n}\hat{z}]. \tag{5}$$

Where $\hat{z}$ is the piloting vector.

The complete expressions for the solenoidal (rotational or transverse) functions are

$$\overline{P}_{\substack{e\\o}n\lambda}(h) = \left\{\begin{array}{c} \mp\frac{n}{r}j_n(\lambda r)^{\sin}_{\cos} n\phi^{\cos}_{\sin} hz\hat{r} \\ -(\frac{\partial j_n(\lambda r)}{\partial r})^{\cos}_{\sin} n\phi^{\cos}_{\sin} hz\hat{\phi} \\ 0 \end{array}\right\} \tag{6}$$

$$\overline{Q}_{\substack{e\\o}n\lambda}(h) = \left\{\begin{array}{c} \mp h[\frac{\partial j_n(\lambda r)}{\partial r}]^{\cos}_{\sin} n\phi^{\sin}_{\cos} hz\hat{r} \\ \frac{hn}{r}[j_n(\lambda r)]^{\sin}_{\cos} n\phi^{\sin}_{\cos} hz\hat{\phi} \\ \lambda^2[j_n(\lambda r)]^{\cos}_{\sin} n\phi^{\cos}_{\sin} hz\hat{z} \end{array}\right\} \frac{1}{k_\lambda} \tag{7}$$

And the complete expressions for the non-solenoidal (irrotational or lamellar) functions are

$$L_{\substack{e\\o}n\lambda}(h) = \left\{\begin{array}{c} \frac{\partial}{\partial r}[j_n(\lambda r)]^{\cos}_{\sin} n\phi^{\cos}_{\sin} hz\hat{r} \\ \mp\frac{n}{r}[j_n(\lambda r)]^{\sin}_{\cos} n\phi^{\cos}_{\sin} hz\hat{\phi} \\ \mp h[j_n(\lambda r)]^{\cos}_{\sin} n\phi^{\sin}_{\cos} hz\hat{z} \end{array}\right\} \tag{8}$$

where $k_\lambda^2 = \lambda^2 + h^2$ and in these vector wave functions one should be careful with the sign of the elements in the matrices when cross-multiplying the terms from "e" to "o" and vice-versa e.g. "sin sin" always remains negative while "cos cos" positive. Also "$-$ cos sin" and "$-$ sin cos" in second elements of matrices in $\overline{P}_{e_{\cdot\cdot}}$ and $\overline{P}_{o_{\cdot\cdot}}$ respectively. In $\overline{L}_{e_{\cdot\cdot}}$ and $\overline{L}_{o_{\cdot\cdot}}$ both "cos sin" and "sin cos" are positive in the first element of their respective matrix. For $\overline{Q}_{e_{\cdot\cdot}}$, "$-$ sin cos" in second element of matrix, while "$+$ cos sin" in the third element. For $\overline{Q}_{o_{\cdot\cdot}}$, "$-$ cos sin" and "$+$ sin cos" in the elements 2 and 3 respectively. "$\mp$" applies the negative to the top line while positive to the bottom line.

Note that in the set of cylindrical vector wave functions only $\overline{P}_{\substack{e\\o}n\lambda}$ do not possess the z component. The $\hat{r}$, $\hat{\phi}$ and $\hat{z}$ are the cylindrical unit vectors. These functions are defined in the entire space, corresponding to $0 \leq r \leq \infty$, $0 \leq \phi \leq 2\pi$ and $0 < z < l$.

The volume integral of the product of the cylindrical vector wave functions is clearly zero if $n \neq n'$ and $h \neq h'$ because of the orthogonal property of the $\cos n\phi$ and $\sin n\phi$ functions and the Fourier integral relation. The derivation of the orthogonal properties of these vector wave functions are very similar to those for infinite circular cylinder discussed by Tai [3] and Collin [4].

3 Formulation of the Problem

Consider a cylinder (fig. 1) of radius "α" concentric along z-axis with length "l" is illuminated by an electromagnetic wave. An electromagnetic field is induced in the system and an electromagnetic wave is scattered by the system.

A time dependence $e^{j\omega t}$ is assumed and suppressed throughout.

3.1 DGF for a finite Length Cylinder of Circular Cross-Section

Because the dyadic $\nabla\times[\bar{\bar{I}}\delta(\overline{R}-\overline{R}')]$ is solenoidal, it can be expanded in terms of solenoidal vector wave functions; $\overline{P}_{\substack{e\\o}mn\lambda}$ and $\overline{Q}_{\substack{e\\o}mn\lambda}$ defined previously.

Applying the method of (G_m) and according to the Ohm-Rayleigh procedure, an EFE for the source function $\nabla\times[\bar{\bar{I}}\delta(\overline{R}-\overline{R}')]$ using the solenoidal vector wave functions can be

$$\nabla\times[\bar{\bar{I}}\delta(\overline{R}-\overline{R}')]=\int_0^\infty d\lambda\int_0^t dh\sum_{n=0}^{\infty}\cdot\begin{bmatrix}\overline{Q}_{\substack{e\\o}n\lambda}(h)\overline{A}_{\substack{e\\o}n\lambda}(h)\\ \overline{P}_{\substack{e\\o}n\lambda}(h)\overline{B}_{\substack{e\\o}n\lambda}(h)\end{bmatrix}, \tag{9}$$

where λ and h are continuous eigen-values and $\overline{A}_{\substack{e\\o}n\lambda}(h)$ and $\overline{B}_{\substack{e\\o}n\lambda}(h)$ are two unknown vector functions to be determined. This is a three-dimensional problem with a dyadic singular function, therefore the above equation can be treated as the Fourier transform and the Fourier-Bessel transform or the Hankel transform of $\nabla\times[\bar{\bar{I}}\delta(\overline{R}-\overline{R}')]$. By taking the anterior scalar product of the above equation with $\overline{Q}_{\substack{e\\o}n'\lambda'}(h')$ and integrating the resultant equation through the entire space and as a result of the orthogonal relationships and repeating the same routine with the $\overline{P}_{\substack{e\\o}n'\lambda'}(h')$ we can obtain the EFE, where we have preserved the Fourier integration. The plane of discontinuity for the magnetic DGF is located at $r=r'$. The expression for ($\bar{\bar{G}}_{e1}$) for a finite cylinder of radius "α" concentric with the z-axis can now be written in the form

$$\bar{\bar{G}}_{e1}(\overline{R},\overline{R}')=-\frac{\hat{r}\hat{r}}{k^2}\delta(\overline{R}-\overline{R}')+\int_0^t dh\sum_{n=0}^{\infty}C_\lambda\cdot\begin{cases}\left\{\begin{matrix}[\overline{P}^{(1)}_{\substack{e\\o}n_\eta}(h;\eta_r)\overline{P}'_{\substack{e\\o}n_\eta}(h;\eta_r)]\\ [\overline{Q}^{(1)}_{\substack{e\\o}n_\eta}(h;\eta_r)\overline{Q}'_{\substack{e\\o}n_\eta}(h;\eta_r)]\end{matrix}\right\}, & r>r',\\ \left\{\begin{matrix}[\overline{P}_{\substack{e\\o}n_\eta}(h;\eta_r)\overline{P}'^{(1)}_{\substack{e\\o}n_\eta}(h;\eta_r)]\\ [\overline{Q}_{\substack{e\\o}n_\eta}(h;\eta_r)\overline{Q}'^{(1)}_{\substack{e\\o}n_\eta}(h;\eta_r)]\end{matrix}\right\}, & r<r'.\end{cases} \tag{10}$$

where

$$C_\lambda=\frac{i(2-\delta_o^n)}{2l\eta_r^2} \tag{11}$$

Coefficient C_λ depends on the value of δ_o^n which is the Kronecker delta functions defined with respect to n, when

$$\delta_o^n=\begin{cases}1, & \text{if } n=o\\ 0, & \text{if } n\neq o\end{cases} \tag{12}$$

Here $\hat{r}\hat{r}$ is a dyad (dyadic product of the unit vectors) and $\delta(\overline{R}-\overline{R}')$ is weighted Dirac delta function in three dimensions. This is included explicitly as a correction to the general solenoidal EFE which is valid outside the source point. The dyadic delta function term at the source point in cylindrical coordinates

$$\delta(\overline{R}-\overline{R}')=\frac{1}{r'}\delta(\overline{r}-\overline{r}')\delta(\overline{\phi}-\overline{\phi}')\delta(\overline{z}-\overline{z}') \tag{13}$$

Comparing the DGFs for a finite cylinder developed here with those presented by other authors e.g. Tai [3] for an infinite cylinder, one can notice that they are similar in mathematical form but different in the calculations of Ps and Qs and the limits of integration for a finite cylinder.

4 Scattering DGF for a Finite Conducting Cylinder of Circular Cross-Section

When a perfectly conducting cylinder of the same size as above is illuminated by an electromagnetic wave, the scattered terms can be written in the form

$$\bar{\bar{G}}_{es}(\overline{R},\overline{R}')=\int_0^t dh\sum_{n=0}^{\infty}C_\lambda\cdot\begin{bmatrix}\alpha_{\substack{e\\o}n_\eta}\overline{P}^{(1)}_{\substack{e\\o}n_\eta}(h;\eta)\overline{P}'^{(1)}_{\substack{e\\o}n_\eta}(h;\eta)\\ \beta_{\substack{e\\o}n_\eta}\overline{Q}^{(1)}_{\substack{e\\o}n_\eta}(h;\eta)\overline{Q}'^{(1)}_{\substack{e\\o}n_\eta}(h;\eta)\end{bmatrix}. \tag{14}$$

Applying the principle of scattering superposition, we obtain

$$\bar{\bar{G}}_{Es}(\overline{R},\overline{R}')=\bar{\bar{G}}_{e1}(\overline{R},\overline{R}')+\bar{\bar{G}}_{es}(\overline{R},\overline{R}') \tag{15}$$

Where we consider the function for a finite circular cylinder in a region $0\leq r\leq\infty$. After applying the boundary condition one can determine the unknown coefficients. In order to satisfy the boundary condition at interface $r=\alpha$,

$$\hat{r}\times\left[\overline{P}_{\substack{e\\o}n_\eta}(h;\eta)\overline{P}'^{(1)}_{\substack{e\\o}n_\eta}(h;\eta)+\alpha_{\substack{e\\o}n_\eta}\overline{P}^{(1)}_{\substack{e\\o}n_\eta}(h;\eta)\overline{P}'^{(1)}_{\substack{e\\o}n_\eta}(h;\eta)\right]_{r=\alpha} \tag{16}$$

$$\hat{r}\times\left[\overline{Q}_{\substack{e\\o}n_\eta}(h;\eta)\overline{Q}'^{(1)}_{\substack{e\\o}n_\eta}(h;\eta)+\beta_{\substack{e\\o}n_\eta}\overline{Q}^{(1)}_{\substack{e\\o}n_\eta}(h;\eta)\overline{Q}'^{(1)}_{\substack{e\\o}n_\eta}(h;\eta)\right]_{r=\alpha} \tag{17}$$

$$\hat{r}\times\left[\overline{P}_{\substack{e\\o}n_\eta}(h;\eta)+\alpha_{\substack{e\\o}n_\eta}\overline{P}^{(1)}_{\substack{e\\o}n_\eta}(h;\eta)\right]_{r=\alpha}=0 \tag{18}$$

$$\hat{r}\times\left[\overline{Q}_{\substack{e\\o}n_\eta}(h;\eta)+\beta_{\substack{e\\o}n_\eta}\overline{Q}^{(1)}_{\substack{e\\o}n_\eta}(h;\eta)\right]_{r=\alpha}=0 \tag{19}$$

substituting for $\overline{P}_{\substack{e\\o}n_\eta}(h;\eta)$ and $\overline{P}^{(1)}_{\substack{e\\o}n_\eta}(h;\eta)$

$$\overline{P}_{\substack{e\\o}n_\eta}(h;\eta)=\nabla\times[j_n(\eta r)^{\cos}_{\sin}n\phi\sin hz\hat{z}], \tag{20}$$

$$\overline{P}^{(1)}_{\substack{e\\o}n_\eta}(h;\eta)=\nabla\times[H^{(1)}_n(\eta r)^{\cos}_{\sin}n\phi\sin hz\hat{z}], \tag{21}$$

in equation (18) produces $\alpha_{\bullet\bullet\eta} = -\frac{[\partial j_n(\eta a)]/\partial(\eta a)}{[\partial H_n^{(1)}(\eta a)]/\partial(\eta a)}$.

Similarly inserting for $\overline{Q}_{\bullet\bullet\eta}(h;\eta)$ and $\overline{Q}^{(1)}_{\bullet\bullet\eta}(h;\eta)$

$$\overline{Q}_{\bullet\bullet\eta}(h;\eta) = \frac{1}{k}\nabla\times\nabla\times[j_n(\eta r)^{\cos}_{\sin} n\phi \cos hz\hat{z}], \qquad (22)$$

$$\overline{Q}^{(1)}_{\bullet\bullet\eta}(h;\eta) = \frac{1}{k}\nabla\times\nabla\times[H_n^{(1)}(\eta r)^{\cos}_{\sin} n\phi \cos hz\hat{z}], \qquad (23)$$

in equation (19) produces $\beta_{\bullet\bullet\eta} = -\frac{[j_n(\eta a)]}{[H_n^{(1)}(\eta a)]}$.

5 Magnetic DGF in the Antenna-Prosthesis Configuration

The principle of duality states that once the electric DGF is obtained, the magnetic DGF is derivable by interchanging the field functions $\overline{P}_{\bullet\bullet} \rightarrow k\overline{Q}_{\bullet\bullet}$ and $\overline{Q}_{\bullet\bullet} \rightarrow k\overline{P}_{\bullet\bullet}$ and omitting the singularity term contribution and vice versa.

On the other hand the corresponding total magnetic DGF at any point in the system can be calculated from $\nabla\times\overline{\overline{G}}_e = \overline{\overline{G}}_m$, bearing in mind the discontinuous nature of magnetic DGF across a point source at $R = R'$ and the Ampere-Maxwell equation relating $\overline{\overline{G}}_e$ and $\overline{\overline{G}}_m$ in the dyadic form i.e.: $\nabla\times\overline{\overline{G}}_m = \overline{\overline{I}}\delta(\overline{R}-\overline{R}') + k^2\overline{\overline{G}}_e$.

6 Electric and Magnetic Field at any Point in the Configuration

The use of DGF technique allows us to determine the expansion of the electric and magnetic fields in a cylinder/antenna configuration in a direct and elegant manner.

For any current source with current density function $\overline{J}(\overline{R}')$ located outside the cylinder, the electric or magnetic field radiated by such a dipole can be calculated using the formulae,

$$\overline{E}(\overline{R}) = i\omega\mu_o\iiint_V \overline{\overline{G}}_{E1}(\overline{R},\overline{R}')\cdot\overline{J}(\overline{R}')dV' \qquad (24)$$

$$\overline{H}(\overline{R}) = i\omega\varepsilon_o\iiint_V \overline{\overline{G}}_{M1}(\overline{R},\overline{R}')\cdot\overline{J}(\overline{R}')dV'. \qquad (25)$$

These signify the computation of the E and H-fields in the structure, which states the superposition of the incident field $\overline{E}_i(\overline{R})$ or $\overline{H}_i(\overline{R})$ and the scattered field $\overline{E}_s(\overline{R})$ or $\overline{H}_s(\overline{R})$ is given by

$$\overline{E}(\overline{R}) = \overline{E}_i(\overline{R}) + \overline{E}_s(\overline{R}) \qquad (26)$$

$$\overline{H}(\overline{R}) = \overline{H}_i(\overline{R}) + \overline{H}_s(\overline{R}). \qquad (27)$$

7 Concluding Remarks

General expressions have been derived in simple form for the finite conducting circular cylinder (medical devices/prostheses) of any size as well as of very small radius (resonant length). The DGFs are obtained by employing the EFE and the method of scattering superposition.

The results of this paper could be useful for a further analysis of the problem as a thin wire or an implant such as heart pace-maker embedded in the body and biotelemetry transmitters for medical applications and could easily be expanded so as to handle any scatterer having finite radius and length.

They can also be applied to problems of optical fibers and waveguides for the investigation of inhomogeneities or obstacles inside them or by considering the cylinder as an excitation or scatterer. They can also be of use in the study and design of antennas of high frequency.

The usefulness of the present technique obviously requires comparison with numerical and experimental results. it is envisaged that a later publication will address this aspect of the problem in more detail.

References:

[1] C. T. Tai, *Dyadic Green Functions in Electromagnetic Theory*, Scranton, Intext Educational Publishers, New York, First Edition, 1971.

[2] W. W. Hansen, A New Type of Expansion in Radiation Problems, *Phys. review*, Vol. 47, 1935, pp. 139-143.

[3] C. T. Tai, *Dyadic Green Functions in Electromagnetic Theory*, IEEE Press, series on Electromagnetic waves, New York, Second Edition, 1994.

[4] R. E. Collin,*Field Theory of Guided Waves*, IEEE Press, New York, Second Edition, 1991.

[5] S. M. S. Reyhani and R. J. Glover, Electromagnetic Dyadic Green's Function for a Human Torso Model for Numerical EMC Investigation, to be presented at *11th International Conference on EMC (IEE EMC York 99)* University of York, UK: 12-13 July 1999.

Electromagnetic Modeling of Implantable Medical Devices Using Cylindrical DGFs

S.M.S. REYHANI AND R.J. GLOVER
FDTD Research Group
Dept. of Elect. & Electronic Eng.,
Brunel University,
Uxbridge, Middlesex, UB8 3PH.
UNITED KINGDOM.
E-mail: Sayed.Salehi-Reyhani@brunel.ac.uk

Abstract

GSM (global system for mobile communication) and PCS's (personal communication services) can interfere with implantable medical devices/prostheses particularly for systems using TDMA (time-division multiple access) and cause possible malfunction. Also the performance of an antenna is significantly altered by the presence of conducting medical devices/prostheses. The objective of this paper is to outline a general expression of dyadic Green's function (DGF) for the problem of electromagnetic radiation from a source of excitation in the presence of a finite length "l" of perfectly conducting thin circular cylinder of radius "a" concentric along z-axis of any size as well as of resonant length, which is valid everywhere, including the source region. The whole structure is assumed to be uniform along the propagation direction. The advantage of the proposed analysis is its simplicity and efficiency in computation.

Key-Words: - Electromagnetic, Circular Cylinder, Implants, Antenna, Dipole, Dyadic Green's function.

1. Introduction

Although electromagnetic scattering by a finite cylinder is a well known canonical problem, published work does not include the effects of arbitrary placed source point. The derivations presented here are motivated by the need to understand the behaviour of antennas near to or embedded in living tissue. Interaction of electromagnetic fields (EMF) with living systems and public concern regarding their allegedly/possible harmful health effects have been of current research interest. These investigations are motivated by two relating factors:

i) a need to evaluate the specific absorption rate (SAR) (the rate of RF energy deposition) in the user's body, in order to evaluate potential health effects and compliance with standards, and;

ii) the antenna performance in the proximity of the user's body and to develop better antenna designs whose performance is less affected by the biological systems and produce lower SAR.

Several theoretical studies have analysed these models in Reyhani [1,2,3]. This paper is organised as follows. The complete set of cylindrical vector wave functions are introduced in section 2. In section 3, we construct the DGF, $\overline{\overline{G}}^{\infty}_{e1}(\overline{R},\overline{R}')$, in terms that constitute the continuous Eigen-function expansion (EFE) in which the Eigen-functions are guided in preferred r and z-coordinate directions, using the procedures described in Tai [4] or Collin [5]. The procedure required to derive the complete EFE of the general scattering DGF for the infinite circular cylinder, in terms of only the solenoidal Eigen-functions is shown to be a simple and straight-forward general expression and is summarised in section 4. The DGF for a semi-infinite cylinder, $\overline{\overline{G}}^{s\infty}_{E1}(\overline{R},\overline{R}')$ is then constructed from the principle of the superposition, where it satisfies the boundary conditions. Section 5, presents the final construction of the DGFs expansions. It is in this development that the principal point of this paper is identified.

Conclusions are then presented in section 8. summarising the important points contained in this work.

2. Cylindrical Vector Wave Functions

The vector wave functions are the building blocks of the EFE of various kinds of DGF. They are solutions of the homogeneous vector Helmholtz equation. The generating functions, which are solutions of the cylindrical scalar wave equation $\nabla^2\Psi + k_\lambda^2\Psi=0$, can be written in the form $\Psi_{\substack{e\\o}n}(h) = j_n(\lambda r)^{\cos}_{\sin} n\phi e^{ihz}$. k_λ is an unde-

termined wave number and subscripts "e" stands for even and "o" is odd character of the generating functions. Where $j_n(\lambda r)$ identifies the cylindrical Bessel functions of the order n to represent both out-going and in-coming waves. λ is the continuous eigen-value. Cylindrical vector wave functions are akin to the Debye potentials. $\overline{P}_{o^e_o n\lambda}(h) = \nabla\times[\Psi_{e^o_o n}\hat{z}]$ and $\overline{Q}_{e^o_o n\lambda}(h) = \frac{1}{k_\lambda}\nabla\times\nabla\times[\Psi_{e^o_o n}\hat{z}]$. Where $\hat{z}$ is the piloting vector. These functions are defined in the entire space, corresponding to $0 \le r \le a$, $0 \le \phi \le 2\pi$ and $-\infty < z < \infty$.

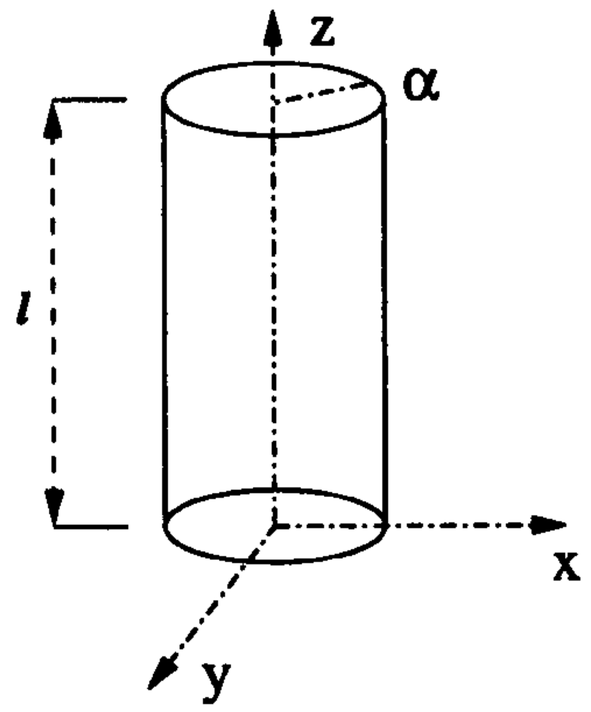

Fig. 1. Diagram of a Finite Circular Cylinder

The orthogonal properties of these vector wave functions have been discussed by Tai [4] and Collin [5].

3. DGF for an Infinite Length Cylinder of Circular Cross-Section

Because the dyadic source function $\nabla \times [\overline{\overline{I}}\delta(\overline{R} - \overline{R}')]$ is solenoidal, it can be expanded in terms of solenoidal vector wave functions $\overline{P}_{e^o_o n\lambda}$ and $\overline{Q}_{e^o_o n\lambda}$. Applying the method of (G_m) and according to the Ohm-Rayleigh procedure, an EFE for the source function

$$\nabla \times [\overline{\overline{I}}\delta(\overline{R} - \overline{R}')] = \int_0^a d\lambda \int_{-\infty}^{\infty} dh \sum_{n=0}^{\infty} \cdot \begin{bmatrix} \overline{Q}_{e^o_o n\lambda}(h)\overline{A}_{e^o_o n\lambda}(h) \\ \overline{P}_{e^o_o n\lambda}(h)\overline{B}_{e^o_o n\lambda}(h) \end{bmatrix}, \quad (1)$$

where λ and h are continuous eigen-values and $\overline{A}_{e^o_o n\lambda}(h)$ and $\overline{B}_{e^o_o n\lambda}(h)$ are two unknown vector functions to be determined. This is a three-dimensional problem with a dyadic singular function, therefore the electric DGF for infinite conducting cylinder can be written as

$$\overline{\overline{G}}^{\infty}_{e1}(\overline{R},\overline{R}') = -\frac{\hat{z}\hat{z}}{k^2}\delta(\overline{R}-\overline{R}') + \int_0^a d\lambda \sum_{n=0}^{\infty} C_\lambda \cdot \begin{bmatrix} \overline{P}_{e^o_o n\lambda}(\pm h_1)\overline{P}'_{e^o_o n\lambda}(\mp h_1) \\ \overline{Q}_{e^o_o n\lambda}(\pm h_1)\overline{Q}'_{e^o_o n\lambda}(\mp h_1) \end{bmatrix}, \quad z \gtrless z', \quad (2)$$

$C_\lambda = \frac{i(2-\delta_o^n)}{4\pi\lambda^2 I_\lambda h_1}$ depends on the value of δ_o^n which are the Kronecker delta functions defined with respect to n and I_λ is the normalisation factor. Poles of integrand are $h = \pm(k^2 - \lambda^2)^{\frac{1}{2}} = \pm h_1$.

4. DGF for a Semi-Infinite Length Cylinder of Circular Cross-Section

The scattered terms for cylinder of infinite length is

$$\overline{\overline{G}}_{es}(\overline{R},\overline{R}') = \int_0^a d\lambda \sum_{n=0}^{\infty} C_\lambda \begin{bmatrix} \alpha_{e^o_o n\lambda}\overline{P}_{e^o_o n\lambda}(h_1)\overline{P}'_{e^o_o n\lambda}(h_1) \\ \beta_{e^o_o n\lambda}\overline{Q}_{e^o_o n\lambda}(h_1)\overline{Q}'_{e^o_o n\lambda}(h_1) \end{bmatrix}. \quad (3)$$

Applying the principle of scattering superposition,

$$\overline{\overline{G}}^{s\infty}_{E1}(\overline{R},\overline{R}') = \overline{\overline{G}}^{\infty}_{e1}(\overline{R},\overline{R}') + \overline{\overline{G}}_{es}(\overline{R},\overline{R}') \quad (4)$$

Where we consider the function for a semi-infinite circular cylinder in region $0 \le z < \infty$. After applying the boundary condition at interface $z = 0$ one can determine the unknown coefficients.

$$\hat{z} \times [\overline{P}_{e^o_o n\lambda}(-h_1) + \alpha_{e^o_o n\lambda}\overline{P}_{e^o_o n\lambda}(h_1)]_{z=0} = 0 \quad (5)$$

$$\hat{z} \times [\overline{Q}_{e^o_o n\lambda}(-h_1) + \beta_{e^o_o n\lambda}\overline{Q}_{e^o_o n\lambda}(h_1)]_{z=0} = 0 \quad (6)$$

Equations (5) and (6) produce $\alpha_{e^o_o n\lambda} = -1$ and $\beta_{e^o_o n\lambda} = 1$ respectively. Furthermore, if we introduce vector wave functions

$$\overline{P}_{e^o_o n\lambda o}(z) = \nabla\times[j_n(\lambda r)^{\cos}_{\sin} n\phi \sin h_1 z\hat{z}], \quad (7)$$

$$\overline{Q}_{e^o_o n\lambda e}(z) = \frac{1}{k}\nabla\times\nabla\times[j_n(\lambda r)^{\cos}_{\sin} n\phi \cos h_1 z\hat{z}]. \quad (8)$$

then the expression for electric DGF for semi-infinite cylinder (4) can be written in the following compact form:

$$\overline{\overline{G}}^{s\infty}_{E1}(\overline{R},\overline{R}') = -\frac{\hat{z}\hat{z}}{k^2}\delta(\overline{R}-\overline{R}') + \int_0^a d\lambda \sum_{n=0}^{\infty}(-2i)C_\lambda \cdot \begin{Bmatrix} \begin{bmatrix} \overline{P}_{e^o_o n\lambda}(h_1)\overline{P}'_{e^o_o n\lambda o}(z') \\ i\overline{Q}_{e^o_o n\lambda}(h_1)\overline{Q}'_{e^o_o n\lambda e}(z') \end{bmatrix} \\ \begin{bmatrix} \overline{P}_{e^o_o n\lambda o}(z)\overline{P}'_{e^o_o n\lambda}(h_1) \\ i\overline{Q}_{e^o_o n\lambda e}(z)\overline{Q}'_{e^o_o n\lambda}(h_1) \end{bmatrix} \end{Bmatrix} z \gtrless z'. \quad (9)$$

5. DGF for a Finite Length Cylinder of Circular Cross-Section

The electric DGF for a finite cylinder (fig. 1) can now be derived with the aid of equation (9) in the form

$$\overline{\overline{G}}^{FL}_{E1}(\overline{R},\overline{R}') = \overline{\overline{G}}^{s\infty}_{E1}(\overline{R},\overline{R}') + \overline{\overline{G}}^{s\infty}_{E1_s}(\overline{R},\overline{R}') \quad (10)$$

The scattered representation $\overline{\overline{G}}^{s\infty}_{E1_s}$ can be assumed

$$\overline{\overline{G}}^{s\infty}_{E1_s}(\overline{R},\overline{R}') = \int_0^a d\lambda \sum_{n=0}^{\infty} -2iC_\lambda \begin{bmatrix} A^{e}_{o}{}_{n\lambda o}\overline{P}^{e}_{o}{}_{n\lambda o}(z)\overline{P}'^{e}_{o}{}_{n\lambda o}(z') \\ B^{e}_{o}{}_{n\lambda e}\overline{Q}^{e}_{o}{}_{n\lambda e}(z)\overline{Q}'^{e}_{o}{}_{n\lambda e}(z') \end{bmatrix}, \quad (11)$$

The boundary condition must also be fulfilled at $z = l$. This yield $A^{e}_{o}{}_{n\lambda o} = -\frac{e^{ih_1 l}}{\sin h_1 l}$ and $B^{e}_{o}{}_{n\lambda e} = -\frac{ie^{ih_1 l}}{\sin h_1 l}$. Substituting into (11) and using (10) with the aid of new vector wave functions, we finally obtain the following representation for

$$\overline{\overline{G}}^{FL}_{E1}(\overline{R},\overline{R}') = -\frac{\hat{z}\hat{z}}{k^2}\delta(\overline{R}-\overline{R}') + \int_0^a d\lambda \sum_{n=0}^{\infty} \frac{2C_\lambda}{i\sin h_1 l} \cdot \begin{cases} \begin{Bmatrix} \overline{P}^{e}_{o}{}_{n\lambda o}(l-z)\overline{P}'^{e}_{o}{}_{n\lambda o}(z') \\ -\overline{Q}^{e}_{o}{}_{n\lambda e}(l-z)\overline{Q}'^{e}_{o}{}_{n\lambda o}(z') \end{Bmatrix}, & z > z', \\ \begin{Bmatrix} \overline{P}^{e}_{o}{}_{n\lambda o}(z)\overline{P}'^{e}_{o}{}_{n\lambda o}(l-z') \\ -\overline{Q}^{e}_{o}{}_{n\lambda o}(z)\overline{Q}'^{e}_{o}{}_{n\lambda o}(l-z') \end{Bmatrix}, & z < z'. \end{cases} \quad (12)$$

6. Magnetic DGF in the Antenna-Prosthesis Configuration

The principle of duality states that once the electric DGF is obtained, the magnetic DGF is derivable by interchanging the field functions $\overline{P}^{e}_{o} \to k\overline{Q}^{e}_{o}$ and $\overline{Q}^{e}_{o} \to k\overline{P}^{e}_{o}$ and omitting the singularity term contribution and vice versa.

On the other hand the corresponding total magnetic DGF at any point in the system can be calculated from $\nabla\times\overline{\overline{G}}_e = \overline{\overline{G}}_m$, bearing in mind the discontinuous nature of magnetic DGF across a point source at $R = R'$ and the Ampere-Maxwell equation relating $\overline{\overline{G}}_e$ and $\overline{\overline{G}}_m$ in the dyadic form i.e.: $\nabla\times\overline{\overline{G}}_m = \overline{\overline{I}}\delta_e(\overline{R}-\overline{R}') + k^2\overline{\overline{G}}_e$.

7. Electric and Magnetic Field at any Point in the Configuration

The use of DGF technique allows us to determine the expansion of the electric and magnetic fields in a cylinder/antenna configuration in a direct and elegant manner.

For any current source with current density function $\overline{J}(\overline{R}')$ located outside the cylinder, the electric or magnetic field radiated by such a dipole can be calculated using the formulae,

$$\overline{E}(\overline{R}) = i\omega\mu_o \iiint_V \overline{\overline{G}}^{FL}_{E1}(\overline{R},\overline{R}')\cdot\overline{J}(\overline{R}')dV' \quad (13)$$

$$\overline{H}(\overline{R}) = i\omega\varepsilon_o \iiint_V \overline{\overline{G}}^{FL}_{M1}(\overline{R},\overline{R}')\cdot\overline{J}(\overline{R}')dV'. \quad (14)$$

These signify the computation of the E and H-fields in the structure, which states the superposition of the incident field $\overline{E}_i(\overline{R})$ or $\overline{H}_i(\overline{R})$ and the scattered field $\overline{E}_s(\overline{R})$ or $\overline{H}_s(\overline{R})$ is given by

$$\overline{E}(\overline{R}) = \overline{E}_i(\overline{R}) + \overline{E}_s(\overline{R}) \quad (15)$$

$$\overline{H}(\overline{R}) = \overline{H}_i(\overline{R}) + \overline{H}_s(\overline{R}). \quad (16)$$

8. Concluding Remarks

General expressions have been derived in simple form for the finite conducting circular cylinder (medical devices/prostheses) of any size as well as of very small radius (resonant length). The DGFs are obtained by employing the EFE and the method of scattering superposition. The advantage of the proposed analysis is its simplicity and efficiency in computation.

The results of this paper could be useful for a further analysis of the problem as a thin wire or an implant such as heart pace-maker embedded in the body and biotelemetry transmitters for medical applications and could easily be expanded so as to handle any scatterer having finite radius and length.

They can also be applied to problems of optical fibers and waveguides for the investigation of inhomogeneities or obstacles inside them or by considering the cylinder as an excitation or scatterer. They can also be of use in the study and design of antennas of high frequency whose performance is less affected by the biological systems and produce lower SAR.

The usefulness of the present technique obviously requires comparison with numerical and experimental results. it is envisaged that a later

publication will address this aspect of the problem in more detail.

References

[1] S. M. S. Reyhani and R. J. Glover, "Electromagnetic Dyadic Green's Function of an Implantable Medical Device Model for Numerical EMC Investigation", to be presented at 3rd IMACS/IEEE International Multiconference on: Circuits, Systems, Communications and Computers (CSCC'99) (IMACS/IEEE CSCC'99), Athens, Greece 4-8 July 1999.

[2] S. M. S. Reyhani and R. J. Glover, "Electromagnetic Dyadic Green's *Function for* a Human Torso Model for Numerical EMC Investigation", to be presented at *11th International Conference on EMC (IEE EMC York 99)* University of York, UK: 12-13 July 1999.

[3] S. M. S. Reyhani and R. J. Glover, "Electromagnetic Dyadic Green's Function for a Multilayered Homogeneous Lossy Dielectric Spherical Head Model for Numerical EMC Investigation", to be published in Journal of Electromagnetics 1999.

[4] C. T. Tai, "*Dyadic Green Functions in Electromagnetic Theory*", IEEE Press, series on Electromagnetic waves, New York, Second Edition, 1994.

[5] R. E. Collin, "*Field Theory of Guided Waves*", IEEE Press, New York, Second Edition, 1991.

Abstract # 1566

INSULATED IMPLANTABLE MEDICAL DEVICE MODEL USING ELECTROMAGNETIC DYADIC GREEN'S FUNCTION

S.M.S. Reyhani, R.J. Glover

FDTD Research Group
Dept. Of Electronic & Computer Eng.,, Kingston Lane, 301F, Howell Building,
Uxbridge, Middlesex, UB8 3PH, UNITED KINGDOM
Email: sayed.salehi-reyhani@brunel.ac.uk

Abstract:

Modern wireless telecommunication devices (GSM Mobile system) can interfere with implantable medical devices/prostheses and cause possible malfunction. Also the performance of an antenna is significantly altered by the presence of these conducting medical devices/prostheses. Although electromagnetic scattering by a finite cylinder is a well known canonical problem, published work does not include the effects of arbitrary placed source point. The derivations presented here are motivated by the need to understand the behaviour of insulated antennas near to or embedded in living tissue. Dielectric-coated medical devices are preferable over bare ones for use in a human body. The reason is that the often undesirable contact (hyperthermic/localised heating effect) between the prostheses and the surrounding tissue is avoided and, more importantly, the radiat ion efficiency of the antenna can be improved by insulating all or part of the medical devices surface.

The principle objective of this paper is to outline a general expression of dyadic Green's function (DGF) for the problem of electromagnetic radiation from a source of excitation in the presence of a finite length of insulated perfectly conducting circular cylinder of any size as well as of resonant length, which is valid everywhere, including the source region. The whole structure is assumed to be uniform along the propagation direction. The DGFs are obtained by employing the method of scattering superposition. The advantage of the proposed analysis is its simplicity and efficiency in computation.

The results of this paper could be useful for a further analysis of the problem as a thin insulated wire or a dielectric-coated implant such as heart pace-maker embedded in the body and biotelemetry transmitters for medical applications and could easily be expanded so as to handle any scatterer having finite radiu s and length.

They can be applied to problems of optical fibers and waveguides for the investigation of inhomogeneities or obstacles inside them or by considering the cylinder as an excitation or scatterer. They can also be of use in the study and design of antennas of high frequency whose performance is less affected by the biological systems and produce lower SAR.

References:

[1] C. T. Tai, "Dyadic Green Functions in Electromagnetic Theory", IEEE Press, series on Electromagnetic waves, New York, Second Edition, 1994.

[2] S. M. S. Reyhani and R. J. Glover, "Electromagnetic Dyadic Green's Function of an Implantable Medical Device Model for Numerical EMC Investigation", In "Recent Advances in Signal Processing and Communications", Edited by Nikos E. Mastorakis. World Scientific and Engineering Society Press, pp. 224-227, July 1999. ISBN:960-8052-03-3.
A[3] S. M. S. Reyhani and R. J. Glover, "Electromagnetic Dyadic Green's Function for a Human Torso Model for Numerical EMC Investigation", proceedings of the 11th International Conference on EMC (IEE EMC York 99) University of York, UK: pp. 21-25, 12-13 July 1999.

Author's presentation preference: Oral

Author's suggested 1st topic: A26: Medical applications and biological effects
Author's suggested 2nd topic: A26: Medical applications and biological effects

Top of the abstract

INSULATED IMPLANTABLE MEDICAL DEVICE MODEL USING ELECTROMAGNETIC DYADIC GREEN'S FUNCTION

S.M.S. Reyhani and R.J. Glover

FDTD Research Group
Dept. of Electronic & Computer Eng.,
Brunel University,
Uxbridge, Middlesex, UB8 3PH.
UNITED KINGDOM.
E-mail : Sayed.Salehi-Reyhani@brunel.ac.uk

Abstract

Modern wireless telecommunication devices (GSM Mobile system and PCS's) can interfere with implantable medical devices/prostheses and cause possible malfunction. Also the performance of an antenna is significantly altered by the presence of these conducting medical devices/prostheses. Dielectric-coated medical devices are preferable over bare ones for use in a human body. The reason is that the often undesirable contact (hyperthermic/heating effect) between the prostheses and the surrounding tissue is avoided and, more importantly, the radiation efficiency of the antenna can be improved by insulating all or part of the medical devices surface. The principle objective of this paper is to outline a general expression of dyadic Green's function (DGF) for the problem of electromagnetic radiation from a source of excitation in the presence of a finite length of insulated perfectly conducting circular cylinder of any size as well as of resonant length, which is valid everywhere, including the source region. The whole structure is assumed to be uniform along the propagation direction. The DGFs are obtained by employing the method of scattering superposition. The advantage of the proposed analysis is its simplicity and efficiency in computation.

1. INTRODUCTION

Although electromagnetic scattering by a finite cylinder is a well known canonical problem, published work does not include the effects of arbitrary placed source point. The derivations presented here are motivated by the need to understand the behaviour of antennas near to or embedded in living tissue. Dielectric-coated medical devices are preferable over bare ones for use in a human body. The reason is that the often undesirable contact (hyperthermic/localised heating effect) between the prostheses and the surrounding tissue is avoided and, more importantly, the radiation efficiency of the antenna can be improved by insulating all or part of the medical devices surface. The Eigen-function expansion (EFE) of DGFs in electromagnetic theory provide a systematic means of constructing and interpreting these dyadics. The pioneering work by Tai [1] has set the stage for most of what has been achieved over the last two and a half decades. The expansion of DGFs in terms of the Hansen [2] vector wave functions must be carried out carefully in order to ensure that one is dealing with a complete expansion. This paper is organized as follows. The complete set of cylindrical vector wave functions are introduced in section 2.

In section 3 we begin to formulate the problem for a finite circular cylinder and in subsection 3.1, we set out with the case, in which we construct the DGF, $\overline{\overline{G}}_{e1}(\overline{R},\overline{R}')$, in terms that constitute the continuous Eigen-function expansion (EFE) in which the Eigen-functions are guided in preferred r and z-coordinate directions, using the procedures described in Tai [1] or Collin [3]. This expansion also contains an explicit dyadic delta function term which is required for completeness at the source point. It is considered as a correction to the general solenoidal EFE which is valid outside the source point.

Subsection 3.2, presents the general scattering DGFs expansions (3) in terms of only the solenoidal Eigen-functions. It is in this development that the principal point of this paper is identified. Magnetic type DGF discussed in section 4, can be found by invoking duality or once the electric field is obtained the magnetic field is derivable by taking the curl of the electric field, and vice versa.

Conclusions are then presented in section 6 summarizing the important points contained in this work and

finally a short bibliography is provided for further research.

2. VECTOR WAVE FUNCTIONS FOR A CIRCULAR CYLINDER OF FINITE LENGTH

The cylindrical vector wave functions are the building blocks of the EFE of various kinds of DGFs. They are solutions of the homogeneous vector Helmholtz equation. The generating or Eigen-functions, which are solutions of the cylindrical scalar wave equation $\nabla^2\Psi + k_\lambda^2\Psi=0$ can be written [4] in the form

$$\Psi_{\substack{e\\o}\substack{e\\o}n}(h) = j_n(\lambda r)^{\cos}_{\sin} n\phi^{\cos}_{\sin} hz, \tag{1}$$

Here subscripts "e" stands for even and "o" is odd character of the generating functions. $h = \frac{q\pi}{l}$ are the eigenvalues in the z-direction with $q = 0, 1, 2, ...$ and l is the length of cylinder. $j_n(\lambda r)$ identifies the cylindrical Bessel functions of the order n to represent both out-going and in-coming waves. λ is the continuous eigen-value. Cylindrical vector wave functions are akin to the Debye potentials. $\overline{P}_{\substack{e\\o}\substack{e\\o}n\lambda}(h) = \nabla\times[\Psi_{\substack{e\\o}\substack{e\\o}n}\hat{z}]$ and $\overline{Q}_{\substack{e\\o}\substack{e\\o}n\lambda}(h) = \frac{1}{k_\lambda}\nabla\times\nabla\times[\Psi_{\substack{e\\o}\substack{e\\o}n}\hat{z}]$. Where $\hat{z}$ is the piloting vector and here $k_\lambda^2 = \lambda^2 + h^2$.

The complete expressions for the solenoidal (rotational or transverse) and the nonsolenoidal (irrotational or lamellar) functions are given in Reyhani [5]. These functions are defined in the entire space, corresponding to $0 \leq r \leq \infty$, $0 \leq \phi \leq 2\pi$ and $0 < z < l$.

3. FORMULATION OF THE PROBLEM

When a conducting cylinder coated by a layer of dielectric of the same length as in (fig. 1) is illuminated by an electromagnetic wave, the scattered functions for a source in open space region "0", corresponding to the exterior region of the coated implant will be denoted by $\overline{\overline{G}}_{E1}^{L0o}$ and for interior region is $\overline{\overline{G}}_{E1}^{L1o}$. Region "1" is within the layer ($\alpha \leq r \leq \beta$) for a conducting implant of radius α with thickness of the layer equal to $t = \beta - \alpha$. The function $\overline{\overline{G}}_{E1}^{L1o}$ must satisfy the Dirichlet boundary condition at $r = \alpha$, the interface of the conducting implant. A time dependence $e^{j\omega t}$ is assumed and suppressed throughout.

3.1 DGF for a Finite Length Cylinder of Circular Cross-Section

Applying the method of (G_m) and according to the Ohm-Rayleigh procedure the expression for ($\overline{\overline{G}}_{e1}$) for a finite cylinder of radius "α" concentric with the z-axis is given in Reyhani [5] in the form

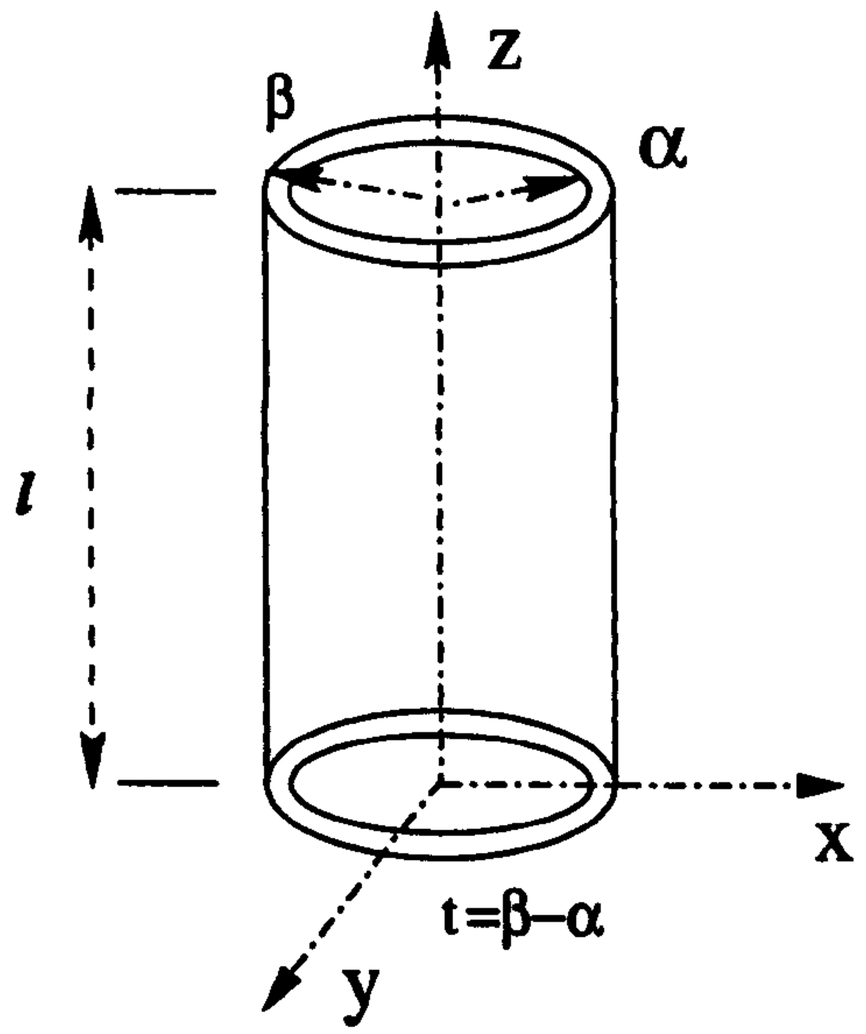

Figure 1. Diagram of a Finite Insulated Circular Cylinder

$$\overline{\overline{G}}_{e1}(\overline{R},\overline{R}') = -\frac{\hat{r}\hat{r}}{k^2}\delta_e(\overline{R}-\overline{R}') + \int_0^l dh \sum_{n=0}^{\infty} C_\lambda \cdot \begin{cases} \left\{ \begin{matrix} [\overline{P}^{(1)}_{\substack{e\\o}\eta_b}(h;\eta_b)\overline{P}'_{\substack{e\\o}\eta_b}(h;\eta_b)] \\ [\overline{Q}^{(1)}_{\substack{e\\e}\eta_b}(h;\eta_b)\overline{Q}'_{\substack{e\\o}\eta_b}(h;\eta_b)] \end{matrix} \right\}, & r > r', \\ \left\{ \begin{matrix} [\overline{P}_{\substack{e\\o}\eta_b}(h;\eta_b)\overline{P}'^{(1)}_{\substack{e\\o}\eta_b}(h;\eta_b)] \\ [\overline{Q}_{\substack{e\\e}\eta_b}(h;\eta_b)\overline{Q}'^{(1)}_{\substack{e\\o}\eta_b}(h;\eta_b)] \end{matrix} \right\}, & r < r'. \end{cases} \tag{2}$$

where coefficient $C_\lambda = \frac{i(2-\delta_o^n)}{2l\eta_o^2}$.

3.2 General Expression of Scattering DGFs for an Electric Dipole in the Presence of a Dielectrically Multi-Layered Coated Implant Model

For a dielectric cylinder, an incident TE mode will excite both a scattered TE and a scattered TM mode. The Scattered DGF term for the exterior and the interior of a dielectrically multi-layered insulated cylindrical implant in this case has the form

$$\overline{\overline{G}}^{Lfo}_{es}(\overline{R},\overline{R}') = \int_0^l dh \sum_{n=0}^{\infty} C_\lambda \cdot \left\{ \begin{Bmatrix} \begin{bmatrix} A^{Lfo}_{\substack{e\\o}\eta_f}\overline{P}^{(1)}_{\substack{e\\o}\eta_f}(h;\eta_f) \\ B^{Lfo}_{\substack{o\\e}\eta_f}\overline{Q}^{(1)}_{\substack{o\\e}\eta_f}(h;\eta_f) \end{bmatrix} \\ (1-\delta_f^o)\begin{bmatrix} a^{Lfo}_{\substack{e\\o}\eta_f}\overline{P}_{\substack{e\\o}\eta_f}(h;\eta_f) \\ b^{Lfo}_{\substack{o\\e}\eta_f}\overline{Q}_{\substack{o\\e}\eta_f}(h;\eta_f) \end{bmatrix} \end{Bmatrix} \overline{P}'^{(1)}_{\substack{e\\o}\eta_b}(h;\eta_b) \right. \\ \left. + \begin{Bmatrix} \begin{bmatrix} C^{Lfo}_{\substack{e\\o}\eta_f}\overline{Q}^{(1)}_{\substack{e\\o}\eta_f}(h;\eta_f) \\ D^{Lfo}_{\substack{o\\e}\eta_f}\overline{P}^{(1)}_{\substack{o\\e}\eta_f}(h;\eta_f) \end{bmatrix} \\ (1-\delta_f^o)\begin{bmatrix} c^{Lfo}_{\substack{e\\o}\eta_f}\overline{Q}_{\substack{e\\o}\eta_f}(h;\eta_f) \\ d^{Lfo}_{\substack{o\\e}\eta_f}\overline{P}_{\substack{o\\e}\eta_f}(h;\eta_f) \end{bmatrix} \end{Bmatrix} \overline{Q}'^{(1)}_{\substack{e\\o}\eta_b}(h;\eta_b) \right\}. \tag{3}$$

Where $k_f^2 = \omega^2(\mu_f\varepsilon_f)$ and $\eta_f^2 = (k_f^2 - h^2)$. "L" is the symbol for last inner layer in the implant model. "f" ($f = 0, 1, 2, ..., L$) is the field point or observer layer. Superscript/subscript "o" stands for source point at open space. Subscript "s" is scattering, while its superscript represents the layer at which the source is located. δ_f^o is the Kronecker delta function, where

$$\delta_f^o = \begin{cases} 1, & \text{if } o = f \\ 0, & \text{if } o \neq f \end{cases}. \tag{4}$$

$A^{Lfo}_{\substack{e\\o}\eta_f}$, $a^{Lfo}_{\substack{e\\o}\eta_f}$, $B^{Lfo}_{\substack{o\\e}\eta_f}$, $b^{Lfo}_{\substack{o\\e}\eta_f}$, $C^{Lfo}_{\substack{e\\o}\eta_f}$, $c^{Lfo}_{\substack{e\\o}\eta_f}$, $D^{Lfo}_{\substack{o\\e}\eta_f}$ and $d^{Lfo}_{\substack{o\\e}\eta_f}$ are the amplitude coefficients of scattered DGF to be determined by applying the boundary condition at the interfaces $r = \alpha_l$ ($l = 1, 2, ..., L$). These boundary conditions are;

$$\hat{r} \times \overline{\overline{G}}^{LLo}_e = 0 \tag{5}$$

$$\hat{r} \times \overline{\overline{G}}^{Lfo}_e = \hat{r} \times \overline{\overline{G}}^{L(f+1)o}_e \tag{6}$$

$$\frac{1}{\mu_f}\hat{r} \times \nabla \times \overline{\overline{G}}^{Lfo}_e = \frac{1}{\mu_{(f+1)}}\hat{r} \times \nabla \times \overline{\overline{G}}^{L(f+1)o}_e \tag{7}$$

We can now obtain the total DGF by applying the principle of scattering superposition,

$$\overline{\overline{G}}^{Lfo}_{E1}(\overline{R},\overline{R}') = \overline{\overline{G}}_{e1}(\overline{R},\overline{R}')\delta_f^o + \overline{\overline{G}}^{Lfo}_{es}(\overline{R},\overline{R}') \tag{8}$$

If our concern is only with the region exterior to the source, then the singular term, which is important only in the source region can be dropped from the expression for the Green's function.

4. MAGNETIC DGF IN THE ANTENNA-PROSTHESIS CONFIGURATION

The principle of duality states that once the electric DGF is obtained, the magnetic DGF is derivable by interchanging the field functions $\overline{P}_{oo}^{ee} \rightarrow k\overline{Q}_{oo}^{ee}$ and $\overline{Q}_{oo}^{ee} \rightarrow k\overline{P}_{oo}^{ee}$ and omitting the singularity term contribution and vice versa.

On the other hand the corresponding total magnetic DGF at any point in the system can be calculated from $\nabla \times \overline{\overline{G}}_e = \overline{\overline{G}}_m$, bearing in mind the discontinuous nature of magnetic DGF across a point source at $R = R'$ and the Ampere-Maxwell equation relating $\overline{\overline{G}}_e$ and $\overline{\overline{G}}_m$ in the dyadic form i.e.: $\nabla \times \overline{\overline{G}}_m = \overline{\overline{I}}\delta_e(\overline{R} - \overline{R}') + k^2\overline{\overline{G}}_e$.

5. ELECTRIC AND MAGNETIC FIELD AT ANY POINT IN THE CONFIGURATION

The use of DGF technique allows us to determine the expansion of the electric and magnetic fields in a cylinder/antenna configuration in a direct and elegant manner. For any current source with current density function $\overline{J}(\overline{R}')$ located outside the cylinder, the electric or magnetic field radiated by such a dipole can be calculated using the formulae,

$$\overline{E}^{Lfo}(\overline{R}) = i\omega\mu_f \iiint_V \overline{\overline{G}}_{E1}^{Lfo}(\overline{R}, \overline{R}') \cdot \overline{J}(\overline{R}')dV' \tag{9}$$

$$\overline{H}^{Lfo}(\overline{R}) = i\omega\varepsilon_f \iiint_V \overline{\overline{G}}_{M1}^{Lfo}(\overline{R}, \overline{R}') \cdot \overline{J}(\overline{R}')dV'. \tag{10}$$

6. CONCLUDING REMARKS

General expressions have been derived in simple form for the finite insulated conducting circular cylinder (insulated medical devices/prostheses) of any size as well as of very small radius (resonant length). The DGFs are obtained by employing the EFE and the method of scattering superposition.

The results of this paper could be useful for a further analysis of the problem as a thin insulated wire or a dielectric-coated implant such as heart pace-maker embedded in the body and biotelemetry transmitters for medical applications and could easily be expanded so as to handle any scatterer having finite radius and length. They can be applied to problems of optical fibers and waveguides for the investigation of inhomogeneities or obstacles inside them or by considering the cylinder as an excitation or scatterer. They can also be of use in the study and design of antennas of high frequency whose performance is less affected by the biological systems and produce lower SAR.

The usefulness of the present technique obviously requires comparison with numerical and experimental results. it is envisaged that a later publication will address this aspect of the problem in more detail.

References

[1] C. T. Tai, *Dyadic Green Functions in Electromagnetic Theory*, IEEE Press, series on Electromagnetic waves, New York, Second Edition, 1994.

[2] W. W. Hansen, A New Type of Expansion in Radiation Problems, *Phys. review*, Vol. 47, 1935, pp. 139-143.

[3] R. E. Collin, *Field Theory of Guided Waves*, IEEE Press, New York, Second Edition, 1991.

[4] S. M. S. Reyhani and R. J. Glover, "Electromagnetic Dyadic Green's Function for a Human Torso Model for Numerical EMC Investigation", proceedings of the *11th International Conference on EMC (IEE EMC York 99)* University of York, UK: pp. 21-25, 12-13 July 1999.

[5] S. M. S. Reyhani and R. J. Glover, "Electromagnetic Dyadic Green's Function of an Implantable Medical Device Model for Numerical EMC Investigation", In "*Recent Advances in Signal Processing and Communications*", Edited by Nikos E. Mastorakis. World Scientific and Engineering Society Press, pp. 224-227, July 1999. ISBN:960-8052-03-3.

emc York 2000

Conference Proceedings

10 - 11 July 2000

The Exhibition Centre, University of York

EMC 2000

Conference Proceedings
10 - 11 July 2000

SMS Reyhani

Brunel University

Far Field Electromagnetic Modelling of Implantable Medical Devices Using Cylindrical DGFs

Far Field Electromagnetic Modeling of Implantable Medical Devices Using Cylindrical DGFs

S.M.S. REYHANI AND R.J. GLOVER
FDTD Research Group
Dept. of Electronic & Computer Eng.,
Brunel University,
Uxbridge, Middlesex, UB8 3PH.
UNITED KINGDOM.
E-mail: Sayed.Salehi-Reyhani@brunel.ac.uk

Abstract: - Electromagnetic pollution is increasing due to massive increase in both mobile and fixed electronic equipments, whilst at the same time, industry is producing devices with ever increasing clock speeds. Modern wireless telecommunication devices (GSM Mobile system) can interfere with implantable medical devices/prostheses and cause possible malfunction. Also the performance of an antenna is significantly altered by the presence of conducting medical devices/prostheses. Hence the need to consider electromagnetic compatibility (EMC) becomes ever more important. Although electromagnetic scattering by a finite cylinder is a well known canonical problem, published work does not include the effects of arbitrary placed source point. The derivations presented here are motivated by the need to understand the behaviour of antennas/insulated antennas near to or embedded in living tissue.

The principle objective of this paper is to outline a far field general expression of dyadic Green's function (DGF) for the problem of electromagnetic radiation from a source of excitation in the presence of a finite length of perfectly conducting circular cylinder of any size as well as of resonant length, which is valid everywhere, including the source region. The whole structure is assumed to be uniform along the propagation direction. The DGFs are obtained by employing the eigenfunction expansion (EFE) and the method of scattering superposition. The advantage of the proposed analysis is its simplicity and efficiency in computation.

The results of this paper could be useful for a further analysis of the problem as a thin wire/insulated wire or an implant/dielectric-coated implant such as heart pace-maker embedded in the body and biotelemetry transmitters for medical applications and could easily be expanded so as to handle any scatterer having finite radius and length.

They can be applied to problems of optical fibers and waveguides for the investigation of inhomogeneities or obstacles inside them or by considering the cylinder as an excitation or scatterer. They can also be of use in the study and design of antennas of high frequency whose performance is less affected by the biological systems and produce lower SAR.

Key-Words: - Electromagnetic, Far Field, Circular Cylinder, Implants, Antenna, Dipole, Dyadic Green's function.

References:

[1] C. T. Tai,*Dyadic Green Functions in Electromagnetic Theory*, IEEE Press, series on Electromagnetic waves, New York, Second Edition, 1994.

[2] S. M. S. Reyhani and R. J. Glover, "Electromagnetic Dyadic Green's Function of an Implantable Medical Device Model for Numerical EMC Investigation", In "*Recent Advances in Signal Processing and Communications*", Edited by Nikos E. Mastorakis. World Scientific and Engineering Society Press, pp. 224-227, July 1999. ISBN:960-8052-03-3.

[3] S. M. S. Reyhani and R. J. Glover, "Electromagnetic Dyadic Green's Function for a Human Torso Model for Numerical EMC Investigation", proceedings of the *11th International Conference on EMC (IEE EMC York 99)* University of York, UK: pp. 21-25, 12-13 July 1999.

[4] S. M. S. Reyhani and R. J. Glover, "Insulated Implantable Medical Device Model Using Electromagnetic Dyadic Green's Function", to be presented at AP2000 Millennium Conference on Antennas and Propagation (AP2000/IEEE, IEE, ICAP, JINA & EUREL), Davos, Switzerland 9-14 April 2000.

Far Field Electromagnetic Modeling of Implantable Medical Devices Using Cylindrical DGFs

S.M.S. REYHANI AND R.J. GLOVER
FDTD Research Group
Dept. of Electronic & Computer Eng.,
Brunel University,
Uxbridge, Middlesex, UB8 3PH.
UNITED KINGDOM.
E-mail: Sayed.Salehi-Reyhani@brunel.ac.uk

Abstract:— Electromagnetic pollution is increasing due to massive increase in both mobile and fixed electronic equipments, whilst at the same time, industry is producing devices with ever increasing clock speeds. Modern wireless telecommunication devices (GSM Mobile system) can interfere with implantable medical devices/prostheses and cause possible malfunction. Also the performance of an antenna is significantly altered by the presence of conducting medical devices/prostheses. Hence the need to consider electromagnetic compatibility (EMC) becomes ever more important. The principle objective of this paper is to outline a far field general expression of dyadic Green's function (DGF) for the problem of electromagnetic radiation from a source of excitation in the presence of a finite length of perfectly conducting circular cylinder of any size as well as of resonant length, which is valid everywhere, including the source region. The whole structure is assumed to be uniform along the propagation direction. The DGFs are obtained by employing the eigenfunction expansion (EFE) and the method of scattering superposition. The advantage of the proposed analysis is its simplicity and efficiency in computation.

Keywords:— Electromagnetic, Far Field, Circular Cylinder, Implants, Antenna, Dipole, Dyadic Green's Function.

1 INTRODUCTION

There is an accelerating growth in the use of radio transmission as the demand for mobile communication expands to embrace data as well as speech. As a result, the mutual interference between transmitting devices and active medical prostheses should be calculated. Analytical solutions are useful for calibrating measurement systems and understanding fundamental propagation mechanisms. We represent here implanted medical devices as conducting cylinders which can be embedded in concentric layered dielectrics.

Although electromagnetic scattering by a finite cylinder is a well known canonical problem, published work does not include the effects of arbitrary placed source point. The derivations presented here are motivated by the need to understand the behaviour of antennas/insulated antennas near to or embedded in living tissue. The eigenfunction expansion (EFE) of DGFs in electromagnetic theory provide a systematic means of constructing and interpreting these dyadics. The pioneering work by Tai [1] has set the stage for most of what has been achieved over the last two and a half decades. The expansion of DGFs in terms of the Hansen [2] vector wave functions must be carried out carefully in order to ensure that one is dealing with a complete expansion. Several theoretical studies have utilized DGFs to analyze the implanted head/body antenna models in Reyhani [4]-[7].

This paper is organized as follows. The complete set of cylindrical vector wave functions are introduced in section 2. This material is included here in order to explicitly define notation and to call attention to a few points in connection with these expansions.

In section 3 we begin to formulate the problem for a finite circular cylinder and in subsection 3.1, we set out with the case, in which we construct the DGF, $\overline{\overline{G}}_{e1}(\overline{R}, \overline{R}')$, in terms that constitute the continuous eigenfunction expansion (EFE) in which the eigenfunctions are guided in preferred r and z-coordinate directions, using the procedures described in Tai [1] or Collin [3]. This expansion also contains an explicit dyadic delta function term which is required for completeness at the source point. It is considered as a correction to the general solenoidal EFE which is valid outside the source point.

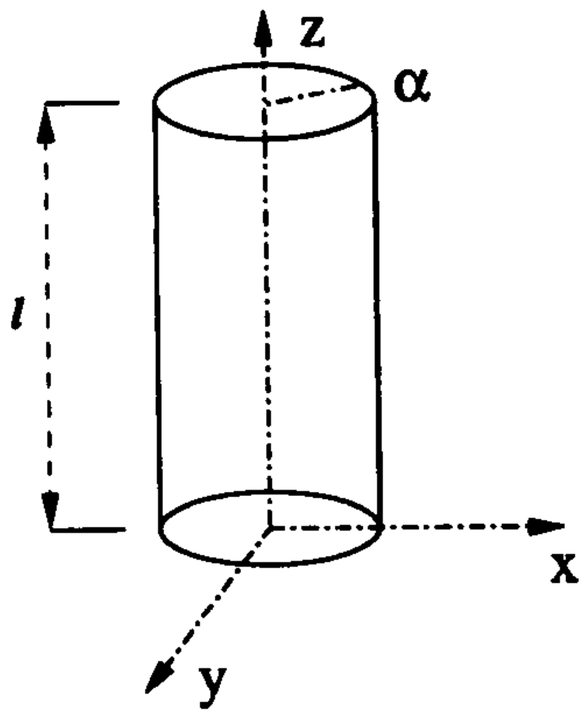

Fig. 1. Diagram of a Finite Circular Cylinder

The procedure required to derive the complete EFE of the scattering DGF for the finite circular cylinder, in terms of only the solenoidal eigenfunctions is shown to be a simple and straight-forward general expression and is summarized in subsection 3.2. The DGF for a finite conducting cylinder, $\overline{\overline{G}}_{E1}(\overline{R},\overline{R}')$ can be constructed from the principle of the superposition, where it satisfies the boundary conditions. The far zone field expression of the prosthesis configuration has been developed in subsection 3.3.

Magnetic type DGF discussed in section 4, can be found by invoking duality or once the electric field is obtained the magnetic field is derivable by taking the curl of the electric field, and vice versa.

Conclusions are then presented in section 6 summarizing the important points contained in this work and finally a short bibliography is provided for further research.

2 VECTOR WAVE FUNCTION FOR A CIRCULAR CYLINDER OF FINITE LENGTH

The cylindrical vector wave functions are the building blocks of the EFE of various kinds of DGFs. They are solutions of the homogeneous vector Helmholtz equation. The generating or eigenfunctions, which are solutions of the cylindrical scalar wave equation $\nabla^2\Psi + k_\lambda^2\Psi{=}0$ can be written [4] in the form

$$\Psi_{\substack{e\\o}\substack{o\\e}n}(h) = j_n(\lambda r)^{\cos}_{\sin} n\phi^{\cos}_{\sin} hz, \qquad (1)$$

Here subscripts "e" stands for even and "o" is odd character of the generating functions. $h = \frac{q\pi}{l}$ are the eigenvalues in the z-direction with $q = 0, 1, 2, ...$ and l is the length of cylinder. $j_n(\lambda r)$ identifies the cylindrical Bessel functions of the order n to represent both out-going and in-coming waves. λ is the continuous eigenvalue. Cylindrical vector wave functions are akin to the Debye potentials. $\overline{P}_{\substack{e\\o}\substack{o\\e}n\lambda}(h) = \nabla\times[\Psi_{\substack{e\\o}\substack{o\\e}n}\hat{z}]$ and $\overline{Q}_{\substack{e\\o}\substack{o\\e}n\lambda}(h) = \frac{1}{k_\lambda}\nabla\times\nabla\times[\Psi_{\substack{e\\o}\substack{o\\e}n}\hat{z}]$. Where $\hat{z}$ is the piloting vector and here $k_\lambda^2 = \lambda^2 + h^2$.

The complete expressions for the solenoidal (rotational or transverse) and the nonsolenoidal (irrotational or lamellar) functions are given in Reyhani [5]. These functions are defined in the entire space, corresponding to $0 \le r \le \infty$, $0 \le \phi \le 2\pi$ and $0 < z < l$.

3 FORMULATION OF THE PROBLEM

Consider a cylinder (fig. 1) of radius "α" concentric along z-axis with length "l" is illuminated by an electromagnetic wave. An electromagnetic field is induced in the system and an electromagnetic wave is scattered by the system.

A time dependence $e^{j\omega t}$ is assumed and suppressed throughout.

3.1 DGF for a finite Length Cylinder of Circular Cross-Section

Applying the method of (G_m) and according to the Ohm-Rayleigh procedure the expression for $(\overline{\overline{G}}_{e1})$ for a finite cylinder of radius "α" concentric with the z-axis is given in Reyhani [5] in the form

$$\overline{\overline{G}}_{e1}(\overline{R},\overline{R}') = -\frac{\hat{r}\hat{r}}{k^2}\delta_\epsilon(\overline{R}-\overline{R}') + \int_0^l dh \sum_{n=0}^{\infty} C_\lambda \cdot \begin{cases} \left\{ \begin{array}{l} [\overline{P}^{(1)}_{\substack{e\\o}\eta}(h;\eta)\overline{P}'_{\substack{e\\o}\eta}(h;\eta)] \\ [\overline{Q}^{(1)}_{\substack{o\\e}\eta}(h;\eta)\overline{Q}'_{\substack{o\\e}\eta}(h;\eta)] \end{array} \right\}, & r > r', \\ \left\{ \begin{array}{l} [\overline{P}_{\substack{e\\o}\eta}(h;\eta)\overline{P}'^{(1)}_{\substack{e\\o}\eta}(h;\eta)] \\ [\overline{Q}_{\substack{o\\e}\eta}(h;\eta)\overline{Q}'^{(1)}_{\substack{o\\e}\eta}(h;\eta)] \end{array} \right\}, & r < r'. \end{cases} \qquad (2)$$

where

$$C_\lambda = \frac{i(2-\delta_o^n)}{2l\eta^2} \qquad (3)$$

Coefficient C_λ depends on the value of δ_o^n which is the Kronecker delta functions defined with respect to n, when

$$\delta_o^n = \begin{cases} 1, & \text{if } n = o \\ 0, & \text{if } n \neq o \end{cases} \qquad (4)$$

Here $\hat{r}\hat{r}$ is a dyad (dyadic product of the unit vectors) and $\delta(\overline{R}-\overline{R}')$ is weighted Dirac delta function in three

dimensions. This is included explicitly as a correction to the general solenoidal EFE which is valid outside the source point. The dyadic delta function term at the source point in cylindrical coordinates

$$\delta(\overline{R}-\overline{R}') = \frac{1}{r'}\delta(\overline{r}-\overline{r}')\delta(\overline{\phi}-\overline{\phi}')\delta(\overline{z}-\overline{z}') \qquad (5)$$

Comparing the DGFs for a finite cylinder developed here with those presented by other authors e.g. Tai [1] for an infinite cylinder, one can notice that they are similar in mathematical form but different in the calculations of Ps and Qs and the limits of integration for a finite cylinder.

3.2 Scattering DGF for a Finite Conducting Cylinder of Circular Cross-Section

When a perfectly conducting cylinder of the same size as above is illuminated by an electromagnetic wave, the scattered terms can be written in the form

$$\overline{\overline{G}}_{es}(\overline{R},\overline{R}') = \int_0^l dh \sum_{n=0}^{\infty} C_\lambda \cdot \begin{bmatrix} \alpha^{e\,o}_{o\,e\,\eta}\overline{P}^{(1)}_{o\,e\,\eta}(h;\eta)\overline{P}'^{(1)}_{o\,e\,\eta}(h;\eta) \\ \beta^{e\,e}_{o\,e\,\eta}\overline{Q}^{(1)}_{o\,e\,\eta}(h;\eta)\overline{Q}'^{(1)}_{o\,e\,\eta}(h;\eta) \end{bmatrix}. \qquad (6)$$

Applying the principle of scattering superposition, we obtain

$$\overline{\overline{G}}_{E1}(\overline{R},\overline{R}') = \overline{\overline{G}}_{e1}(\overline{R},\overline{R}') + \overline{\overline{G}}_{es}(\overline{R},\overline{R}') \qquad (7)$$

Where we consider the function for a finite circular cylinder in a region $0 \le r \le \infty$. After applying the boundary condition one can determine the unknown coefficients. In order to satisfy the boundary condition at interface $r = \alpha$,

$$\hat{r}\times\left[\overline{P}^{e\,o}_{o\,e\,\eta}(h;\eta)\overline{P}'^{(1)}_{o\,e\,\eta}(h;\eta) + \alpha^{e\,o}_{o\,e\,\eta}\overline{P}^{(1)}_{o\,e\,\eta}(h;\eta)\overline{P}'^{(1)}_{o\,e\,\eta}(h;\eta)\right]_{r=\alpha} \qquad (8)$$

$$\hat{r}\times\left[\overline{Q}^{e\,e}_{o\,e\,\eta}(h;\eta)\overline{Q}'^{(1)}_{o\,e\,\eta}(h;\eta) + \beta^{e\,e}_{o\,e\,\eta}\overline{Q}^{(1)}_{o\,e\,\eta}(h;\eta)\overline{Q}'^{(1)}_{o\,e\,\eta}(h;\eta)\right]_{r=\alpha} \qquad (9)$$

$$\hat{r}\times\left[\overline{P}^{e\,o}_{o\,e\,\eta}(h;\eta) + \alpha^{e\,o}_{o\,e\,\eta}\overline{P}^{(1)}_{o\,e\,\eta}(h;\eta)\right]_{r=\alpha} = 0 \qquad (10)$$

$$\hat{r}\times\left[\overline{Q}^{e\,e}_{o\,e\,\eta}(h;\eta) + \beta^{e\,e}_{o\,e\,\eta}\overline{Q}^{(1)}_{o\,e\,\eta}(h;\eta)\right]_{r=\alpha} = 0 \qquad (11)$$

substituting for $\overline{P}^{e\,o}_{o\,e\,\eta}(h;\eta)$ and $\overline{P}^{(1)}_{o\,e\,\eta}(h;\eta)$

$$\overline{P}^{e\,o}_{o\,e\,\eta}(h;\eta) = \nabla\times[j_n(\eta r)^{\cos}_{\sin} n\phi \sin hz\hat{z}], \qquad (12)$$

$$\overline{P}^{(1)}_{o\,e\,\eta}(h;\eta) = \nabla\times[H^{(1)}_n(\eta r)^{\cos}_{\sin} n\phi \sin hz\hat{z}], \qquad (13)$$

in equation (10) produces $\alpha^{e\,o}_{o\,e\,\eta} = -\frac{[\partial j_n(\eta\alpha)]/\partial(\eta\alpha)}{[\partial H^{(1)}_n(\eta\alpha)]/\partial(\eta\alpha)}$.

Similarly inserting for $\overline{Q}^{e\,e}_{o\,e\,\eta}(h;\eta)$ and $\overline{Q}^{(1)}_{o\,e\,\eta}(h;\eta)$

$$\overline{Q}^{e\,e}_{o\,e\,\eta}(h;\eta) = \frac{1}{k}\nabla\times\nabla\times[j_n(\eta r)^{\cos}_{\sin} n\phi \cos hz\hat{z}], \qquad (14)$$

$$\overline{Q}^{(1)}_{o\,e\,\eta}(h;\eta) = \frac{1}{k}\nabla\times\nabla\times[H^{(1)}_n(\eta r)^{\cos}_{\sin} n\phi \cos hz\hat{z}], \qquad (15)$$

in equation (11) produces $\beta^{e\,e}_{o\,e\,\eta} = -\frac{[j_n(\eta\alpha)]}{[H^{(1)}_n(\eta\alpha)]}$.

3.3 Far Zone Field Expression of the Prosthesis Configuration

The far field of this medical device in the presence of a source can be computed using the asymptotic expression for $\overline{\overline{G}}_{E1}(\overline{R},\overline{R}')$, utilizing the saddle-point integration method. Assuming $\eta r \ggg 1$, the Hankel function in $\overline{P}^{(1)}_{o\,e\,\eta}(h;\eta)$ and $\overline{Q}^{(1)}_{o\,e\,\eta}(h;\eta)$ can be approximated to its asymptotic expression

$$H^{(1)}_n(\eta r) \simeq \left(\frac{2}{\pi\eta r}\right)^{\frac{1}{2}}(-i)^{n+\frac{1}{2}}e^{i\eta r} \qquad (16)$$

$$\overline{P}^{(1)}_{o\,e\,\eta}(h;\eta) \simeq (-i)^{n+\frac{3}{2}}\eta\left(\frac{2}{\pi\eta r}\right)e^{i(\eta r+hz)}{}^{\cos}_{\sin} n\phi \sin hz\hat{\phi} \qquad (17)$$

$$\overline{Q}^{(1)}_{o\,e\,\eta}(h;\eta) \simeq (-i)^{n+\frac{1}{2}}\frac{\eta}{k}\left(\frac{2}{\pi\eta r}\right)^{\frac{1}{2}}e^{i(\eta r+hz)} \cdot \begin{Bmatrix} {}^{\cos}_{\sin} n\phi \sin hz(-h\hat{r}) \\ {}^{\cos}_{\sin} n\phi \cos hz(\eta\hat{z}) \end{Bmatrix} \qquad (18)$$

The expression for $\overline{\overline{G}}_{E1}(\overline{R},\overline{R}')$ can be approximated with the functions $\overline{P}^{(1)}_{o\,e\,\eta}(h;\eta)$ and $\overline{Q}^{(1)}_{o\,e\,\eta}(h;\eta)$ replaced by (17) and (18), can be written in the form

$$\overline{\overline{G}}_{E1}(\overline{R},\overline{R}') \simeq \int_0^l dh \sum_{n=0}^{\infty} C_\lambda \frac{2\eta}{(2\pi\eta r)^{\frac{1}{2}}}(-i)^{n+\frac{1}{2}}e^{i(\eta r+hz)} \cdot \begin{Bmatrix} -i^{\cos}_{\sin} n\phi \sin hz\hat{\phi}\begin{bmatrix} \overline{P}'^{e\,o}_{o\,e\,\eta}(h;\eta) \\ \alpha^{e\,o}_{o\,e\,\eta}\overline{P}^{(1)}_{o\,e\,\eta}(h;\eta) \end{bmatrix} \\ \frac{1}{k}{}^{\cos}_{\sin} n\phi \sin hz(-h\hat{r})\begin{bmatrix} \overline{Q}'^{e\,e}_{o\,e\,\eta}(h;\eta) \\ \beta^{e\,e}_{o\,e\,\eta}\overline{Q}^{(1)}_{o\,e\,\eta}(h;\eta) \end{bmatrix} \\ \frac{1}{k}{}^{\cos}_{\sin} n\phi \cos hz(\eta\hat{z})\begin{bmatrix} \overline{Q}'^{e\,e}_{o\,e\,\eta}(h;\eta) \\ \beta^{e\,e}_{o\,e\,\eta}\overline{Q}^{(1)}_{o\,e\,\eta}(h;\eta) \end{bmatrix} \end{Bmatrix} \qquad (19)$$

where terms of the order $\ge (\eta r)^{-\frac{3}{2}}$ have been ignored.

4 MAGNETIC DGF IN THE ANTENNA-PROSTHESIS CONFIGURATION

The principle of duality states that once the electric DGF is obtained, the magnetic DGF is derivable by interchanging the field functions $\overline{P}_{\rho\rho}^{\phi\phi} \rightarrow k\overline{Q}_{\rho\rho}^{\phi\phi}$ and $\overline{Q}_{\rho\rho}^{\phi\phi} \rightarrow k\overline{P}_{\rho\rho}^{\phi\phi}$ and omitting the singularity term contribution and vice versa.

On the other hand the corresponding total magnetic DGF at any point in the system can be calculated from $\nabla \times \overline{\overline{G}}_e = \overline{\overline{G}}_m$, bearing in mind the discontinuous nature of magnetic DGF across a point source at $R = R'$ and the Ampere-Maxwell equation relating $\overline{\overline{G}}_e$ and $\overline{\overline{G}}_m$ in the dyadic form i.e.: $\nabla \times \overline{\overline{G}}_m = \overline{\overline{I}}\delta_e(\overline{R} - \overline{R}') + k^2\overline{\overline{G}}_e$.

5 ELECTRIC AND MAGNETIC FIELD AT ANY POINT IN THE CONFIGURATION

The use of DGF technique allows us to determine the expansion of the electric and magnetic fields in a cylinder/antenna configuration in a direct and elegant manner.

For any current source with current density function $\overline{J}(\overline{R}')$ located outside the cylinder, the electric or magnetic field radiated by such a dipole can be calculated using the formulae,

$$\overline{E}(\overline{R}) = i\omega\mu_o \iiint_V \overline{\overline{G}}_{E1}(\overline{R}, \overline{R}') \cdot \overline{J}(\overline{R}')dV' \qquad (20)$$

$$\overline{H}(\overline{R}) = i\omega\varepsilon_o \iiint_V \overline{\overline{G}}_{M1}(\overline{R}, \overline{R}') \cdot \overline{J}(\overline{R}')dV'. \qquad (21)$$

These signify the computation of the E and H-fields in the structure, which states the superposition of the incident field $\overline{E}_i(\overline{R})$ or $\overline{H}_i(\overline{R})$ and the scattered field $\overline{E}_s(\overline{R})$ or $\overline{H}_s(\overline{R})$ is given by

$$\overline{E}(\overline{R}) = \overline{E}_i(\overline{R}) + \overline{E}_s(\overline{R}) \qquad (22)$$

$$\overline{H}(\overline{R}) = \overline{H}_i(\overline{R}) + \overline{H}_s(\overline{R}). \qquad (23)$$

6 CONCLUDING REMARKS

General far field expressions have been derived in simple form for the finite conducting circular cylinder (medical devices/prostheses) of any size as well as of very small radius (resonant length). The DGFs are obtained by employing the EFE and the method of scattering superposition.

The results of this paper could be useful for a further analysis of the problem as a thin wire/insulated wire or an implant/dielectric-coated implant such as heart pace-maker embedded in the body and biotelemetry transmitters for medical applications and could easily be expanded so as to handle any scatterer having finite radius and length. They can be applied to problems of optical fibers and waveguides for the investigation of inhomogeneities or obstacles inside them or by considering the cylinder as an excitation or scatterer. They can also be of use in the study and design of antennas of high frequency whose performance is less affected by the biological systems and produce lower SAR (specific absorption rate, the rate of electromagnetic energy deposition) and as a result contribute to the efficiency of handheld/mobile phones.

Numerical simulation techniques developed for the comprehensive analysis of the human exposure to electromagnetic waves and estimating the SAR may require considerable time and large computer memory for calculation. Analytical methods provide valuable tools in evaluating the interaction between canonical head/body models and antenna sources. The usefulness of the present technique obviously requires comparison with numerical and experimental results. it is envisaged that a later publication will address this aspect of the problem in more detail.

REFERENCES

[1] C. T. Tai, *Dyadic Green Functions in Electromagnetic Theory,* IEEE Press, series on Electromagnetic waves, New York, *Second Edition,* 1994.

[2] W. W. Hansen, A New Type of Expansion in Radiation Problems, *Phys. review,* Vol. 47, 1935, pp. 139-143.

[3] R. E. Collin, *Field Theory of Guided Waves,* IEEE Press, New York, Second Edition, 1991.

[4] S. M. S. Reyhani and R. J. Glover, "Electromagnetic Dyadic Green's Function for a Human Torso Model for Numerical EMC Investigation", proceedings of the *11th International Conference on EMC (IEE EMC York 99)* University of York, UK: pp. 21-25, 12-13 July 1999.

[5] S. M. S. Reyhani and R. J. Glover, "Electromagnetic Dyadic Green's Function of an Implantable

Medical Device Model for Numerical EMC Investigation", In "*Recent Advances in Signal Processing and Communications*", Edited by Nikos E. Mastorakis. World Scientific and Engineering Society Press, pp. 224-227, July 1999. ISBN:960-8052-03-3.

[6] S. M. S. Reyhani and R. J. Glover, "Insulated Implantable Medical Device Model Using Electromagnetic Dyadic Green's Function", proceedings of the AP2000 Millennium Conference on Antennas and Propagation (AP2000/IEEE, IEE, ICAP, JINA & EUREL), Davos, Switzerland: paper no. p1566, 9-14 April 2000.

[7] S. M. S. Reyhani and R. J. Glover, "Electromagnetic Dyadic Green's Function for a Multilayered Homogeneous Lossy Dielectric Spherical Head Model for Numerical EMC Investigation", *Journal of Electromagnetics* Vol. 20, no.2, pp. 141-153, March-April 2000.

IEE Science, Education and Technology

Seminar

Electromagnetic assessment and antenna design relating to health implications of mobile phones

Monday, 28 June 1999

IEE
Savoy Place
London
WC2R 0BL

99/043

IEE

IEE Science, Education and Technology

Seminar

Electromagnetic assessment and antenna design relating to health implications of mobile phones

Monday, 28 June 1999

IEE
Savoy Place
London
WC2R 0BL

99/043

ELECTROMAGNETIC MODELING OF SPHERICAL HEAD USING DYADIC GREEN'S FUNCTION

S.M.S. Reyhani* and R.J. Glover

Abstract

Antenna radiation pattern and other characteristics are significantly altered by the presence of the human head. When considering possible biological effects of electromagnetic (EM) fields, it is important to distinguish between field strengths outside the subject, and those within the body. The relationship of fields outside and within the body (called coupling) varies greatly with frequency. This paper aims to express an exact general representation of dyadic Green's function (DGF) for the problem of electromagnetic radiation from a source of excitation in the presence of a human head model (multi-layered homogeneous lossy dielectric spherical model), which is valid everywhere, including the source region. The medium is assumed to be homogeneous, isotropic, linear, non-dispersive and stationary. The DGFs are obtained by employing the method of scattering superposition. Alternatively a compact general expression has been developed to determine the electric and magnetic type DGFs giving clarity as well as more efficient and economical computation in terms of speed, time and memory.

1. INTRODUCTION

Interaction of electromagnetic fields (EMF) with living systems and public concern regarding their allegedly/possible harmful health effects have been of current research interest. These investigations are motivated by two relating factors:

i) a need to evaluate the specific absorption rate (SAR) (the rate of RF energy deposition) in the user's body, in order to evaluate potential health effects and compliance with standards, and;

ii) the antenna performance in the proximity of the user's body and to develop better antenna designs whose performance is less affected by the biological systems and produce lower SAR.

The Eigen-function expansion (EFE) of DGFs in electromagnetic theory provide a systematic means of constructing and interpreting these dyadics. The pioneering work by Tai [1] has set the stage for most of what has been achieved over the last two and a half decades. The expansion of DGFs in terms of the Hansen [2] vector wave functions must be carried out carefully in order to ensure that one is dealing with a complete expansion.

This paper is organised as follows. The complete set of spherical vector wave functions are introduced in section 2.

In section 3, we start with the unbounded case, in which the point source radiates with no interface present and construct the corresponding DGF, $\overline{\overline{G}}_{ee}^{00}(R,R')$, in terms of an integral over the spectra of plane waves that constitute the continuous Eigen-function expansion (EFE) in which the Eigen-functions are guided in preferred R-coordinate direction, using the procedures described in Tai [1] or Collin [3]. This expansion also contains an explicit dyadic delta function term which is required for completeness at the source point. It is considered as a correction to the general solenoidal EFE which is valid outside the source point.

Subsection 3.2, presents the general scattering DGFs expansions (5) in terms of only the solenoidal Eigen-functions. It is in this development that the principal point of this paper is identified.

Magnetic type DGF can be found by invoking duality or once the electric field is obtained the magnetic field is derivable by taking the curl of the electric field, and vice versa.

*The authors are with the FDTD Research Group, Dept. of Elect. & Electronic Eng., Brunel University, Uxbridge, Middlesex, UB8 3PH. United Kingdom. E-mail: Sayed.Salehi-Reyhani@brunel.ac.uk.

Conclusions are then presented in section 4 summarising the important points contained in this work and finally a short bibliography is provided for further research.

2. SPHERICAL HANSEN VECTOR WAVE FUNCTIONS

The spherical vector wave functions are the building blocks of the EFE of various kinds of DGF. They are solutions of the homogeneous vector Helmholtz equation. The generating functions, which are solutions of the spherical scalar wave equation $\nabla^2\Psi + k^2\Psi=0$, can be written in the form

$$\Psi_{emn}(k) = j_n(kR)F_n^m(\cos\theta)\begin{matrix}\cos\\ \sin\end{matrix}m\phi, \tag{1}$$

Here k is an undetermined wave number and R is the piloting radial vector. Subscripts "e" stands for even and "o" is odd character of the generating functions. Where $F_n^m(\cos\theta)$ identifies the Associated Legendre functions of the first kind with order (n,m) and $j_n(kR)$ denotes the spherical Bessel functions of the order n to represent both out-going and in-coming waves. Spherical vector wave functions are akin to the Debye potentials. $\overline{P}_{emn}(k) = \nabla\times[\Psi_{emn}\overline{R}]$ and $\overline{Q}_{emn}(k) = \frac{1}{k}\nabla\times\nabla\times[\Psi_{emn}\overline{R}]$. These functions are defined in the entire space, corresponding to $0 \le R \le \infty$, $0 \le \phi \le 2\pi$ and $0 \le \theta \le \pi$. The orthogonal properties of these vector wave functions have been discussed by Tai [1] and Collin [3].

3. FORMULATION OF THE PROBLEM

Before developing the expressions of electromagnetic wave propagation in multi-layered head model, one should examine the media firstly with no scatterer present. Consider a multi-layered homogeneous lossy dielectric concentric sphere with radii as shown in (fig. 1) is illuminated by an electromagnetic wave. An electromagnetic field is induced in the system and an electromagnetic wave is scattered by the system. A time dependence $e^{j\omega t}$ is assumed and suppressed throughout.

3.1 Free Space DGF for an Electric Dipole in Unbounded Medium

The electric and magnetic fields due to an electric dipole located at R' in an infinite homogeneous space without the presence of an scatterer (obstacle) can be computed in spherical co-ordinates. There are various methods that can be utilised to achieve this. The expansion of the electric field requires both the transverse and longitudinal vector Eigen-functions and hence the DGF must also have both sets of Eigen-functions in its expansion [1].

$$\overline{\overline{G}}_{eo}^{00e}(\overline{R},\overline{R}') = -\frac{\hat{R}\hat{R}}{k_o^2}\delta(\overline{R}-\overline{R}') + \frac{ik_o}{4\pi}\sum_{n=1}^{\infty}\sum_{m=0}^{n} C_{mn}$$
$$\begin{cases} \begin{Bmatrix} [\overline{P}_{emn}^{(1)}(k_o)\overline{P}'_{emn}(k_o)] \\ [\overline{Q}_{emn}^{(1)}(k_o)\overline{Q}'_{emn}(k_o)] \end{Bmatrix}, & R > R', \\ \\ \begin{Bmatrix} [\overline{P}_{emn}(k_o)\overline{P}'^{(1)}_{emn}(k_o)] \\ [\overline{Q}_{emn}(k_o)\overline{Q}'^{(1)}_{emn}(k_o)] \end{Bmatrix}, & R < R'. \end{cases} \tag{2}$$

where

$$C_{mn} = (2-\delta_o^m)\frac{2n+1}{n(n+1)}\frac{(n-m)!}{(n+m)!} \tag{3}$$

Coefficient C_{mn} depends on the value of m and n where δ_o^m is the Kronecker delta functions, when

$$\delta = \begin{cases} 1, & \text{if } m = o \\ 0, & \text{if } m \neq o \end{cases} \tag{4}$$

Subscripts "o" and "e" stand for unbounded (open) space and electric respectively. Here $\hat{R}\hat{R}$ is a dyad (dyadic product of unit vectors) and $\delta(\overline{R}-\overline{R}')$ is weighted Dirac delta function in three dimensions. This is included explicitly as a correction to the general solenoidal EFE which is valid outside the source point.

3.2 General Expression of Scattering DGFs for an Electric Dipole in the Presence of a Spherical Head Model

When a biological system is illuminated by an electromagnetic wave, an electromagnetic field is induced inside the system and an electromagnetic wave is scattered externally by the system. Since the biological system is an irregularly shaped heterogeneous imperfectly conducting medium with frequency dependent permittivity and conductivity, the distribution of the internal electromagnetic field and the scattered electromagnetic wave will depend on the body's physiological parameters and geometry, as well as the frequency and polarisation of the incident wave. The mathematical complexity of the problem has led researchers to investigate simple models. Several theoretical studies have analysed these models in Reyhani [4,5]. In this paper the medium is assumed to be homogeneous, isotropic, linear, non-dispersive and stationary. An efficient formulation of the general scattering DGF for a multi-layer spherical head (fig. 1) is:

$$\overline{\overline{G}}_{es}^{Lfo}(\overline{R},\overline{R}') = \frac{ik_o}{4\pi}\sum_{n=1}^{\infty}\sum_{m=0}^{n} C_{mn}\cdot\begin{Bmatrix} A_{:P}^{Lfo}(1-\delta_f^L)\overline{P}_{:mn}^{(1)}(k_f)\overline{P}'^{(1)}_{:mn}(k_o) \\ A_{:Q}^{Lfo}(1-\delta_f^L)\overline{Q}_{:mn}^{(1)}(k_f)\overline{Q}'^{(1)}_{:mn}(k_o) \\ B_{:P}^{Lfo}(1-\delta_f^o)\overline{P}_{:mn}(k_f)\overline{P}'^{(1)}_{:mn}(k_o) \\ B_{:Q}^{Lfo}(1-\delta_f^o)\overline{Q}_{:mn}(k_f)\overline{Q}'^{(1)}_{:mn}(k_o) \end{Bmatrix}. \tag{5}$$

"L" is the symbol for last inner layer in the head. "f" is the field point or obeserver layer. Superscript/subscript "o" stands for source point at open space while subecript "s" is scattering. δ_f^L and δ_f^o are the Kronecker delta functions, where

$$\delta = \begin{cases} 1, & \text{if } L/o = f \\ 0, & \text{if } L/o \neq f \end{cases} \tag{6}$$

$A_{:P}^{Lfo}$, $A_{:Q}^{Lfo}$, $B_{:P}^{Lfo}$ and $B_{:Q}^{Lfo}$ are the amplitude coefficients of scattered DGF to be calculated by applying the boundary condition at the surface ($f = 0, 1, 2, ..., L$) of the sphere. These boundary conditions are;

$$\hat{R}\times\overline{\overline{G}}_e^{Lfo} = \hat{R}\times\overline{\overline{G}}_e^{L(f+1)o} \tag{7}$$

and

$$\frac{1}{\mu_f}\hat{R}\times\nabla\times\overline{\overline{G}}_e^{Lfo} = \frac{1}{\mu_{(f+1)}}\hat{R}\times\nabla\times\overline{\overline{G}}_e^{L(f+1)o} \tag{8}$$

For more details on the evaluation of coefficients, readers are referred to Li et-al [6].

We can now obtain the total DGF by applying the principle of scattering superposition,

$$\overline{\overline{G}}_e^{Lfo}(\overline{R},\overline{R}') = \overline{\overline{G}}_{eo}^{00o}(\overline{R},\overline{R}')\delta_f^o + \overline{\overline{G}}_{es}^{Lfo}(\overline{R},\overline{R}') \tag{9}$$

If our concern is only with the region exterior to the source, then the singular term, which is important only in the source region can be dropped from the expression for the Green's function.

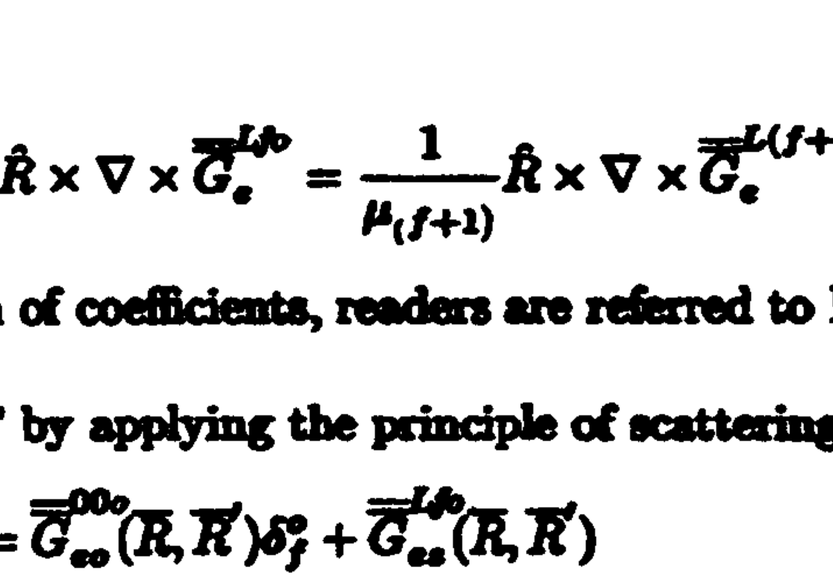

Figure 1. Test Position of a Dipole and Cross Section of Spherical Head Model

4. A NOVEL GENERAL EXPRESSION OF SCATTERING DGFS FOR AN ELECTRIC DIPOLE IN THE PRESENCE OF A SPHERICAL HEAD MODEL

The integral equation methods have the disadvantage of being difficult to implement for complex objects, and generally result in the use of full matrices, whose treatment requires a large amount of memory and CPU time. The computational difficulties can be surmounted by more convenient and compact general equation. General formulations for scattering DGFs can be expressed by introducing the $\overline{\odot}$ operator which exploits the symmetry of the principle terms in the DGF expansion to give a general formulation applicable to a wide range of geometrical configurations [my unpublished paper] when one can significantly reduce the number of field samples needed for the field calculation. As shown below

$$\overline{\overline{G}}_{es}^{Lfo}(\overline{R},\overline{R}') = \frac{ik_o}{4\pi}\sum_{n=1}^{\infty}\sum_{m=0}^{n} C_{mn}\begin{bmatrix} A_{eP}^{Lfo}\,\overline{\overline{\odot}}_{esM}^{Lfo} \\ A_{eQ}^{Lfo}\,\overline{\overline{\odot}}_{esN}^{Lfo}\end{bmatrix} \tag{10}$$

We give a direct and conceptually simple algorithm whose main benefit is great computational efficiency. Where

$$\overline{\overline{\odot}}_{esp}^{L0o} = 0, \qquad \text{for } L = 0$$

(This means that, there is only infinite open space in the absence of a scattering body.) and

$$\overline{\overline{\odot}}_{esp}^{L0o} = \overline{P}_{emn}^{(1)}(k_f)\overline{P}_{emn}^{(1)}(k_o), \qquad \text{for } f = 0 \text{ and } L > 0$$

$$\overline{\overline{\odot}}_{esp}^{Lfo} = \begin{bmatrix}\alpha\overline{P}_{emn}^{(1)}(k_f)\overline{P}_{emn}^{\prime(1)}(k_o) \\ \beta\overline{P}_{emn}(k_f)\overline{P}_{emn}^{\prime(1)}(k_o)\end{bmatrix}, \qquad \text{for} f \neq \begin{cases}0\\ \text{or}\\ L\end{cases}$$

and

$$\overline{\overline{\odot}}_{esp}^{LLo} = \overline{P}_{emn}(k_f)\overline{P}_{emn}^{\prime(1)}(k_o), \qquad \text{for } f = L$$

$\overline{\overline{\odot}}_{esQ}^{Lfo}$ can be calculated from the same procedure as for $\overline{\overline{\odot}}_{esp}^{Lfo}$.

5. MAGNETIC DGF IN THE ANTENNA-HEAD CONFIGURATION

The principle of duality state that once the electric DGF is obtained, the magnetic DGF is derivable by interchanging the field functions $\overline{P}_{emn} \to k\overline{Q}_{emn}$ and $\overline{Q}_{emn} \to k\overline{P}_{emn}$ and omitting the singularity term contribution and vice versa.

On the other hand the corresponding total magnetic DGF at any point in the system can be calculated from $\nabla \times \overline{\overline{G}}_e^{Lfo} = \overline{\overline{G}}_m^{Lfo}$, bearing in mind the discontinuous nature of magnetic DGF across a point source at $R = R'$ and the Ampere-Maxwell equation relating $\overline{\overline{G}}_e^{Lfo}$ and $\overline{\overline{G}}_m^{Lfo}$ in the dyadic form i.e.: $\nabla \times \overline{\overline{G}}_m^{Lfo} = \overline{\overline{I}}\delta(\overline{R}-\overline{R}') + k^2\overline{\overline{G}}_e^{Lfo}$

6. ELECTRIC AND MAGNETIC FIELD AT ANY POINT IN THE CONFIGURATION

The use of DGF technique allows us to determine the expansion of the electric and magnetic fields in a head/antenna configuration in a direct and elegant manner. For any current source with current density function $\overline{J}(\overline{R}')$ located outside the head, the electric or magnetic field radiated by such a dipole can be calculated using the formulae,

$$\overline{E}^{Lfo}(\overline{R}) = i\omega\mu_f \iiint_V \overline{\overline{G}}_{e1}^{Lfo}(\overline{R},\overline{R}')\cdot\overline{J}(\overline{R}')dV' \tag{11}$$

$$\overline{H}^{Lfo}(\overline{R}) = i\omega\epsilon_f \iiint_V \overline{\overline{G}}_{m1}^{Lfo}(\overline{R},\overline{R}')\cdot\overline{J}(\overline{R}')dV'. \tag{12}$$

7. CONCLUDING REMARKS

We have proposed general electromagnetic representations for a human head model (in simple form for the multi-layered homogeneous lossy dielectric sphere) for numerical EMC investigation in order to evaluate deterioration of the antennas performance and obtain the rates of RF energy deposition (SAR) inside the head. The representations may be used to optimise antenna design, ascertain potential health hazards, and compliance with standards legislation. The DGFs are obtained by employing the EFE and the method of scattering superposition.

Furthermore, by defining a symmetry operator the required memory for efficient numerical computations using the method of moments can be reduced drastically by formulating a new compact general expression. The validity of general model is verified by the DGF of the specific models which was in agreement with other authors' study.

The results of this study could be useful for a further analysis of the problem. Both GSM (global system for mobile communication) and PCS (personal communication services) pose potential problems with regard to interactions with the human body and implanted medical devices. Interaction/interference-free antennas design is useful and, increasingly, is becoming necessary. Since anything that conducts can be considered as an antenna and two antennas interact with each other, the interaction problem could potentially be solved by using the mobile phone (handset transceiver) user (human body) as an antenna and transmitting at frequency levels (for example, noise) unharmful to humans. This would make possible the design of antenna-less PCS, receiving/transmitting signals only in close proximity to biological antennas (users).

The usefulness of the present technique obviously requires comparison with numerical and experimental results. it is envisaged that a later publication will address this aspect of the problem in more detail.

References

[1] C. T. Tai, "Dyadic Green Functions in Electromagnetic Theory". IEEE Press, series on Electromagnetic waves, New York, Second Edition, 1994.

[2] W. W. Hansen, "A New Type of Expansion in Radiation Problems". Phys. review, Vol. 47, pp. 139-143, 1935.

[3] R. E. Collin, "Field Theory of Guided Waves". IEEE Press, New York, Second Edition, 1991.

[4] S. M. S. Reyhani and R. J. Glover, "Electromagnetic Dyadic Green's Function of an Implantable Medical Device Model for Numerical EMC Investigation", to be presented at 3rd IMACS/IEEE International Multiconference on: Circuits, Systems, Communications and Computers (CSCC'99) (IMACS/IEEE CSCC'99), Athens, Greece 4-8 July 1999.

[5] S. M. S. Reyhani and R. J. Glover, "Electromagnetic Dyadic Green's Function for a Human Torso Model for Numerical EMC Investigation", to be presented at 11th International Conference on EMC (IEE EMC York 99) University of York, UK: 12-13 July 1999.

[6] L. W. Li, J. A. Bennett and P. L. Dyson, "Some Method for Solving the Coefficients of Dyadic Green's Function in Isotropic Stratified Media". Int. J. Electronics, Vol. 70, no.4, pp. 803-814, 1991.